internal combustion engines

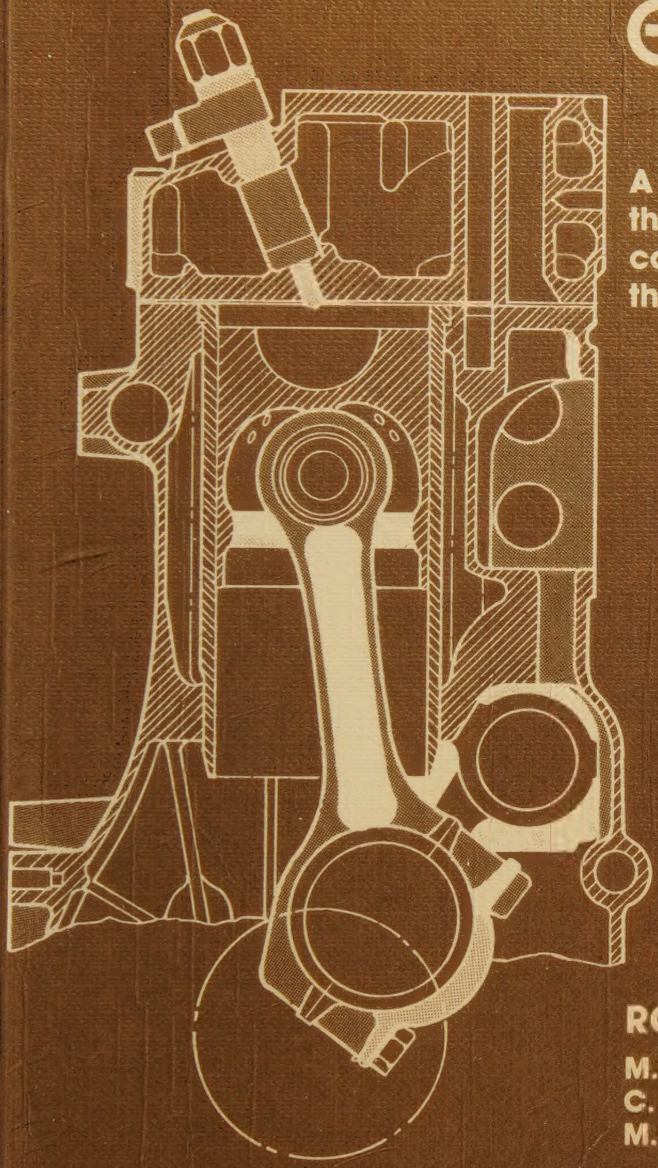

A detailed introduction to the thermodynamics of spark and compression ignition engines, their design and development

ROWLAND S. BENSON

M.Sc., D.Sc.(Eng.), Ph.D., Dr.h.c., C. Eng., F. I. Mech. E., F.I.Mar.E., M.S.A.E.

N. D. WHITEHOUSE

M.Sc., C.Eng., M.I.Mech.E.

University of Manchester Institute of Science and Technology

VOLUME 1

PERGAMON INTERNATIONAL LIBRARY

23/07/79

Digitized by the Internet Archive
in 2025

https://archive.org/details/internalcombusti0001rowl

Internal Combustion Engines

IN 2 VOLUMES

A detailed introduction to the thermodynamics of spark and compression ignition engines, their design and development

VOLUME 1

ROWLAND S. BENSON
Late Professor of Mechanical Engineering, University of Manchester Institute of Science and Technology

AND

N. D. WHITEHOUSE
Reader in Internal Combustion Engines, University of Manchester Institute of Science and Technology

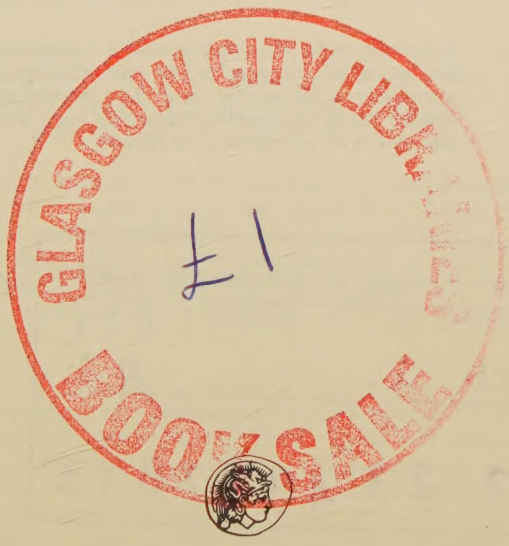

PERGAMON PRESS

OXFORD · NEW YORK · TORONTO · SYDNEY · PARIS · FRANKFURT

U.K.	Pergamon Press Ltd., Headington Hill Hall, Oxford OX3 0BW, England
U.S.A.	Pergamon Press Inc., Maxwell House, Fairview Park, Elmsford, New York 10523, U.S.A.
CANADA	Pergamon of Canada, Suite 104,150 Consumers Road, Willowdale, Ontario M2J 1P9, Canada
AUSTRALIA	Pergamon Press (Aust.) Pty. Ltd., P.O. Box 544, Potts Point, N.S.W. 2011, Australia
FRANCE	Pergamon Press SARL, 24 rue des Ecoles, 75240 Paris, Cedex 05, France
FEDERAL REPUBLIC OF GERMANY	Pergamon Press GmbH, 6242 Kronberg-Taunus, Pferdstrasse 1, Federal Republic of Germany

---

Copyright © 1979 R. S. Benson and N. D. Whitehouse

All Rights Reserved. No part of this publication may be reproduced, stored in a retrieval system or transmitted in any form or by any means: electronic, electrostatic, magnetic tape, mechanical, photocopying, recording or otherwise, without permission in writing from the publishers.

First edition 1979

British Library Cataloguing in Publication Data

Benson, Rowland Seider
Internal combustion engines.
Vol. 1
1. Internal combustion engines
I. Title II. Whitehouse, Norman Dan
621.43 TJ785 79-40361

ISBN 0 08 022717 1 hard (Vols 1 & 2 combined)
ISBN 0 08 022718 X flexi (Vol 1)
ISBN 0 08 022720 1 flexi (Vol 2)

In order to make this volume available as economically and as rapidly as possible the typescript has been reproduced in its original form. This method unfortunately has its typographical limitations but it is hoped that they in no way distract the reader.

GLASGOW DISTRICT COUNCIL – LIBRARIES DEPARTMENT

LIBRARY	DATE RECEIVED	CLASS
DHW	Feb '82	621 43

STOCK

C1 2 23 43178 03

Printed and bound at William Clowes & Sons Limited Beccles and London

Preface

The ever present energy crisis and the need for environmental controls has had a major impact on the development of the internal combustion engine. In this development a closer understanding of the thermodynamic processes occurring within the engine is necessary. Both authors have been continuously involved in industry and the universities over the past 30 years in the design, development, research and the teaching of internal combustion engines. The present text represents the fruits of some of their labours. Much of the material is original and some has not been published heretofore. The material has been used in the authors' department in the final year's BSc courses and in the MSc course.

The text has been written as a companion to one of the authors (R.S. Benson's) text in the same series entitled *Advanced Engineering Thermodynamics* (2nd edition). A novel feature in the text is the presentation of FORTRAN listings of two programs for simple cycle calculations—one for a compression ignition engine cycle and the other for a spark ignition engine cycle. Methods are also outlined for more complex cycle calculations of the type which are now normally carried our in design offices. The quantitative material for combustion processes in compression ignition engines and some of the data for spark ignition engines are based on the latest research carried out in the authors' laboratories.

The text is divided into two volumes to suit the convenience of students. The first volume contains material suitable for an undergraduate course in internal combustion engines, whilst the second volume is more relevent to postgraduate courses.

The book is primarily concerned with the thermodynamics of internal combustion engines but inevitably we have included hardware features. Since the successful understanding of the processes in which the engine operates is dependent on experimental work, a section is included on experimental methods which is appended to Volume I although some of the techniques are only used in advanced research establishments.

The authors wish to acknowledge with thanks the help of the numerous research students, research assistants and technical staff in producing the data used in the text. They wish to thank the various publishers and institutions for the reproductions of figures, due acknowledgement of which is given in the appropriate place. They also wish to thank Mrs. M. McDonnell and Mrs. P. Shepherd for typing the draft and Mrs. J.A. Munro for typing the camera ready copy of the text.

Finally, they wish to thank their respective wives and families for their patience and forbearance for the many evenings and weekends spent in preparing the text.

Acknowledgements

The authors wish to thank Mr. J.G.G. Hempson for permission to reproduce figures from the well-known text The High Speed Internal Combustion Engine by Sir Harry Ricardo and J.G.G. Hempson. Thanks are also due to Mr. W. Tipler and Perkins Engine Company for providing a sketch of the squish lip combustion chamber, Doxford Engines Ltd., for a sketch of an opposed piston engine combustion chamber and British Leyland Truck and Bus Division for the drawing used as the basis of the cover. The authors also wish to thank the following publishers for permission to reproduce figures from the texts indicated below:

Ann Arbor Science Publications Inc.
Emissions from Combustion Engines and their Control
by D.J. Patterson and N.A. Henein

Blackie & Son
The High Speed Combustion Engine (4th and 5th editions)
by Sir Harry Ricardo and J.G.G. Hempson

Chapman & Hall
Internal Combustion Engine
by Fritz A.F. Schmidt

Oxford University Press
Internal Combustion Engine, Vol. I (2nd edition)
by D.R. Pye

International Text Book Co.
Principles of Heat Transfer (2nd edition)
by Frank Kreith

The authors have reproduced a number of figures from papers by themselves and other authors in the Journals of Combustion and Flame, Chemical Society, The Royal Society, The International Journal of Mechanical Sciences (IJMS), The International Journal of Mechanical Engineering Education (IJMEE), The Transactions of the Society of Automobile Engineers (SAE), The Congress International des Machines a Combustion (CIMAC) and The Diesel and Gas Turbine Progress and Automobile Engineer. The authors wish to thank the publishers, editors and the societies responsible for these journals for permission to reproduce these figures in accordance with the international convention for acknowledgement.

Contents of Volume 1

Preface v

Acknowledgements vi

Chapter 1 Description of Internal Combustion Engines 1

1.1 Introduction 3
1.2 The Compression Ignition Engine 4
1.2.1 Compression Ignition Engine Combustion Chambers 5
1.2.1.1 Subdivided Combustion Chamber 6
1.2.1.2 Direct Injection Combustion Chamber 8
1.2.1.3 The Quiescent Combustion Chamber 12
1.3 Indirect or Spark Ignition Engines 15
1.3.1 Indirect or Spark Ignition Engine Combustion Chambers 15
1.3.1.1 Automotive Engine Combustion Chambers 18
1.3.1.2 High Compression Ratio Gas Engine 18
1.3.2 Stratified Charge Engines 20
1.3.3 Torch Ignition Engines 22
1.4 Rotary Engines 22
1.4.1 The Wankel Engine 22
References 24

Chapter 2 Basic Thermodynamics and Gas Dynamics 25

Notation 26
2.1 State Equation 27
2.2 The First Law of Thermodynamics 28
2.2.1 Closed Systems 28
2.2.2 Open Systems 29
2.3 The Second Law of Thermodynamics 32
2.4 Homentropic Flow 34
2.4.1 Continuity Equation 34
2.4.2 Momentum Equation 35
2.5 Gas Mixtures 37
2.6 Internal Energy and Enthalpy Diagrams 38
2.7 Dissociation 44
References 50

Chapter 3 Air Standard Cycles 51

Notation 52
3.1 Air Standard Cycle Efficiencies 53
3.2 Limitations 61

Chapter 4 Combustion in Compression Ignition Engines 69

Notation 70
4.1 Description of Combustion Process 71
4.2 Models for Compression Ignition Combustion Calculations 75
4.2.1 Single-zone Combustion Models 75
4.2.1.1 Lyn's Method 77

4.2.1.2 Whitehouse-Way's Method 79
4.2.2 Two-zone Combustion Model 84
4.2.2.1 The Conical/Annular Burning Zone Model 86
4.2.2.2 The Swirling-wall Jet-burning Zone Model 88
4.2.3 Multi-zone Combustion Models 88
4.2.4 Turbulent Flow Prediction Models 88
4.3 Combustion-generated Emissions 89
4.3.1 Soot 90
4.3.2 Gaseous Pollutants 92
References 93

Chapter 5 Combustion in Spark Ignition Engines 97

Notation 98
5.1 Definitions of Controlled, Uncontrolled, Normal and Abnormal Combustion 99
5.2 Normal Combustion 99
5.3 Abnormal Combustion-Engine Knock 105
5.3.1 Combustion Research in Hydrocarbon-Oxygen Mixtures 106
5.3.2 Engine Research 111
5.3.3 Influence of Fuel Additives on Knock 117
5.4 Uncontrolled Combustion, Pre-ignition and Running-on 118
5.4.1 Pre-ignition 119
5.4.2 Running-on 119
5.4.3 Rumble 119
5.5 Chemical Thermodynamic Models for Normal Combustion 119
5.6 Combustion-generated Emissions 123
5.6.1 Carbon Monoxide 123
5.6.2 Nitric Oxide 124
5.6.3 Hydrocarbons 134
References 136

Chapter 6 Heat Transfer in Engines 139

Notation 140
6.1 Basic Principles 141
6.1.1 Radiation 141
6.1.2 Radiation from Clouds of Solid Particles Such as Soot 146
6.1.3 Convective Heat Transfer 147
6.2 Heat Transfer in Internal Combustion Engines – A Survey 149
6.3 Heat Transfer in Internal Combustion Engines – Some Practical Considerations 152
6.4 Instantaneous Heat Transfer Calculations 155
6.4.1 Single-zone Heat Transfer Calculations 155
6.4.2 Multi-zone Heat Transfer 161
6.5 Numerical Values 163
References 165

Appendix I Experimental Methods 169

Notation 170
I.1 Pressure Measurement and Recording 171
I.2 Temperature Measurement and Recording 177
I.2.1 Component Temperature Measurement 177
I.2.2 Gas Temperature Measurement 186
I.3 Combustion Photography and Flame Speed Detection 189
I.4 Spectrographic Methods 191

I.5 Chemical Analysis Techniques 193
I.5.1 Sampling Valve 193
I.5.2 Orsat Apparatus 194
I.5.3 Non-dispersive Infrared (NDIR) 195
I.5.4 Flame Ionization Detector (FID) 196
I.5.5 Gas Chromatography 198
I.5.6 Chemiluminescence 199
References 200

Subject Index xiii

Contents of Volume 2

Preface v

Chapter 7 Gas Exchange Process 203

Notation 204
7.1 The Gas Exchange Process in Four-stroke and Two-stroke Cycle Engines 205
7.2 Definitions 209
7.3 Thermodynamics of the Gas Exchange Process 215
7.3.1 Exhaust Blowdown Period 216
7.3.2 Exhaust Stroke 219
7.3.3 Suction Stroke 221
7.4 Scavenge Process 230
7.4.1 Isothermal Scavenge Models 231
7.4.2 Non-isothermal Scavenge Models 239
7.5 Flow Processes in the Gas Exchange Period 246
7.5.1 Exhaust Valve or Port Area 246
7.5.2 Air Port Area in Two-stroke Cycle Engine 254
7.5.3 Reduced Port Area 258
7.5.4 Air Valve Area for Four-stroke Engine 260
7.6 Spark Ignition Gasoline Engine Intake System – Carburettor 263
7.7 Non-steady Flow Wave Action 267
References 269

Chapter 8 Compression Ignition Engine Cycle Calculations 271

Notation 272
8.1 Introduction 273
8.2 Thermodynamics of Combustion Process 274
8.3 The Ideal Dual-combustion Cycle 278
8.3.1 Isentropic Compression 278
8.3.2 Adiabatic Combustion at Constant Volume 280
8.3.3 Adiabatic Combustion at Constant Pressure 284
8.3.4 Isentropic Expansion 285
8.3.5 Cycle Studies 287
8.4 Real Cycle with Single-zone Combustion Model 290
8.5 Multi-zone Modelling 301
8.5.1 Thermodynamics of Two-zone Models 301
8.5.2 Multi-zone Models 302

Chapter 9 Spark Ignition Engine Cycle Calculations 303

Notation 304
9.1 Ideal Otto Cycle with Hydrocarbon-Air Mixture 305
9.1.1 Adiabatic Compression 308
9.1.2 Adiabatic Combustion at Constant Volume 311
9.1.3 Adiabatic Expansion 317
9.1.4 Cycle Studies 321
9.2 Cycle Calculations with Allowance for Combustion Time, Heat Loss and Rate Kinetics 328
References 336

Chapter 10 Supercharging 337

Notation 338
10.1 Relationship Between Trapped Conditions and Mean Effective Pressure 339
10.2 Mechanical Supercharging 341
10.3 Turbocharger 344
10.4 Mean Exhaust Temperature 349
10.5 Simple Turbocharging System 354
10.6 Ideal Turbocharging System 358
10.6.1 Two-stroke Engine 360
10.6.2 Four-stroke Engine 368
10.7 Actual Turbocharger System 374
10.8 Efficiency of Exhaust Systems 377
10.8.1 Constant Pressure Charging 380
10.8.2 Pulse Turbocharging 384
10.9 Matching Turbocharger to Engine 392
10.10 High Pressure Turbocharging 396
10.11 Some Turbocharged Engine Performance Characteristics 396
References 404

Appendix II 405

A Thermodynamic Properties of Mixtures 407
B Dual Combustion Cycle Program 413
C Otto Cycle Program 420

Subject Index xiii

Chapter 1

Description of Internal Combustion Engines

1.1 INTRODUCTION

This first chapter is intended to set the stage for and to indicate the general scope and limitations of the succeeding chapters. To make the discussion intelligible some terms and descriptive material on the combustion process will be introduced. These will be amplified in later chapters.

The title Internal Combustion Engines may be somewhat misleading as it suggests too much. This work deals with internal, intermittent combustion engines, thus excluding the gas turbine, an internal continuous combustion engine. It excludes turbomachinery in general except for that important auxiliary the exhaust driven turbocharger.

Another important limitation is that the intention is to deal with the thermodynamics and gas dynamics of engines-not the mechanical design. Some reference to the mechanical design is unavoidable because it impinges on the application of thermodynamics. So some general descriptive matter is given in this chapter-but look elsewhere for detailed information on the structure and mechanics of engines.

Internal, intermittent combustion engines are familiar to most people due to their ubiquity as the prime mover in motor vehicles. Usually these engines are reciprocating engines in which a major moving part is a piston which moves in a straight line, backwards and forwards, with an infinitesimal period at each extreme when it is stationary. Contrary to some popular opinion these reverses of direction of motion do not affect efficiency—there are no losses inherently involved in this process. The advantages of rotary over reciprocating action are primarily a matter of compactness, of geometry, and do not directly involve thermodynamics and gas dynamics.

The succeeding chapters may be applied to either rotary or reciprocating engines if the appropriate spatial characteristics are invoked-notably combustion chamber volumes, port areas and surface areas and their changes with time.

The genus of engines being considered may be subdivided into different categories in a number of ways. One way is in accordance with use. Marine engines for the propulsion of ships at sea; industrial engines for power generation on land; automotive engines for land transport. This may be important to the designer: the limitations and performance criteria for success are obviously different for an engine used very occasionally for short periods only, as in a standby set than for an engine used continuously for

main power generation. For our purposes, however, the main divisions will be based upon combustion, thermodynamics and gas dynamics.

The division based upon combustion characteristics is primarily a matter of ignition—either self-ignition or indirect ignition may be used. With indirect ignition a rapid rise of temperature at a particular point in the combustion chamber ignites a mixture of fuel and air near that point. Typically this is achieved by means of an electric spark, hence usually referred to as "spark ignition", though it will be appreciated that other forms of ignition achieving the same end would make little, if any, difference to our treatment of the engine.

With self-ignition the fuel/air mixture is heated to a high temperature and spontaneous ignition takes place—possibly more or less simultaneously throughout the mixture.

1.2 THE COMPRESSION IGNITION ENGINE

In practice self-ignition is achieved by compression, which being rapid and so almost adiabatic, produces a rise in temperature of the air or air/fuel mixture to a point above the self-ignition temperature of the fuel. The term compression ignition conveys the substance of this process and is more expressive than the more popular term "diesel" engine.

The compression ignition engine could be made in a rotary form and Wankel-type diesels have been developed, but at the moment reciprocating engines predominate. They are made in a vast range of sizes and speeds, from small, high speed auxiliary and automotive engines of around 6-10 cm bore and 4000-5000 rev/min to large, slow speed engines used for main propulsion in ships, of around 100 cm bore and 100 rev/min. These figures are in no way definitive merely illustrative. It may be noted that the apparently wide range of speeds indicated above camouflages a comparative uniformity the actual maximum velocity of the piston is of the same order of magnitude for all reciprocating engines.

All of these engines have much in common. They need high compression ratios to achieve the temperatures and pressures necessary for self-ignition. This results in high cylinder pressures, which requires robustness of mechanical design, but the high compression ratio also leads to a high expansion ratio which gives the high indicated efficiency characteristic of the diesel engine. The self-igniting fuel has to be injected late in the compression process to avoid the dangers of pre-ignition, and this fuel must be capable of being ignited at the pressures and temperatures achieved within the short time that they exist. Finally, to enable combustion to be completed rapidly, to suit the time available, the injection and mixing of the fuel with the air in the combustion chamber needs to be achieved very rapidly. These requirements dictate an interaction between fuel injection and air motion in the cylinder which controls combustion chamber design.

1.2.1 Compression Ignition Engine Combustion Chambers

In addition to the mixing requirements mentioned above a combustion chamber should be designed to minimize heat losses from the burning gases to the combustion chamber walls and must also, of course, provide space for valves and fuel injection equipment. These different requirements need compromises, and a vast variety of combustion chambers have been and many still are used. It is not the purpose of this work to illustrate this complexity but rather to indicate the main types and suggest some broad principles which differentiate between them.

The preferred solution tends to differ with engine size and speed, though with considerable overlap. It is also affected by commercial requirements. Thus small engines are used in automotive applications where maximum power is required relative to size: so the amount of excess air permissible may well be small and the engine speed high. This places a premium on the rapid mixing of fuel and air. In the large engine used for industrial or marine purposes the engine speed is relatively low and more time is available for mixing. Also fuel consumption rather than maximum power tends to be important, so that larger amounts of excess air are acceptable.

In the compression ignition engine, fuel is injected under high pressure through nozzles with one or several holes. This produces a finely divided spray of fuel so that combustion of individual droplets is not too prolonged. Large engines usually have nozzles with a number of holes each of moderate size, i.e. 6 holes of 0.4 mm diameter, 8 holes of 0.5 mm diameter, etc., depending upon the quantity of fuel to be injected per cycle and the injection pressure used. Small engines using the same principle need less total hole area, leading to smaller hole sizes and fewer holes. This makes it more difficult to use the spray pattern to distribute the fuel uniformly through the combustion chamber.

The net effect of these factors is that in small engines air movement is likely to be needed to ensure adequate mixing of fuel and air, and this becomes less true as engine size is increased, ultimately resulting in engines with little or no air motion deliberately designed into the combustion chamber.

Combustion chambers may therefore be ordered logically in accordance with the air velocities in the combustion chamber during the combustion process. At one extreme are subdivided combustion chambers in which the process of combustion itself is used to generate violent air motion. In the middle may be placed single chambers, or as usually referred to, direct injection engines, with air movement provided for by direction of the incoming air and the combustion chamber shape and at the other extreme the direct injection engine with no deliberate design for air motion—the quiescent combustion chamber engines. This progression is illustrated below.

1.2.1.1 Subdivided Combustion Chamber

Pre-chamber. These tend to have been favoured chiefly on the Continent of Europe; typical are those shown in Fig. 1.1.

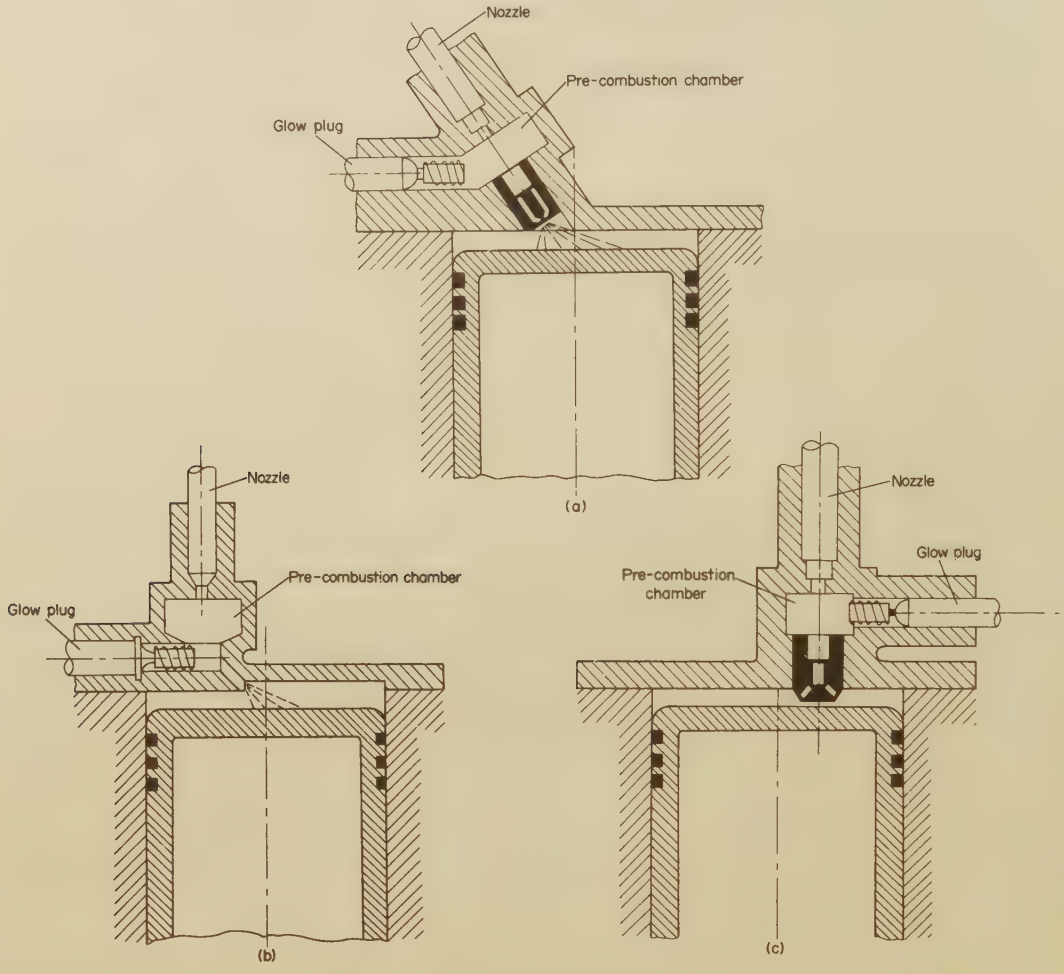

FIG. 1.1. Typical pre-chamber combustion chambers. (From Schmidt[4] by courtesy of Chapman & Hall.)

In the pre-chamber designs the idea is that combustion starts in the pre-chamber, which contains a proportion of the total air only and causes a rise in pressure which forces fuel and air violently through a passage into the main chamber. The passage(s) is/are small in cross-sectional area to ensure high velocities and efficient distribution. This passage is designed to distribute the fuel/air mixture throughout the main chamber and may have several passages or holes. This method achieves rapid, violent mixing of the air and fuel in the main chamber without demanding a great deal of the fuel injection equipment.

Design of these types are said to be critical as to sizes, etc.

Turbulence Chamber. In the designs shown previously the air motion in the pre-chamber before combustion is not ordered-as far as can be seen. Another type of chamber may be used in which air motion is available to mix the air and fuel in the chamber before and during combustion. The Ricardo Comet combustion chamber design illustrates this type (Fig. 1.2).

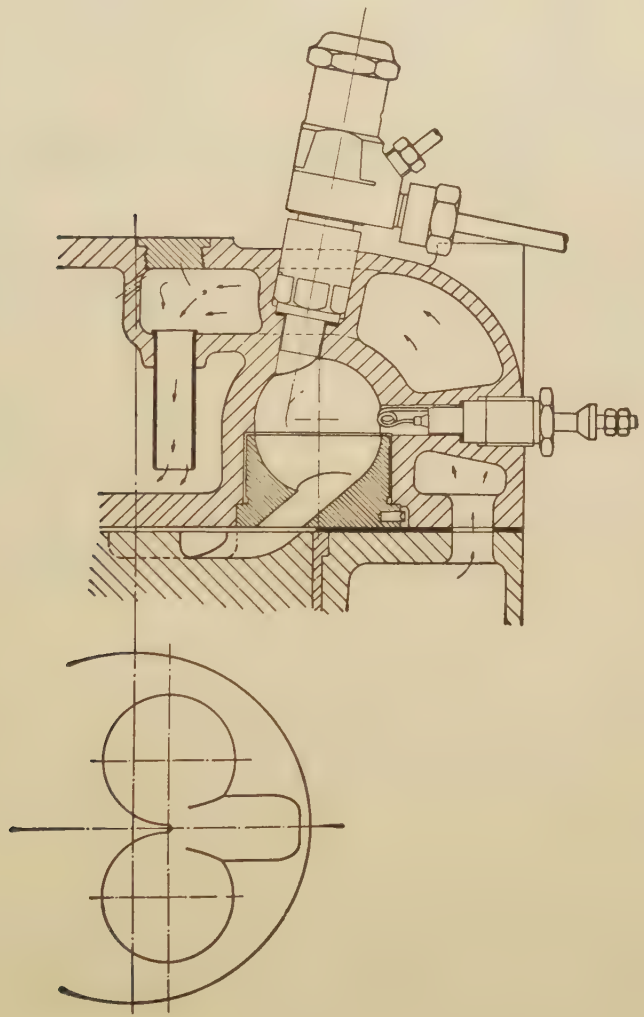

FIG. 1.2. Ricardo Comet Mark III combustion chamber (From Ricardo and Hempson[5].)

In this type of chamber the piston compresses air tangentially into the spherical chamber producing a swirling air mass. The fuel is sprayed downstream into the air (maybe with a small preliminary spray along a diameter).

After ignition the rise in pressure due to combustion forces the mixture into the main chamber where a double swirl is obtained due to the shape of the cavity in the piston. The throat between main chamber and swirl chamber is larger than is the case in the pre-chamber designs so that pressure difference between the chambers is more moderate. The swirl in the swirl chamber ensures quite good mixing there,and the process is rapidly completed in the main chamber.

The swirl chamber has a volume about equal to that in the main chamber at top dead centre (or in other types, more than).

Ricardo & Co. (1926) Ltd., of Shoreham by Sea, near Brighton, run a very successful diesel engine design and consultancy business and have continuously developed this combustion chamber.

The difference between the pre-chamber and turbulence chamber is primarily that the pre-chamber is relatively small and burns only a small part of the fuel while most of the fuel may be burnt in the turbulence chamber. Both allow the use of comparatively simple, undemanding fuel injection equipment, and due to high air velocities can operate with low excess air.

The difference between the two types is often not very marked.

Air cell. Another type of divided combustion chamber injects the fuel into the main chamber but has a secondary chamber; movement of air and fuel from the main chamber into the secondary chamber occurs, followed by some combustion and reverse flow which in turn causes secondary turbulence in the main chamber to complete combustion effectively.

The MAN air cell indicates the action (Fig. 1.3).

The Lanova type (Fig. 1.4) is intermediate between an air cell and a pre-chamber as the core of the spray from the nozzle enters the air cell. Combustion probably starts in the main chamber, spreads to the major part of the fuel in the air cell and then the air/fuel is forced back into the main cell.

1.2.1.2 Direct Injection Combustion Chamber

In a sense the air cell combustion chamber is a direct injection type also, but the latter term is restricted to single-combustion chambers. They have the advantage of comparatively low surface area, and so lower heat losses, and this tends to be improved even more by the use of lower air velocities.

Usually fuel is injected through a multi-hole nozzle—probably placed at or near the centre of the top of the combustion chamber, i.e. through the cylinder head. Mixing of fuel and air is achieved by a combination of air movement and of distribution by the fuel sprays. Air movement is, in general, less violent than in the divided combustion chamber.

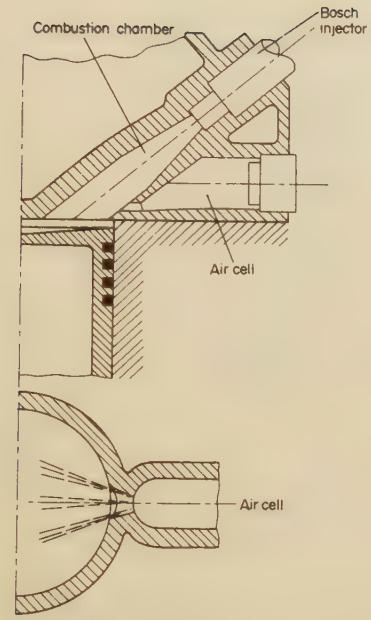

FIG. 1.3. MAN air cell combustion chamber. (From Schmidt[4] by courtesy of Chapman & Hall.)

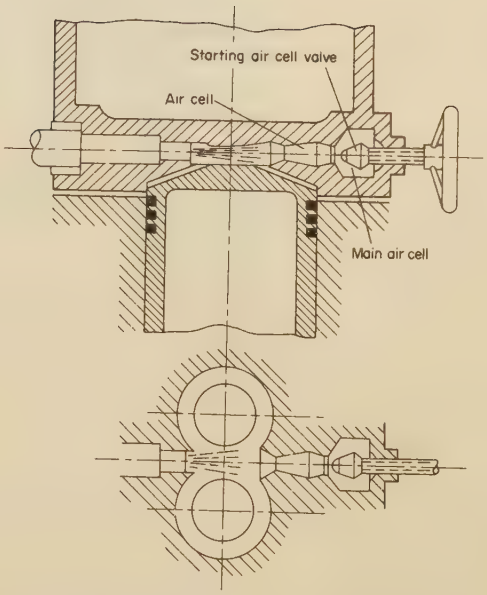

FIG. 1.4. Lanova combustion chamber. (From Schmidt[4] by courtesy of Chapman & Hall.)

Meurer System MAN - "M" Engine. Some mention should be made of the "M" engine combustion chamber (Fig. 1.5) although it does not quite fit into the general pattern. It is a direct injection engine with a lot of swirl, but with a difference. The fuel is almost entirely injected tangentially onto the bowl in the piston and thus is not reacted or evaporated on its way to the bowl. A small amount is sprayed into the air charge to provide self-ignition, but the rest evaporates off the bowl comparatively slowly so that there is very little fuel/air mixture available for rapid combustion immediately after ignition has taken place. This eliminates diesel knock, the rapid pressure rise that can occur in the early stage of combustion, and combustion noise is low. Cold starting is more difficult than

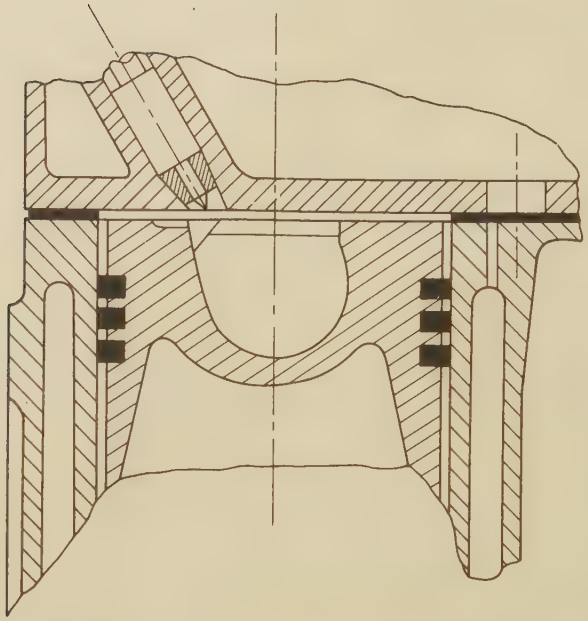

FIG. 1.5. MAN "M" engine combustion chamber.
(From Schmidt[4] by courtesy of Chapman & Hall.)

in most direct injection engines, and special measures may be necessary for a quick cold start because the fuel on the bowl of the piston does not evaporate rapidly enough when the piston is cold.

Perkins "Squish Lip" Combustion System. This new development (Fig. 1.6) by the Perkins Engine Co. although similar to the deep bowl direct injection engine dealt with next, is in some ways similar to the turbulence chamber type of subdivided combustion chamber already mentioned in that there is a somewhat restricted throat between a pre-chamber, in the piston and the main chamber. This feature promotes vigorous air motion and rapid combustion. Ordered air motion also exists due to the conservation of swirl as in the deep bowl type dealt with next.

Information about this engine is as yet limited, but it is likely to enjoy to some extent the advantages and disadvantages of the Comet combustion chamber-high air utilization, rapid combustion and high heat transfer. A major difference is that the design of the cylinder head is not affected by the inclusion of a pre-combustion chamber, giving the designer more freedom for inlet and exhaust valve arrangement.

Deep Bowl with Swirl and Squish. This type of combustion chamber is used for the smaller direct injection type engines. A deep bowl of small diameter is situated in the piston, and at top dead centre the clearance between piston and cylinder head is small. Most of the air is thus concentrated in the bowl. The fuel sprays

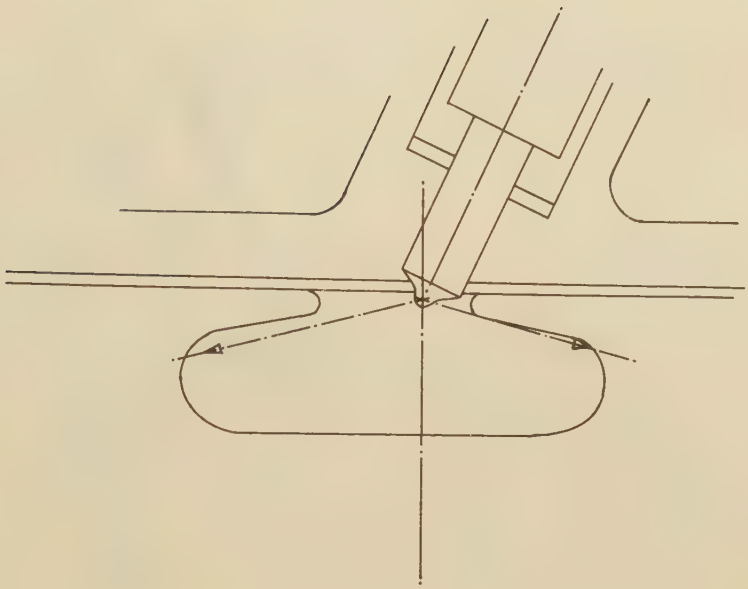

FIG. 1.6. Perkins "squish lip" combustion chamber.
(By courtesy of Perkin Engine Co.)

will impinge on the walls of the cylinder bowl very shortly after injection, probably before ignition occurs. The air is introduced into the combustion chamber more or less tangentially by inlet passage shape or by "masks" on the inlet valves. The forcing of this air into the bowl during compression not only concentrates the air into the vicinity of the fuel sprays but, due to conservation of angular momentum, the angular velocity of the air is increased. This promotes mixing of the fuel and air, particularly at the interface between the fuel in the vicinity of the wall of the bowl and the rotating air. Any liquid fuel deposited on the bowl would be evaporated and removed by this air motion. As the mixed fuel burns the hot combustion products near the bowl surface, being of lower density than the rest of the cylinder contents, move inwards as convection currents and unburnt cooler air moves out from the centre due to centripetal and centrifugal effects. Due to this action, distribution by sprays is less important than in the quiescent chamber. This makes the requirements for the fuel injection equipment less demanding so that costs can be kept down-important for small engines. Fewer nozzle holes are required, and this is a particular advantage in small engines as holes would

otherwise tend to be very small, and a few large holes will last longer between overhauls, being less likely to become blocked or eroded than would many small holes (Fig. 1.7).

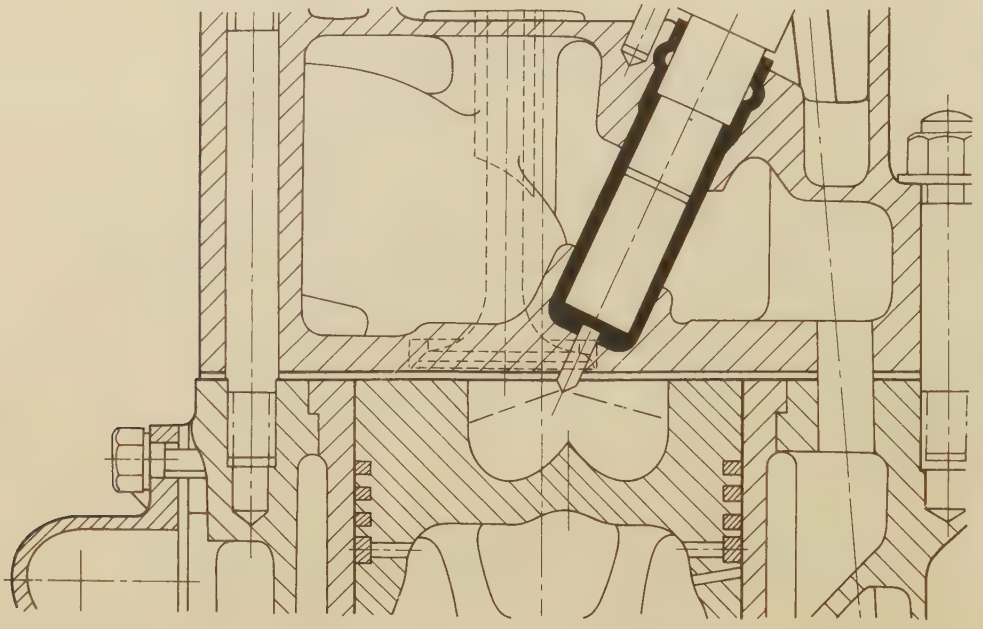

FIG. 1.7. Deep bowl combustion chamber.

Opposed Piston Engine Combustion Chamber. This type (Fig. 1.8) is rather out of the direct progression as the geometric design limits make it rather special. A central injector cannot be used, so one, two or more on the periphery have to be used. Air swirl is obtained quite easily by shaped inlet ports. Sprays are directed downstream—with the air swirl—otherwise the fuel would be swept back into the spray and mixing would be less easily obtained.

1.2.1.3 The Quiescent Combustion Chamber

The quiescent type combustion chamber is the most extreme in the direction of minimizing air motion and depending on fuel distribution by means of many sprays from a multi-hole nozzle.

As there is little air movement any fuel that reaches the piston, or even worse the cool liner walls, will not readily burn off. So this type of combustion chamber is only suitable for engines above a certain size to prevent premature impingement of a spray onto a wall before ignition. The exact size is dependent

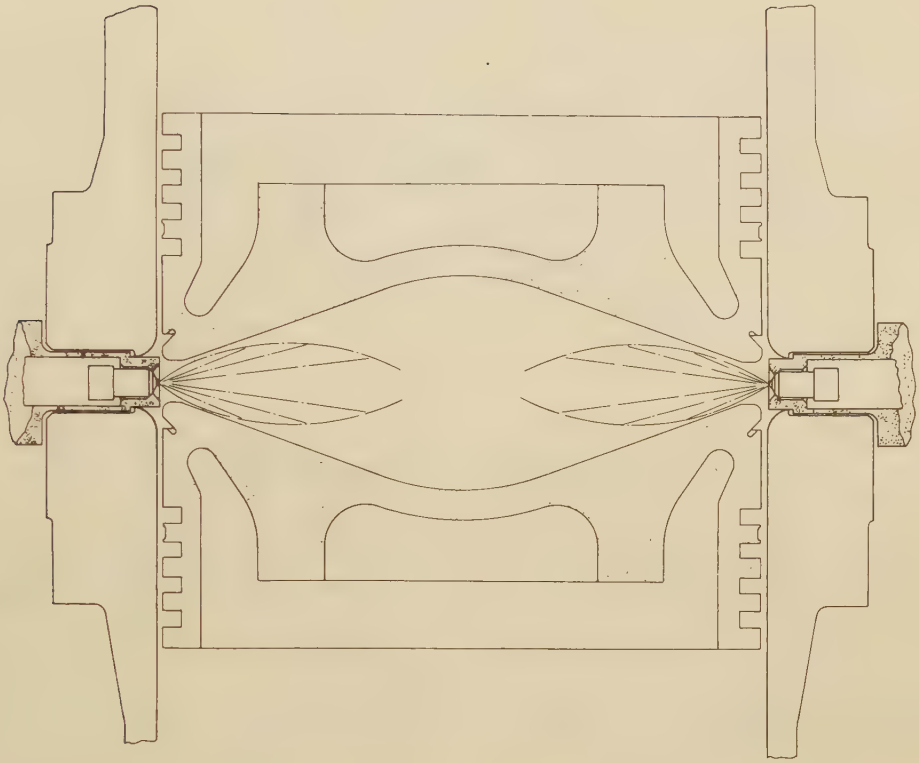

FIG. 1.8. Opposed piston engine combustion chamber.
(By courtesy of Doxford Engines Ltd.)

upon a number of factors but most engines of this type tend to be 20 cm bore or above.

Fuel distribution is provided by a large number of sprays-nozzles have six or more holes.

A shallow bowl-shaped combustion chamber is typical (Fig. 1.9).

Summary of Advantages and Disadvantages. The advantages and disadvantages of these different types of combustion chamber may be deduced from various remarks made above and from general thermodynamic and gas dynamic principles but they are summarized in Table 1.1. Generalizations only! They may not all be true for any particular engine.

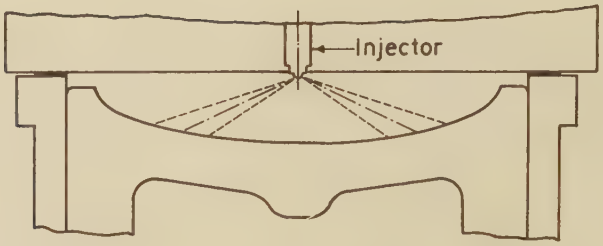

FIG. 1.9. Quiescent combustion chamber

TABLE 1.1

Divided combustion chamber		Single combustion chamber	
Pre-combustion	Swirl chambers	Air swirl	Quiescent
High heat losses Very good air utilization		Moderate Moderate air utilization	Low heat losses Fairly moderate utilization
Poorer starting		Good starting	
Some restrictions on valves	Limits on valve area	Good valve area	Best valve area
Throttling losses in passages	Some throttling losses	No throttling losses	
Easy fuel injection requirements		Moderate fuel injection requirements	More difficult fuel injection
Low pressure rises in main chamber		Higher pressure rises	
High speeds		Moderately high speeds	Medium/low speeds
		Better fuel consumption	

1.3 INDIRECT OR SPARK IGNITION ENGINES

A rapid rise of temperature at a particular point in the combustion chamber causes ignition of a small volume of the air and fuel mixture at that locality but ignition elsewhere is not as automatic as in the compression ignition engine. This produces special design problems based on flame propagation requirements. To effect combustion of the fuel the ignition source must be surrounded by a mixture of gaseous fuel and air to produce a kernel of flame, and this in turn must be in contact with succeeding layers of combustible mixture reaching out to encompass all the fuel used. Flame will only propagate, however, if the ratio of air and fuel is within certain limits-not too weak and not too rich. Although the range can be widened by increasing pressure and temperature, in practice the limits impose considerable restrictions on engine design. The thermodynamics of these processes will be discussed in Chapters 5 and 9.

Usually spark ignition engines are designed to mix the fuel (gas or vapour) with the air comparatively early, before the compression stroke, in the air inlet passages during the suction stroke, although separate admission of fuel and air into the cylinder is used in a few cases. The mixture is usually intended to be as uniform in composition as possible. To keep within the acceptable limits for flame propagation then requires a restriction of the air supply at part loads obtained by throttling the air inlet. Difficulties arise from the practice of having a combustible mixture always present from suction through compression and on through combustion. The mixture may ignite prematurely or some part of it may auto-ignite after normal combustion has raised pressures and temperatures in the cylinder. These phenomena are dealt with in Chapter 5. Here it suffices to say that these dangers make necessary the use of low compression ratios. This in turn leads to lower indicated efficiencies than obtained with compression ignition engines, and this disadvantage is intensified at part loads by air restriction, which increases air-pumping work losses.

Some of the disadvantages of the spark ignition engine may be reduced by deliberately avoiding the uniform composition norm and designing for a charge divided into two parts of different composition, e.g. the stratified charge engine. In these engines excess unmixed air can be admitted as it does not reduce the mixture strength of the combustible mixture below the flammability limit. This avoids the excessive pumping losses mentioned above. It is also possible to so control mixture strengths to avoid significant quantities at those mixture ratios found to produce the largest quantities of pollutants.

1.3.1 Indirect or Spark Ignition Engine Combustion Chambers

Many of the remarks made earlier about compression ignition engine combustion chambers could be repeated here. Such problems as heat losses and the geometry of inlet and exhaust valves recur. The mixing problem is largely avoided; instead the time for combustion is controlled by the speed of the flame front through the mixture. Pre-ignition and auto-ignition have to be avoided. A design for minimum surface area to reduce heat losses will also tend

to reduce losses and pollution from wall quenching.

These various factors may be considered in rather more detail before looking at a few actual designs.

Auto-ignition of a part of the fuel/air mixture before the flame front reaches it is often an overriding consideration in a spark ignition engine. It is a chemical reaction caused by high temperature and pressure and it takes time to develop. The flame path from the ignition point to the end of the flame travel needs to be kept small to keep the time in which these chemical reactions may occur down to a minimum, but it would also be desirable that any last part of mixture to be burnt should be of minimum volume so that auto-ignition would give little energy and thus knocking would be minor. For reasons given later, it is desirable that the end gas should be located near cool surfaces rather than hot ones, e.g. not near a hot exhaust valve. Combustion chamber shape will also affect the pattern of combustion of the fuel/air mixture. Detailed investigation of such effects could best be made by cycle calculations, such as those mentioned later in this book, which could also be used to indicate the dangers and severity of knock due to auto-ignition of the end gas. For the present the general trends to be expected are interesting and will suffice.

For this purpose we may consider a very simple combustion chamber shape, a hemisphere, with the spark plug at the centre of the flat side (Fig. 1.10).

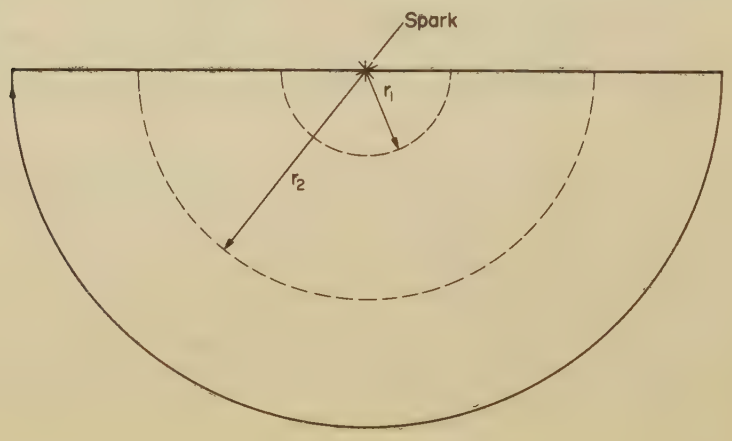

FIG. 1.10. Diagram of simple hemispherical spark ignition combustion chamber.

Initially flame speed is generally low; turbulence is reduced by the proximity of the surface. In addition a given movement r_1 of the flame front represents a volume of gas equal to $\frac{2}{3}\pi r_1^3$, which for a small value of r_1 is very small. So the initial rate of combustion will be very low.

Later, the flame speed will increase due to the effect of increased turbulence at a distance from the wall, and the surface area of the flame front also increases, so that in a similar increment of time, centred about the time when the flame front has reached r_2, the volume burnt will be about $2\pi r_2^2 \times r_1 \times k$, where k is the ratio of the flame speeds. As the pressure in the cylinder will probably have been increased due to combustion, the density of the unburnt gas will also have been increased. Consequently the rate of combustion of fuel will have increased considerably. This trend will persist until very near the end of combustion, when the presence of the walls again reduces turbulence and flame speed. Thus the rate of combustion would have a pattern as in Fig. 1.11.

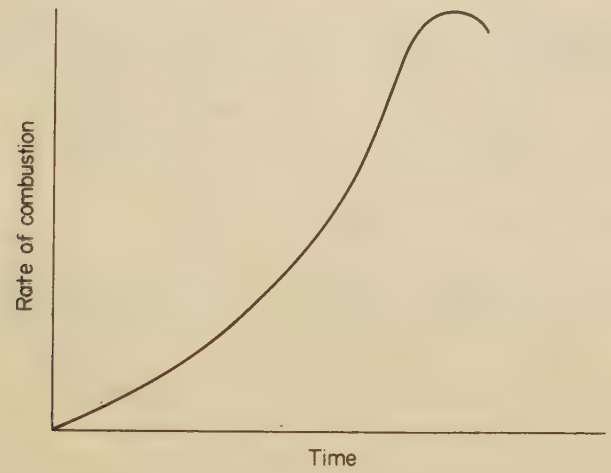

FIG. 1.11. Typical rate of combustion curve (hemispherical chamber)

The actual shape will depend upon the changes in flame speed, density and radius. It must be remembered that the flame speed considered above is relative to the unburnt gases immediately ahead of the flame front. The movement of the flame front relative to the spark plug also includes an effect due to the expansion of the burning gases due to their increase in temperature, and similar effects due to pressure changes. This is important because of the influence of the surface area of the flame front.

This analysis has assumed a constant volume of the combustion chamber. In practice, movement of the piston will distort the pattern, the effect depending upon time of ignition and duration of combustion. Duration of combustion is usually about 30-40 degrees crankangle, so that if divided approximately about top dead centre

the actual movement of the piston in a reciprocating engine is not large.

As the efficiency of utilization of the energy released by combustion depends primarily on the effective expansion ratio relevant to the time of that combustion, the most efficient combustion pattern will be one that concentrates combustion near top dead centre. Assuming ideal ignition timing, this requires a short duration of combustion, and for a given duration, the most rapid rate at the middle of the duration.

This hemispherical shape has good features, therefore, as the short flame path will lead to low duration, which helps efficiency and reduces the probability of auto-ignition. It also has some disadvantages. The main rate of combustion occurs near the end of combustion, which tends to reduce the efficiency, will make auto-ignition severe, should it occur, and the rapid peak combustion rate is quite likely to produce rapid rates of cylinder pressure rise and so engine roughness.

It can be seen that combustion chamber designs must be compromises among and between these thermodynamic considerations and the need to accommodate valves, spark plugs and the piston.

This is illustrated by a few sketches and comments on some of the designs that have been or are used.

1.3.1.1 Automotive Engine Combustion Chambers

It may be deduced that although the T head design (Fig. 1.12) could provide geometric advantages, the flame paths would be rather long if the spark plug was central with auto-ignition likely near the hot exhaust valve, or very long if the plug was near the exhaust valve with auto-ignition likely near the inlet valve. The low compression ratio and the long duration of combustion lead to low efficiency.

The combustion chamber for the side valve engine (Fig. 1.13) with underhead valves is convenient geometrically but it gives fairly long flame paths. Rates of combustion will peak fairly early and auto-ignition—if it occurs—is likely to be of fairly small quantities. This will lead to a smoother and more efficient engine than would the previous design.

The overhead valve-in-head engine (Fig. 1.14) has a compact combustion chamber with short flame paths. This improves resistance to auto-ignition and increases efficiency by reducing combustion duration. Maximum combustion rate would tend to be late (but not so intense as with the hemispherical example mentioned earlier).

1.3.1.2 High Compression Ratio Gas Engine

Gas engines, often based on medium speed diesel engines, may have a central spark plug or place two plugs on a diameter. This latter design would not reduce the flame path length but would tend

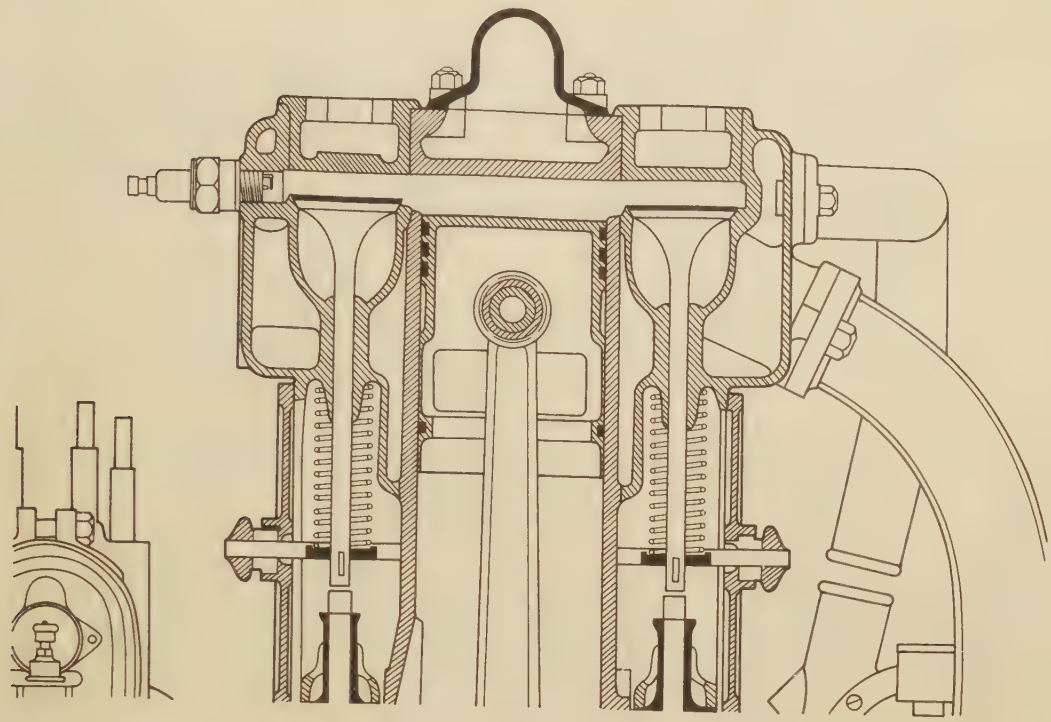

FIG. 1.12. T head combustion chamber.
(By courtesy of Automobile Engineer[6].)

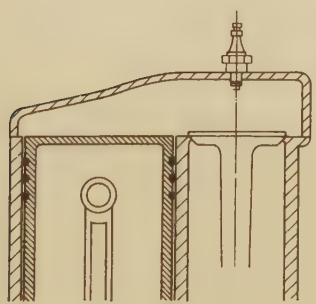

FIG. 1.13. Side valve engine combustion chamber.

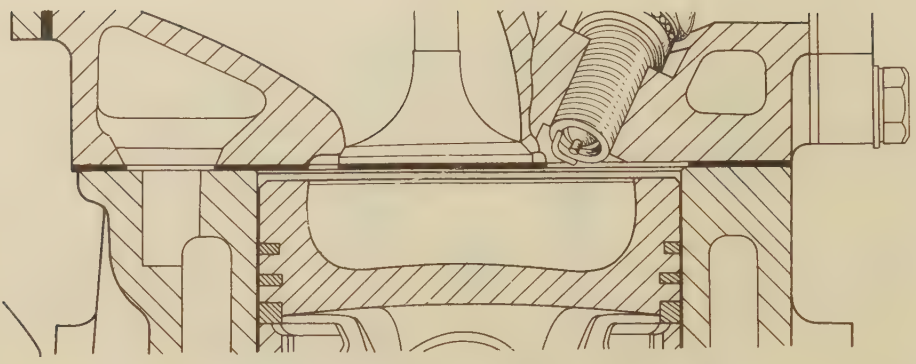

FIG. 1.14. Overhead valve engine bowl-type combustion chamber. (By courtesy of Automobile Engineer[7].)

to reduce the magnitude of the late rate of combustion and increase it earlier, giving some improvement in efficiency and a reduction in the danger of serious auto-ignition. As the fuel used in these engines is usually mainly methane, which is resistant to auto-ignition, high compression ratios can be used, giving high efficiency. similar to the comparable diesel engine (Fig. 1.15).

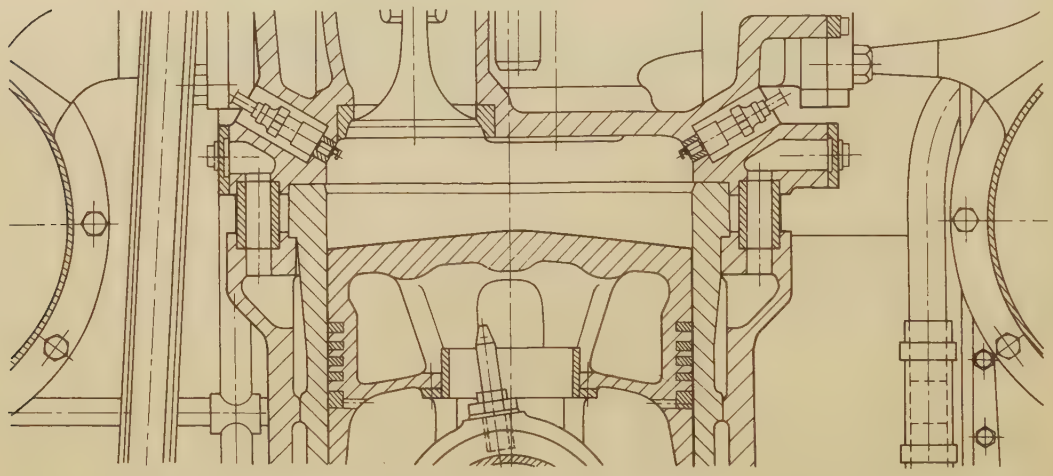

FIG. 1.15. Combustion chamber for medium speed gas engine

1.3.2 Stratified Charge Engines

In a stratified charge combustion system part of the cylinder contents consist of air unmixed with fuel while simultaneously fuel is being mixed with air in another part of the combustion chamber, while combustion of already mixed fuel and air can be proceeding in

some other part. This makes possible the use of excess air in the engine combustion chamber without producing an excessively weak mixture for combustion purposes. In the Texaco controlled combustion system one of the earliest and best known, shown diagrammatically in Fig. 1.16, the intake port is designed to promote high air swirl. The fuel is injected towards the end of

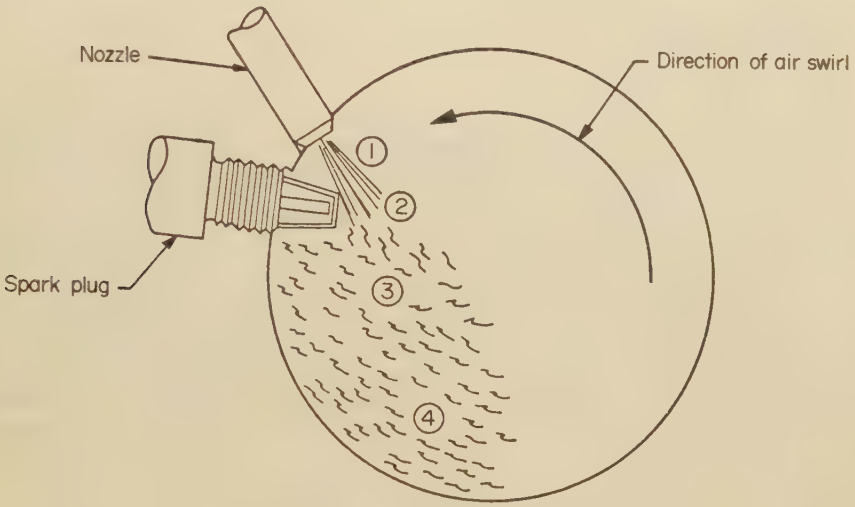

FIG. 1.16. Stratified charge engine combustion chamber. (1) Fuel spray. (2) Fuel/air mixing zone. (3) Flame front area. (4) Combustion products.

(By courtesy of Diesel and Gas Turbine Progress.[1])

the compression stroke and mixes with air. The mixture is swept downstream by the air swirl to the spark plug where it is immediately ignited. A flame front is formed and continued injection supplies fuel as the air swirl supplies air to provide mixture to this flame front. Combustion products are swept on by the swirl. Power is thus controllable by fuel alone, without air throttling. Pre-ignition and knock are avoided and higher compression ratios may be used than typical of carburetted spark ignition engines. High octane or high cetane fuels are alike unnecessary. Ample supplies of air can be available for completion of combustion, yet during the major duration of combustion the mixture may be controlled to avoid that combination of oxygen availability and high temperature that produces high quantities of nitric oxide. The stratified charge engine is claimed, therefore, to be more efficient and to emit less pollutant than most spark ignition engines. However, the fuel injection system required to inject late in the compression stroke is relatively expensive. The Texaco ignition system is also relatively expensive, being an oscillator type giving high voltages and long spark duration (e.g. 25 degrees crankangle)[1].

C1 2 23 43178 03

1.3.3 Torch Ignition Engines

Charge separation may also be achieved by using a pre-chamber for a rich mixture of fuel and air and the main chamber for a weak mixture. Two fuel supply systems, which may be carburettor or injection systems, may now be used. Similar advantages are claimed as for the open chamber stratified charge engines[2].

1.4 ROTARY ENGINES

1.4.1 The Wankel Engine

As mentioned earlier, rotary engines are not intrinsically different from reciprocating engines in thermodynamic terms. Variations may arise, however, due to special differences. Taking the Wankel spark ignition engine as typical of a relatively successful rotary engine, several such differences may be noted. Firstly, and perhaps most importantly, sealing of the combustion chamber in the reciprocating engine used several piston rings in series, operating against a cylindrical surface giving favourable conditions for low leakage. The Wankel engine uses only one sequence of seals and that operates against a more complicated surface—troichoidal—making leakage control difficult. Lawton et al.[3] suggests up to 20% of the charge is leaked in cases they have investigated.

Secondly, the effect of combustion chamber shape on the progress of combustion could be explored. A typical shape is shown in Fig. 1.17. It can be seen that the combustion chamber shape at minimum volume tends to be rather long and thin, which would be expected to prolong the time required for combustion.

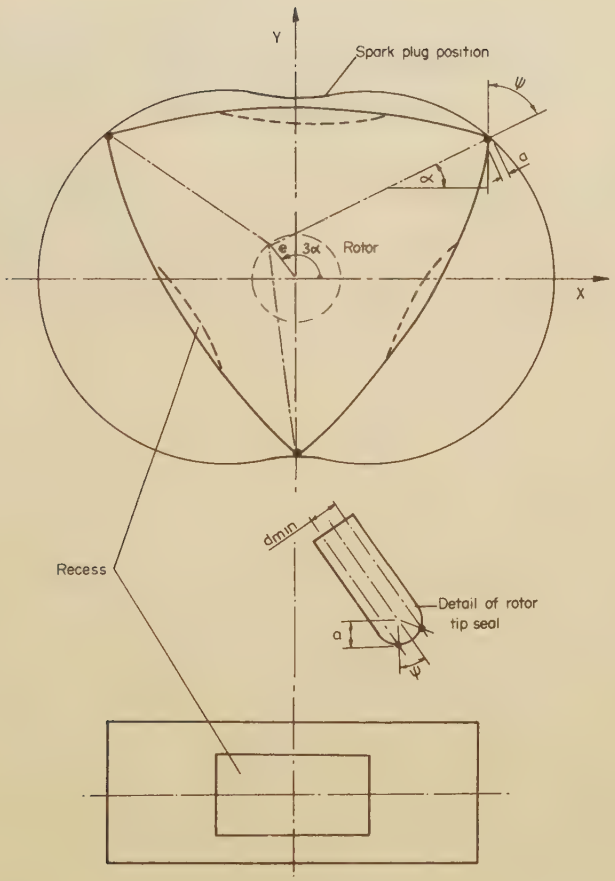

FIG. 1.17. Combustion chamber for Wankel engine. a, radius of seal, 2ψ, contact angle of seal, α, crankangle, e, eccentricities.

REFERENCES

1. Developments in military stratified charge engines, Diesel Gas Turb. Prog., xli, 60 (1975).

2. Eisele, E., Hiereth, H. and Charzinski, P., A study of a charge stratification system for heavy commercial vehicle engines, Combustion in Engines, p.197, Institution of Mechanical Engineers, (1975).

3. Lawton, B. and Millar, D.H., Recent research on rotary piston engine, J1 Manchester Assc. Engrs No.3(1973-74).

4. Schmidt, F.A.F., The Internal Combustion Engine, Chapman & Hall, 1965.

5. Ricardo, H.R. and Hempson, J.G.G., The High Speed Internal Combustion Engine, 5th edn., Blackie, London, 1968.

6. Ricardo, H.R., Story of the engine, Auto. Engr 50, 236 (1960).

7. Wilson-Jones, R.A., Engines, Auto. Engr 58, 202 (1968).

Chapter 2

Basic Thermodynamics and Gas Dynamics

Notation

a_n	constants
b_n	constants
C	velocity
C_p	specific heat at constant pressure
C_v	specific heat at constant volume
e	specific internal energy
E	internal energy
F	area
g	specific Gibbs function
G	Gibbs function
h	specific enthalpy
H	enthalpy
k_f	forward velocity coefficient
k_b	backward velocity coefficient
K_C	equilibrium constant
K_P	equilibrium constant
m	mass
M	number of mols
p	pressure
P	normalized pressure = (p/reference pressure)
Q	heat
Q_{VS}	heat of reaction at constant volume
R	characteristic gas constant
R_f	one-way equilibrium rate for reaction
R_{mol}	universal gas constant
s	specific entropy
S	entropy
T	temperature
u	velocity
$u_{i,j}$	enthalpy coefficient for species i-th,j-th term
v	specific volume
V	volume
w_m	molecular weight
W	work
x_i	mol fraction of species i
κ	specific heat ratio
α	see equation (2.161)
β	see equation (2.161)
γ	see equation (2.161)
ν	stoichiometric coefficient
ρ	density
Δ_{EO}	heat of reaction absolute zero

Suffixes

R	reactant
P	product
O	level at zero temperature
1	calculation step 1
2	calculation step 2
S	reference

In this chapter we shall review the basic thermodynamics and gas dynamics used in internal combustion engine studies. A full development of the subject is given elsewhere.[1,2]

2.1 STATE EQUATION

In internal combustion engine thermodynamics we use the generalized state equation for an ideal gas

$$pV = MR_{mol}T, \tag{2.1}$$

where p is the pressure (N/m^2), V the volume (m^3), M the number of kg-mols, R_{mol} the universal gas constant, 8314.3 J/kg-mol ^oK, and T is the temperature ^oK. It should be noted that 1 kg-mol occupies 22.41 m^3 at 1.01325E^5 N/m^2 and 273^oK.

An alternative form of (2.1) is

$$pV = mRT \tag{2.2}$$

In this case m is the mass in kilograms and R the characteristic gas constant given by

$$R = \frac{R_{mol}}{w_m} \tag{2.3}$$

where the molecular weight of the gas is w_m kg-mol.

For unit mass of gas the specific volume v is V/m and the state equation becomes

$$pv = RT \tag{2.4}$$

or

$$\frac{p}{\rho} = RT, \tag{2.5}$$

where ρ is the density of the gas.

Unless otherwise stated we shall use the kg-mol as a unit of mass and (2.1) for the state equation.

2.2 THE FIRST LAW OF THERMODYNAMICS

In cycle calculations and studies of combustion, heat transfer and gas movement, the first law of thermodynamics is frequently used in both closed and open systems.

2.2.1 Closed Systems

For a closed system the first law states that

$$dQ - dW = dE, \tag{2.6}$$

where dQ is the net heat energy transfer to the system, dW is the net work energy transfer from the system and dE is the change in internal energy.

Although the internal energy is dependent on the composition, temperature, motion and position of the system, in internal combustion engines, closed cycle analysis, the internal energy is a function of temperature and composition only, so that we can write

$$E = E \text{ (temperature, composition)} \tag{2.7}$$

The work transfer W is related to the pressure p and volume V in the cylinder by

$$dW = p\, dV. \tag{2.8}$$

An alternate form of the first law is then

$$dQ - p\, dV = dE \tag{2.9}$$

or per unit mass or mol,

$$dq - p\, dv = de, \tag{2.10}$$

where

$$q = \frac{Q}{m}; \quad e = \frac{E}{m}. \tag{2.11}$$

For unit mass or mol of a system of constant composition the specific internal energy is a function of temperature only,

$$e = e(T). \tag{2.12}$$

The specific heat at constant volume C_v is defined as

$$C_v = \left(\frac{\partial e}{\partial T}\right)_v. \tag{2.13}$$

For a system subject to heat energy transfer at constant volume, the work transfer is zero, dW = 0, and the first law states (2.10)

$$dq = de = C_v dT \tag{2.14}$$

whence $$C_v = \frac{dq}{dT} . \tag{2.15}$$

Since e is a function T, so is the specific heat C_v.

Hence $$C_v = C_v(T). \tag{2.16}$$

The internal energy and the specific heats may be expressed in a number of forms. The exact form used in a calculation will depend on the degree of accuracy required and the temperature range. The most general form of the internal energy e is as a polynomial function of temperature T. Thus

$$e = a_1 T + a_2 T^2 + a_3 T^3 + a_4 T^4 + a_5 T^5 + e_0, \tag{2.17}$$

where a_1 to a_5 are constants and e_0 is the internal energy at the absolute zero T = 0.

The specific heat is then

$$C_v = a_1 + 2a_2 T + 3a_3 T^2 + 4a_4 T^3 + 5a_5 T^4$$

or $$C_v = b_0 + b_1 T + b_2 T^2 + b_3 T^3 + b_4 T^4, \tag{2.18}$$

where b_0 to b_5 are constants.

There are two special approximations used in internal combustion engine studies; namely, a gas of constant specific heats and a gas with a specific heat varying linearly with temperature.

For a gas of constant specific heat,

$$C_v = a_1 = b_0 \tag{2.19}$$

and the internal energy is

$$e = a_1 T + e_0. \tag{2.20}$$

For a gas with specific heat varying linearly with temperature,

$$C_v = b_0 + b_1 T \tag{2.21}$$

and $$e = a_1 T + a_2 T^2 + e_0. \tag{2.22}$$

For changes in state without change in composition the constants e_0 may be eliminated and the internal energy is then $C_v T$.

2.2.2 Open Systems

For an open system the first law of thermodynamics states

$$\dot{Q}-\dot{W}_s-\dot{W}_p = \frac{\partial (E)_{cv}}{\partial t} + \left(\dot{H}_0\right)_{outflow} - \left(\dot{H}_0\right)_{inflow}, \tag{2.23}$$

where $\dot{Q}$ is the net rate of heat energy transfer <u>into</u> the system, $\dot{W}_s$ is the net <u>shear</u> work energy transferred <u>out</u> of the system, W_p is the net rate of work energy due to change in the volume of the system, $\frac{\partial (E)_{cv}}{\partial t}$ is the time rate of change of internal energy within the system, $\left(\dot{H}_0\right)_{outflow}$ is the total rate of stagnation enthalpy leaving the system and $\left(\dot{H}_0\right)_{inflow}$ is the total rate of stagnation enthalpy entering the system.

The work energy due to the change in volume of the system is

$$dW_p = pdV \tag{2.24}$$

and the rate of work energy or power is

$$\dot{W}_p = \frac{dW_p}{dt} = p\frac{dV}{dt}. \tag{2.25}$$

The internal energy of the system $(E)_{cv}$ is given by

$$(E)_{cv} = (me)_{cv}, \tag{2.26}$$

where m is the mass of the system and e the specific internal energy.

Hence $$\frac{\partial (E)_{cv}}{\partial t} = \frac{\partial (me)_{cv}}{\partial t}. \tag{2.27}$$

The static enthalpy h is defined as

$$h = \int_o^T C_p dT = C_p T \quad \text{(where } C_p \text{ taken to be a constant)} \tag{2.28}$$

If C is the gas velocity crossing the open system surface, then the stagnation enthalpy h_0 per unit mass per unit time is

$$h_0 = h + \frac{C^2}{2}. \tag{2.29}$$

The total rate of stagnation enthalpy leaving the open system is

$$\left(\dot{H}_0\right)_{out} = \left(\frac{dH_0}{dt}\right)_{out} = \left(\frac{dm}{dt}\right)_{out}\left(h + \frac{C^2}{2}\right)_{out}, \tag{2.30}$$

where $\left(\frac{dm}{dt}\right)_{out}$ is the mass flow rate out of the system. The total rate of stagnation enthalpy entering the open system is

$$\left(\dot{H}_0\right)_{in} = \left(\frac{dH_0}{dt}\right)_{in} = \left(\frac{dm}{dt}\right)_{in}\left(h + \frac{C^2}{2}\right)_{in}, \tag{2.31}$$

where $\left(\frac{dm}{dt}\right)_{in}$ is the mass flow rate entering the system; we can then write the first law for an open system as

$$\frac{dQ}{dt} - \frac{dW_s}{dt} - p\frac{dV}{dt} = \frac{\partial (me)_{cv}}{\partial t} + \left(\frac{dm}{dt}\right)_{out}\left(h+\frac{C^2}{2}\right)_{out} - \left(\frac{dm}{dt}\right)_{in}\left(h+\frac{C^2}{2}\right)_{in}. \quad (2.32)$$

For mass continuity across an open system,

$$\left(\frac{dm}{dt}\right)_{cv} = \left(\frac{dm}{dt}\right)_{in} - \left(\frac{dm}{dt}\right)_{out}, \quad (2.33)$$

where $\left(\frac{dm}{dt}\right)_{cv}$ is the rate of change of mass in the system.

For an open system with steady flow and constant volume,

$$\left(\frac{dm}{dt}\right)_{cv} = 0; \qquad \left(\frac{dV}{dt}\right) = 0. \quad (2.34)$$

The first law becomes

$$\frac{dQ}{dt} - \frac{dW_s}{dt} = \frac{dm}{dt}\left(\left(h+\frac{C^2}{2}\right)_{out} - \left(h+\frac{C^2}{2}\right)_{in}\right). \quad (2.35)$$

This expression is called the steady flow energy equation.

The static enthalpy h is related to the internal energy e. For a closed system,

$$dq - dw = de. \quad (2.36)$$

If heat is added at constant pressure,

$$dq = C_p\, dT = dh \quad (2.37)$$

and

$$dw = p\, dV \quad (2.38)$$

Hence

$$dh - p\, dV = de \quad (2.39)$$

or

$$dh = de + p\, dV \quad (2.40)$$

or

$$h = e + pV. \quad (2.41)$$

For an ideal gas, $pV = RT$ or $pV = R_{mol}T$, whence

$$h = e + RT \qquad (J/kg) \quad (2.42)$$

or

$$h = e + R_{mol}T \qquad (J/kg\text{-}mol) \quad (2.43)$$

It follows that the static enthalpy is a function of temperature

$$h = h(T), \tag{2.44}$$

and from (2.17) and (2.43) we can write for the enthalpy h in J/kg-mol as

$$h = a_1T + a_2T^2 + a_3T^3 + a_4T^4 + a_5T^5 + R_{mol}T + e_0 \tag{2.45}$$

and the specific heat C_p in J/kg-mol ^oK,

$$C_p = \left(\frac{\partial h}{\partial T}\right)_p = a_1 + 2a_2T + 3a_3T^2 + 4a_4T^3 + 5a_5T^4 + R_{mol}$$

or

$$C_p = b_0 + b_1T + b_2T^2 + b_3T^3 + b_4T^4 + R_{mol}. \tag{2.46}$$

For a gas with constant specific heat,

$$C_p = a_1 + R_{mol} = b_0 + R_{mol} \tag{2.47a}$$

or for a gas with specific heat varying linearly with temperature T,

$$C_p = a_1 + R_{mol} + 2a_2T = b_0 + R_{mol} + b_1T. \tag{2.47b}$$

In practice the polynomial coefficients a_n or b_n will be given either for internal energy or enthalpy functions (e or h) or for specific heat function (C_v or C_p). In this book we will use enthalpy functions (see section 2.6). The specific heats will then follow from the derivatives of these functions. Finally, we note that C_p and C_v are related though

$$C_p - C_v = R_{mol}, \tag{2.48}$$

so that only one set of coefficients are required.

2.3 THE SECOND LAW OF THERMODYNAMICS

The general form of the second law for a closed system is

$$dS = \left(\frac{dQ}{T}\right)_{rev}, \tag{2.49}$$

where dS is the entropy change associated with an energy transfer dQ at temperature T.

For unit mass of the system,

$$ds = \left(\frac{dq}{T}\right)_{rev}. \tag{2.50}$$

Substituting for dq from the first law for a closed system,

$$ds = \frac{de - p\,dv}{T}. \tag{2.51}$$

Now $de = C_v\,dT.$

Hence
$$ds = C_v \frac{dT}{T} - p\frac{dv}{T} \tag{2.52}$$

or
$$ds = C_v \frac{dT}{T} + R_{mol}\frac{dv}{v}. \tag{2.53}$$

Other forms are:
$$ds = C_p \frac{dT}{T} - R_{mol}\frac{dp}{p}, \tag{2.54}$$

$$ds = C_p \frac{dv}{v} + C_v \frac{dp}{p}. \tag{2.55}$$

For an isentropic process ds = 0 and

$$pv^{\left(\frac{C_p}{C_v}\right)} = \text{constant}. \tag{2.56}$$

For gases with constant specific heats, the ratio C_p/C_v is the isentropic index κ.

Hence
$$pv^{\kappa} = \text{constant}. \tag{2.57}$$

In terms of the density ρ,

$$\frac{p}{\rho^{\kappa}} = \text{constant}. \tag{2.58}$$

Now $C_p - C_v = R_{mol}.$

Hence
$$C_p = \frac{\kappa}{\kappa-1} R_{mol}, \tag{2.59}$$

$$C_v = \frac{1}{\kappa-1} R_{mol}. \tag{2.60}$$

For the general case of e = e(T), h = h(T) the usual form of the second law is

$$ds = \frac{dh}{T} - R_{mol}\frac{dp}{p} \tag{2.61}$$

since $dh = C_p\,dT.$

Integrating (2.61) between limits p, T, s and p_0, T_0, s_0 we have

$$s = \int_{T_0}^{T} \frac{dh}{T} - R_{mol}\,\ell n\,\frac{p}{p_0} + s_0. \tag{2.62}$$

The first term is a function of temperature only

$$s(T) = \int_{T_0}^{T} \frac{dh}{T} . \tag{2.63}$$

If we define $P = p/p_0$, called the normalized pressure, then

$$s = s(T) - R_{mol} \ln P + s_0. \tag{2.64}$$

It is usual to set $s_0=0$ (see Advanced Engineering Thermodynamics[1]),

$$s = s(T) - \ln P. \tag{2.65}$$

The pressure p_0 is usually set at 1 atm, i.e. 1.01325 bar.

2.4 HOMENTROPIC FLOW

For simple problems of flow we can assume that the entropy of a gas is constant and uniform in the whole flow field. This type of flow is called homentropic flow.

We shall consider the control volume in Fig. 2.1.

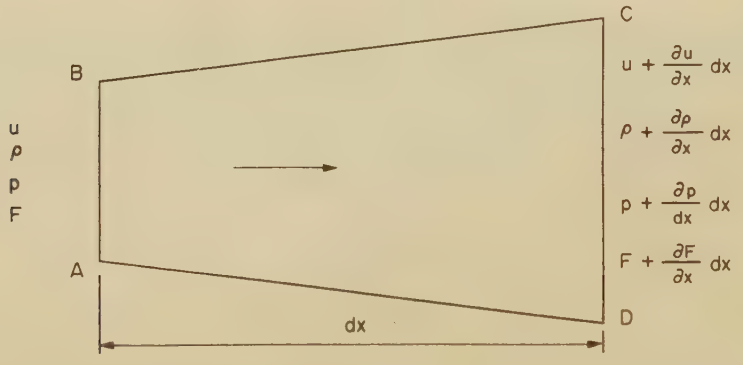

FIG. 2.1. Control volume.

We shall assume the flow is one-dimensional with velocity u, density ρ, pressure p and cross-sectional area F.

2.4.1 Continuity Equation

The rate of mass flow entering the control surface AB is

$$\rho u F. \tag{2.66}$$

The rate of mass flow leaving the control surface CD is

$$\left(\rho + \frac{\partial \rho}{\partial x}\, dx\right)\left(u + \frac{\partial u}{\partial x}\, dx\right)\left(F + \frac{dF}{dx}\, dx\right). \tag{2.67}$$

The rate of decrease of mass within the control surface ABCD is

$$-\frac{\partial}{\partial t}\,(\rho F\, dx). \tag{2.68}$$

The continuity equation states: The net rate of flow out of the control volume equals the rate of decrease in mass in the control volume.

Substituting (2.66), (2.67) and (2.68) into the continuity equation and simplifying, we obtain

$$\frac{\partial(\rho u F)}{\partial x}\, dx = -\frac{\partial}{\partial t}(\rho F\, dx) \tag{2.69}$$

or

$$\frac{\partial p}{\partial t} + \rho\,\frac{\partial u}{\partial x} + u\,\frac{\partial \rho}{\partial x} + \frac{\rho u}{F}\,\frac{dF}{dx} = 0. \tag{2.70}$$

This is the general continuity equation for flow through a control volume. We have a number of special cases:

For a constant area duct $dF/dx = 0$

and

$$\frac{\partial \rho}{\partial t} + \rho\,\frac{\partial u}{\partial x} + u\,\frac{\partial \rho}{\partial x} = 0. \tag{2.71}$$

For steady flow $\partial\rho/\partial t = 0$

and

$$\rho\,\frac{\partial u}{\partial x} + u\frac{\partial \rho}{\partial x} + \frac{\rho u}{F}\,\frac{dF}{dx} = 0, \tag{2.72}$$

which integrated gives

$$\rho u F = \text{constant}. \tag{2.73}$$

2.4.2 Momentum Equation

The momentum equation states that the pressure forces on the control surface ABCD equals the rate of change of momentum within the control volume ABCD plus the net efflux of momentum out of the control surface ABCD. For homentropic flow we ignore the shear forces on the wall.

The pressure forces on the control surface are

$$pF - \left(p + \frac{\partial p}{\partial x}\, dx\right)\left(F + \frac{dF}{dx}\, dx\right) + p\,\frac{dF}{dx}\, dx \tag{2.74}$$

which simplifies to

$$-\frac{\partial}{\partial x}\,(pF)dx + p\,\frac{dF}{dx}\, dx. \tag{2.75}$$

The rate of change of momentum in the control volume is

$$\frac{\partial}{\partial t} (\rho F u \, dx). \tag{2.76}$$

The net efflux of momentum from control surfaces is

$$\left(\rho + \frac{\partial \rho}{\partial x} dx\right)\left(u + \frac{\partial u}{\partial x} dx\right)^2 \left(F + \frac{dF}{dx} dx\right) - \rho u^2 F. \tag{2.77}$$

Substituting (2.74)-(2.77) into the momentum equation and simplifying, we obtain

$$\frac{\partial u}{\partial t} + u \frac{\partial u}{\partial x} + \frac{1}{\rho} \frac{\partial p}{\partial x} = 0. \tag{2.78}$$

For steady flow we have $\partial u/\partial t = 0$ and

$$\frac{\partial p}{\partial x} = - \rho u \frac{\partial u}{\partial x}, \tag{2.79}$$

which on integration gives for incompressible flow, ρ = constant,

$$p + \frac{\rho u^2}{2} = \text{constant}. \tag{2.80}$$

This is Bernoulli's equation in the usual form

$$\frac{p}{\rho} + \frac{u^2}{2} = \text{constant}. \tag{2.81}$$

For isentropic compressible flow with constant specific heats,

$$\frac{p}{\rho^\kappa} = \text{constant}. \tag{2.58}$$

Substituting for p in (2.79) and integrating, we obtain after simplification,

$$\frac{\kappa}{\kappa - 1} \frac{p}{\rho} + \frac{u^2}{2} = \text{constant}. \tag{2.82}$$

The first term equals $C_p T$, and if we set $h = 0$ at $T = 0$, then $h = C_p T$ and we have the expression

$$h + \frac{u^2}{2} = \text{constant} = h_0. \tag{2.83}$$

Thus the momentum equation for isentropic compressible flow reduces to the steady flow energy equation with no heat transfer and work transfer.

2.5 GAS MIXTURES

We consider the mixture comprising ideal gases which obeys the following:

(a) The gas mixture as a whole obeys the equation of state $pV = MR_{mol}T$, where M is the total number of mols of all kinds.

(b) The total pressure of the mixture is the sum of the pressures which each component would exert if it alone occupied the whole volume of the mixture at the same temperature.

(c) The internal energy, enthalpy and entropy of the mixture are respectively equal to the sums of the internal energies, enthalpies and entropies which each component of the mixture would have if each alone occupied the whole volume of the mixture at the same temperature.

If we have a mixture of three gases A, B and C at temperature T and volume V, we define the mole fraction x as

$$x_a = \frac{M_a}{M}, \quad x_b = \frac{M_b}{M}, \quad x_c = \frac{M_c}{M}, \tag{2.84}$$

where the total number of mols M is

$$M = M_a + M_b + M_c. \tag{2.85}$$

We define the partial pressure p_i of gas i as

$$p_i = x_i p \tag{2.86}$$

It follows then that for the mixture of gases A, B and C

$$p = p_a + p_b + p_c = \Sigma p_i, \tag{2.87}$$

where p is the pressure of the mixture given by

$$p = \frac{MR_{mol}T}{V}. \tag{2.88}$$

If $$v_i = \frac{M_i R_{mol} T}{p} = \frac{x_i M R_{mol} T}{p} \tag{2.89}$$

and $$\%v_i = \frac{100\ v_i}{V} \tag{2.90}$$

then, since

$$p_i = x_i p, \tag{2.86}$$

it follows that

$$p_i = \frac{\% v_i}{100} p. \tag{2.91}$$

The specific energy of the mixture e is given by

$$e = x_a e_a + x_b e_b + x_c e_c \tag{2.92}$$

or

$$e = \Sigma x_i e_i, \tag{2.93}$$

and the specific static enthalpy of the mixture h is given by

$$h = \Sigma x_i h_i, \tag{2.94}$$

and for systems at rest,

$$h - e = \Sigma x_i \left(h_i - e_i \right) \tag{2.95}$$

$$= \Sigma x_i R_{mol} T = R_{mol} T \tag{2.96}$$

or

$$h = e + R_{mol} T \quad \text{for the mixture.} \tag{2.97}$$

The total internal energy E is

$$E = Me = M \Sigma x_i e_i = \Sigma M_i e_i \tag{2.98}$$

and

$$H = E + R_{mol} T. \tag{2.99}$$

Note M_i equals the number of mols of gas i in the mixture.

2.6 INTERNAL ENERGY AND ENTHALPY DIAGRAMS

Although constant specific heats enable cycle studies to be carried out with relative ease, these studies have limited accuracy and we must allow for the variation of the specific heats with temperature. We shall use the internal energy or enthalpy rather than the specific heats.

We define the specific internal energy as

$$e = e_0 + e(T) \tag{2.100}$$

and the specific enthalpy as

$$h = h_0 + h(T), \tag{2.101}$$

where e_0 and h_0 are the specific internal energies and specific enthalpy at the absolute zero.

Hence $h_0 = e_0$. (2.102)

In this book we shall define the specific enthalpy h(T) of a gas of species i as $h_i(T)$ and the corresponding internal energy as $e_i(T)$. The numerical value of $h_i(T)$ is given by

$$h_i(T) = R_{mol}\left[u_{i,1}T + u_{i,2}T^2 + u_{i,3}T^3 + u_{i,4}T^4 + u_{i,5}T^5\right], \quad (2.103)$$

where $u_{i,1}$, $u_{i,2}$, $u_{i,3}$, $u_{i,4}$, $u_{i,5}$ are the polynomial coefficients for the species i. We can generalize these to $u_{i,j}$ (j = 1 to 5), The numerical value of $h_i(T)$ is then

$$h_i(T) = R_{mol}\left[\sum_{j=1}^{j=5} u_{i,j}\, T^j\right]. \quad (2.104)$$

The corresponding value of $e_i(T)$ will be

$$e_i(T) = h_i(T) - R_{mol}\, T$$

and $$e_i(T) = R_{mol}\left[\left[\sum_{j=1}^{j=5} u_{i,j}\, T^j\right] - T\right]. \quad (2.105)$$

The coefficients $u_{i,j}$ (j = 1 to 5) are given in Table 2.1 for a number of gases and two fuels.

The absolute specific enthalpy h_i is given by

$$h_i = h_i(T) + h_{0i},$$

where h_{0i} is the enthalpy at absolute zero and is given by $u_{i,7}$ in Table 2.1.

The absolute specific internal energy h_i is given by

$$e_i = e_i(T) + e_{0i},$$

where e_{0i} is the internal energy at absolute zero. This is equal to h_{0i} and is given by $u_{i,7}$ in Table 2.1.

Note that in Table 2.1 the units of the coefficients $u_{i,1}$ to $u_{i,5}$ are dimensionless and $u_{i,7}$ is in J/kg-mol. The reference pressure for the data is 1.01325×10^5 N/m^2.

TABLE 2.1. Polynomial Coefficients ($u_{i,j}$)

Temperature Range 500-3000 ^{o}K

Reference Pressure, p_o = 1.01325 x 10^5 N/m^2

i	Species	j	1	2	3	4	5	6	7
1	CO_2		3.09590	2.73114×10^{-3}	-7.88542×10^{-7}	8.66002×10^{-11}	0.00000	6.58393	-3.93640×10^{8}
2	CO		3.31700	3.76970×10^{-4}	-3.22080×10^{-8}	-2.19450×10^{-12}	0.00000	4.63284	-1.13950×10^{8}
3	H_2O		3.74292	5.65590×10^{-4}	4.95240×10^{-8}	-1.81802×10^{-11}	0.00000	9.65140	-2.39225×10^{8}
4	H_2		3.43328	-8.18100×10^{-6}	9.66990×10^{-8}	-1.44392×10^{-11}	0.00000	-3.84470	0.00000
5	O_2		3.25304	6.52350×10^{-4}	-1.49524×10^{-7}	1.53897×10^{-11}	0.00000	5.71243	0.00000
6	N_2		3.34435	2.94260×10^{-4}	1.95300×10^{-9}	-6.57470×10^{-12}	0.00000	3.75863	0.00000
7	C_8H_{18}		-0.71993	4.64260×10^{-2}	-1.68385×10^{-5}	2.67009×10^{-9}	0.00000		-4.9298×10^{8}
8	C_3H_8		1.13711	1.45532×10^{-2}	-2.95876×10^{-6}	0.00000	0.00000		-0.90510×10^{8}

Q_{VS} (heat of reaction) for:

C_8H_{18} at 298^{o}K = -4.788 x 10^9 J/kg-mol.

C_3H_8 at 298^{o}K = -2.0372 x 10^9 J/kg-mol.

The enthalpy h_{Oi} at absolute zero is coefficient u_{i7}.

This is in units of J/kg-mol.

For a mixture of gases,

$$E = E_0 + E(T), \tag{2.106}$$

$$H = H_0 + E(T), \tag{2.107}$$

where
$$H_0 = E_0 = M \Sigma x_i e_{0i} = \Sigma M_i e_{0i} \tag{2.108}$$

and
$$E(T) = M \Sigma x_i e_i(T) = \Sigma M_i e_i(T), \tag{2.109}$$

$$H(T) = M \Sigma x_i h_i(T) = \Sigma M_i h_i(T), \tag{2.110}$$

where E_0 and H_0 are the internal energy and enthalpy at absolute zero. In Volume II, Appendix II.A, numerical methods for computing (2.108) to (2.110) are given. The internal energy and enthalpy may be plotted in the form of the diagram shown in Fig. 2.2.

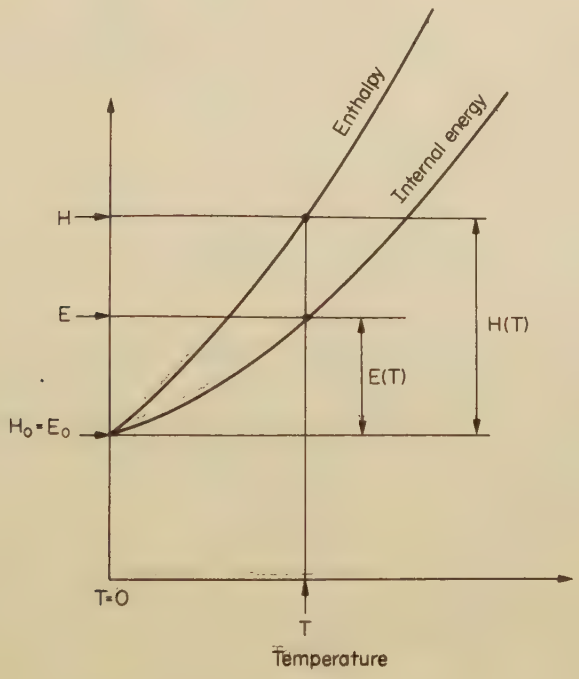

FIG. 2.2. Internal energy and enthalpy diagram.

$$M_R \longrightarrow M_P$$

where M_R is the total number of mols of the reactants and M_P the total number of mols of the products.

The first law of thermodynamics for the process is

$$dQ - dW = dE.$$

Now for adiabatic constant volume combustion, $dQ = 0$ and $dW = 0$. It follows therefore that

$$dE = 0 \tag{2.111}$$

or
$$E_P - E_R = 0. \tag{2.112}$$

That is, the internal energy of the products equals the internal energy of the reactants.

Now
$$E_P = M_P \Sigma \left(x_i e_i\right)_P = M_P \left(\Sigma \left(x_i e_{Oi}\right)_P + \Sigma \left(x_i e_i(T)\right)_P\right) \tag{2.113}$$

and
$$E_R = M_R \Sigma \left(x_i e_i\right)_R = M_R \left(\Sigma \left(x_i e_{Oi}\right)_R + \Sigma \left(x_i e_i(T)\right)_R\right). \tag{2.114}$$

We let
$$\left(E_O\right)_R = M_R \Sigma \left(x_i e_{Oi}\right)_R = M_R e_{OR}, \tag{2.115}$$

$$E(T)_R = M_R \Sigma \left(x_i e_i(T)\right)_R = M_R e_R(T_R), \tag{2.116}$$

$$\left(E_O\right)_P = M_P \Sigma \left(x_i e_{Oi}\right)_P = M_P e_{OP}, \tag{2.117}$$

$$E(T)_P = M_P \Sigma \left(x_i e_i(T)\right)_P = M_P e_P(T_P). \tag{2.118}$$

Then, for an adiabatic constant volume combustion process from (2.112) the internal energy of the product equals the internal energy of the reactants

$$E_P = E_R \tag{2.119}$$

whence

$$M_P e_{OP} + M_P e_P(T_P) = M_R e_{OR} + M_R e_R(T_R). \tag{2.120}$$

If we let

$$\Delta E_O = M_P e_{OP} - M_R e_{OR} \tag{2.121}$$

it follows therefore that for adiabatic constant volume combustion

$$M_P e_O(T_P) = M_R e_R(T_R) - \Delta E_O. \tag{2.122}$$

If the temperature of the reactants T_R is known, then the temperature of the products can be obtained from the above expression. This is illustrated in Fig. 2.3.

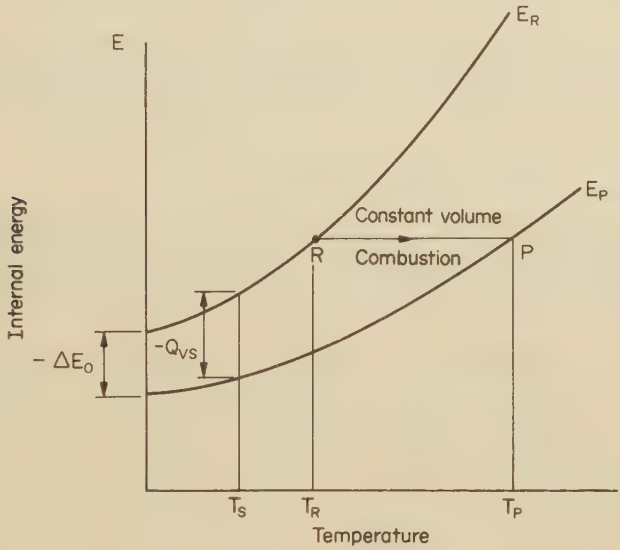

FIG. 2.3. Internal energy diagram for adiabatic constant volume combustion.

The term ΔE_0 is the heat of reaction at the absolute zero. This can be obtained from the heat of reaction at some temperature T_S in a constant volume calorimeter (e.g. a bomb calorimeter).

In a constant volume calorimeter the reaction takes place in a container surrounded by a water jacket. The initial temperature of the reactants is T_S. After combustion the products are brought back to the temperature T_S by heat transfer between products and water jacket. The heat transfer from the water jacket to the products is called the heat of reaction Q_{VS}, and is negative for an exothermic reaction. From the first law of thermodynamics for the process, $dW = 0$ since $dV = 0$.

Hence
$$Q_{VS} = E_P - E_R. \tag{2.123}$$

The internal energy of the products and reactants will be

$$E_P = M_P e_{OP} + M_P e_P(T_S) \tag{2.124}$$

and
$$E_R = M_R e_{OR} + M_R e_R(T_S). \tag{2.125}$$

Hence the first law for the reaction will be

$$Q_{VS} = \left(M_P e_{OP} - M_R e_{OR}\right) + M_P e_P(T_S) - M_R e_R(T_S) \tag{2.126}$$

or

$$Q_{VS} = \Delta E_O + M_P e_P(T_S) - M_R e_R(T_S). \tag{2.127}$$

This is shown in Fig. 2.3. Notice the heat of reaction is a function of temperature T_S. If we rearrange (2.127) in terms of ΔE_O

$$\Delta E_O = Q_{VS} - M_P e_P(T_S) + M_R e_R(T_S), \tag{2.128}$$

and substitute into (2.122) we can obtain a general expression for adiabatic constant volume combustion in terms of the reaction temperature T_R and the heat of reaction Q_{VS} of the reactants.

$$M_P e_P(T_P) = M_R\left(e_R(T_R) - e_R(T_S)\right) + M_P e_P(T_S) - Q_{VS}. \tag{2.129}$$

Typical values of Q_{VS} are given in Table 2.1.

For the general case of combustion with heat loss and volume change, the first law is

$$dQ - dW = dE$$

or

$$\int_1^2 dQ - \int_1^2 p\, dV = E_2 - E_1. \tag{2.130}$$

This expression will be used later in cycle analysis. The internal energy terms E_1 and E_2 will vary according to temperature and composition during the course of the combustion process.

2.7 DISSOCIATION

A chemical reaction is usually of the form

$$A + B = C + D \tag{2.131}$$

For example,

$$CO + \tfrac{1}{2}O_2 = CO_2 \tag{2.132}$$

or

$$CO + \tfrac{1}{2}O_2 + \tfrac{1}{2} \times \frac{79}{21} N_2 = CO_2 + \tfrac{1}{2} \times \frac{79}{21} N_2 \tag{2.133}$$

or

$$CH_4 + 3O_2 + 3 \times \frac{79}{21} N_2 = CO_2 + 2H_2O + O_2 + 3 \times \frac{79}{21} N_2. \tag{2.134}$$

In the first example (2.132) there is sufficient oxygen to change the CO to CO_2. In the second example (2.133) the CO is burnt in air. The mols of N_2 in air per mol of O_2 is 79/21. In the third example (2.134) we have excess air.

The chemical equation for the CO - O_2 - CO_2 reaction

$$1CO + \tfrac{1}{2}O_2 = 1CO_2$$

is called the stoichiometric equation. The numbers 1, $\frac{1}{2}$ and 1 are called the stoichiometric coefficients. Thus

$$\nu_{CO} = 1, \ \nu_{O_2} = \tfrac{1}{2}, \ \nu_{CO_2} = 1.$$

We shall refer to these later.

The total number of mols of the reactants M_R and products M_P in the examples given above are:

eqn. (2.132) $M_R = 1.5$, $M_P = 1$;

eqn. (2.133) $M_R = 3.38$, $M_P = 2.88$;

eqn. (2.134) $M_R = 15.29$, $M_P = 15.29$.

Notice it is not necessary for the stoichiometric coefficients ν or the number of mols M to be integer numbers.

All the above reactions are ideal reactions. In practice the rate of formation of the products from the reactants is retarded by the rate of dissociation of the products back to the original reactants. We represent this process by the stoichiometric equation. For example, for the CO - O_2 - CO_2 reaction,

$$CO + \tfrac{1}{2}O_2 \rightleftharpoons O_2. \qquad (2.135)$$

The forward reaction is

$$CO + \tfrac{1}{2}O_2 \longrightarrow CO_2. \qquad (2.136)$$

At the same time some α of the CO is dissociated so that there is a backward reaction.

$$\alpha CO_2 \longrightarrow \alpha CO + \frac{\alpha}{2} O_2. \qquad (2.137)$$

During the course of the reaction α may vary. Equilibrium is established when α is constant and does not change. The final composition of the products of the reaction is then

$$(1-\alpha)\ CO_2 + \alpha CO + \frac{\alpha}{2} O_2. \qquad (2.138)$$

The chemical reaction will be represented by the chemical equation

$$CO + \tfrac{1}{2}O_2 \longrightarrow (1-\alpha)CO_2 + \alpha CO + \frac{\alpha}{2} O_2. \qquad (2.139)$$

To determine the degree of dissociation α we apply equilibrium thermodynamics (see Advanced Engineering Thermodynamics[1]). The system is in chemical and thermodynamic equilibrium when the Gibbs function (G = H-TS) reaches a minimum value. When this occurs for the above reaction we find that the normalized partial pressures of CO_2, CO and O_2 are related by the equilibrium equation

$$K_P = \frac{P_{CO_2}}{P_{CO}\sqrt{P_{O_2}}} \tag{2.140}$$

where K_P is called the equilibrium constant and the normalized partial pressure P_i is given by

$$P_i = \frac{p_i}{p_0}, \tag{2.141}$$

In the reaction (2.133)

$$CO + 0.5O_2 + 1.88N_2$$

the final products will be

$$(1-\alpha)\ CO_2 + \alpha CO + 0.5\alpha O_2 + 1.88N_2.$$

In the general case for a CO - O_2 - CO_2 reaction,

$$CO + aO_2 + bN_2,$$

the final products will be

$$dCO_2 + eCO + fO_2 + bN_2$$

The proportions d, e, f will be dependent on the equilibrium constant. So that if

$$P_{CO_2} = \frac{d}{M_P}P, \quad P_{CO} = \frac{e}{M_P}P, \quad P_{O_2} = \frac{f}{M_P}P,$$

then

$$K_P = \frac{\left(\frac{d}{M_P}P\right)}{\left(\frac{e}{M_P}\right)\left(\frac{f}{M_P}P\right)^{\frac{1}{2}}} = \frac{d}{e}\left(\frac{M_P}{fP}\right)^{\frac{1}{2}}$$

For the general case of a stoichiometric reaction,

$$\nu_a A + \nu_b B \rightleftharpoons \nu_c C + \nu_d D, \tag{2.142}$$

where ν_a, ν_b, ν_c, ν_d are the stoichiometric coefficients the equilibrium is

$$K_P = \frac{(P_c)^{\nu_c}\ (P_d)^{\nu_d}}{(P_a)^{\nu_a}\ (P_b)^{\nu_b}} \tag{2.143}$$

where P_a, P_b, P_c, P_d are the normalized partial pressures of A, B, C and D. In terms of the partial pressures p_a, p_0, p_c, p_d the equilibrium equation is

$$K_P = \frac{(p_c)^{\nu_c}\ (p_d)^{\nu_d}}{(p_a)^{\nu_a}\ (p_b)^{\nu_b}}\ p_0^{\ \nu_c+\nu_b-\nu_c-\nu_d}\ . \tag{2.144}$$

If the units of pressure are atmosphere then p_0 is 1 atm; if the units of pressure are bars then p_0 is 1.10325 bar or in N/m^2, then p_0 is 1.10325×10^5 N/m^2.

The equilibrium constant K_P is obtained from considering the thermodynamic equilibrium of chemical reactions. A full treatment of the subject is given in Advanced Engineering Thermodynamics.(1) We shall only state here the expression for determining K_P. This is

$$\ell n\, K_P = \left[\Sigma\left(\frac{\nu_i g_i(T)}{R_{mol}T}\right)_R - \Sigma\left(\frac{\nu_i g_i(T)}{R_{mol}T}\right)_P\right] - \frac{\Delta H_0}{R_{mol}T}\ . \tag{2.145}$$

In this expression subscripts R and P refer to reactants and products respectively in the stoichiometric equation, is the stoichiometric coefficient and $\Delta H_0 = \Delta E_0$ the heat of reaction at absolute zero. The function $g_i(T)$ is called the relative Gibbs function and is given by

$$\frac{g_i(T)}{R_{mol}T} = u_{i,1}(1-\ell n\ T) - u_{i,2}T - \frac{u_{i,3}}{2}T^2 - \frac{u_{i,4}}{3}T^3 - \frac{u_{i,5}}{5}T^4 - u_{i,6}$$

or

$$\frac{g_i(T)}{R_{mol}T} = u_{i,1}\ (1-\ell n\ T) - \sum_{j=2}^{j=5}\frac{u_{i,j}}{j-1}T^{j-1} - u_{i,6}. \tag{2.146}$$

The coefficients $u_{i,j}$ (j = 1 to 6) are given in Table 2.1 for a number of species i. The coefficient $u_{i,6}$ is reference pressure, p_0 dependent. The value given is for $p_0 = 1.01325E^5$ N/m^2. In Volume II, Appendix II.A a numerical method for computing the equilibrium constant (2.145) is given.

It will be seen from (2.145) that the equilibrium constant K_P is a function of temperature. It follows that the degree of dissociation is also a function of temperature. The higher the temperature the greater the degree of dissociation. The effect

of dissociation is to reduce the temperature rise during the chemical reaction.

Another way of looking at dissociation is to consider the rate of the forward and backward reactions. Consider the reaction

$$A + B \rightleftharpoons C + D. \tag{2.147}$$

This may be thought of as a forward reaction

$$A + B \xrightarrow{k_f} C + D \tag{2.148}$$

and a backward reaction

$$A + B \xleftarrow{k_b} C + D, \tag{2.149}$$

where k_f and k_b are called the reaction velocities.

The rate of formation of C or D is given by

$$k_f(A)(B), \tag{2.150}$$

where ( ) represents the molar concentration in mols per unit volume.

The rate of formation of A or B is given by

$$k_b(C)(D). \tag{2.151}$$

The rate of dissociation of A or B due to the forward reaction is

$$-k_f(A)(B). \tag{2.152}$$

The rate of dissociation of C or D due to the backward reaction is

$$-k_b(C)(D). \tag{2.153}$$

By combining the forward and backward rates of the reaction we can obtain the net rate of formation of the reactants A, B, C and D. These are:

For A:

$$\frac{d(A)}{dt} = -k_f(A)(B) + k_b(C)(D). \tag{2.154}$$

For B:

$$\frac{d(B)}{dt} = -k_f(A)(B) + k_b(C)(D). \tag{2.155}$$

For C:

$$\frac{d(C)}{dt} = k_f(A)(B) - k_b(C)(D). \tag{2.156}$$

For D:

$$\frac{d(D)}{dt} = k_f(A)(B) - k_b(C)(D), \tag{2.157}$$

Equilibrium is obtained in the reaction when there are no further changes in A, B, C or D. That is when

$$\frac{d(A)}{dt} = \frac{d(B)}{dt} = \frac{d(C)}{dt} = \frac{d(D)}{dt} = 0.$$

We shall call the equilibrium concentrations $(\ )_e$. It follows that equilibrium is established when

$$k_f(A)_e(B)_e = k_b(C)_e(D)_e = R_f \tag{2.158}$$

or

$$\frac{(C)_e(D)_e}{(A)_e(B)_e} = \frac{k_f}{k_b} = K_C. \tag{2.159}$$

K_C is called the <u>equilibrium constant</u> and is related to K_P by the expression

$$K_C = K_p(R_{mol}T)^{\left(\nu_a+\nu_b\right)-\left(\nu_c+\nu_d\right)}. \tag{2.160}$$

In some reactions the rate of the forward reaction does <u>not</u> equal the rate of the backward reaction and vice versa. In these cases the reaction will not be in equilibrium. These reactions cover an important area of combustion in internal combustion engines which we shall refer to later.

If we define

$$\alpha = \frac{(A)}{(A)_e}, \quad \beta = \frac{(B)}{(B)_e}, \quad \gamma = \frac{(C)}{(C)_e}, \quad \delta = \frac{(D)}{(D)_e}, \tag{2.161}$$

then the rate of equations (2.153)-(2.156) can be expressed in the general form

$$\pm k_f\alpha\beta(A)_e(B)_e \mp k_p\gamma\delta(C)_e(D)_e \tag{2.162}$$

or

$$(\pm\alpha\beta \mp \gamma\delta)R_f. \tag{2.163}$$

The constant R_f is obtained through one of the reaction velocities, either k_f or k_b, and the equilibrium constant K_c. We shall use the general form later in examining emissions.

The forward reaction velocity k_f is usually quoted in the form

$$k_f = aT^b \exp\left(\frac{-\Delta E_o}{R_{mol}T}\right). \qquad (2.164)$$

The term ΔE_o is called the activation energy. The constant a is usually fairly large and b can be positive, negative or zero. It is usually an integer number. The index $(-\Delta E_o/R_{mol}T)$ is strongly dependent on temperature.

We shall discuss the time dependent reactions later when examining emissions. Equations of the type given in (2.164) are called Arrhenius equations.

REFERENCES

1. Benson, R.S., Advanced Engineering Thermodynamics Pergamon Press, 2nd edn., Oxford, 1976.

2. Shapiro, A.H., The Dynamics and Thermodynamics of Compressible Fluid Flow, Vols. I and II, Ronald Press, 1954.

Chapter 3

Air Standard Cycles

Notation

H_T	total heat energy input
p	pressure
Q	heat transfer per unit mass
r_c	volumetric compression ratio or compression ratio
r_e	volumetric expansion ratio or expansion ratio
r_p	equation (3.5)
r_t	rate of heat release (Fig. 3.7)
t	time
T	temperature
V	volume
W	work done per unit mass
W_T	total work done
α	equation (3.3)
β	equation (3.8)
κ	ratio of specific heats
η_{TH}	cycle thermal efficiency

Air standard cycles are well covered in numerous undergraduate texts on thermodynamics and it is not the intention to repeat such information extensively here. Some knowledge of them is, however, useful as an introduction to the more detailed calculations of engine cylinder pressure diagrams developed later; they can also give an insight into some of the important parameters influencing engine performance. Practical engineers use these cycles to provide a short description of real engines. Thus the idea of using an expansion ratio that is greater than the compression ratio is immortalized in the Atkinson cycle and the term may be often used by engineers as a description for any engine that uses the idea, however achieved. In our analysis we shall differentiate between the real Atkinson cycle and the modified cycle.

Three of the air standard cycles are particularly relevant to the reciprocating internal combustion engine and a fourth to a combination of engine and turbine. The four cycles are illustrated in Fig. 3.1; they are the constant volume (or Otto) cycle (Fig. 3.1(b)); the constant pressure combustion (or Diesel) cycle (Fig. 3.1(a)); a combination of the two, the dual combustion cycle (Fig. 3.1(c)); and the modified Atkinson cycle (Fig. 3.1(d)). We have pointed out that these ideal cycles give a valuable insight into real effects and possibilities. Some shortcomings are obvious; we shall refer to these later, but they should not be allowed to obscure the value of such idealization. We shall discuss in the next section air standard cycle efficiency and then follow with a section on the limitations of air standard cycles.

3.1 AIR STANDARD CYCLE EFFICIENCIES

Air standard cycles assume that the working fluid in the engine is always an ideal gas; namely, pure air with constant specific heats and that:

(a) A fixed mass of air is the working fluid throughout the entire cycle, i.e. there are no intake and exhaust processes.

(b) The combustion process is replaced by a heat transfer process from an external source.

(c) The cycle is completed by heat transfer to the surrounding until the air temperature and pressure correspond to the initial conditions (in contrast to the exhaust and intake processes in an actual engine).

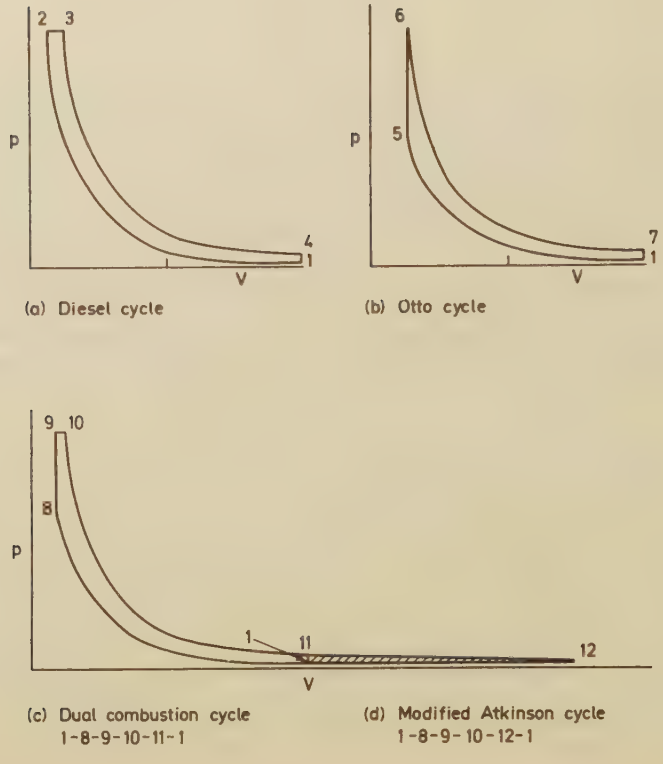

FIG. 3.1. Air standard cycles.

(d) All compression and expansion processes are internally reversible.

The ideal cycles shown in Fig. 3.1 all include isentropic compression, a simulation of combustion by means of heat transfer, isentropic expansion and, finally, heat transfer to close the cycle. As energy transfers only occur during the heat transfer processes the work done is the difference between heat addition and heat lost under the specified conditions and is calculated from the temperature at the various key points. From the work and heat transfer to the cycle we can compute the cycle efficiency. We shall illustrate the method by reference to the dual combustion cycle (Fig. 3.1(c)).

The initial temperatures and pressures are T_1 and p_1 respectively. For isentropic compression from 1 to 8 the temperature at 8, T_8, is given by

$$T_8 = \left(\frac{V_1}{V_8}\right)^{\kappa-1} T_1 = T_1 r_c^{\kappa-1}, \tag{3.1}$$

where κ is the ratio of the specific heats, r_c is the volumetric compression ratio (V_1/V_8) and is often simply called the compression ratio.

Heat is transferred at constant volume from 8 to 9. The temperature T_9 is then given by

$$T_9 = \frac{p_9}{p_8} T_8. \tag{3.2}$$

The ratio of the pressures p_9/p_8 is given the symbol α, i.e.

$$\alpha = \frac{p_9}{p_8} = \frac{T_9}{T_8}, \tag{3.3}$$

whence if we substitute for T_8 from (3.1) into (3.2) we obtain

$$T_9 = T_1 \alpha r_c^{\kappa-1}. \tag{3.4}$$

The temperature T_9 can be expressed in terms of the maximum to minimum pressure ratio r_p,

$$r_p = \frac{p_9}{p_1} \tag{3.5}$$

Then (3.2) will be replaced by

$$T_9 = \frac{p_9}{p_1} \frac{V_9}{V_1} T_1 = \frac{p_9}{p_1} \frac{V_8}{V_1} T_1 = T_1 \frac{r_p}{r_c}. \tag{3.6}$$

Heat is transferred at constant pressure from 9 to 10. The temperature T_{10} is then given by

$$T_{10} = \frac{V_{10}}{V_9} T_9. \tag{3.7}$$

The volume ratio (V_{10}/V_9) is given the symbol β, i.e.

$$\beta = \frac{V_{10}}{V_9} = \frac{T_{10}}{T_9} . \tag{3.8}$$

If we substitute (3.8) and (3.4) into (3.7) we then obtain

$$T_{10} = T_1 \alpha \beta r_c^{\kappa-1}. \tag{3.9}$$

In terms of the maximum pressure ratio r_p, we can write in place of (3.7)

$$T_{10} = \frac{p_{10}}{p_1} \frac{V_{10}}{V_1} T_1 = T_1 \frac{r_p}{r_e} \tag{3.10}$$

where r_e is the final volumetric ratio of expansion V_1/V_{10} or simply the expansion ratio.

The final temperature T_{11} is obtained from isentropic expansion from the state 10.

Thus $$T_{11} = \left(\frac{V_{10}}{V_{11}}\right)^{\kappa-1} T_{10} = \frac{T_{10}}{r_e^{\kappa-1}} . \tag{3.11}$$

If we substitute for T_{10} from (3.10), we obtain

$$T_{11} = T_1 \frac{r_p}{r_e^{\kappa}} . \tag{3.12}$$

It is convenient to express T_{11} in terms of α and β. If we note that

$$\beta = \frac{V_{10}}{V_9} = \frac{V_{10}}{V_8} = \frac{V_{10}}{V_1} \frac{V_1}{V_8} = \frac{r_c}{r_e} , \tag{3.13}$$

then, substituting for r_e from (3.13) and for T_{10} from (3.9) into (3.11), we obtain after simplification,

$$T_{11} = T_1 \alpha \beta^{\kappa}. \tag{3.14}$$

We can summarize the temperatures at the salient points as:

1: T_1.

8: $T_8 = T_1 r_c^{\kappa-1}$.

9: $T_9 = T_1 \alpha r_c^{\kappa-1} = T_1 \frac{r_p}{r_e}$.

10: $$T_{10} = T_1 \alpha\beta r^{\kappa-1} = T_1 \frac{r_p}{r_e}.$$

11: $$T_{11} = T_1 \alpha\beta^{\kappa} = T_1 \frac{r_p}{r_e^{\kappa}}.$$

The heat transfer per unit mass from state 8 to state 10 is given by

$$Q_{in} = C_v(T_9-T_8) + C_p(T_{10}-T_9) \tag{3.15}$$

or
$$Q_{in} = C_v T_1 \left[\kappa\left(\frac{T_{10}}{T_1}\right) - (\kappa-1)\left(\frac{T_9}{T_1}\right) - \left(\frac{T_8}{T_1}\right)\right]. \tag{3.16}$$

Substituting for the temperature ratios we obtain

$$Q_{in} = C_v T_1 r_c^{\kappa-1} \left((\alpha-1) + \alpha\kappa(\beta-1)\right) \tag{3.17}$$

or
$$Q_{in} = C_v T_1 \left[\left(\frac{r_p}{r_c} - r_c^{\kappa-1}\right) + \kappa\left(\frac{r_p}{r_e} - \frac{r_p}{r_c}\right)\right]. \tag{3.18}$$

The heat transfer per unit mass from state 11 to 1 is given by

$$Q_{out} = C_v(T_{11}-T_1) = C_v T_1 \left[\frac{T_{11}}{T_1} - 1\right]. \tag{3.19}$$

Substituting for the temperature ratio we obtain

$$Q_{out} = C_v T_1 (\alpha\beta^{\kappa}-1) \tag{3.20}$$

or
$$Q_{out} = C_v T_1 \left[\frac{r_p}{r_e^{\kappa}} - 1\right]. \tag{3.21}$$

The work done W in the cycle is

$$W = Q_{in} - Q_{out}. \tag{3.22}$$

The cycle efficiency η is given by

$$\eta = \frac{W}{Q_{in}} = \frac{Q_{in}-Q_{out}}{Q_{in}} = 1 - \frac{Q_{out}}{Q_{in}} \tag{3.23}$$

Substituting for Q_{out} and Q_{in} we obtain the cycle efficiency as

$$\eta = 1 - \frac{1}{r_c^{\kappa-1}} \left[\frac{\alpha\beta^{\kappa}-1}{(\alpha-1) - \alpha\kappa\,(\beta-1)}\right] \tag{3.24}$$

or
$$\eta = 1 - \frac{\left(\frac{r_p}{r_e^{\kappa-1}} - 1\right)}{\left(\frac{r_p}{r_c} - r_c^{\kappa-1}\right) + \kappa\left(\frac{r_p}{r_e} - \frac{r_p}{r_c}\right)}. \qquad (3.25)$$

If we examine (3.24) in conjunction with Fig. 3.1 we observe that for the Otto cycle (Fig. 3.1(b)) $\beta = 1.0$ and (3.24) becomes

$$\eta = 1 - \frac{1}{r_c^{\kappa-1}} \qquad (3.26)$$

and for the diesel cycle (Fig. 3.1(a)) $\alpha = 1.0$ and (3.24) becomes

$$\eta = 1 - \frac{1}{r_c^{\kappa-1}}\left(\frac{\beta^\kappa - 1}{\kappa(\beta-1)}\right). \qquad (3.27)$$

We observe that the Otto cycle efficiency is independent of the heat transfer to the cycle, whilst the diesel cycle is dependent on the heat transfer ($\beta > 1.0$). Expression for the efficiency (3.24), (3.25) and (3.26) can be written in the form

$$\eta = 1 - \frac{1}{r_c^{\kappa-1}} f(\alpha,\beta). \qquad (3.28)$$

The function $f(\alpha,\beta)$ is unity for the Otto cycle and greater than unity for the diesel and dual combustion cycles. It is often said that for the same compression ratio the Otto cycle is therefore the most efficient cycle and its efficiency is called the air standard efficiency. This is true, but in practice the picture is not so simple as design limitations and friction alter the basis for comparison. It may also be argued that efficiency is dependent upon expansion ratio rather than compression ratio.

The engine designer may be expected to work to two basic criteria: these are mechanical loading, or maximum cylinder pressure and thermal loading, often intuitively based upon exhaust temperature or, somewhat more scientifically, on heat transfer concepts, but in either case largely dependent upon air/fuel ratio. Maximum cylinder pressure is dependent upon compression ratio and the timing and rate of combustion, that is how much combustion occurs before or near top dead centre. The work output must also be considered in any true comparison as the brake thermal efficiency will largely depend on by how much the indicated work exceeds the frictional losses. In Fig. 3.2 the three cycles are superimposed for the same work and maximum pressure. For these conditions we find that

$$\eta_{Diesel} > \eta_{Dual} > \eta_{Otto}$$

This may be seen more clearly from Fig. 3.3, where the Otto cycle efficiencies are compared with diesel cycle efficiencies. Each Otto cycle condition was calculated for two maximum cylinder

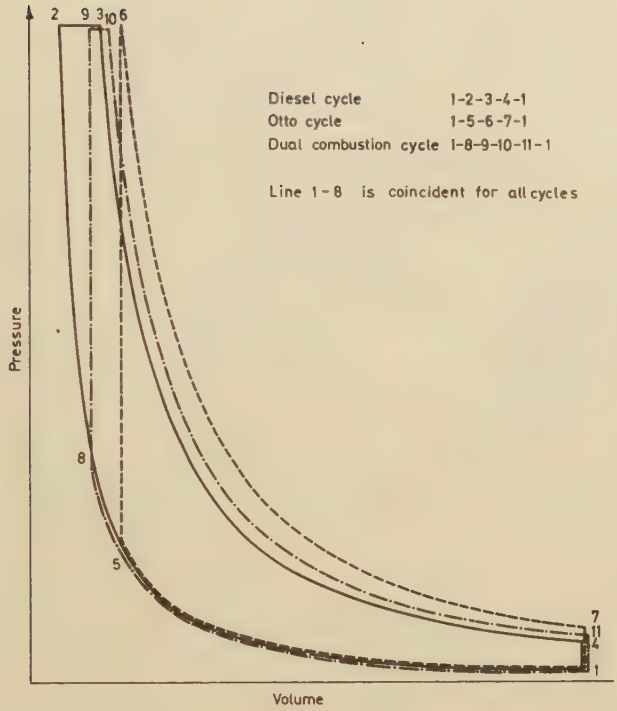

FIG. 3.2. Diesel, Otto and dual combustion cycles with same maximum pressure and work.

pressure conditions, which would give different indicated work, and for each of these a corresponding diesel cycle of same output and cylinder pressure is plotted. The thermal efficiency, maximum pressure and expansion ratio are plotted against the Otto cycle compression ratio. We notice that the diesel cycles are more efficient than the corresponding Otto cycle and that the efficiency increases with maximum cylinder pressure. The diesel expansion ratio r_e is in each case itself greater than the Otto compression (and expansion) ratio. However, this is not the full explanation as cross-checking from one curve to another shows that the same expansion ratio does not give the same efficiency either. It may be noted that efficiency depends upon some sort of mean expansion ratio for the heat transfer process. This expansion ratio will be between the compression ratio r_c and the expansion ratio r_e, as previously defined for the diesel cycle. As r_c is a function of the ratio of the maximum cylinder pressure to the initial pressure ($p_{max}/p_1 = r_p$); an increase in this ratio may be expected to increase the efficiency, as shown in Fig. 3.3.

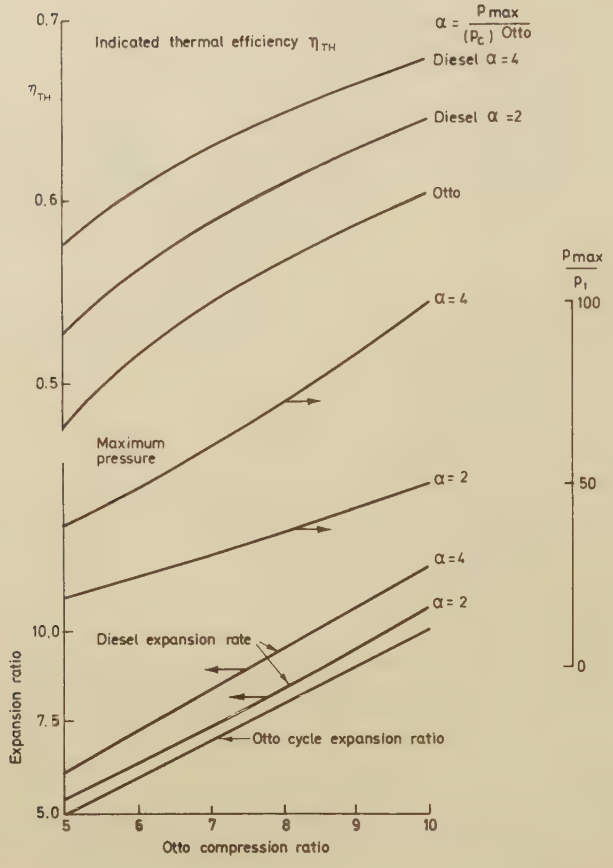

FIG. 3.3. Comparison of diesel and Otto cycles for same indicated work and maximum pressure.

In Fig. 3.4 the thermal efficiency is plotted for the diesel cycle (α = 1.0) and the dual combustion cycle (α = 1.5, 2.0) against the expansion ratio, for constant maximum pressures. On each graph the equivalent Otto cycle efficiency is shown. Here we clearly see the superiority of the diesel cycle and the dual combustion cycle over the Otto cycle. If we compare the diesel and dual combustion cycle as α approaches unity, so the efficiency increases. Finally, we note, as before, that as we raise the maximum pressure so we shall improve the cycle efficiency, although the law of diminishing returns is clearly in evidence.

If the cylinder contents could be expanded to the initial pressure p_1 more work might be obtained and the efficiency raised. The modified Atkinson cycle (Fig. 3.1(d)) shows the increased work represented by area 11-12-1. A large increase in volume is required to reduce the pressure to p_1. The work could be obtained

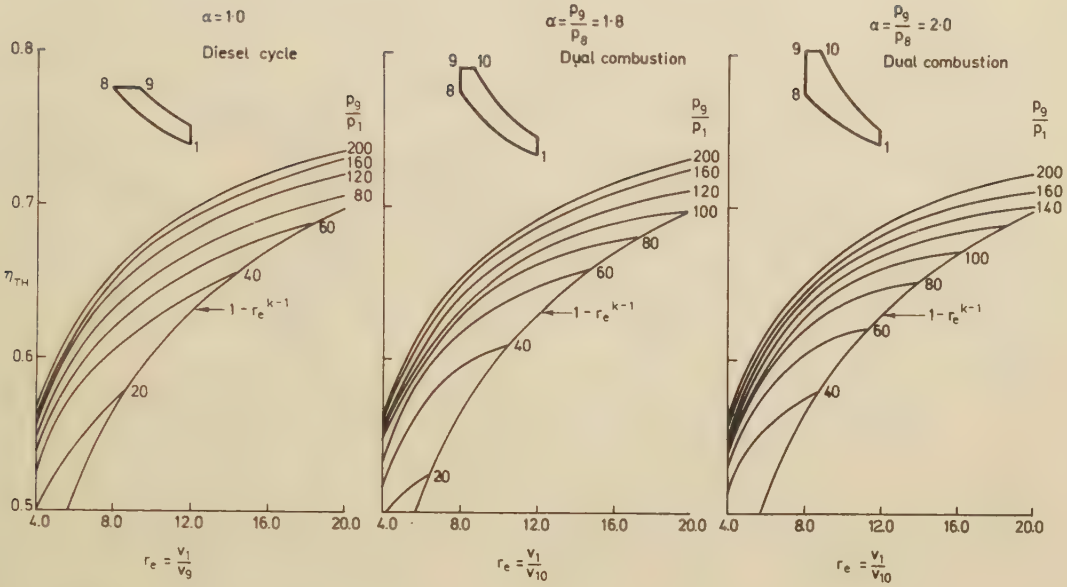

FIG. 3.4. Indicated efficiencies for diesel and dual combustion cycles.

in a gas turbine coupled directly to the internal combustion reciprocating engine but at the usual rather low value of pressure p; this turbine is used to drive a compressor, so modifying the cycle further. The modified Atkinson cycle efficiency is given by

$$\eta = 1 - \frac{1}{r_c^{\kappa-1}} \frac{\alpha^{\frac{1}{\kappa}} \beta - 1}{(\alpha-1) + \alpha\kappa(\beta-1)} . \qquad (3.29)$$

In Fig. 3.5 the efficiency of the dual combustion and modified Atkinson cycles are compared for the same $\alpha = (p_{max}/p_{compression})$ and β(= volume ratio of expansion during combustion). The modified Atkinson efficiency is almost, but not completely, independent of β. For $\beta = 1$ we have the Otto cycle and $\alpha = 1$ the diesel cycle. In Chapter 10 we will explore the utilization of the work represented by the area 11-12-1 (Fig. 3.1(d)).

3.2 LIMITATIONS

Although these air standard cycles give useful indications of the trends likely to follow from a change in some engine variable or other, they also give extremely optimistic numerical estimates of the output obtainable from an engine, and the quantitative conclusions need to be treated with caution. Some obvious reasons

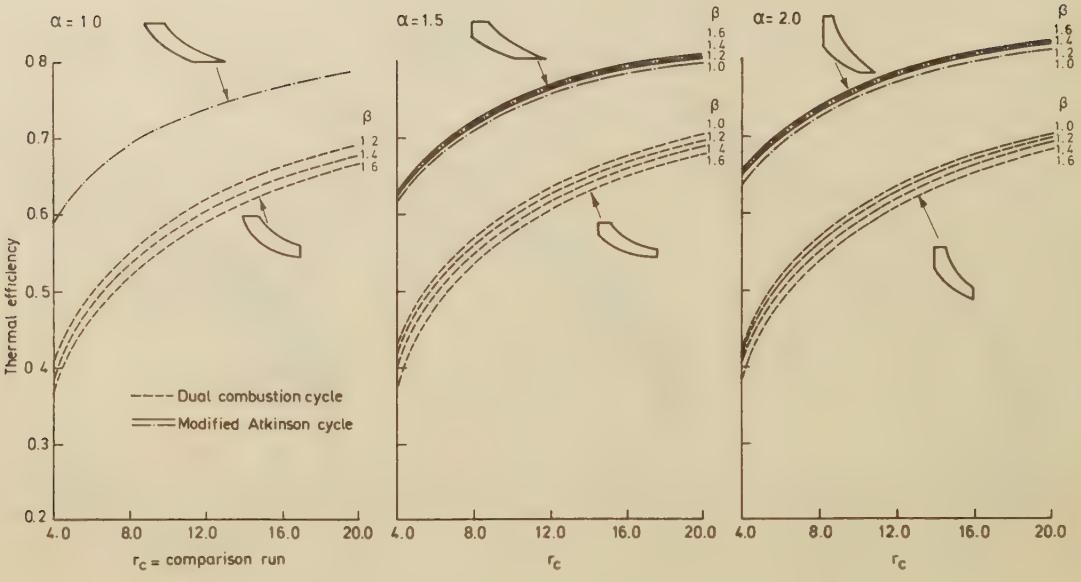

FIG. 3.5. Comparison of diesel, dual combustion and modified Atkinson cycles.

for this may be derived from a study of the assumptions listed earlier, and later chapters of this book will give methods for computing more realistic information. We shall review in this chapter some of these limitations before giving the fuller treatment later.

Real gases have variable specific heats, and in particular the variation is more extreme when the products of combustion are taken into account. At air/fuel ratio near the stoichiometric dissociation becomes significant. The effect of dissociation and the variation in the specific heats is to give a smaller temperature change during heat addition than would be anticipated if these phenomena were neglected. Thus the pressure changes are lower and there is lower work output and lower efficiency. A closer approximation to the real cycle may be obtained if mean specific heats are used over the temperature range. In Chapters 8 and 9 a comparison is made between the air cycle efficiency and the real cycle efficiency for ideal fluids with variable specific heats and dissociation, if present.

An important difference between the real cycle and the ideal cycle is due to the effect of heat transfer from the cylinder gases to the combustion chamber walls, which occurs just before, during and after the combustion process. Much of it occurs during the combustion process itself and directly reduces the effective heat input and so work output and efficiency of the engine. Although some correction could be made by using a factor relating the actual

(fuel) input and the effective heat input the factor would be arbitrary—needing to be based on experience of engine type and relevant conditions of operation. This is a significant factor, contributing of the order of a 20% reduction in output.

In the real engine the simple constant volume heat rejection process is replaced by a gas exchange process which modifies the beginning and end parts of the pressure/volume diagram, reducing power output. In the four-stroke engine there is also an exhaust stroke and suction stroke which provide an air-pumping loop. These processes are dealt with in some detail in Chapter 7. The effects are not insignificant but not very drastic. The gas exchange process is most important, of course, in determining the trapped conditions (point 1 in Fig. 3.1) in the cylinder at the beginning of the compression stroke, which determines oxygen availability.

There are two other important factors that affect the accuracy of the air standard cycle analysis very considerably but which do not derive from the assumptions specified. Firstly, the work output, derived from the diagram area or heat balance considerations, gives an indicated work while commercially the net output after deducting frictional losses in the engine is important. It is easy to calculate the indicated work, express it as an indicated mean effective pressure, take away an estimate of the frictional mean effective pressure and so arrive at a net output. Allowing for friction in this way emphasizes the importance of output, sometimes neglected in elementary analysis, which concentrates on ideal thermodynamic efficiency. This is illustrated in Fig. 3.6. Here the ideal i.m.e.p. and indicated thermal efficiency for an Otto cycle is shown for a fixed maximum cylinder pressure against compression ratio. Superimposed is a constant f.m.e.p. line (a reasonable first approximation). Brake mean effective pressure is the intercept above this line and brake thermal efficiency is then obtainable and is also shown. It can be seen that the ideal compression ratio for a "real" Otto cycle engine would be quite low, well below that for maximum indicated efficiency (which corresponds to zero i.m.e.p.!). The second factor relates to realistic combustion rates and patterns. No engine can burn large quantities of fuel instantaneously at top dead centre. This would require infinite rates of combustion. Nor can combustion rates be controlled to give the constant pressure conditions required by the dual combustion or diesel cycles.

At this point it might be useful to discuss the different methods of representing the combustion process in cycle calculations. For a constant volume combustion process the absolute internal energy of the reactants, namely the fuel and air, will equal the absolute internal energy of the products of combustion plus the heat losses to the walls. Similarly, for a constant pressure combustion process absolute enthalpies would need to be used.

In a real engine the combustion processes usually occur with both pressure and volume changes and the absolute internal energy of the reactants equals the absolute internal energy of the products plus the heat losses and the work done by the cylinder contents on the moving boundary (the piston in reciprocating engines).

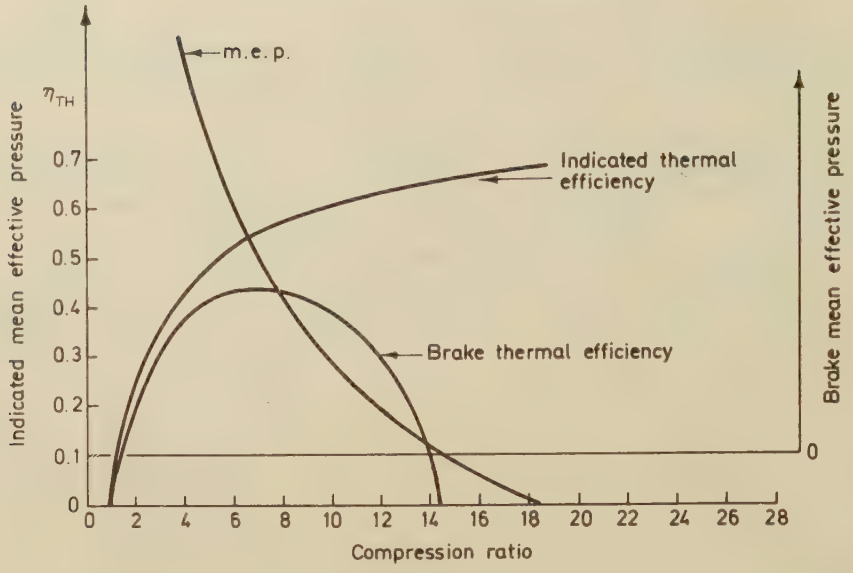

FIG. 3.6. Ideal Otto cycle performance with fixed maximum cylinder pressure. Allowing for f.m.e.p. (typical).

If the absolute value of the internal energies (or enthalpies) of all the chemical species taking part are known, then we can refer to the combustion process in a quantitative manner by plotting a diagram which expresses either the rate of conversion of fuel (and air) to the products with respect to time against time or the actual quantity of fuel burnt against time. These types of diagrams are called the rate diagram and the cumulative diagram respectively. This procedure is conventionally used in spark ignition engine calculations and can be applied in diesel engine calculations; however, an alternative convention has become normal, paralleling the "heat addition" used in the air standard cycles to represent combustion. The combustion process is expressed as a "heat release" diagram. In this case the combustion parameter is the quantity of fuel burnt multiplied by the lower calorific value of the fuel, using a positive value for an exothermic reaction. This is more in line with normal commercial practice, where the quality of a fuel is normally quoted in terms of calorific value. This parameter is called the "heat release" and may be expressed in energy units (J or kJ) in cumulative diagrams or energy units per degree crankangle (J/°CA or kJ/°CA) in rate diagrams.

To calculate the heat release pattern the relative internal energies of the reactants and products are measured from the same reference temperature, the temperature at which the calorific value is specified. With this convention the "heat released" in a given time interval is the change in the difference between the relative internal energies of the products and the reactants with adjustment for heat transfer to the walls and the work transfer using the appropriate sign. A typical heat release rate diagram is shown in Fig. 3.7. These types of diagram will be extensively used in Chapter 4.

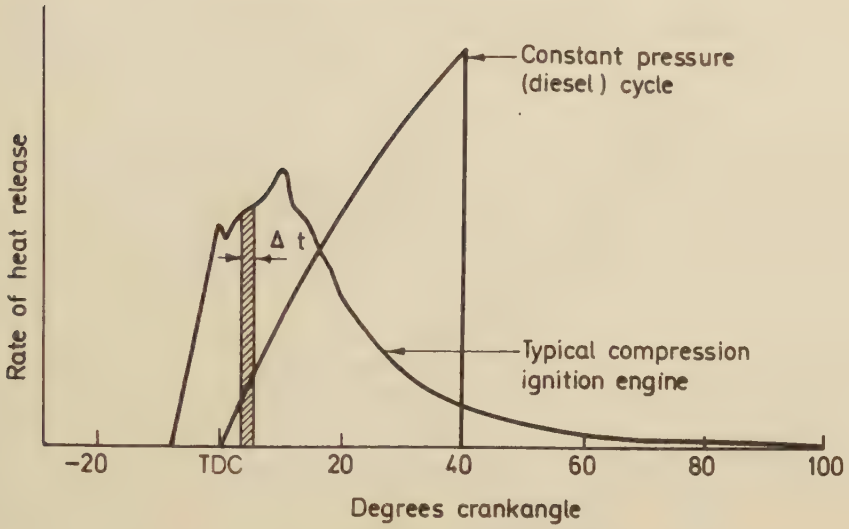

FIG. 3.7. Typical and ideal rate of heat release for a diesel engine

It may also be noted that the formula heat release equals fuel mass burnt times lower calorific value, assumes perfect combustion of the fuel.

In line with the convention for representing the combustion process in diesel engines in the form of heat release diagrams it is customary to discuss the process in terms of heat addition producing a temperature rise. From the thermodynamic point of view this is strictly a misuse of the term "heat addition", since no heat is added during the combustion process in the cylinder; there is a transfer of energy of one form into energy of another form producing a rise in the temperature of the cylinder contents. Because almost all the literature on diesel engine combustion uses the heat addition convention we shall use this practice.

Referring now to our previous discussion, of the three cycles mentioned the dual combustion cycle is perhaps somewhat nearer to reality than either of the other two, but it is essentially unreal. The combustion process is partially controllable, but no more than that, and it does not reproduce the rates required by an ideal cycle. Figure 3.7 compares a realistic diesel engine combustion rate diagram with a diesel cycle combustion rate diagram.

Although the usual air standard cycles, being based upon artificial pressure/volume diagrams, cannot deal with realistic combustion rates, it is easy to devise a method of doing so. The realistic rate, such as in Fig. 3.7, would produce a pressure/volume diagram as in Fig. 3.8.

If we consider an element of time Δt, during the combustion process, the heat addition due to combustion will be proportional to the shaded area on the rate diagram $r_t \Delta t$, and the total heat input will be similarly proportional to the sum of all such areas. The

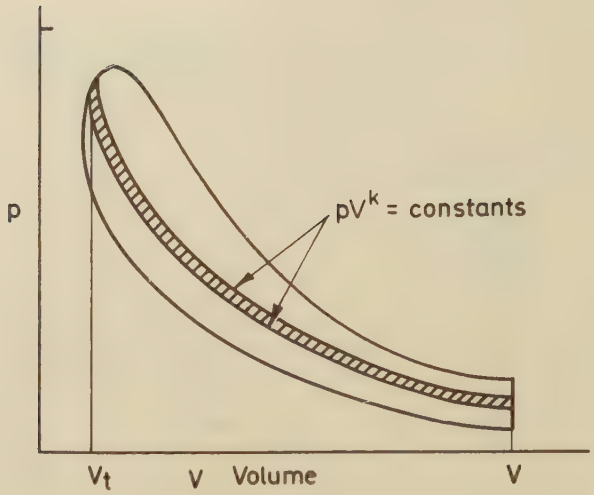

FIG. 3.8. Air standard cycle for realistic heat release rate.

same time period Δt is shown on the pressure/volume diagram and a small pressure/volume diagram is formed by drawing isentropic pressure/volume curves from the two end points of the period down to the constant volume heat rejection line. This small shaded area may be regarded as a small constant volume cycle with volumetric ratio $V/V_t = r_e$, so that the efficiency of utilization of the heat input will be $1-(1/(r_e^{\kappa-1}))$.

Thus work done by that fuel will be

$$r_t \, \Delta t \left(1 - \frac{1}{r_e^{\kappa-1}}\right).$$

Total work done will then be

$$\sum_a^b r_t \left(1 - \frac{1}{r_e^{\kappa-1}}\right) \Delta t = W_T$$

and total heat energy input will be

$$\sum_a^b r_t \, \Delta t = H_T.$$

Then efficiency of cycle will be W_T/H_T.

These equations may be solved by using the known geometry of the engine concerned, and the effect of combustion pattern and duration can be explored without other considerations. As the

efficiency of each interval depends on its expansion ratio it can be seen that for an engine with a given geometric expansion ratio the efficiency will be higher the more combustion is concentrated near top dead centre.

Having discussed the ideal cycles and their limitations we are now in a position to continue our study into the thermodynamics of the real engine. For these engines we can separate the closed part of the cycle from the open part. In the open part of the cycle we have the gas exchange process in which the products of combustion are exhausted and replaced by a fresh charge. This process is common to all engine cycles and will be discussed in Chapter 7.

In principle the closed part of the cycle is thermodynamically similar for both the compression ignition and the spark ignition engine but the details are often dissimilar. Both approximate to the dual combustion cycle in practice even though ideally the spark ignition engine would have an infinite flame speed and become an Otto cycle and the compression ignition engine would have a high compression ratio and controlled combustion to approximate to a diesel cycle.

The combustion process for the spark ignition engine is examined in Chapter 5 and the cycle analysis dealt with in Chapter 9.† The combustion process for the compression ignition engine is examined in Chapter 4 and the cycle analysis dealt with in Chapter 8.†

---

† In Volume II.

Chapter 4

Combustion in Compression Ignition Engines

Notation

act	constant in rate equation
A	surface or cross-sectional area
d	nozzle hole diameter (mm)
D	droplet diameter
h	number of holes in injector nozzle
K, K'	constants in rate equations
m	index in rate equation or mass of fuel droplet
M	mass of fuel injected during injection period (g)
M_i	total mass of fuel injected
M_u	total mass of unprepared fuel
n	number of fuel droplets
N	engine speed (rev/min)
p	pressure
p_i	injection period (^{o}crankangle)
p_{O_2}	partial pressure of oxygen
P	preparation rate
Q	fuel mass flow rate
R	instantaneous heat release rate or reaction rate
R'	reaction rate
R_{mol}	universal gas constant
t	time
T	temperature
x	index in rate equation
ΔH_o	heat of reaction at absolute zero
α	crankangle degree
ν	kinematic viscosity

4.1 DESCRIPTION OF COMBUSTION PROCESS

As mentioned in Chapter 1, in the typical compression ignition (CI) engine air alone is compressed and so raised to a high temperature during the compression stroke, so that rapid spontaneous ignition of the fuel is possible after it has been injected into the combustion chamber.

Because of the heterogeneities of the combustion process in a CI engine, in-cylinder studies of the combustion process, at the time of writing, have not been so detailed as in the spark ignition (SI) engine. Our understanding has been mainly achieved from combustion photography and an analysis of cylinder pressure diagrams. From these studies a picture of the combustion process has been obtained from which models have been developed to compute the pressure/time changes in the cylinder. In this chapter it is intended to discuss modern developments in this field. Because of the limited space, attention will be mainly, but not entirely, given to the authors' work.

Liquid fuel is injected, towards the end of the compression stroke, so that the fuel is distributed in a jet, or in several jets, throughout all or part of the combustion chamber. Distribution of the fuel, mixing with air, evaporation and diffusion to produce a gaseous mixture and chemical reactions to burn the fuel all have to be accomplished in an extremely short period of time if the engine is to be efficient. Thus an engine of 1000 rev/min would have about 10 ms for this sequence of events. The fuel is, therefore, supplied to the nozzle, which directs the jets into the combustion chamber, at very high pressure. This produces rapid injection through a small nozzle area and a high velocity of the jet relative to the air. Due to this high velocity the jet disintegrates into fuel droplets forming a spary. This spray, together with any air movement present, distributes the fuel through the air. There is little time for mixing and evaporation, and the different processes referred to above are not separate but tend to overlap. The cylinder contents are not homogeneous but vary from fuel, fuel/air combustion product mixtures to air alone in different regions. These regions may exist close to each other, in the vicinity of individual droplets, for example, as well as occurring on a larger scale.

From the commencement of injection the combustion process, as deduced from a study of cylinder pressure diagrams, may be divided into several stages (Fig. 4.1).

I. Ignition delay. No noticeable deviation of the pressure diagram from the compression curve (if late enough from the expansion curve).

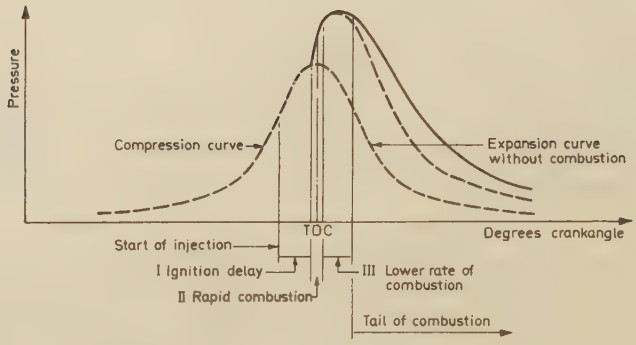

FIG. 4.1. Stages of diesel engine combustion.

II. Rapid (uncontrolled) combustion. A rapid rise in cylinder pressure.

III. A lower rate of combustion. This gives a moderate increase in cylinder pressure over that to be expected in the absence of continuing combustion.

IV. A very low rate of combustion, sometimes referred to as the tail of combustion, occurring well down the expansion stroke of the engine.

Although the ignition delay period is one where pressure is apparently unaffected by the presence of the injected fuel, this does not signify a period of uneventfulness. A great deal is happening; the fuel has to be broken down into droplets, heated and so vaporised, and mixed with air, a physical delay, and there is also a chemical delay during which chemical reactions are proceeding so slowly that no effect is discernible. It is incorrect to think of these two delays, the physical and the chemical,—as additive. They will overlap, the rate of chemical reaction increasing as the fuel and air becomes intimately mixed.

As conditions in the CI engine are so heterogeneous, it might be thought that delay would be variable and indeterminate but this is not so. Fuel on the periphery of a spray usually reaches ignition first and presumably ignition occurs in a region where a mixture near stoichiometric has been achieved. Formulae for ignition delay in CI

engines have been obtained, usually on a semi-empirical basis, but differences in engines, in fuel properties, in uncertainties as to actual temperatures and pressures in the engine and wall temperature effects all contribute to make such a calculation rather approximate. However the pattern of combustion is considerably affected by this delay period, and if anything more than purely empirical, or descriptive, information is required, as it is in modern cycle calculations by computer, some estimate has to be made.

One estimate has been given by Wolfer[1] as

$$t = \frac{0.44 e^{\left(\frac{4650}{T}\right)}}{p^{1.19}} \quad (\text{ms}),$$

where p is in atm and T in ^{o}K at the point of ignition.

This formula does emphasize the importance of the temperature in the cylinder: it might well be thought, however, that the way in which the temperature changes during the delay would also matter. To allow for these effects and others, some computer programs[2,3] have incorporated the Arrhenius type reaction calculations into their step-by-step combustion calculations. Such calculations have been mentioned earlier in Chapter 2 (eqn. (2.173)). These are mentioned where appropriate later. It should be mentioned that any such estimate also depends on the fuel properties, notably the cetane number.

During the delay period a considerable amount of fuel may have entered the combustion chamber. Some of this fuel will have become heated and evaporated and mixed with air so that it is ready for rapid combustion, that is it can take part in chemical reaction. These processes may be referred to collectively as preparation. Ignition in one place will be followed by ignition elsewhere, so rapid combustion of prepared fuel follows the first ignition. The rate and quantity of combustion in the second phase is thus dependent on the duration of the delay period and the rate of preparation of fuel during this period. This stage is one of premixed combustion and it may therefore be expected to give comparatively little radiation and to produce little carbon. Expectations supported by experimental evidence by Lyn and Valdamis[4].

Once the prepared fuel accumulated during the delay period has been consumed, the rate of consumption falls to a value that can be maintained by preparation of fresh fuel. The major controlling factor is the need for the fuel to find oxygen. Fuel may well be injected into the burning mixture so that combustion is in part regulated by the injection process as well as by the mixing and diffusion processes.

Finally, after all the fuel has been injected, combustion continues at a diminishing rate as the fuel and oxygen are each consumed. This last stage, referred to as the tail of combustion, and the previous one, are both characterized by diffusion combustion, with production and combustion of carbon particles and a high rate of heat transfer by radiation.

Because of this dependence of combustion on the process of fuel finding oxygen, CI engines require excess air to a greater extent than does the SI engine if high efficiency and, particularly, if low smoke levels are to be achieved. The minimum excess varies with type—as low as 15% for some highly turbulent pre-chamber engines to over 50% for some quiescent chamber engines.

The combustion described above may be shown graphically on a rate diagram, as in Fig. 4.2.

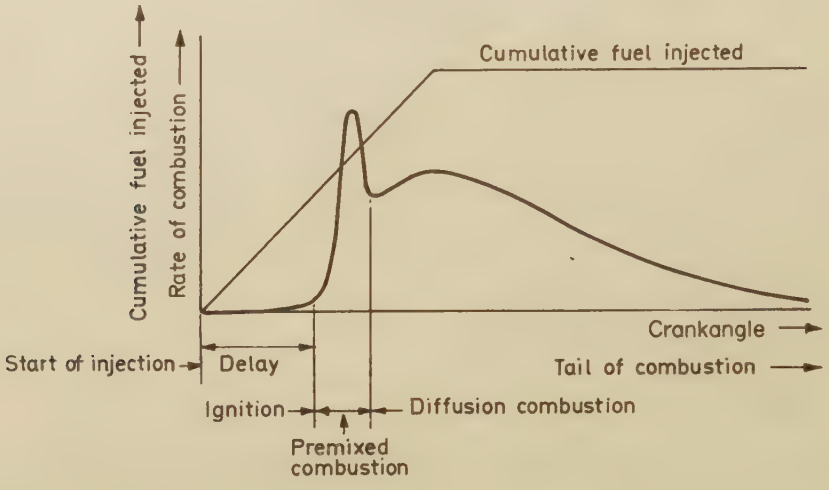

FIG. 4.2. Typical rate of heat release diagram.

This diagram is typical only. The magnitude of the various parts will depend upon the delay period, the fuel injection characteristics, on oxygen availability and the vigour of the mixing process. These divisions of the combustion process, although conventional and to some extent useful, may be thought to be illogically discontinuous. The physical and chemical processes proceed continuously from the start of injection. The effects vary because of differences in magnitude rather than of principle.

Knock in the Compression Ignition Engine. As there is no flame front progressing into a region of premixed fuel vapour and air—no end gas to auto-ignite—knock cannot occur as it does in the SI engine. However, very rapid pressure rises which produce knocking sounds, and other deleterious results can occur if the first peak in the combustion rate diagram is high enough. Although this is an auto-ignition phenomenon it has opposite causes to knock in SI engines. It is due primarily to too long a delay period and requires cures diametrically opposite to those required for the SI engine. Diesel knock is worse at high speeds, at low compression ratios, at low ambient temperatures and with fuels that are resistant to ignition.

Hence the better a fuel is for SI engines the worse it is likely to be for the CI engine.

If diesel knock is experienced in an engine a cure may be by means that either reduce the delay period or reduce the rate of injection during the delay period. A fuel with a higher cetane number will reduce the delay period as would a hot spot in the engine combustion chamber such as a glow plug, or the engine may be designed with a greater compression ratio. The fuel injection equipment may be designed to inject a small quantity of fuel a little before the main injection, a method known as pilot injection.

4.2 MODELS FOR COMPRESSION IGNITION COMBUSTION CALCULATIONS

In Chapter 3 air standard cycle calculations were described and their limitations mentioned. A major limitation is that the combustion process is taken to be a heat addition process, and in almost all examples the heat addition is considered to take place at unnatural and impossible rates. The use of modern computers for engine cycle calculations makes more realistic, complex cycle calculations possible, and these in turn require mathematical modelling of the combustion processes. The nature and complexity of the combustion model depends upon the type and purpose of the cycle calculation. Thus an early, and still major purpose, was to estimate overall engine performance by calculating a cylinder pressure diagram, and this has been achieved by a modest improvement on the air standard cycle, using small steps, spatially uniform cylinder conditions of composition, pressure and temperature, and considering combustion as a "heat release" process. This may be called a "single-zone" model. In some cases the model has been made more complex by considering the way in which fuel and air mix inside the cylinder and expressing the result as if the cylinder contents consisted of a volume of air and a volume of air, fuel and combustion products-a two-zone model.

An alternative, or additional, purpose for making cycle calculations is to arrive at estimates of the chemical nature of the products of combustion, especially of certain pollutants that are emitted in the exhaust gases, e.g. carbon monoxide, nitric oxide and soot. These calculations are as yet in an early stage of development but they require complex multi-zone models for any hope of success.

4.2.1 Single-zone Combustion Models

The simplest single-zone model specifies the heat release, or combustion, pattern in advance, so that the cycle calculation merely involves adding energy to the cylinder contents in accordance with this pattern at the appropriate points in the calculation. The pattern used is based upon experience with similar engines, having been obtained by analysing experimental cylinder pressure diagrams. The analysis of such diagrams is based upon identical calculations to those used for the calculation of cylinder pressure diagrams, called "synthesis", except that the unknown factor in any step is the heat release instead of the pressure change. The thermodynamics and

method of calculation are dealt with in greater detail in Chapter 8. Typical heat release diagrams have been published by early workers in this field, notably by Austen and Lyn[5], and an example is reproduced in Fig. 4.3.

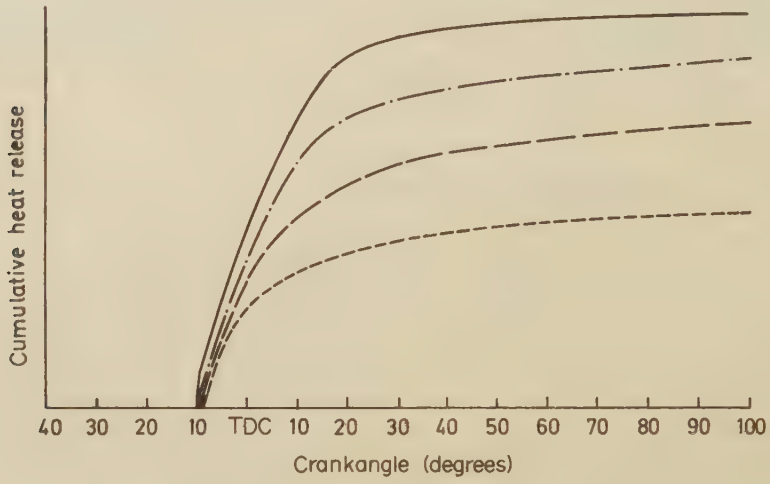

FIG. 4.3. Typical cumulative heat release patterns for different b.m.e.p.s. (From Austen and Lyn[5] by courtesy of the Institution of Mechanical Engineers.)

These heat release patterns may be simplified for calculation purposes, with little loss, if the purpose of the calculation is merely to explore the effect of changes in some design variables—such as compression ratio, valve timing, combustion timing, boost pressure and even duration of combustion, as long as the change does not itself produce additional significant changes in the combustion pattern. One such simplification, used by one of the authors in industry some years ago, is to replace the heat release curve by two straight lines one comprising rapid combustion of the bulk of the injected fuel and the other slow combustion, continuing down the expansion stroke of the remainder of the fuel (Fig. 4.4). Table 4.1 gives a few examples of appropriate values for the different parts.

Combustion rates of this type have advantages for computer work because they can be specified easily, but they suffer from severe limitations if the effect of changes which will affect combustion are to be investigated. It might be argued that the single-zone model is so unreal that significant improvement would be unsoundly based. It is necessary to consider the limitations of any method and the single-zone model is inadequate in many ways, notably when combustion is likely to be affected by lack of air, but some changes of value have been published.

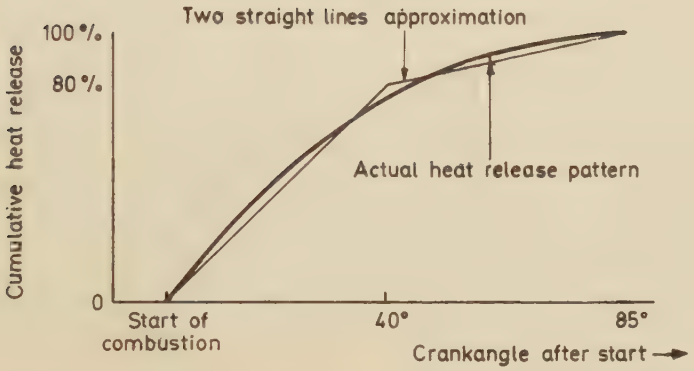

FIG. 4.4. Typical simplified heat release pattern.

TABLE 4.1. Table of Heat Release Data

Reference No.	Stage I Amount %	Stage I Duration (°C/A)	Duration	Total b.m.e.p.	Rev/min
5	85	30-35	110	90	1485
6	80	40	85	-	750
6	80	20	60	100	900
-	80	30	65	180	428

4.2.1.1 Lyn's Method

One such change is the method published by Austen and Lyn[6] which emphasizes the importance of the rate of fuel injection and also indicates how the various stages of the combustion process, already mentioned, may be dealt with mathematically. The fuel injection process may be divided into a number of short steps. The fuel injected during one such step is considered to be prepared and then burnt in a particular way, to accord with a simple mathematical formula. Summing all such steps would then give the preparation rate diagram for all of the injected fuel. However, there is a delay period before the fuel ignites. During this period the prepared fuel is assumed to accumulate to form a quantity of mixture of air and fuel which on ignition burns rapidly as a premixed flame. Once this mixture has been consumed, combustion would continue as fuel is prepared as a diffusion flame. These processes are shown diagrammatically in Fig. 4.5, where the area

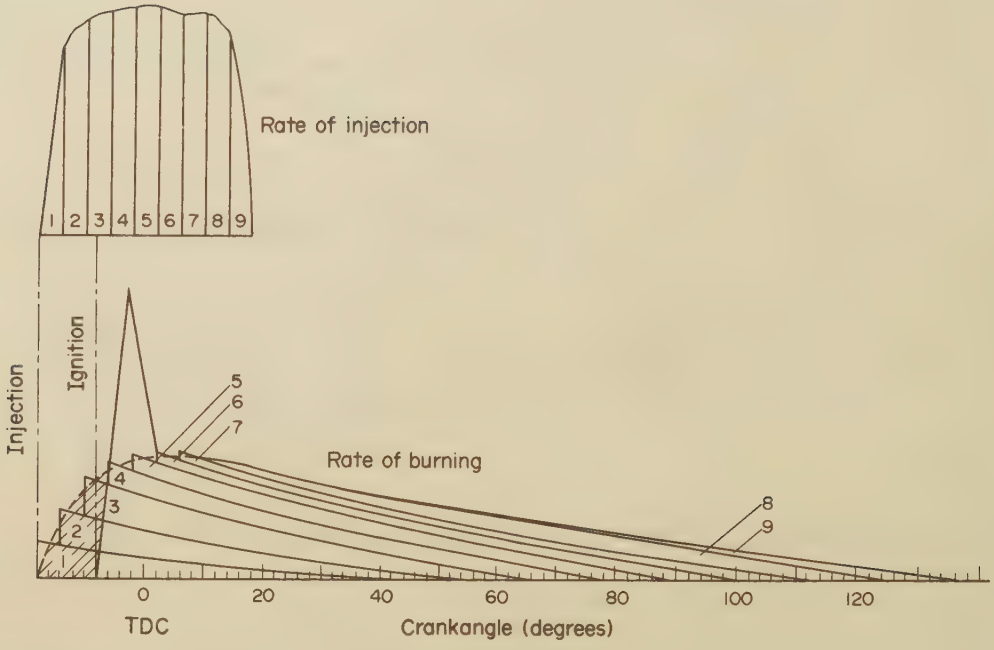

FIG. 4.5. Lyn's method of estimating heat release pattern. (From Lyn,[33] by courtesy of the Institution of Mechanical Engineers.)

under the curve represents the fuel quantity.

The envelope of the bottom figure represents the preparation rate curve. The fuel prepared during the delay period is burnt in the area enclosed by the first peak.

On this theory an ideal combustion rate diagram would show two peaks-one due to premixed combustion and one due to the maximum rate of preparation (which would be likely to occur towards the end of the injection period). Thus this theory does produce a rate diagram similar to that mentioned earlier. Such rate diagrams have been obtained from an analysis of cylinder pressure diagrams obtained experimentally.

Each element may be determined from a few simple formulae, i.e.

$$R = R_o\left(1 - \frac{t}{t_b}\right), \qquad t_b = t_o + a\, t_i,$$

where R_o is the initial rate, R is the instantaneous rate, t_o is the burning time for first element, t_b is the burning time of element, t is the time at rate R, t_i is the time of injection of element, after first element, and a is a constant.

The values of the various factors have to be determined by correlation with empirical data to give the best fit.

4.2.1.2 Whitehouse-Way's Method

Cycle calculations are of particular value when a new engine is being designed. In this case values of factors must be estimated before the calculation can be made, and guidance on this is not readily available. Also the formulae so far mentioned neglect oxygen availability, which is important particularly in assessing the effect of turbocharging on engine performance. Research on a number of engines by Whitehouse et al.[2, 3] led to semi-empirical formulae for calculating rates of combustion in turbocharged direct injection engines which allowed for fuel injection rates and the amount of oxygen available in the cylinder during the combustion process.

As with Lyn's proposals above, after injection the fuel is prepared for combustion by a mixing and diffusion process, but in this hypothesis the rate of mixing was assumed to be dependent upon the total surface area of the droplets forming the fuel spray.

For a single droplet of constant density the surface area is proportional to the diameter squared, the volume to the diameter cubed, and the mass m to the diameter cubed. It follows that for a single droplet the surface area is proportional to the mass to the two-thirds power, i.e. $m^{2/3}$. The total surface area A for all the droplets, at any time, assuming that they would all be the same size, would then be given by

$$A \propto n m^{\frac{2}{3}}$$

where n is the number of droplets.

The mass of the droplet m is related to the yet unprepared mass M_u of the fuel by

$$m = \frac{M_u}{n} .$$

The mass of fuel injected M_i, up to the time under consideration, is related to the number of droplets injected and the original diameter D_o of the droplets by

$$M_i \propto n D_o^3 \propto n$$

It follows, then, that the total surface area A of the droplets is

$$A \propto n \left(\frac{M_u}{n}\right)^{\frac{2}{3}} \quad n^{\frac{1}{3}} \quad M_u^{\frac{2}{3}}$$

or

$$A \propto M_i^{\frac{1}{3}} \quad M_u^{\frac{2}{3}} .$$

Thus the preparation rate is proportional to $M_i^{1/3}$ $M_u^{2/3}$, where M_i is the total mass of fuel injected in the cylinder up to the time of

calculation and M_u is that part of the fuel still available for preparation.

Allowing for an effect of oxygen availability on mixing, Whitehouse et al. suggest that the preparation rate P is given by

$$P = KM_i^{\frac{1}{3}} M_u^{\frac{2}{3}} p_{O_2}^m,$$

where P is the preparation rate (kg per degree crankangle), p_{O_2} is the partial pressure of oxygen and K and m are constants. The indices for the masses M_i and M_u are doubtful.

In his model for combustion of single droplets, Spalding[7] suggests that rate of combustion should be proportional to diameter of the droplet, not area, while if the uniformity of droplet size is replaced by a droplet distribution the effect is to prolong the life of some droplets (the larger ones) which is similar to the effect produced by increasing the value of the index of M_u. This latter point is shown in the paper by Whitehouse and Way[3]. These effects may be generalized by representing the preparation rate formula by

$$P = KM_i^{(1-x)} M_u^x p_{O_2}^m.$$

The values of the constants may be obtained from the analysis of experimentally obtained pressure diagrams and some values have been published,[3] i.e. if pressure is measured in bars (Table 4.2).

TABLE 4.2

Engine type	Bore (cm)	x	m	K.bars^{-m}
Foden two-stroke FD6	9.14	1	0.4	0.0175
RR K60 two-stroke	8.64	1	0.4	0.0175
Dorman 4LBT four-stroke	12.45	0.01	0.4	0.0115
	until after Z^o after top dead centre then			
		1	0.4	0.0115τ
	where $\tau = (M_i/M_u)^{0.99}$ at Z^o ATDC			
Mirrlees National FV2 four-stroke	30.48	2/3	0.4	0.008-0.020

The variations in value of the constants could be related to the type of combustion chamber. Thus the first two engines were both two-stroke engines with swirl, the Dorman engine was a deep bowl combustion chamber with swirl and squish, and the last was a medium speed quiescent combustion chamber diesel. For the Dorman engine the value of Z is given as from 12 to 20, and the formula was thought to be consistent with a layer of fuel vapour centrifuged to the outside of the bowl as shown on Fig. 4.6. This layer was believed to be disrupted by reverse squish at the time indicated by Z. The

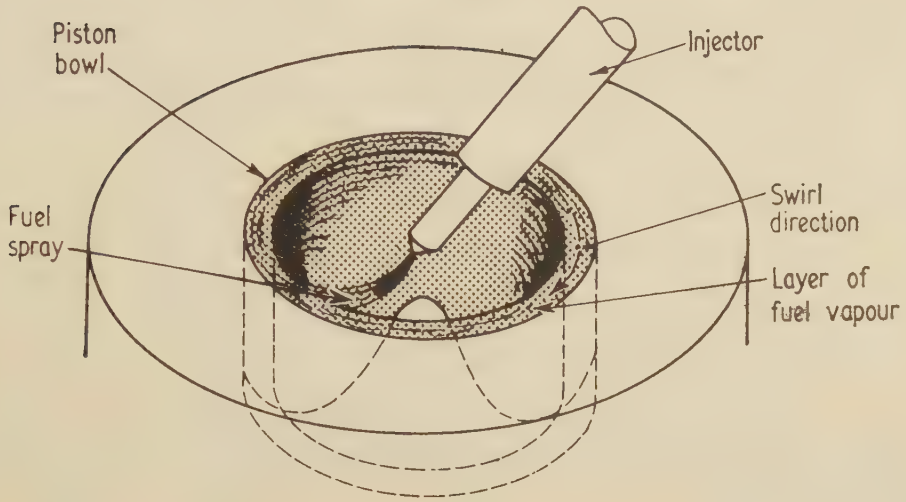

FIG. 4.6. Presumed fuel distribution in Dorman engine.

least satisfactory correlation seems to have been for the quiescent combustion chamber case. This is thought to be because of a critical mixing process which makes a two-zone model essential.

The effect of the delay period has still to be allowed for. This was achieved by introducing a chemical reaction rate using an Arrhenius type expression:

$$R' \quad (\text{velocity of gas molecules}) \quad (\text{oxygen density}) \quad (\text{mass of unburnt fuel}) \quad e^{\frac{-\Delta E_o}{R_{mol}T}}$$

where R' is the reaction rate (kg per unit time) and $\Delta E_o/(R_{mol}T)$ is the activation energy at temperature T.

If we assume that velocity of the gas molecules is proportional to the square root of the temperature, the density of oxygen is proportional to the partial pressure divided by the temperature, the unburnt fuel is given by $\int(P-R)d\alpha$, where P is the rate of preparation and R is the rate of burning per degree crankangle, then the above expression can be written in the form

$$R = \frac{K' \, p_{O_2}}{N\sqrt{T}} \; e^{-\frac{act}{T}} \int (P-R) \, d\alpha,$$

where N is engine speed in rev/min.

The constants K' and act are obtained from analysis of indicator diagrams. For R (kg per degree), T (^{o}K), p_{O_2} (bars), the constants

obtained from analyses of indicator diagrams are as shown in Table 4.3.

TABLE 4.3

Engine type (units)	K' ($K^{\frac{1}{2}}$/bar s)	act (^{o}K)
Foden FD6	1.2×10^{10}	1.5×10^{4}
Rolls-Royce K60	1.2×10^{10}	1.5×10^{4}
Dorman 4LBT	1.2×10^{10}	1.5×10^{4}
Mirrlees National FV2 (single zone)	65×10^{10}	1.5×10^{4}

These formulae lead to similar heat release patterns to those already described; for their application to cycle calculations, see Vol.II, Chapter 8.

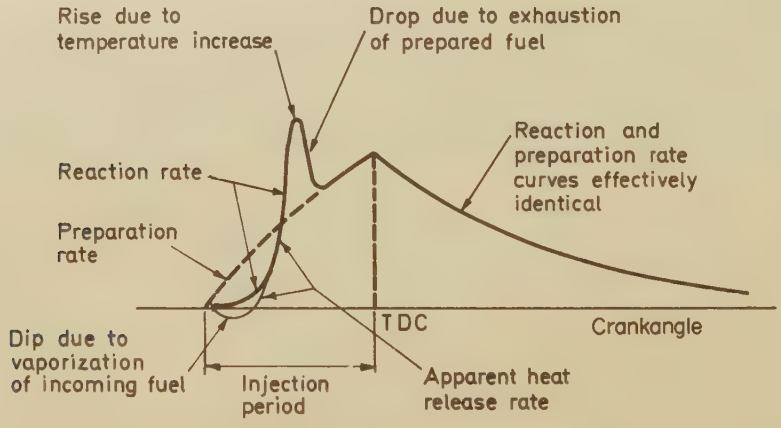

FIG. 4.7. Heat release rates calculated by Whitehouse-Way formulae.

Figure 4.7 illustrates the results of calculations using the Whitehouse-Way preparation and reaction models. In addition accurate experimental data indicates that there is an apparent negative heat release during the early part of the delay period. This is thought to be due to vaporization of the cold fuel. The effect is small and is shown in an exaggerated form on Fig. 4.7.

During the delay period preparation takes place, reaction also occurs but extremely slowly until towards the end of the period,

when it speeds up to produce the rapid heat release which defines the end of delay. This rapid rise is primarily due to the temperature dependence of the reaction rate. This rate then falls as the prepared fuel is consumed. The reaction and preparation rates are effectively identical for the remaining stages of combustion. Typical experimental curves are shown in Fig. 4.8.

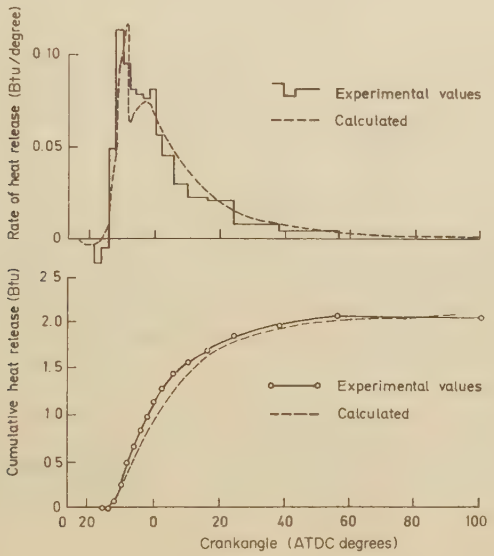

FIG. 4.8. Comparison of experimental and calculated heat release curves.

It should be noted that the meaning of the term "heat release rate" is dependent upon the mathematical model used for cycle calculation. This is dealt with in detail in Vol.II, Chapter 8. The values obtained from experimental pressure diagrams are usually based upon a simple chemical reaction involving perfect combustion of hydrocarbon fuel to carbon dioxide and water vapour. Even so there are too many unknowns, and the calculation cannot be solved except by supplying additional information, i.e. the amount of heat transfer from the cylinder contents to the wall. If this is ignored a net heat release would be obtained which does not indicate the amount of fuel burnt. Usually, therefore, an estimate of heat transfer is made so that the gross amount of fuel burnt can be estimated. In addition the usual analysis calculation assumes uniformity throughout the cylinder contents. Under normal diesel engine conditions this gives weak mixtures and makes any assumption other than perfect combustion an unnecessary and unrewarding refinement. Nonetheless the heat release pattern obtained from a

given cylinder pressure diagram would differ if calculated by different investigators using their particular assumptions. The main pattern, fortunately, does not differ very appreciably because the net heat release is some 80-90% of the total, but it is desirable, nonetheless, to ensure consistency when applying experimental findings.

The assumption of uniformity of conditions throughout the combustion chamber at any given time was at one time so habitual that the obvious heterogeneity of the cylinder contents could almost be forgotten. More recently, however, the inadequacy has proved increasingly irksome for two main reasons.

For performance calculations the single-zone model has been made more complicated and more sophisticated by the methods outlined above or by the accumulation of empirical knowledge, correlations and factors, as by Woschni[8] but even so the methods are dubious when applied to engines where fuel/air mixing on the macroscopic scale is a major factor and, in particular, for such engines under off-design conditions. An example of this would be the quiescent combustion chamber medium speed diesel engine where jet entrainment is of major importance. In this case the single-zone model cannot estimate the effect of the number of holes in the nozzle, yet this is known to be a significant factor to be assessed during development. Other examples may be quoted, e.g. the single-zone model cannot indicate lack of air that occurs while the overall air/fuel ratio is weaker than stoichiometric, so it cannot indicate a likely maximum power, and in particular it cannot calculate the production of noxious substances, such as nitric oxide, carbon monoxide and soot, which are dependent upon local temperatures and chemical concentrations. For this reason multi-zone models are being developed.

4.2.2 Two-zone Combustion Model

The simplest alternative to uniformity is to divide the combustion chamber contents into two parts and assume uniformity within each part. Such two-zone models have been developed both for quiescent combustion chamber engines[9] and for the case of an engine with air swirl.[10]

The problem may be divided into two parts-one of thermodynamics, including combustion, and one of gas dynamics-the mixing of gas from one zone with the other zone.

Thermodynamically the problem is not substantially different from the single-zone model. One zone may be considered to consist of fuel (often ignored chemically and volumetrically) and combustion products (again often simplified to ideal products as in the single-zone case). Combustion formulae may be of the same form as in the single-zone case, although with different values for any empirical constants. The temperature and composition of this zone, which may be called the "burning zone", is obtained from the masses, combustion rates and energy balance and results in a pressure/volume relationship. The other "non-burning zone" consists of that part of the gases originally trapped, mainly pure air, that has not yet been incorporated into the burning zone. The first law of

thermodynamics, the perfect gas equation and the volume/time relationship for the combustion chamber, determine the pressure, temperature and volume relationships.

The two zones must have a combined volume equal to the volume of the combustion chamber and have the same pressure. This cylinder pressure will be the unknown and may be obtained by iteration, being adjusted until the volume equality is satisfied. Heat transfer now has to be calculated for each zone separately, and, as the burning zone temperature is now much higher than the average, radiation effects become somewhat more significant than for the single-zone model.

The thermodynamics of the two-zone model presents no great difficulty once the masses contained in each zone are known. This second problem, that of gas dynamics, is still far from being solved, in a fundamental sense, though some useful advances have been made.

For the simpler case of fuel spraying into quiescent air, the development of the jet of fuel plus air, prior to impingement on the walls, has been investigated by numerous research workers.[11-13] There is also extensive literature about steady state jets.[14, 15] Jets may be compared on a basis of conservation of momentum[16-18] and comparatively simple formulae for the penetration, and so the volume of the jet can be obtained, as given in Vol.II, Chapter 8.

These investigations and semi-empirical formulae have validity up to impingement on the walls provided that combustion does not affect the volume and density of the jet and on the assumption that the jet is a cone of known cone angle and that the shape of the front of the jet is known.

Once the jet has struck the combustion chamber wall the rate of entrainment of fresh air from the non-burning zone into the burning zone becomes even more uncertain, and this usually occurs very early in the injection and combustion process. After impingement the jet will spread sideways until it again impinges-on other walls or on other jets, and it billows back filling the sector of combustion chamber available to it. This process is very complex. The first interaction of jet and wall may be calculated by wall jet theory,[19-20] and such theories have been incorporated in cycle calculations,[10] but this still leaves uncertain the subsequent interaction between wall jet and other surfaces.

Apart from these difficulties the exact limits of the burning (or jet) zone is a matter of some uncertainty. In experimental work the limit is often determined by visibility and its exact position depends upon the sensitivity with which a weak fuel vapour/air mixture can be seen. In the cycle calculation all of the air in the burning zone is assumed to be available for combustion. This will be true in rich areas but not in weak ones. Hence the effective boundary that encloses the air available for combustion does not necessarily coincide with the boundary that encloses all of the fuel that can be seen, still less all of the fuel that exists.

For this reason the use of a simple semi-empirical model may well be justified. Such a model is described below and formulated mathematically in Vol.II, Chapter 8.

4.2.2.1 The Conical/Annular Burning Zone Model

The combustion chamber shape is assumed to be cylindrical, with flat top and bottom, as it would be if the piston were flat-topped. The volume and diameter are the true volume and the cylinder bore diameter, so that the clearance between piston and head is the mean value. The fuel sprays are placed symmetrically. Figure 4.9(a) shows the conditions a little before spray impingement on the walls and Fig. 4.9(b) a little after impingement. In this case the presumably confused and billowing shape of the sprays is replaced by a simple annulus.

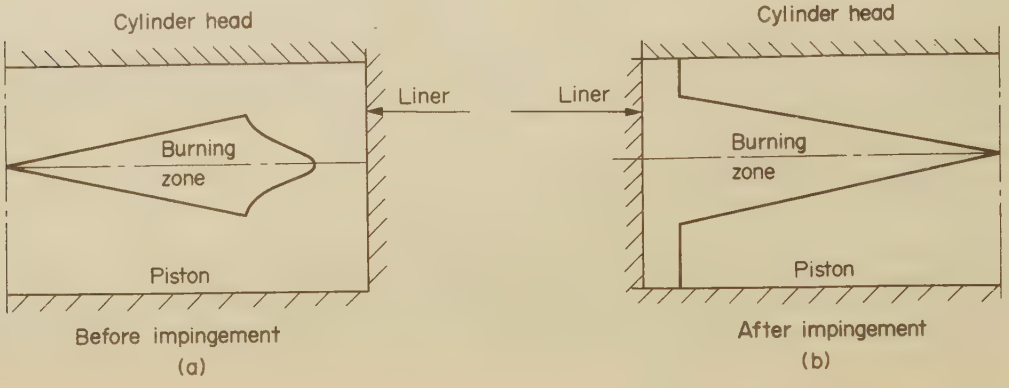

FIG. 4.9. Conical/annular two-zone model for quiescent combustion chamber.

In any step, prior to impingement the entrainment of air into the burning zone is taken as equal to the increase in volume of the jet due to jet penetration, and after impingement as equal to the volume that would pass through the base of the cone, where it meets the annulus, assuming the jet now to be a fully developed steady state jet. This would be determined from the area of cross-section of the cone at that base and the steady state jet velocity profile. After completion of injection the cone becomes a truncated cone, with the inner end moving outwards so that air entrainment becomes the difference between volume flow through base and change in volume at the inner truncation. When the truncation reaches the base entrainment of air into the burning zone would cease, although in the real engine continued mixing at a decaying rate presumably occurs.

In the first published work using this model[9] this was all that was done, with the volumes based upon a jet with a 20^{o} cone angle. However, experimental work with a water rig simulating jet growth in a combustion chamber indicated that the rate of air entrainment after impingement would be greater than calculated from

this theory, but calculations based upon such rig results showed that to make more air available for combustion reduced the agreement between calculation and engine experiment.

Using the idea given earlier that some of the air entrainment into a jet, near its limits, would not be used for combustion owing to the weakness of the fuel/air mixture, a trial and error process led to a reformulation of this model, wherein the burning zone is based upon a cone angle of $17\frac{1}{2}^{o}$ and the momentum conservation/velocity/penetration on a 20^{o} cone angle. In addition the constant K in the preparation formula was made dependent upon droplet size as determined by the Sauter mean diameter of the droplets. However, in a number of cases investigated it was found that the rate of combustion was largely controlled by the rate of air entrainment into the burning zone-large changes in the value of K produced very small changes in the cylinder pressure diagram.

Entrainment after impingement in this later model is assumed to be a constant times the volume passing through the base of the cone. This constant would depend upon the shape of the real combustion chamber, on the number of holes in the nozzle and possibility on other factors. Values for the various constants as used in the work at UMIST and the relevant conditions are as shown in Table 4.4.

TABLE 4.4 Factors Used in Two-zone Quiescent Combustion Chamber Model

Jet cone angle, for penetration calculations (deg.)	20
Jet cone angle, for combustion calculations (deg.)	17.5
Index x	2/3
Index m	0.4
K' (in Arrhenius equation) ($K^{\frac{1}{2}}$/bar s)	87×10^{10}
act (in Arrhenius equation) (K)	1.65×10^{4}

The value of K in the preparation rate equation is based upon the Sauter mean diameter using the equation quoted by Shipinski:[21]

$$SMD = 220(\Delta p)^{-0.458} Q^{0.209} (\nu)^{0.215} \left(\frac{A_{orf}}{A(t)_{eff}} \right),$$

where Δp is the injection pressure, Q is the mass flow rate through the nozzle, ν is the kinematic viscosity of fuel, A_{orf} is the exit orifice area, and $A(t)_{eff}$ is the effective orifice area across which Δp is measured.

Then $$K \alpha \left(\frac{1}{SMD} \right)^{2}.$$

In the cases where this model has been used so far the value of K has been based on an original empirical value and modified on the SMD basis for other cases using the assumption that the values for

Δp and Q are the mean values that would be applicable for a steady rate of injection throughout the injection period. Taking ν and $A_{orf}/A(t)_{eff}$ as constants has reduced the equation to

$$K = 0.085\, N^{0.414}\, M^{1.414}\, p_i^{-1.414}\, h^{-1.414}\, d^{-3.644}$$

where N = RPM, M = mass of fuel injected, grams/cycle/cylinder, p_i = injection period, degrees crankangle, h = number of holes in injector nozzle, d = nozzle hole diameter, mm.

It must be emphasized that all such values are very tentative and are dependent upon the exact formulation of the model used. Research is continuing and values will be modified accordingly. It is also noteworthy that the model is based upon fuel injection at a constant rate.

4.2.2.2 The Swirling-Wall Jet-Burning Zone Model

The two-zone quiescent combustion chamber model is a simple formulation when compared with that needed to deal with the more general case, where air motion, as well as fuel jet motion, has to be incorporated. A number of attempts have been made to consider the effect of air swirl. Adler et al.[22] calculated jet deflection by the use of drag coefficients but did not calculate the volume of jet. Grigg and Syed[23] developed "doughnut" and "conical plume" two-zone models in which air entrainment rates were based on the Schweitzer formula. Whitehouse and Abugheres[10] used jet entrainment to calculate the growth of the jet. As this entrainment is of swirling air, conservation of momentum gives jet deflection, although a limited amount of drag was also incorporated into the model. Drag at the front of the jet was also used in place of a penetration coefficient to allow for the transient nature of the jet. Wall jet theories were used for entrainment after impingement. Apart from these gas dynamic effects the model is basically the same as in the quiescent case.

4.2.3 Multi-zone Combustion Models

Although two-zone models give a zone of comparatively hot gas which might be thought to be appreciably more realistic than the mean value obtained from a single zone, the main advantage is found to be the control on heat release due to oxygen availability (or unavailability) rather than for calculation of chemical species, whether by equilibrium or reaction kinetic methods. For this reason the comparatively simple perfect combustion/heat release calculation is adequate. If chemistry is to be explored so as to obtain emission data, more zones need to be dealt with. This is now being done and a little has been published. [24, 25]

4.2.4 Turbulent Flow Prediction Models

In the two-zone and multi-zone models described above the major problem is to estimate the rate of mixing of the gas outside one zone into that zone. Empirical or semi-empirical estimates or simple assumptions, or guesswork, are used because of the absence of any

known alternative. However, the development of more fundamental methods of predicting mixing and turbulent flow has led to useful applications in other fields including steady flow combustion chambers and the development of jets. These theoretical methods of predicting turbulent flows are under intensive development. Such methods make use of a turbulence model which enables the numerical solution of the basic equations of fluid motion to be carried out using a computer. If heat transfer is involved the solution of the energy equation can be included through the additional assumption of a relation between the turbulent diffusion of momentum and that of heat.

For flows without recirculation, such as in non-separated boundary layers or in ducts, the equations are parabolic, and some success has been achieved with single-turbulence models such as the Prandtl mixing length theory[26]. The mixing length variation is specified empirically to yield the turbulent or eddy diffusivity, which is a function of the local shear rate and the distance from the wall, and this permits the solution of the boundary layer momentum equation.

This model, however, has been shown to be unsuitable for recirculating flows and more complex models have been proposed which involve using further partial differential equations to describe the turbulence characteristics. A promising method uses the equations of turbulence kinetic energy and the rate of dissipation of turbulence energy to obtain an eddy diffusivity which is not a function of local position and shear rate but which includes the influence of the upstream history of the flow.[27] However, the properties of the individual terms of these equations are not fully understood physically and they must be simplified, using empirical information, to enable a solution to be achieved. Applications have been made with some success to recirculating flows in gas turbine combustion chambers and to three-dimensional flows over bluff bodies.

More complex models, involving a large number of partial differential equations to describe the turbulence properties, have been proposed, but it is doubtful whether any gain in reliability results.

A number of workers are now attempting to apply these methods to the problem of combustion in diesel engines.

4.3 COMBUSTION-GENERATED EMISSIONS

A comparison of a typical diesel engine exhaust with a typical petrol engine exhaust, without any of the special measures now often incorporated into petrol engines to meet legislative requirements, used to be favourable to the diesel engine except for particulate matter (smoke). The production of oxides of nitrogen is similar in both engines. This comparison is made in Table 4.5 taken from reference (28).

However, despite this comparison the diesel engine exhaust is often considered even more offensive than is that from the petrol engine because it can be seen and also because it can be smelt.

TABLE 4.5

	Diesel engine	Petrol engine
Particulate matter	0.5 g/m^3	0.01 g/m^3
Carbon monoxide	<0.1% by volume	<10% by volume
Hydrocarbons	< 300 ppm	< 1000 ppm
Oxides of nitrogen	1000-4000 ppm	2000-4000 ppm

Apart from its contribution to atmospheric pollution and the need to meet legislative requirements for general use, the diesel engine owing to the low carbon monoxide of its exhaust—is often used in confined spaces such as mines. This reinforces the need to reduce pollutants even further, particularly the nitric oxide content.

4.3.1 Soot

The presence of soot in the exhaust of the CI engine has been of concern to engine designers, manufacturers, users and the general public for very many years. The maximum output of an engine has often been limited, primarily by the need to avoid a visibly contaminated exhaust. This has been particularly true of the smaller, automotive type engine and has been a factor in favour of the pre-chamber diesel engine which can utilize a greater proportion of the air charge before the exhaust becomes visibly dirty and also is thought to be rather less demanding of good maintenance of the fuel injection equipment than is the single chamber direct injection engine.

A dirty exhaust is usually one with black smoke, or soot, from the combustion process in the engine. The exact mechanisms by which soot is formed may be unknown but a general picture has been put forward in a number of published papers[29-31] This is summarized below.

In the CI engine soot is formed on the fuel rich side of the combustion zone of a diffusion flame by the pyrolysis of hydrocarbons. The term pyrolysis can cover a multitude of reactions, but molecular splitting, or cracking, is prevalent at high temperatures while polymerization and molecular addition are favoured at lower temperatures. Figure 4.10 shows a simplified scheme of such reactions as suggested by Broome and Khan.

The type of carbon produced in the diesel engine is dry, greyish carbon formed in the vapour phase at high temperatures. Fast reactions at temperatures of 2000-3500°K, as found in turbulent diffusive flames in diesel engines, involve decomposition of the fuel molecule, then nucleation or formation of precursors and then formation of small soot particles which aggregate to form larger particles either by adding polyacetylenes or other hydrocarbons or by agglomeration. After leaving these hottest zones the soot particles can grow by coagulation. These soot particles can react with oxygen, or other products of combustion, so the final rate of soot release is

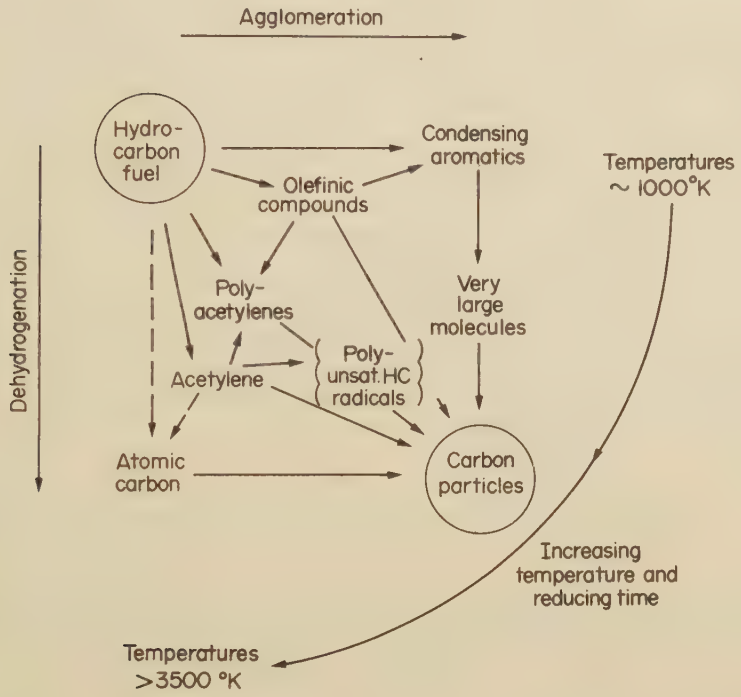

FIG. 4.10. Simplified scheme of reactions producing soot. (From Broome and Khan,[30] by courtesy of the Institution of Mechanical Engineers.)

the difference between rate of formation and rate of combustion. Figure 4.11 shows diagrammatically how the quantity of soot in the combustion chamber may be expected to vary with time, primarily being dependent upon the rate of combustion of fuel or the heat release rate.

It may be noted that even when the diesel exhaust appears black the carbon present as soot is a very small proportion of the carbon in the fuel—of the order of 1% or less.

While the normal visible exhaust in a diesel engine is due to black smoke from carbon, as above, the exhaust may be white or blue under abnormal conditions that result in unburnt fuel or lubricating oil passing through the engine. This may occur if temperatures are too low for adequate combustion as at starting at low ambient temperatures when some or all cylinders may not reach ignition temperature. Continuous operation for lengthy periods at very low loads may also result in lubricating oil passing through to the exhaust manifold, particularly if one or more cylinders has no injection of fuel due to mistuning. Such oil will vaporize when load is increased and be discharged from the exhaust as a blue smoke, perhaps including actual drops of oil. Such behaviour is, however, not expected in normal operation and will not be dealt with further.

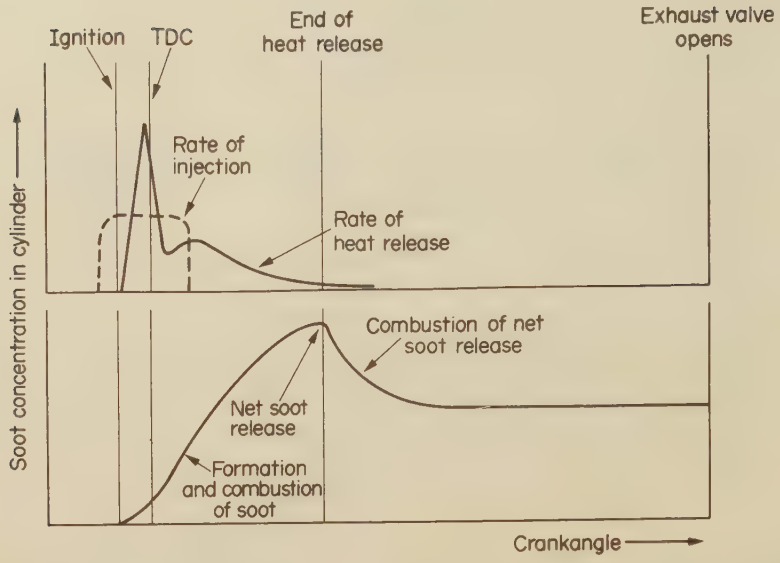

FIG. 4.11. Variation of quantity of soot with time. (From Khan,[29] by courtesy of the Institution of Mechanical Engineers.)

4.3.2 Gaseous Pollutants

As may be seen from Table 4.5 the diesel engine may be expected to produce less gaseous pollutants than does the unmodified petrol engine, but the amounts are not negligible. There is no reason to believe that the basic reaction kinetics involved are different from those detailed in Chapter 5 for SI engine calculations; the differences must be due to the differences in physical processes which affect the processes of combustion. That is, combustion in the diesel engine is primarily controlled by the mixing process, whereas the conventional SI engine relies on flame propagation through a premixed mixture of fuel and air.

The formation of nitric oxide may therefore be calculated by one of the modified Zeldovich mechanisms (see page 126). It is expected to be formed in or near to the mixing zone between air and fuel vapour where combustion will take place and temperatures will be high. As combustion is generally limited by the rate of supply of oxygen, the nitric oxide formation will be similarly somewhat inhibited-though a stoichiometric combustion zone is generally assumed as oxygen would be reacted with before it could penetrate into the rich fuel in the core and fuel vapour would be reacted before it could penetrate into the oxygen rich zones surrounding the flame. Experience with SI engines with homogeneous charges has shown that maximum nitric oxide formation occurs with a somewhat weak charge (see Fig. 5.17) so the diffusion flame process may explain why the CI engine forms slightly less nitric oxide than does

the typical SI engine. However, an exception to this process must be made for the combustion of the fuel prepared during the delay period. This fuel, which produces the first peak of the heat release diagram, burns as a premixed flame and consequently will include a range of mixtures including the range for maximum nitric oxide production. It has therefore been claimed that the proportion of premixed combustion should be small if nitric oxide emissions are to be minimized. As premixed combustion produces little soot it can also be claimed that any reduction in it will tend to increase soot formation.

Usually the diesel engine produces very much less carbon monoxide than does the SI engine, and the use of rate-controlled reactions for calculation purposes—although no doubt theoretically ideal—are unlikely to be of practical value until the physical mixing processes are better understood. Equilibrium thermodynamics are claimed to be reasonably adequate for some calculations[32].

REFERENCES

1. Wolfer, H.H., Ignition lag in the diesel engine, VDI Forshung 392 (1938).

2. Whitehouse, N.D. and Way, R.J.B., Rate of heat release in diesel engines and its correlation with fuel injection data, Proc. Instn. Mech. Engrs. 184, Part 3J, 17 (1969-70).

3. Whitehouse, N.D. and Way, R.J.B., A simple method for the calculation of heat release rates in diesel engines based on the fuel injection rate, SAE Paper 710134 (1971).

4. Lyn, W.T. and Valdamis, E., The application of high speed Schlieren photography to diesel combustion research, Jl. Photogr. Sci. 10, 74 (1962).

5. Austen, A.E.W. and Lyn, W.T., Relation between fuel injection and heat release in a direct-injection engine and the nature of the combustion processes, Proc. Instn. Mech. Engrs. (AD) 1, 47 (1960-1).

6. Austen, A.E.W. and Lyn, W.T., The application of heat release analysis to engine combustion study, 1067, CIMAC (1962).

7. Spalding, D.B., Some Fundamentals of Combustion, Butterworths Scientific Publications, 1955.

8. Woschni, G. and Anisits, F., Experimental investigation and mathematical representation of the rate of heat release in diesel engines dependent on engine operating conditions, SAE Paper 740086 (1974).

9. Whitehouse, N.D. and Sareen, B.K., Prediction of heat release in a quiescent chamber diesel allowing for fuel air mixing, SAE Paper 740084 (1974).

10. Whitehouse, N.D. and Abughres, S.M., Calculation of fuel/air mixing in a diesel engine with swirl for the purpose of heat release prediction, in Combustion in Engines, p.147, Institution of Mechanical Engineers, London and New York, 1975.

11. Schweitzer, P.H., Penetration of oil sprays, Pennsylvania State Coll. Bull. No.46 (1937).

12. Parks, M.V., Polanski, C. and Roye, R., Penetration of diesel fuel sprays in gases, SAE, Paper 660747 (1966).

13. Taylor, D.H. and Walsham, B.E., Combustion processes in a medium speed diesel engine, Proc. Instn. Mech. Engrs., 184, Part 3J, 67 (1969-70).

14. Abramovitch, G.N., The Theory of Turbulent Jets, MIT Press, Cambridge, Massachusetts, 1963.

15. Schlichting, H., Boundary Layer Theory, McGraw-Hill, New York, 1960.

16. Dent, J.C., A basis for the comparison of various experimental methods for studying spray penetration, SAE, Paper 710571 (1971).

17. Hay, N. and Jones, P.L., Comparison of the various correlations for spray penetration, SAE, Paper 720776 (1972).

18. Williams, T.J., Parameters for correlations of penetration results for diesel fuel sprays, Proc. Instn. Mech. Engrs. 187, 771 (1973).

19. Hycak, P. and Lee, D.T., Evaluation of maximum velocity decay in wall jets, Jl. Spacecraft Rockets 7, No. 5, (1970).

20. Sridhar, K. and Tu, P.K.C., Experimental investigations of curvature effects on turbulent wall jets, Aeronaut. Soc. 73, No. 707 (1969).

21. Shipinski, J., Myers, P.S. and Uyehara, O.A., A spray droplet model for diesel combustion, Proc. Instn. Mech. Engrs. 184, Part 3J, 28 (1969-70).

22. Adler, D. and Lyn, W.T., The evaporation and mixing of a liquid fuel spray in a diesel air swirl, Proc. Instn. Mech. Engrs. 184, Part 3J, 171 (1969-70).

23. Grigg, J.C. and Syed, M.H., The problem of predicting rate of heat release in diesel engines, Proc. Instn. Mech. Engrs. 184, Part 3J, 192 (1969-70).

24. Shahed, S.M., Chiu, W.S. and Lyn, W.T., A mathematical model of diesel combustion, in Combustion in Engines, p.119, Institution of Mechanical Engineers, 1975.

25. Hodgetts, D. and Shroff, H.D., More on the formation of nitric oxide in a diesel engine, in Combustion in Engines, Institution of Mechanical Engineers, 1975.

26. Pantankar, S.V. and Spalding, D.B., Heat and Mass Transfer in Boundary Layers, 2nd edn., Intertext, London, 1970.

27. Launder, B.E. and Spalding, D.B., Mathematical Models of Turbulence, Academic Press, London, 1972.

28. Jellings, W., An Elementary Approach to the Computation of I.C. Engine Exhaust Gas Emissions, UMIST Internal Report, 1971.

29. Khan, I.M., Formation and combustion of carbon in a diesel engine, Proc. Instn. Mech. Engrs., 184, Part 3J, 36 (1969-70).

30. Broome, D. and Khan, I.M., The mechanisms of soot release from combustion of hydrocarbon fuels with particular reference to the diesel engine. Conference on Air Pollution Control in Transport Engines, Proc. Instn. Mech. Engrs., 185 (1971).

31. Khan, I.M., Greeves, G. and Probert, D.M., Prediction of soot and nitric oxide concentrations in diesel engine exhaust. Conference on Air Pollution Control in Transport Engines, Proc. Instn. Mech. Engrs., 205 (1971).

32. Baluswamy, N., Spatial and temporal distribution of gaseous pollutants in a diesel engine combustion chamber, PhD Thesis UMIST, 1976.

33. Lyn, W.T., The spectrum of diesel combustion research, Proc. Instn. Mech. Engrs., 184, Part 3J, 1 (1969-70).

Chapter 5

Combustion in Spark Ignition Engines

Notation

ff	flame factor	u_t	turbulent flame speed
p	pressure	α	crankangle
u_ℓ	laminar flame speed	ϕ	equivalence ratio

The combustion process in a spark ignition engine is complex. The process depends to a great extent on the engine conditions. After a great deal of research we are now obtaining a clearer understanding of the processes involved. Before describing these, a few definitions will be presented which will clarify the later discussions.

5.1 DEFINITIONS OF CONTROLLED, UNCONTROLLED, NORMAL AND ABNORMAL COMBUSTION

We distinguish between controlled combustion when combustion is initiated by a spark, and uncontrolled combustion when combustion is initiated by a hot spot. There is a third type of combustion, called abnormal combustion, in which the fuel/air mixture spontaneously ignites without an ignition source, i.e. auto-ignition.

Under normal combustion conditions the combustion is controlled and this is the designer's objective. Abnormal combustion can take place after normal combustion has been initiated in a controlled manner. Abnormal combustion will occur in the unburnt gas zone ahead of the flame initiated by the spark and causes "engine knock". Uncontrolled combustion is associated with pre-ignition and running-on.

We shall first discuss normal combustion, then abnormal combustion and, finally, uncontrolled combustion. There has been extensive published work on engine combustion; the interested reader is recommended to study the source papers for a detailed understanding. We shall only review some of the work highlighting some of the fundamental results of recent research. The source literature referred to in the text are the papers by Downs and his colleagues on engine research excellently described in the two most recent editions of Sir Harry Ricardo's book[1,2]. The fundamental chemistry of combustion reviewed by Minkoff and Tipper,[3] has been used to describe the oxidation processes.

5.2 NORMAL COMBUSTION

Towards the end of the compression stroke the cylinder contains a more or less homogeneous mixture of fuel vapour and air. A spark is fired, and as it passes from one electrode to the other it leaves a thin thread of flame. Combustion spreads to the envelope of the mixture containing the thread at a rate depending primarily on the temperature of the flame front and secondarily on the temperature and density of the surrounding envelope. As the flame front expands it travels across the chamber until finally the whole of the mixture is engulfed. Depending on the degree of turbulence in the cylinder, the flame front wrinkles and perhaps breaks into eddies which speed up the process.

In a typical indicator diagram taken in the cylinder we should distinguish two stages in the combustion process (Fig. 5.1). The first stage (AB) corresponds to the time for the formation of the self-propagating nucleus of the flame, and the second stage (BC) to the propagation of the flame throughout the combustion chamber.

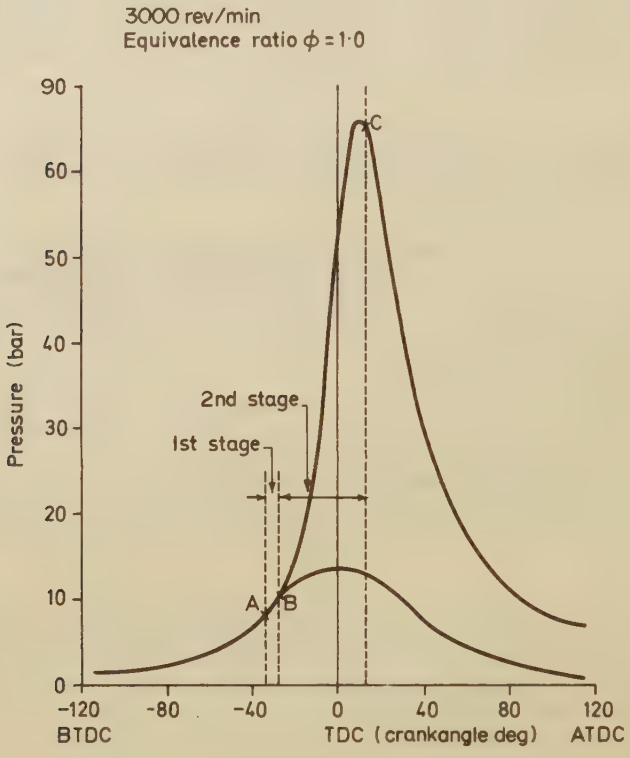

FIG. 5.1. Indicator diagram showing two stages of combustion in a spark ignition engine.

The first stage (AB) is mainly a chemical process and depends on the nature of the fuel, on the temperature and pressure of the fuel/air mixture, the concentration of residuals from the previous cycle present in the cylinder and the chemical reaction rate. It is also influenced by local turbulence.

In Fig. 5.2 the time for the formation of a nucleus some 0.1% of the cylinder volume is shown for various flame temperatures based on calculations carried out by the authors for a commercial gasolene engine with a representative hydrocarbon fuel. The corresponding temperature variation with air/fuel ratio and variation in time with air/fuel ratio are shown in Fig. 5.3. Details of the calculation

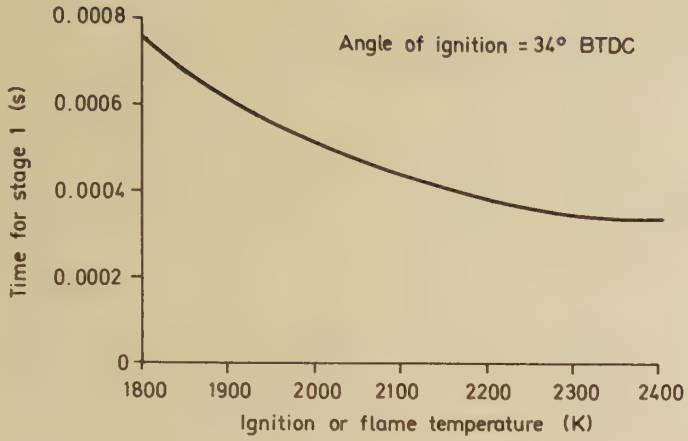

FIG. 5.2. Approximate relationship between flame (ignition) temperature and time for stage 1 (AB).

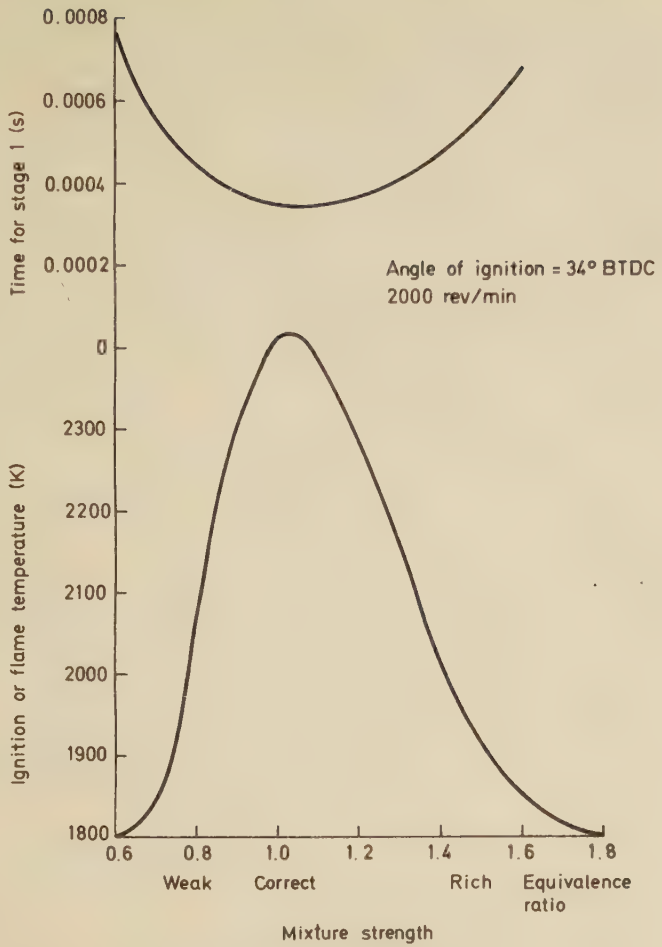

FIG. 5.3. Approximate relationship between mixture flame temperature (ignition temperature) and duration of stage 1 (AB).

procedures will be outlined later. It will be seen from Fig. 5.3 that the minimum period for the first stage of combustion (AB) lies slightly on the rich side, and this normally corresponds to maximum power output. As the mixture is made either richer or weaker, the time for the first stage increases.

The second stage of combustion (BC) corresponds to the propagation of the flame from the initial nucleus to the consumption of all the fuel. This is both a chemical and physical process and depends on the chemical composition, the prevailing temperatures and pressures and the degree of turbulence in the cylinder. Methods for calculating this stage of the combustion process are somewhat empirical and will be discussed in another chapter. Using these methods it is possible to establish the influence of mixing strength and engine speed on stage 2. Some typical results are shown in Fig. 5.4.

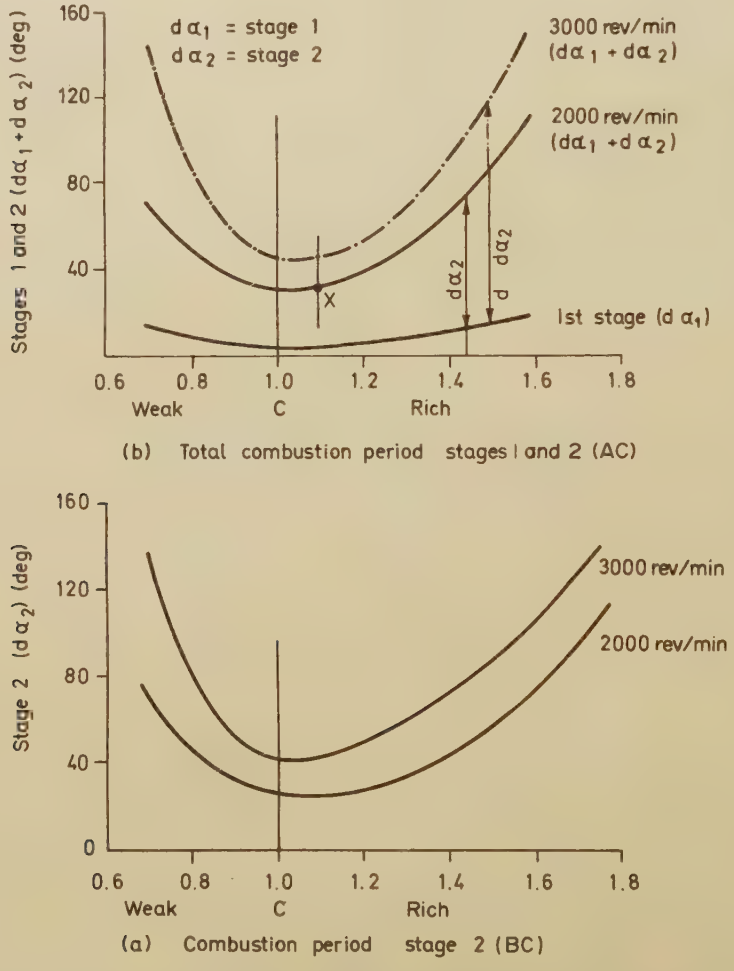

FIG. 5.4. Approximate relationship between combustion periods, mixture strength and engine speed.

In Fig. 5.4(a) the crankangle $d\alpha_2$ in degrees for stage 2 is shown for two engine speeds. For a mixture strength from 0.8-1.2 equivalence the time in degrees is about constant, but for further weakness or richness time for stage 2 increases. This is due to the chemico-thermodynamic affects (pressure and temperature). The total combustion time for stages 1 and 2 in crankangle degrees is shown in Fig. 5.4(b). Here we observe that the total time in degrees increases, with increase in richness and increase in weakness about a certain equivalence and increases with engine speed. The maximum duration for stable combustion (to avoid flame cut out) is about 50^{o} crankangle. The maximum time available for combustion is also limited by the exhaust valve opening. It will be seen from Fig. 5.4(b) that there is therefore a limit to the operating range for the mixture strength and that this is reduced with increasing speed. The end of stage 2 in a well-designed engine is close to the point of maximum cylinder pressure, and this might be used on a test-bed to adjust the engine timing for optimum efficiency. Accepting this criterion it is found in practice that for optimum performance and efficiency the maximum pressure should occur between $5\text{-}20^{o}$ after top dead centre. If we set the ignition timing to obtain maximum efficiency at X in Fig. 5.4(b), it will be seen that as we vary the mixture strength it will be necessary to advance the ignition timing to obtain the same location for the maximum pressure. Similarly, if we increase the engine speed we must also advance the ignition time. In practice the angle corresponding to the maximum pressure does not remain constant with ignition advance and drifts with the advance timing. The magnitude of the maximum pressure varies with the ignition timing. As the ignition time is advanced, the pressure and temperature at the spark time are reduced, but, on the other hand, more heat is released before top dead centre. The combined effect of the compression conditions and the heat release is to raise the maximum pressure as the ignition is advanced until at some point the maximum pressure reaches a maximum value and then decreases with further advance in the ignition timing. As the ignition is advanced there will be an increase in efficiency due to the increase in the effective expansion stroke until a maximum is reached when further increase in advance produces a reduction in efficiency due to increase in heat loss and reduction in effective expansion (see Chapter 2). The trends just described are clearly seen in Fig. 5.5 drawn from results presented by Ricardo.[1] Here we should note that for a given mixture strength and engine volumetric efficiency the thermal efficiency is directly proportioned to the indicated power (i.m.e.p.).

The ignition timing and the mixture strength influence the level of exhaust emissions; these will be described in section 5.6.

In multi-cylinder engines with single carburettors it is difficult to ensure a uniform distribution of fuel between cylinders, and the weak mixture limit is critical if misfiring is not to occur. In practice, therefore, the ignition advance is limited to ensure that all cylinders fire; it follows that the air/fuel ratio is also limited at the weak end of the range. The ignition timing is also controlled by the knock limit, as explained in section 5.3.

In our discussions so far we have implied a more or less homogeneous fuel vapour/air mixture in the cylinder which is ignited

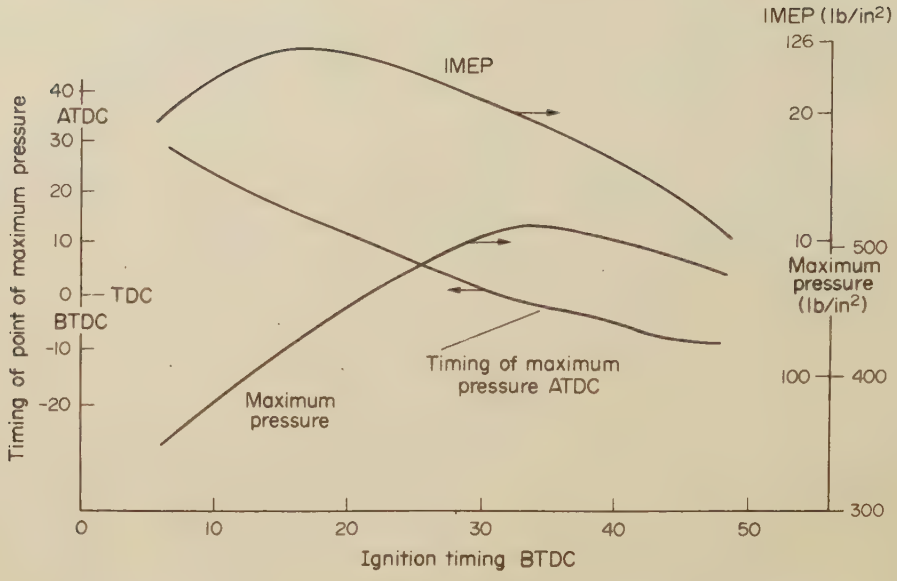

FIG. 5.5. Influence of ignition advance on maximum pressure and power.

by a spark. If the mixture was completely homogeneous there would be a uniform air/fuel ratio and the combustion process would be more repetitive from cycle to cycle. In practice, however, we observe that no two successive cycles are the same. This is manifest in two forms: first, fluctuations in maximum pressure, and second, fluctuations in "heat" released with time. This phenomenon is called cyclic dispersion. We know that cyclic dispersion can be reduced by control of the mixture movement and the addition of more than one spark. Analysis of indicator diagrams indicates that cyclic dispersion is associated with the period immediately after the spark is ignited. It must be affected by micro-heterogeneity of the mixture which possibly affects the oxidation process. Whilst the physical parameters which influence cyclic dispersion are fairly well known, the detailed fundamental processes are still not clear. The phenomenon may be very serious in gas engines where cyclic irregularity might affect electrical synchronization in power stations.

We have seen that the mixture strength and engine speed influence the combustion process under normal combustion. Another important variable is the compression ratio. From the theoretical cycle analysis we know that increasing the compression ratio increases the thermal efficiency and hence, for a given mixture strength, the engine power. Engine tests confirm these predictions up to a certain critical compression ratio when it is observed that there is a slight fall off in power. This is accompanied by an audible knock from the combustion chamber. Increase in compression ratio above this critical value produces a further fall in power with increased intensity of knock. Sustained running above the critical compression ratio might eventually produce uncontrolled combustion with dramatic loss in power.

The audible knock in the combustion chamber is due to spontaneous ignition in part of the charge or abnormal combustion. In the early development of the gasolene engine the most formidable hurdle to its progress was this phenomenon, and much research was directed to its understanding and elimination. It is so important in our understanding of the combustion process in spark ignition engines that we propose to devote a section to describing the phenomenon and the factors which influence it.

5.3 ABNORMAL COMBUSTION-ENGINE KNOCK

In normal combustion after the flame is ignited at the spark the flame front travels in a fairly uniform manner across the chamber compressing the unburnt gas before it. The gas ahead of the flame is called the end gas. The end gas receives heat due to compression by expanding gases and by radiation from the advancing flame front. Under abnormal combustion conditions the end gas spontaneously ignites ahead of the flame front. Shortly after the spontaneous ignition of the end gas a characteristic high pitch "knocking" sound is heard: this is called "knock". Until recently it was generally considered that the knocking sound was due to the impingement of a shock wave at the chamber wall, the shock wave being initiated by the spontaneous ignition source in the end gas. Evidence of the impingement of a shock wave is surface pitting at the wall, associated with the breakdown of the boundary layer, together with an increase heat transfer rate at the wall, the latter producing a slight drop in engine power. More recently the characteristic noise has been considered to be due to the acoustic vibration of the combustion chamber contents at the appropriate resonant frequency.

Under certain conditions the knock intensity can create hot spots in the cylinder which can cause pre-ignition of the fuel/air mixture before the spark timing. This may cause catastrophic loss in power and possible mechanical failure, particularly in a multi-cylinder engine when one cylinder might be knocking and the other running normally.

Engine tests show that the tendency to knock is related to the fuel composition, the compression ratio, the inlet temperature, the mixture strength, the ignition timing, the throttle setting and the engine speed.

Because knock limits the engine performance, considerable research has been directed to an understanding of the fundamental factors that cause knock and the methods for eliminating the phenomena. It is only proposed to briefly outline some of the results based on this work. The source references are the texts by Ricardo and Hempson,[2] Lewis and von Elbe[4] and Minkoff and Tipper,[3] together with papers by Downs and his colleagues listed in Ricardo and Hempson[2]. References (3) and (4) also have extensive bibliographies.

Before examining the conditions in the engine cylinder it is proposed briefly to review some fundamental research on combustion that will lead to an understanding of the engine phenomena.

5.3.1 Combustion Research in Hydrocarbon-Oxygen Mixtures

In order to understand the reactions in the end gas we must examine the fundamental oxidation reactions in hydrocarbon-oxygen mixtures. Studies of these reactions may be made in static or continuous flow apparatus or in rapid compression machines or in motored engines. The simplest experiments are in static and continuous flow apparatus. The phenomena discovered in these experiments have been confirmed in rapid compression machines and motored engines; we shall describe the static experiments. In these experiments the hydrocarbon-oxygen mixture is admitted to a heated quartz or silica vessel at a fixed temperature and pressure and the reactions studied both visually and quantitatively. From these experiments the pressure and temperature for auto-ignition of the mixture can be observed. An ignition diagram can be constructed from which the auto-ignition pressure/temperature characteristics for the mixture can be determined. Such a diagram is shown for a 1:1 propane-oxygen mixture in a silica vessel (Fig. 5.6).

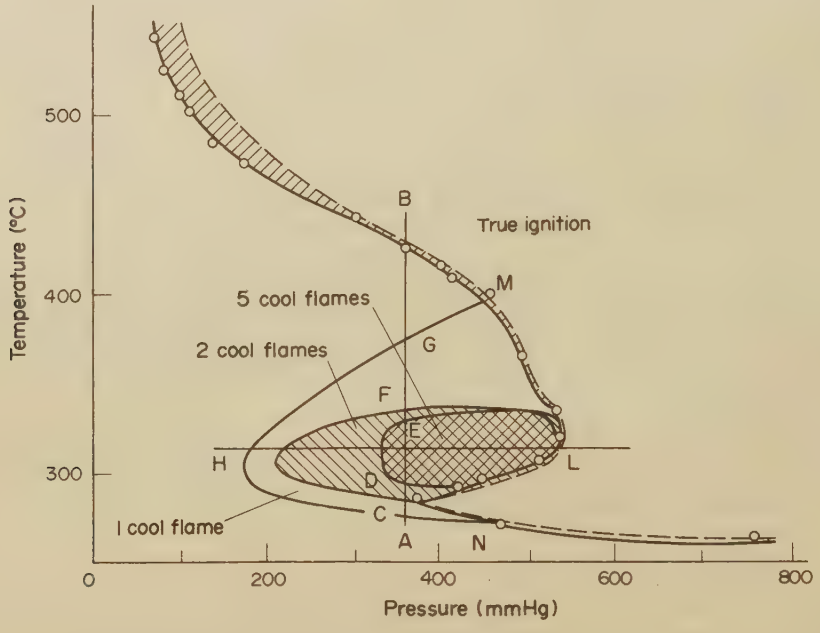

FIG. 5.6. Spontaneous ignition temperatures of a $C_3H_8 + O_2$ mixture. (From Hewitt and Thornes,[5] by courtesy of the Chemical Society.)

These results were obtained by Hewitt and Thornes.[5] We shall examine the conditions along a constant pressure line (AB) corresponding to a pressure of 360 mm. Below 275°C slow oxidation reactions are observed; between 275-285°C a faint luminosity develops after several minutes and remains until the reaction is nearly complete. At 290°C (point A) the luminosity is followed by a pale blue "cool" flame of low intensity which starts near the

centre of the vessel and spreads outwards giving rise to a pressure pulse. After the passage of the flame, the luminosity persists for several seconds. Between 300°C (D) and 340°C (E) the luminosity appears immediately on filling the vessel and is succeeded by three to five "cool" flames at intervals of several seconds, each of which traverses the whole vessel before its extinction gives rise to a pressure pulse. Between 340°C (E) and 345°C (F) only two cool flames, and between 345°C (F) and 385°C (G) only one cool flame, are observed. The intensity of the cool flames is increased as the number diminishes. Above 350°C the single cool flame become less intense as the reaction temperature is raised; on the other hand, the general luminosity increases in intensity until at 425°C (B) a bright blue flame appears. At a slightly higher temperature this changes to the characteristic yellow flame associated with true ignition.

Outside the cool flame and ignition region the chemical reactions proceed at a rate corresponding to the pressure and temperature.

In traversing the cool flame region to the true ignition point there may be several seconds delay between the appearance of a cool flame and true ignition at the point L, e.g. along an isothermal HL. The region NHM is called the cool flame peninsula. In this experiment the hydrocarbon-oxygen reaction exhibited two types of auto-ignition, a low temperature ignition-cool flames and a high temperature ignition-normal flames. To distinguish between the two types of ignition the region below 350-400°C is called the low temperature region and above 350-400°C the high temperature region. The chemical mechanism for the reactions in the two regions is different. Not all hydrocarbon-oxygen mixtures exhibit the two types of ignition and not all mixtures which exhibit cool flames generate five cool flames; the number varies from one to five. Hydrocarbon-oxygen mixtures with low temperature and high temperature ignition regions include the higher paraffinics, such as n-heptane and iso-octane, to which we shall refer to later.

When a hydrocarbon-oxygen mixture has only one ignition temperature at a given pressure this temperature is in the high temperature region. The ignition curves for these mixtures are monotonic functions of pressure. Typical hydrocarbons exhibiting high temperature ignition only are benzene and methane whose ignition curves are shown in Fig. 5.7, together with the ignition curves for typical hydrocarbons n-heptane and iso-octane. Cool flames are not observed for methane and benzene.

In hydrocarbon-oxygen mixtures the blue cool flames are identified with the fluorescence spectrum of formaldehyde. Aldehydes are always present in cool flame regions. The concentrations vary with time reaching a maximum on the appearance of the cool flame (Fig. 5.8).

Significant quantities of peroxide are also present in the reacting mixture reaching a maximum just before the appearance of the cool flame and then dropping as shown in Fig. 5.8. In some experiments[7] the drop in peroxide concentration is not observed.

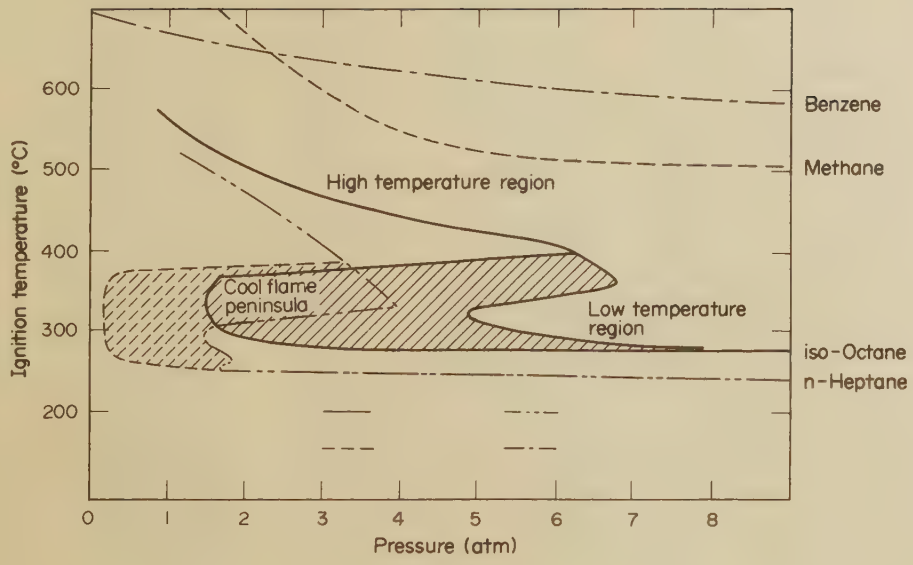

FIG. 5.7. Typical ignition temperature pressure curves.

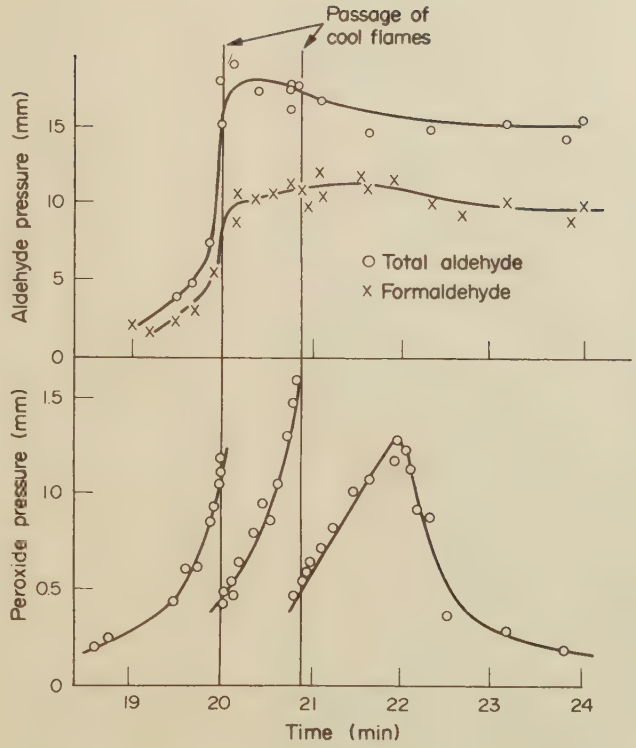

FIG. 5.8. Variation of peroxide and aldehyde concentration during cool flame oxidation of butanone at 283°C. (From Bardwell and Hinshelwood[6] by courtesy of the Royal Society.)

For hydrocarbon-oxygen mixtures not exhibiting cool flames the concentrations of aldehydes and peroxides are very much lower than in cool flame reactions.

The extinction of the cool flame is followed by a pressure pulse (Fig. 5.9).

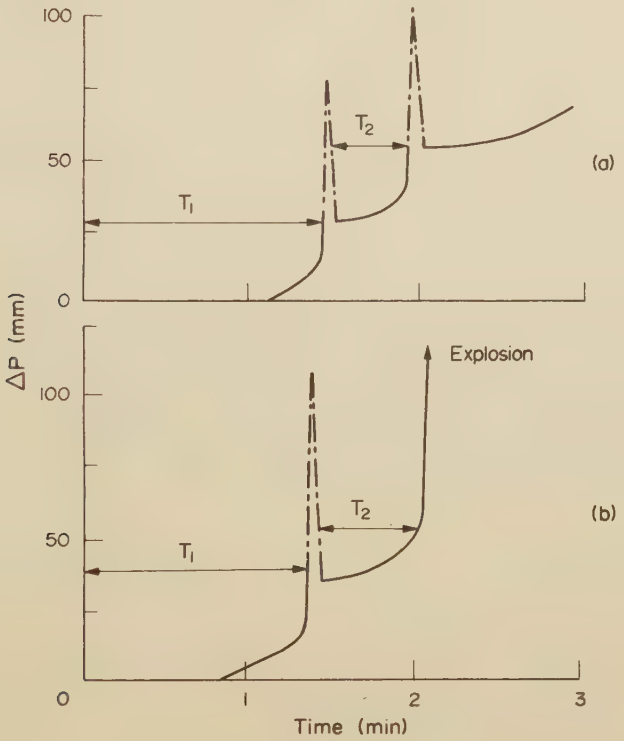

FIG. 5.9. Pressure time record during cool flames of butanone at 290°C. (a) Two cool flames; (b) one cool flame followed by ignition. (From Bardwell and Hinshelwood[6], by courtesy of the Royal Society.

The time intervals between the start of a reaction and the appearance of cool flames and the period between cool flames and normal ignition are called induction periods. In Fig. 5.9(b) we can identify two periods-the first period T_1 up to the appearance of the cool flame and the second period T_2 from the appearance of the cool flame to the appearance of a normal flame explosion. This is a two-stage combustion process and the two separate periods have significance in our discussion later on knock. For high temperature ignition, with no cool flames, there is only one induction period.

We can therefore summarize the phenomena observed in laboratory experiments on the oxidation of hydrocarbon mixtures.

We have observed that there are two types of auto-ignition—a low temperature ignition and a high temperature ignition. Some hydrocarbon-oxygen mixtures exhibit both types of ignition; others only high temperature ignition. In the case of hydrocarbon-oxygen mixture with low and high temperature ignition there are significant concentrations of aldehydes and peroxides which peak just before the low temperature ignition (cool flame). For mixtures with high temperature ignition only, the concentrations of aldehydes and peroxides are small and almost insignificant in some cases.

The presence of the aldehydes and peroxides in the end gas in the engine cylinder are important clues in identifying the mechanism of knock, so we shall now review the possible mechanism of their appearance in a very simple manner. A typical hydrocarbon which knocks under certain conditions in an engine is heptane C_7H_{16}. The overall combustion reaction for a heptane-oxygen mixture is

$$C_7H_{16} + 11O_2 \longrightarrow 7CO_2 + 8H_2O.$$

We can picture this as a reaction between one molecule of heptane and eleven molecules of oxygen. Such a reaction is called a twelve-body reaction. The collision between the twelve molecules will not form the seven molecules of carbon dioxide and eight molecules of water vapour in one step, it must take place by successive collision of oxygen molecules with the heptane molecule degrading the heptane molecule to intermediate bodies before the formation of the final products carbon dioxide and water vapour. This is called a chain process.

Although the complete process is not known we can suggest possible intermediates. Downs[9] and Wheeler[8] have suggested the following reactions.

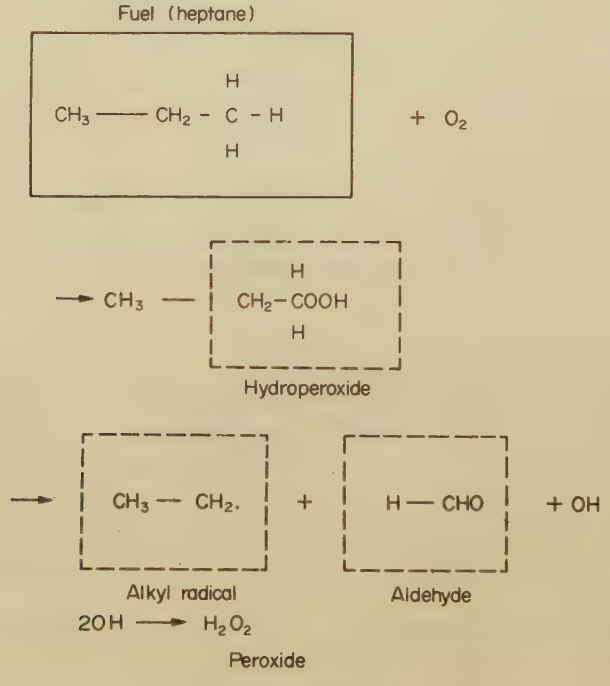

In this model we see that hydroperoxide is produced in the first stage of the reaction and aldehyde in the subsequent stages. Thus by this relatively simple model we can identify the presence of aldehydes and peroxides in the oxidation processes.

Our description of the oxidation processes has been based on laboratory tests in bench-type experiments under static conditions. Experiments under conditions more close to engine conditions such as in rapid compression machines confirm the same processes occurring in hydrocarbon-oxygen reactions. We are therefore in a position to use these results in assessing the processes occurring in engines. We shall now turn to engine research.

5.3.2 Engine Research

We have already noted that knock is due to spontaneous or auto-ignition of the end gas. The bench experiments showed that there are two types of auto-ignition-a low temperature ignition in which cool flames are observed with significant aldehyde and peroxide concentrations, and a high temperature ignition in which low aldehyde and peroxide concentrations are observed. The engine experiments have been devised to establish which form of ignition takes place in the end gas in the engine cylinder. It would be impossible to observe cool flames in the end gas under power conditions because the normal combustion process would generate an intense yellow flame. Therefore, under power conditions gas sampling only is used. To ascertain the relationship between the aldehyde and peroxide concentrations and cool flames, motoring tests are carried out. In these tests quartz windows are fitted and the cylinder contents are observed visually and photometrically.

Downs and Wheeler[8] have reported extensive experiments. By sampling in the region of the end gas during the combustion period they were able to measure the variation of the aldehyde and peroxide concentrations with crankangle. Some typical results are shown in Figs. 5.10 and 5.11. In Fig. 5.10 the experiments were carried out under power with iso-octane with compression ratios well below the knock limit to a compression ratio giving heavy "knock". These curves show that a rise in pre-flame peroxide concentration before top dead centre is followed by a higher peak value just before the flame. With increase of compression ratio there is an earlier rise in peroxide concentration and a much higher peak value. There is a point of inflexion just after top dead centre. Downs suggests that the shape of the curves are two-stage in nature. In passing we might note that the addition of enough tetraethyl lead to suppress knock lowers the peroxide concentration considerably. We will refer to this result shortly.

The aldehyde concentration starts to increase at about top dead centre and the curves show a smooth rise up to the time of flame arrival, achieving a peak concentration some twenty times greater than the peak peroxide value. The effect of increasing the compression ratio on the aldehyde concentration parallels the effect on the peroxide curve. Tetraethyl lead decreases the aldehyde concentration.

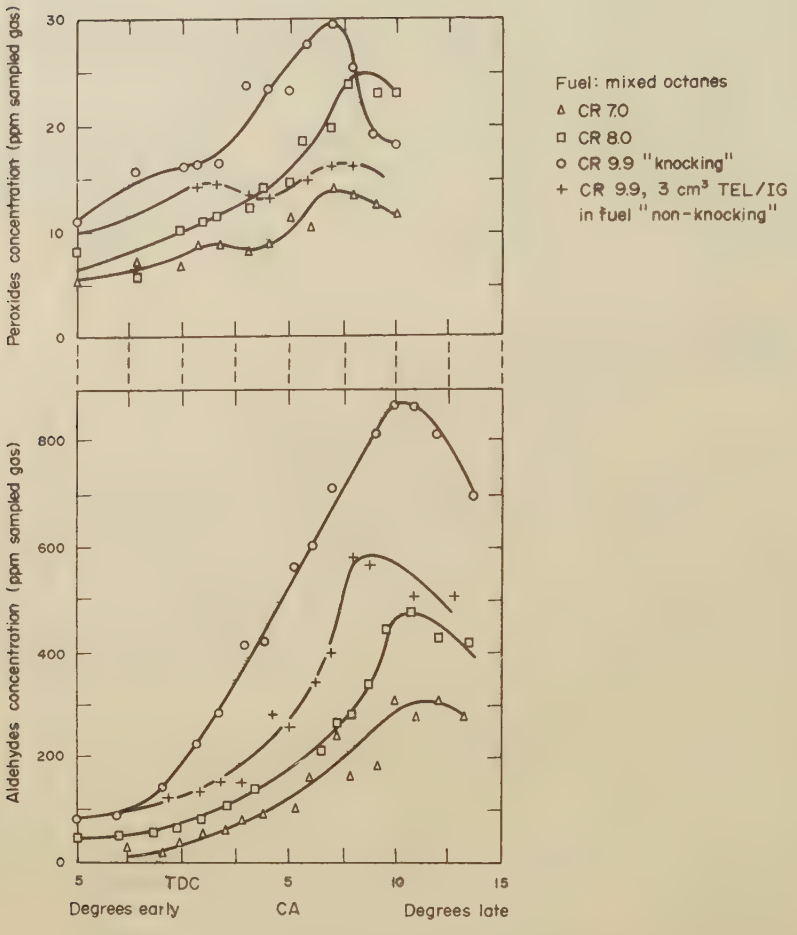

FIG. 5.10. Peroxide and aldehyde concentrations in gases sampled from the engine at various crankangle. (From Downs and Wheeler,[8] by courtesy of the Institution of Mechanical Engineers.

In Fig. 5.11 the experiments were carried out under power with methane as a fuel. It will be seen that the results are somewhat different from the iso-octane results. Raising the compression ratio to cause knock results in a peak in the peroxide curve; this peak is eliminated by the addition of tetraethyl lead to the fuel. There is not a great deal of difference between the knocking and non-knocking aldehyde curves. Both the peroxide and aldehyde concentrations were well below those obtained with iso-octane under comparable conditions. Tests with benzene as a fuel gave negligible concentrations of both peroxide and aldehydes.

In the motoring tests with iso-octane, cool flames were observed when the compression ratio was raised. Photometric experiments showed that the cool flame passed in the region of top

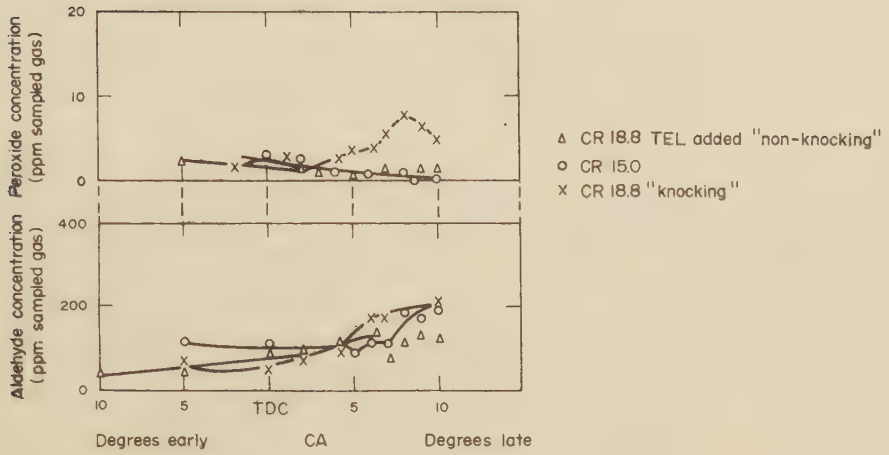

FIG. 5.11. Peroxide and aldehyde curves with methane as fuel. (From Downs and Wheeler,[8] by courtesy of the Institution of Mechanical Engineers.)

dead centre, the timing of the cool flame was in agreement with the point of inflexion of the sampling curves (Fig. 5.10). The hot flame started in the wake of the cool flame. No cool flames were observed with methane and benzene fuels.

From these experiments it is clear that the spontaneous ignition in the end gas with iso-octane fuel is a two-stage ignition phenomenon, whilst the spontaneous ignition in the end gas with methane is a single-stage ignition phenomenon. The results with iso-octane are typical of those obtained with the higher paraffinic components of commercial gasolene, and the knocking compression ratios are of the same order. Thus knock in commercial engines is of the two-stage low temperature type since this is associated with spontaneous ignition in the low temperature region of the ignition curve (Fig. 5.7). We normally call this type of knock low temperature knock.

The mechanism for low temperature knock can therefore be described in the light of the above experiments. As the normal combustion flame traverses the cylinder, the pressure and temperature in the end gas increase until they reach values when, firstly, there is low temperature auto-ignition followed after a short delay by high temperature auto-ignition which produces a rapid increase in pressure generating a shock wave.

Whether under normal combustion conditions the end gas will spontaneously ignite before the flame arrives at the combustion chamber walls will depend on:

(1) the composition of the fuel;

(2) the pressure and temperature in the end gas;

(3) whether there is sufficient time for the two stages of ignition to take place.

We are now in a position to relate these conditions to the observed engine parameters which influence knock. Before doing so we shall very briefly refer to fuel composition. Fuels with ignition curves similar to the higher paraffinics show a greater tendency to knock than fuels with ignition curves similar to methane and benzene. We shall shortly refer to how the fuel quality is assessed. Table 5.1 summarizes the influence of a number of operating factors on the tendency to knock. We shall examine these.

TABLE 5.1. Summary of Factors Influencing Tendency to Knock

Factor	Effect	Pro-knock	Anti-knock
Compression ratio	Increase	✓	
Ignition timing	Advance	✓	
Throttle setting	Full open	✓	
	Partially open		✓
Mixture strength	Weak		✓
	Slightly rich	✓	
	Over rich		✓
Engine speed	Increase		✓
Inlet air temperature	Increase	✓	
Inlet air pressure	Decrease		✓
Cooling water temperature	Increase	✓	

Compression Ratio. The higher the compression ratio the higher the pressure and temperature in the end gas during normal conditions; this increases the tendency to knock. For a given engine setting and fuel there will be a critical compression ratio above which knock occurs. This compression ratio is called the highest useful compression ratio (HUCR).

Ignition Timing. Advancing the ignition timing raises the cylinder pressure and temperature which in turn raises the end gas pressure and temperature thus increasing the tendency to knock. If the ignition is advanced too much the cylinder pressures fall and the tendency to knock is reduced. If in a given engine the fuel quality is changed and knock takes place, retarding the ignition may eliminate the knock; it will also reduce the engine power.

Throttle Setting. This controls the cylinder inlet pressure and mixture strength. If we consider mixture strength under a separate heading the effect of opening the throttle is to raise the cylinder pressure, thus increasing the pressure in the end gas and increases the tendency to knock.

Mixture Strength. This controls the combustion temperature and pressure, hence influencing the end gas temperature and pressure. The tendency to knock follows the power variation with mixture strength. That is at maximum power there is a greater tendency to knock; this is reduced as the mixture is strengthened or weakened.

Engine Speed. The lower the engine speed the longer the absolute time for the flame to traverse the cylinder, the longer the time available for the end gas reaction to take place and the greater the tendency to knock.

Inlet Air Temperature. Raising the air inlet temperature raises the cylinder temperature, thus raising the end gas temperature and increasing the tendency to knock.

Cooling Water Temperature. Raising the cooling water temperature raises the overall cycle temperature, hence increasing the end gas temperature and increasing the tendency to knock.

As well as the engine operating conditions certain design factors also influence the tendency to knock; two of these are the locations of the sparking plug and the exhaust valve. The spark plug should be located to allow for the minimum distance for the normal flame to traverse the combustion chamber thus reducing the time for the end gas reactions. The exhaust valve should be located close to the spark plug so that it is not in the end gas region, otherwise there will be a tendency to knock.

Another important factor influencing the knock limit is the geometric form of the combustion chamber shape including the dimensions of the clearance space between the cylinder head and piston crown. For the interested reader an extensive review of the influence of engine design and operating conditions on the knock limits and performance of motor vehicle gasolene engines has been presented by Caris et al.[23]

Although the designer has a wide range of variables at his disposal to eliminate knock, ultimately his final design will be dependent on the fuel quality. To assess the knock quality of a fuel, special engine tests are carried out under set engine conditions. The engine is a variable compression engine, i.e. an engine whose compression ratio can be varied whilst running. The fuel under test is supplied to the engine and the compression ratio increased until there is incipient knock as measured by an instrument sensitive either to rate of pressure rise, temperature or some other knock sensitive parameter. The fuel is then cut off and a mixture of n-heptane and iso-octane is supplied to the engine. The composition of the mixture is adjusted until incipient knock takes place at the same compression ratio. The fuel is rated by the

percentage of iso-octane in the n-heptane and iso-octane mixture. Iso-octane has a lower tendency to knock than n-heptane, so that the higher the octane rating of a fuel the lower the tendency to knock.

The standard engine used in these tests is the CFR engine; this is a variable compression ratio engine similar to the Ricardo E6 (Fig. 5.12). There are two basic tests called the motor method

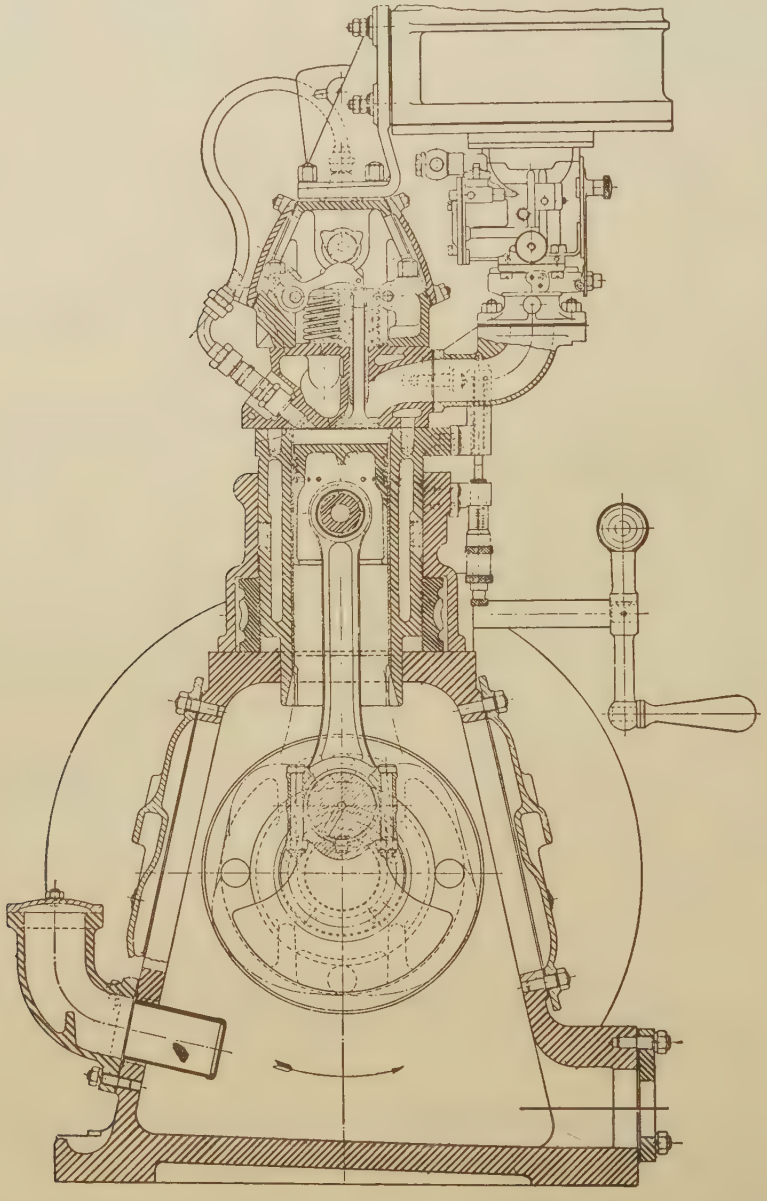

FIG. 5.12. Ricardo E6 cross-sectional arrangement of variable-compression ratio research engine of 3 in. bore by 4⅜ in. stroke (petrol engine).

and the research method. The test conditions for the two tests are summarized below:

Method	Motor	Research
Engine speed (rev/min)	900	600
Mixture temperature (^{o}C)	149	51.7

The sensitivity of a fuel to knock is measured by the difference in the two knock ratings; the greater the difference the greater the fuel sensitivity. The octane rating of fuel is lower in the motor method than in the research method.

Although the numerical value of the sensitivity has no physical meaning, it does give an indication of the relative merits of fuels used in automobile gasolene engines on the road. It might be expected that a fuel with a high sensitivity would tend to knock with the wide range of engine operating conditions experienced in normal traffic, whilst a fuel with low sensitivity would be relatively insensitive to the same conditions. Other methods have been developed to define the fuel quality using motor vehicle tests; the reader is referred to Ricardo and Hempson[1] for a discussion of these methods.

We have mainly discussed low temperature knock. It was shown by Downs and Wheeler[8] that certain fuels knock at high compression ratios. These fuels do not exhibit cool flames. The auto-ignition mechanism is therefore of the high temperature type. This is a single-stage auto-ignition and the phenomenon is called high temperature knock. Modern fuels contain components which exhibit both low temperature and high temperature knock. Experiments show that sensitive fuels knock more by a high temperature process than by low temperature knock.

5.3.3 Influence of Fuel Additives on Knock

Up to this point we have examined the knock mechanism in engines and related these to the engine operating conditions and the fuel. There has been much research to develop fuels with high knock ratings (high octane number). These are mainly achieved by refining processes, but they are in general expensive fuels. Alternative methods have therefore been sought, the most promising of which are fuel additives. Research has shown that, in general, an anti-knock additive in a fuel which inhibits low temperature knock enhances knock in a fuel which exhibits high temperature knock, and vice versa. Hence the selection of the correct additive for a particular fuel is most important. The most effective additive for commercial fuels at the time of writing is tetraethyl lead (TEL). There has in recent years been criticism of this additive since environmentalists claim it pollutes the atmosphere, although at present there is no direct evidence of resulting damage. Nevertheless, an increasing number of legislatures throughout the world are specifying reduction in the lead content in fuels with its eventual elimination. Since TEL is so effective there has been much research on the mechanism of its action. It is probable from

this work that alternative, and less obnoxious, additives might be developed. The exact mechanism of the action of TEL is not clear and there is some controversy in scientific circles on the mechanisms, but it is possible to identify some of the probable facets of its action.

The chemical formula of TEL is $Pb(C_2H_5)_5$, i.e. it is a metallorganic salt. It is mixed with the fuel and is present in the cylinder in the fuel vapour. It is generally accepted that it is decomposed thermally during the compression stroke and reacts with oxygenated intermediates to give lead oxides. There are two opposing theories as to whether the lead oxide is in vapour form or in particulate form (fog). The lead oxide acts as a chain-breaking agent (this was observed in Figs. 5.10 and 5.11). It does not appear to influence the reaction in the first stage of combustion nor to have any influence on the cool flames, but it does have an inhibiting action in the second stage by increasing the induction time T_2.

The suggested chain-breaking mechanism is:

$$PbO + OH \longrightarrow PbO(OH),$$

$$PbO(OH) + OH \longrightarrow PbO_2 + H_2O.$$

or

$$PbO_2 + R \longrightarrow PbO + RO,$$

where R is a radical.

The vital point, not clearly understood, is whether the chain termination is a surface or a gas phase effect, since if it is the former the anti-knock effectiveness of TEL might be increased by adding other organometallic compounds so that mixed oxides could be formed which would be more efficient than solid PbO itself in destroying the HO_2 radicals or peroxides. Downs et al.[9] have claimed to have observed PbO_2 fog in the cylinder indicating possible surface reactions. In addition to the pollution effect of lead it also poisons catalytic reactors used to reduce emissions from gasolene engines, so that the intense research directed to improve fuel quality with alternative additions might, by the time this book is in print, have the effect of rendering TEL to the history book. Whatever new additive is used, however, its mechanism will have to have the same effect as TEL, i.e. to act as a chain terminator.

5.4 UNCONTROLLED COMBUSTION, PRE-IGNITION AND RUNNING-ON

Under certain conditions the fuel/air mixture is ignited by a hot spot in the cylinder. The hot surface might be the spark plug insulator or electrode, or combustion deposits, or when knock occurs the exposed surface, where the boundary layer is scored by the shock wave. When the ignition occurs before the spark is ignited the phenomenon is called pre-ignition. When the phenomenon occurs after the ignition is switched off it is called running-on. Combustion deposit ignition is called rumbling.

5.4.1 Pre-ignition

This is the most severe form of uncontrolled combustion. Under severe operating conditions some part of the cylinder surface may be hot enough to ignite the charge. If there is insufficient time for hot spot ignition to take place before the spark ignites the mixture, normal combustion will take place. As the temperature of the hot spot increases, a condition may be reached when the engine would run normally with the ignition switched off. This is often called auto-ignition. Further increase in hot spot temperature would cause the mixture to ignite before the spark ignites. This is equivalent to advancing the ignition, but since the hot spot surface is larger than the spark the combustion rate would be faster than normal combustion creating very high cylinder pressures and temperatures resulting in excessive negative compression work and increased heat loss to the walls, the overall effect being a loss in power. Under certain conditions the engine could stall and possibly cause mechanical failure.

Pre-ignition normally follows heavy knocking due to the breakdown of the cylinder wall boundary layer. The combustion mechanism for pre-ignition corresponds to high temperature ignition, and it is noteworthy that although benzene does not knock it has a strong tendency to pre-ignite. Methods have been developed for pre-ignition ratings for different fuels. Descriptions of these methods are given by Downs and Pigneguy.[10]

5.4.2 Running-on

When the ignition is switched off and the throttle closed the engine may continue to fire. This might be due to a hot surface in the cylinder. It is considered, however, that the major cause is spontaneous ignition of the fuel/air mixture. The tendency to spontaneous ignition is dependent on the temperature/pressure ignition curve (Fig. 5.7) for the fuel, reflected in the octane rating of the fuel. Physical factors influencing spontaneous ignition are an elevated inlet temperature of the mixture, poor cooling of the combustion chamber surface, duration of valve overlap and high compression ratio.[29]

5.4.3 Rumble

This is ignition associated with the combustion deposits. This might occur with sudden power demand from the engine causing the deposit to glow and ignite the fuel/air mixture. The tendency of deposits to form and to cause ignition depends on the fuel composition. By adding phosphorus compounds the deposits become chemically inactive and do not cause ignition.

5.5 CHEMICAL THERMODYNAMIC MODELS FOR NORMAL COMBUSTION

In the previous discussions we have directed our attention to describing the combustion porcess from the point of view of the various modes of combustion and their influence on the engine performance. We now propose to describe a chemical-thermodynamic

model for the combustion process which will enable us to predict the engine performance. In Chapter 9 we shall develop these methods further from the view point of cycle analysis; in this section we shall outline the model and the assumptions leading on to the important new subject of combustion-generated emissions in the next section.

It is clear from the previous discussion that the chemical reactions during combustion are complex. For the predictions of the pressure and temperature in the cylinder and the overall composition of the products of combustion we can make fairly simple assumptions to obtain a broad picture of the overall process under normal combustion conditions. For this purpose we use equilibrium thermodynamics,† the major principles of which were reviewed in Chapter 2.

The combustion chamber may contain a heterogeneous mixture of burnt and unburnt products. For calculation purposes the combustion chamber is subdivided into zones. Lavoie et al.[18] and Blumberg[20] assumed a multi-zone model for the combustion process with a uniform temperature in each zone giving a variable temperature distribution in the combustion chamber. A burning rate is assumed for the combustion process. This is usually in the form of fraction of fuel/air burnt as a function of crankangle.[20]†† Another model[12], which will be outlined in Chapter 9, assumes that the combustion chamber is subdivided into two zones—a burnt zone and an unburnt zone. The two zones are separated by a flame front which is spherical in form and centred on the spark plug. With the second model a relationship is required between the flame speed and the cylinder conditions. The selection of an appropriate relationship is critical to the modelling of the combustion process. In practice the flame will be turbulent; unfortunately there is no clear model for a turbulent flame, so that attention has been drawn to computing the laminar flame speed with a suitable modification to allow for turbulence called the flame factor ff.

Benson et al.[12] suggest the following expression for the turbulent flame speed u_t:

$$u_t = ff \times u_\ell,$$

where u_ℓ is the laminar flame speed. This model is due to Annand.[19]

The laminar flame speed can be calculated by a number of methods which are reviewed by Phillips and Orme[11] and Benson et al.[12]

---

†For accurate predictions of the chemical composition reaction rate, equations must be included.

††More recently a turbulent flame combustion model has been developed by the same research group to predict the burning rate. Full details are given by Blizard and Keck[27] and Tabaczynski et al.[28]

The flame factor ff is adjusted to assume the combustion time is symmetrical about top dead centre. A calculation of the flame speed using the Annand model is shown in Fig. 5.13.

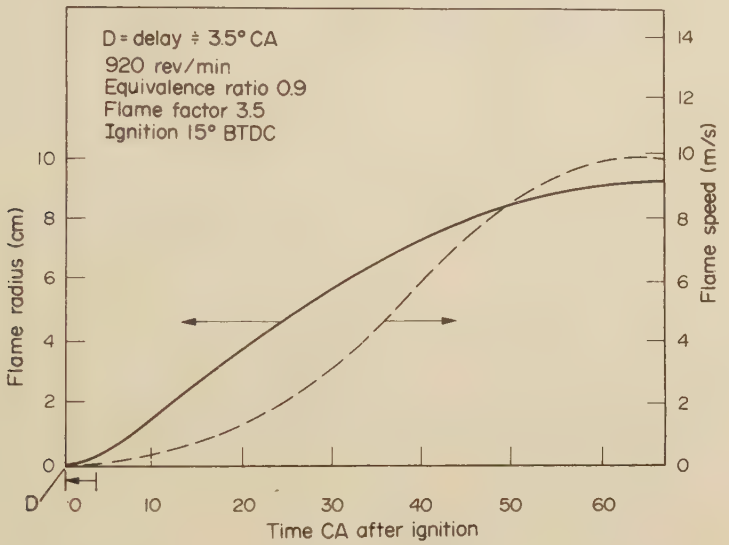

FIG. 5.13. Computed flame speed and radius

An outline of the calculation procedure is given in Chapter 9. In the Annand model it is assumed that in the unburnt zone there are no chemical reactions, whilst in the burnt zone reactions that satisfy chemical and thermodynamic equilibrium, including the appropriate reaction rate equations, take place.

For a correct mixture of a hydrocarbon C_nH_m and air the overall chemical reaction can be expressed as

$$C_nH_m + \left(n + \frac{m}{4}\right)O_2 + 3.76\left(n + \frac{m}{4}\right)N_2 \longrightarrow n\,CO_2 + m\,H_2O + 3.76\left(n + \frac{m}{4}\right)N_2.$$

At the elevated temperatures in the burnt gas zone the carbon dioxide (CO_2) and water vapour (H_2O) dissociate to form carbon monoxide (CO), oxygen (O_2) and hydrogen (H_2). Furthermore, the molecular oxygen (O_2), hydrogen (H_2) and nitrogen (N_2), dissociate to form atomic oxygen (O), hydrogen (H) and nitrogen (N). In addition there will be equilibrium concentrations of hydroxide (OH) and nitrous oxide (NO). Thus in the burnt gas zone we have the following species:

$$CO_2,\ CO,\ H_2O,\ OH,\ H_2,\ O_2,\ N_2,\ NO,\ H,\ O,\ N.$$

The concentration of these various species will depend on the air/fuel ratio and the prevailing pressure and temperature. By setting

up the appropriate equations and the equilibrium constants, the numerical concentrations can be computed by the methods outlined in Chapter 2 and Chapter 9 of Vol. II. The overall effect of the dissociation processes is to reduce the maximum temperature of the burnt gas below the value which would have been reached if dissociation had not been allowed for. This is illustrated in Fig. 5.14 for a benzene/air mixture. The maximum temperature occurs with a mixture about 10-20% on the rich side of stoichiometric.

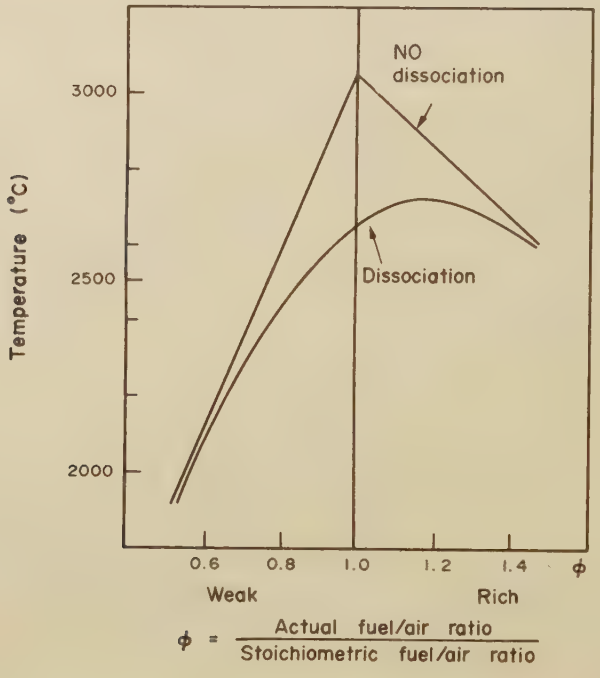

FIG. 5.14. Calculated maximum temperature for benzene-air mixtures.

It will be seen that dissociation effects are quite strong either side of the stoichiometric mixture. A full discussion on the influence of dissociation on the combustion temperature and the engine power is given in Chapter 9.

The gas composition in the cylinder changes during the expansion stroke, some of the dissociating species combine; others, however, remain in concentrations above the equilibrium values. We shall discuss this in the important topic of combustion-generated emissions in the next section.

5.6 COMBUSTION-GENERATED EMISSIONS

In recent years public attention has been directed to the problem of exhaust emissions from automobiles. The problem was first highlighted in the United States in the Los Angeles area where air pollution caused plant damage, eye and throat irritation, cracking of stressed rubber and decrease in visibility (smog). In the United State legislation has been implemented to limit the concentrations of hydrocarbon (HC), carbon monoxide (CO), nitric oxides (NOX) and particulates in the automobile exhaust gases. Although some of the emissions are due to the lubricating oil, the main source is the combustion process of the hydrocarbon/air mixture.

In Europe the attention of legislatures has been directed mainly to the reduction of lead in the exhaust gases by limiting the lead content of the fuel.

An excellent review of the current knowledge of pollutant formation and control in spark ignition engines has been given by Heywood.[24] In this section we will outline the possible mechanisms of the formation of the combustion-generated emissions and indicate the thermodynamic factors which influence the concentrations. We shall see that for carbon monoxide and nitric oxide the evidence indicates that during the expansion process recombination does not take place. In these circumstances the rate of the forward reaction is different from the rate of the backward reaction. The chemical reactions are therefore rate-controlled. A brief discussion of the thermodynamics of rate-controlled reactions is given in Chapter 2 (section 2.7).

5.6.1 Carbon Monoxide

Carbon monoxide (CO) is always present in the exhaust gases due to the dissociation processes. With rich mixtures the CO concentration is further increased due to the incomplete combustion to carbon dioxide. Some typical results are shown in Fig. 5.15 for a four-cylinder engine at full throttle. The measured concentrations of CO are greater than the equilibrium concentrations. This indicates that recombination is not complete in the expansion stroke. The reactions in the expansion stroke must therefore be rate-controlled. The full mechanism for the formation of CO is at the time of writing (1976) not fully known, although some of the rate-controlled reactions are known, so it is not possible at present to predict the CO concentrations. A review of the present position for CO predictions is given by Heywood[24] and Benson.[25]

To reduce CO emissions the engine may run with a weak mixture with loss of power; or devices may be appended to the exhaust to oxidize the CO. One such group of devices are thermal reactors in which air is injected into the exhaust stream and a flame is produced which aids in the combustion of CO to CO_2. Another method is to oxidize the CO in the presence of a catalyst. A number of these methods are described in the symposium on Air Pollution in Transport Engines[4] (Proc. Instn. Mech. Engrs. 1971) and in the review paper by Heywood.[24]

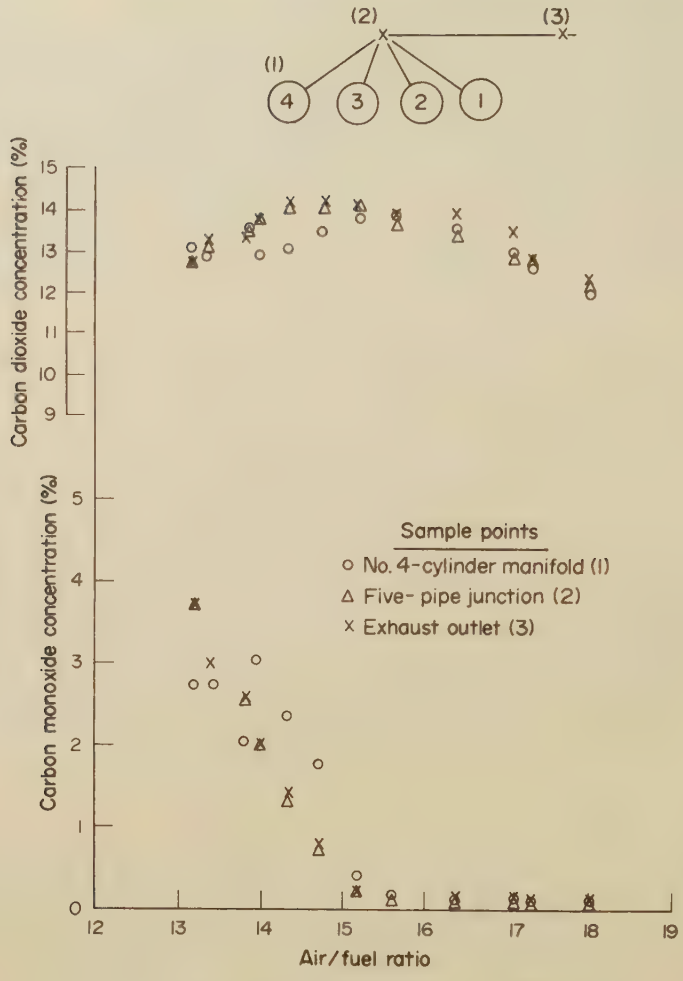

FIG. 5.15. Measured carbon monoxide and carbon dioxide in exhaust pipe of a four cylinder gasolene engine. Full throttle at 3000 rev/min.

5.6.2 Nitric Oxide

Whilst the obnoxious effects of CO are well known the significance of the nitric oxide (NO) emissions has only recently been discovered. It is the NO and hydrocarbon emissions which react in sunlight to cause photochemical smog which caused the peculiar pollution problem in the Los Angeles area. There has been intensive research to understand the source of the NO emissions and to develop methods to reduce them. The pioneering work was carried out by Starkman and Newhall.[15] There have been numerous publications. We have already indicated that NO is present in the products of combustion due to dissociation of the molecular oxygen and nitrogen. Under equilibrium conditions one would expect that the concentrations of NO would fall with pressure and temperature

during the expansion stroke to negligible proportions at exhaust valve opening. All experiments on engines indicate that the NO concentrations in the exhaust gases are well above the equilibrium values. It is therefore deduced that the NO reactions are rate-controlled. In order to calculate the quantity of NO to be expected it is necessary to establish the chemical mechanism so that the appropriate rate equations can be used. There have been a number of models suggested. Experiments by Newhall and Shahed[16] using spectroscopic techniques to record the time rate of formation of NO in a hydrogen-oxygen reaction in a closed vessel showed that NO formation occurred predominantly in the post-flame combustion products. Lavoie[17,18] showed that substantial temperature and NO gradients occurred behind the flame in an engine combustion chamber. In Fig. 5.16 some of Lavoie's results are shown from spectrographic measurements. It will be seen that after the flame arrives at the window the NO concentration increases up to a maximum and then remains steady. Different concentration curves were observed at each window.

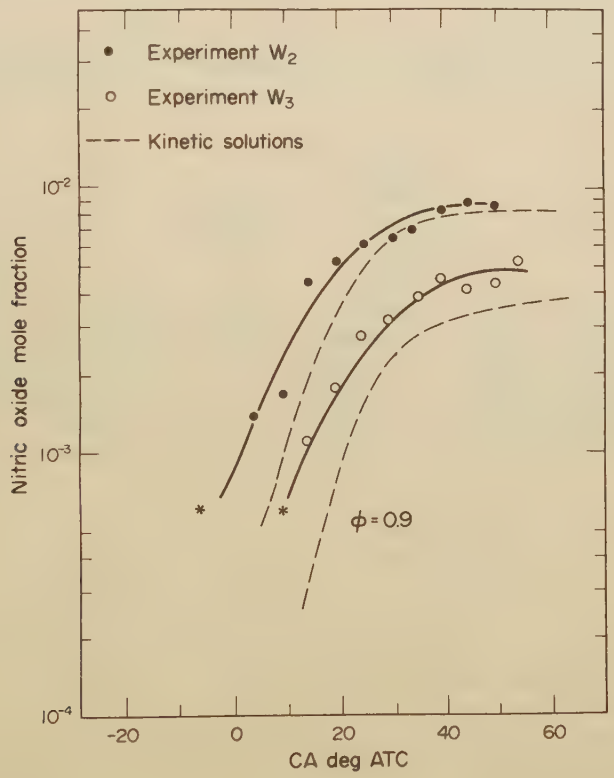

FIG. 5.16. Nitric oxide concentrations in engine cylinder. Experimental NO concentration versus crankangle for ϕ = 0.9 for two windows, W_2 being closer to the spark than W_3. The asterisks mark estimated initial conditions and flame arrival times. The dotted lines are theoretical kinetic solutions for parts of the charge burning at the corresponding times and starting with zero NO concentrations. (From Lavoie,[17] by courtesy of Combustion and Flame).

Because the detailed experiments on engines are difficult, computer models have been set up to study the effect of engine operating variables on the NO emissions and to identify the important parameters which influence the formation of NO. Lavoie et al.[18] subdivide the combustion chamber into a number of elements and assume that each element is burnt separately. This method enables the temperature gradient to be computed and the variation in NO concentration to be determined. The average value of NO concentration is then taken as the NO at exhaust valve opening. The rate of combustion of the elements is called the burning law, and this is taken from an analysis of the measured indicator diagram.† Annand,[19] on the other hand, has suggested a simple two-zone model with an unburnt and burnt region with uniform temperatures in each region. In this method the indicator diagram is synthesized by assuming a spherical flame front separating the two zones and calculating the temperature, pressure and composition of the burnt zone from a combination of the equilibrium equations for a number of reactions and the rate-controlled equations for the oxides of nitrogen simultaneously.

Both methods require a mechanism for the formation of NO. In their original work, Newhall and Starkman[15] suggested the so-called Zeldovich chain reaction:

$$O_2 \rightleftharpoons 2O,$$

$$O + N_2 \rightleftharpoons NO + N,$$

$$N + O_2 \rightleftharpoons NO + O.$$

It is suggested that at elevated temperatures in the cylinder the molecular oxygen (O_2) dissociates to atomic oxygen which reacts with the molecular nitrogen (N_2) to form NO and atomic nitrogen (N) the latter reacting with O_2, forming NO and atomic oxygen (O). There have been suggestions that this model is not complete and Lavoie et al.[18] have proposed a modified Zeldovich reaction with the hydroxide (OH) radical:

$$N + OH \rightleftharpoons NO + H,$$

$$H + N_2O \rightleftharpoons N_2 + OH,$$

$$O + N_2O \rightleftharpoons N_2 + O_2,$$

$$O + N_2O \rightleftharpoons NO + NO.$$

Using this model, Lavoie compared his experimental results with the predicted concentration of NO (Fig. 5.16).

---

†More recently Blizard and Keck[27] and Tabaczynski et al.[28] have developed turbulent flame combustion models to predict the burning law

Annand[19] has suggested a further group of reactions to be added to the modified Zeldovich reaction, these are:

$$N + NO \rightleftharpoons N_2 + O_2,$$

$$N + O_2 \rightleftharpoons NO + O,$$

$$N_2O + M \rightleftharpoons N_2 + O + M.$$

Benson et al.,[20] using Annand's method, predicted the NO emissions for a single-cylinder gas engine operating with propane/air as shown in Fig. 5.17. It will be seen that the predictions agree with the experiment. It should be pointed out that the flame factor ff was adjusted to give agreement between the experimental and predicted value of NO at the maximum emission. It was then kept constant and the predictions made over the whole air/fuel ratio range shown.

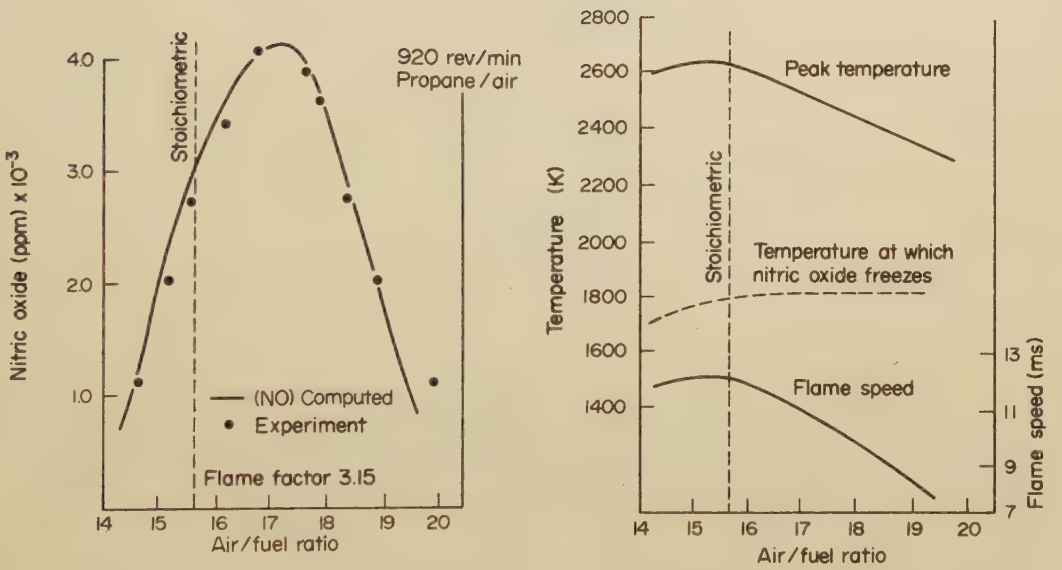

FIG. 5.17. Influence of mixture strength on nitric oxide and maximum and freezing temperatures. (From Benson et al.[12].)

The variation in NO with crankangle is shown in Fig. 5.18. The same trends as noted by Lavoie (Fig. 5.16) will be observed.

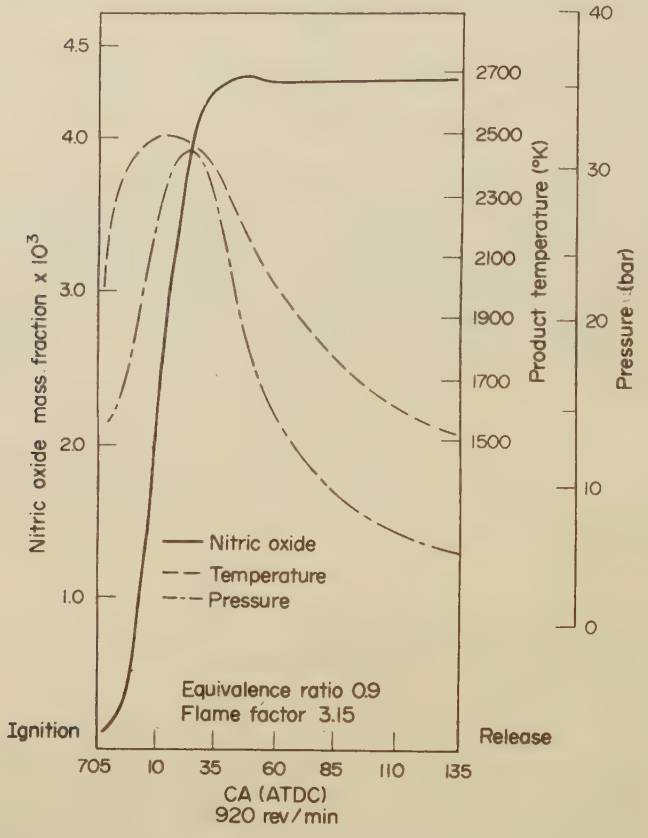

FIG. 5.18. Variation in pressure, temperature and nitric oxide concentration. (From Benson et al.[12].)

From these calculations it could be observed that after ignition the NO concentration increases rapidly, then there is a slight fall and the NO concentration remains constant, even though the temperature and pressure are falling. This phenomenon is called "freezing" and is due to the slow rate of the backward reactions, i.e., the dissociation of NO to N_2 and O_2 through the chain given above.

Lavoie et al.[18] have shown for their multi-element model and the modified Zeldovich reaction, that, depending on the time of burning of a particular element, even the forward rate of some of the reactions are not fast enough to achieve equilibrium conditions. This is illustrated in Fig. 5.19. Here we notice that the element burning 30^o before top dead centre ($\theta_b = -30^o$) reaches the peak value at about the equilibrium concentrations, but the element burning at 10^o after top dead centre ($\theta_b = 10^o$) does not reach the peak equilibrium value. In Fig. 5.19 we clearly see the difference

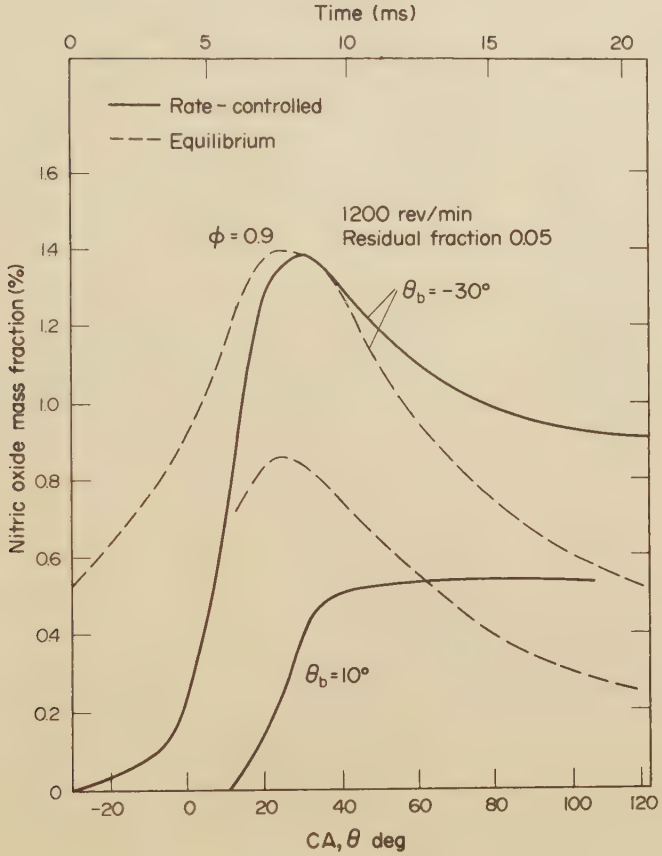

FIG. 5.19. Variation in nitric oxide concentration. Nitric oxide mass fractions as a function of time in the burnt gas for two elements which burn at different times: $\theta_b = -30^\circ$ is the first part of the charge to burn; at $\theta_b = 10^\circ$, one-third of charge is burnt. From Lavoie et al.,[18] by courtesy of the Massachusetts Institute of Technology.)

between the equilibrium concentration and the predicted frozen concentration at the end of the expansion.

If we turn to Fig. 5.17 again we see that for weak mixtures the temperature at which NO freezes is almost constant; and even on the rich side there is only a slight drop in temperature. The peak NO concentration occurs on the weak side and falls off considerably over a few air/fuel ratios. This trend is observed in engines of all types. The NO concentration may vary in the exhaust pipe. Some results obtained by the authors in a four-cylinder engine are shown in Fig. 5.20.

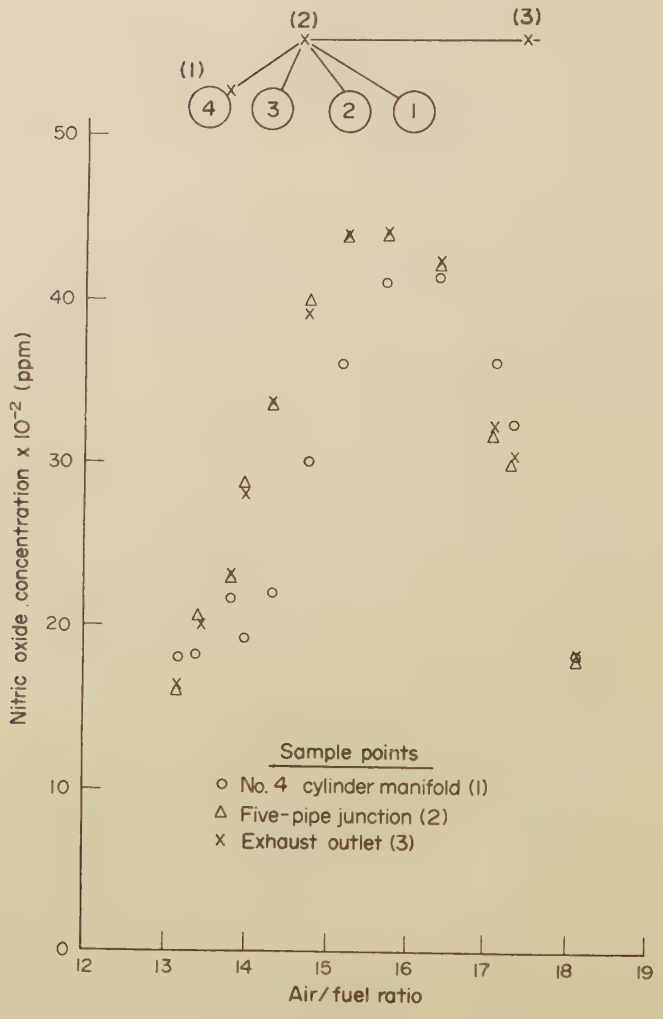

FIG. 5.20. Measured nitric oxide concentrations in exhaust pipe of a four-cylinder gasolene engine. Full throttle at 3000 rev/min.

Thus we may conclude that the NO formation in the cylinder is associated with the rate-controlled combustion processes. It is therefore related to the thermodynamic conditions in the cylinder at ignition. To minimize the NO concentration the problem has to be attacked by controlling the combustion process. It would seem from Fig. 5.19 that the NO concentration is related to the peak temperature and the flame speed. The higher the peak temperature the higher the concentration, and the lower the flame speed the longer the time for the NO to dissociate to molecular nitrogen and oxygen. This does not completely hold since we should expect the peak NO to be on the rich side, but the general trend is in these directions. Therefore

any parameter that can reduce the peak temperature or decrease the flame speed or both will reduce the NO emission. Blumberg and Kummer[2] have carried out a large number of calculations based on the Lavoie et al.[18] model to investigate a number of engine parameters. This work identified the leading factors which influenced the NO emissions. In Figs. 5.21-5.24 the results are given of calculations by the authors based on the methods developed by Benson et al.[12] These calculations differ from those of Blumberg and Kummer not only in the combustion model, which is simpler, but also because allowance was made for the influence of the intake and exhaust systems on the trapped engine conditions. The same broad trends as Blumberg and Kummer were observed.

We have already noted that retarding the ignition timing reduces the maximum pressure (and hence peak temperature) (Fig. 5.5). It would therefore be expected that decreasing the spark advance would also reduce NO emissions. In Fig. 5.21 this effect is observed but the magnitude will depend on the air/fuel ratio. Reducing NO by this method, however, will reduce the engine power.

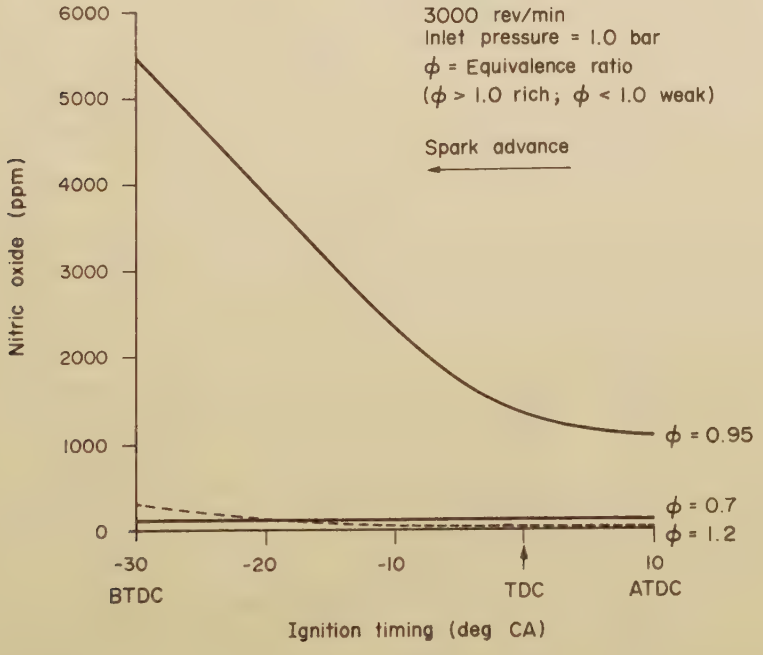

FIG. 5.21. Influence of ignition timing on nitric oxide emissions.

The effect of engine operating conditions such as speed and manifold pressure are shown in Figs. 5.22 and 5.23. The lower the engine speed, the longer the time available for the dissociation of NO, but the magnitude of the change in NO concentration will depend on the ignition timing, mixture strength and heat losses. Finally, running very lean will also reduce the NO emission (Fig. 5.7). Here we are faced with a practical problem of ensuring a uniform distribution of fuel between cylinders in multi-cylinder operation and ignition stability already referred to earlier in our discussion of ignition timing.

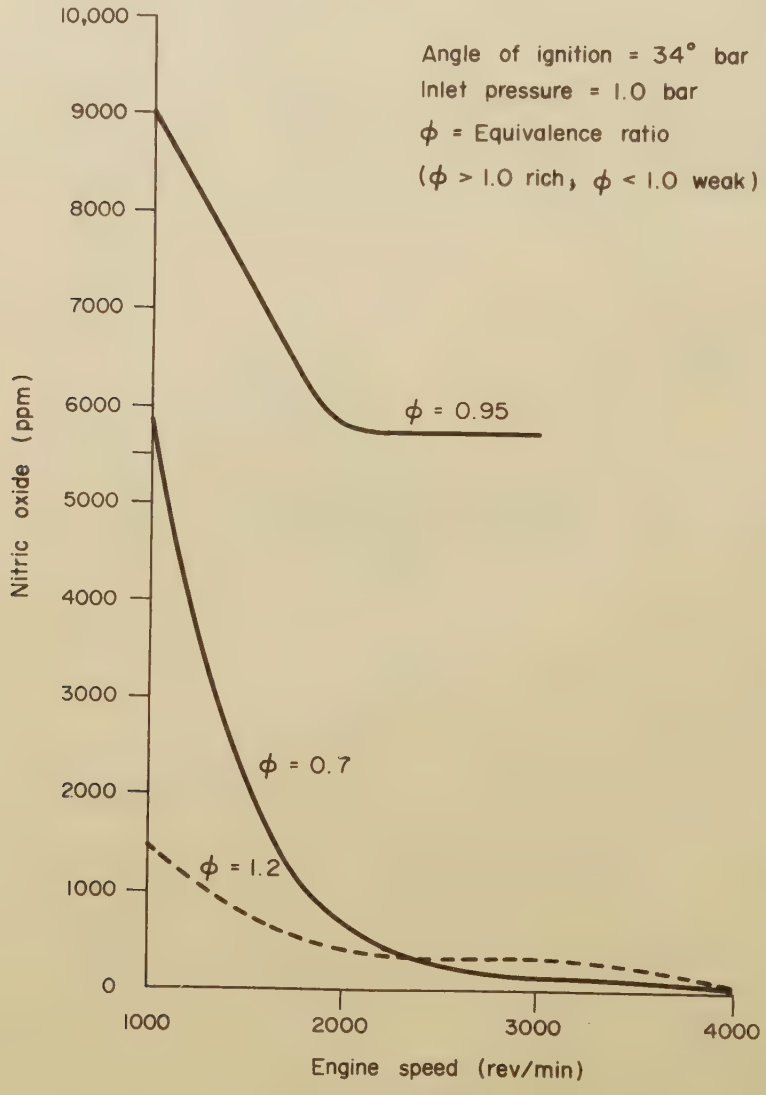

FIG. 5.22. Influence of engine speed on nitric oxide emissions.

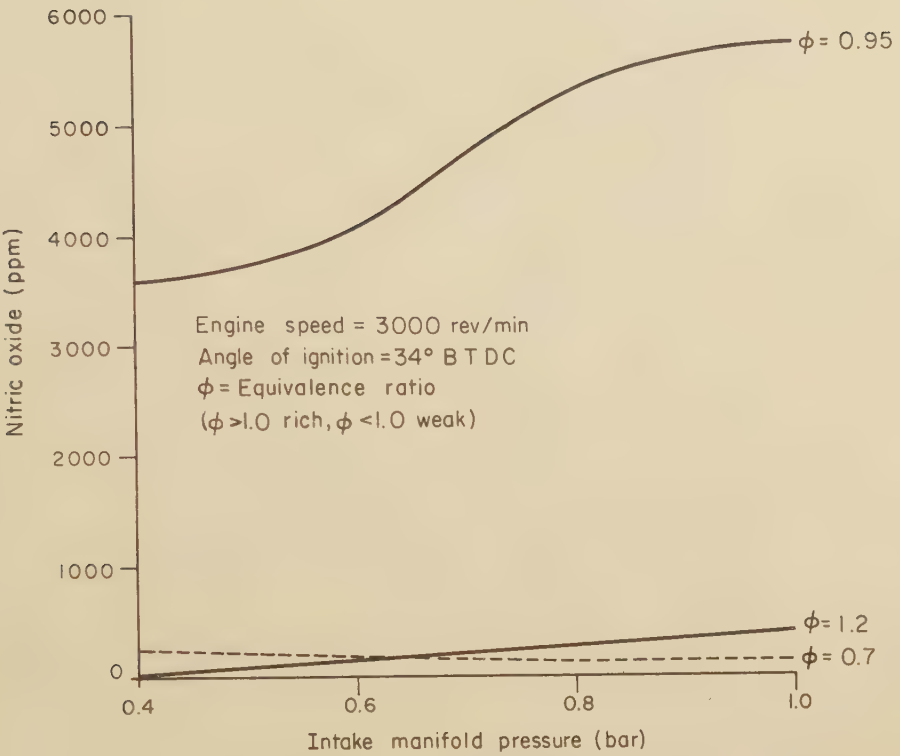

FIG. 5.23. Influence of intake manifold pressure on nitric oxide emissions.

Another method of reducing the maximum temperature and flame speed is to increase the residual fraction of the products of combustion from the previous cycle. In Fig. 5.24 it will be seen that a small change in the residual fraction has a marked significance on the peak NO.

A practical method of implementing this is to recirculate some of the exhaust gas back to the inlet manifold. This method is called exhaust gas recirculation (EGR). Some typical results obtained in the authors' laboratories on a four-cylinder engine with EGR are shown in Fig. 5.25. Here it will be seen that a reduction in peak NO concentration from about 4000 ppm to 2500 ppm was obtained with approximately 3.5% EGR. The percentage EGR decreases with increase in air/fuel ratio for a fixed valve setting. In practice, the EGR valve is shut off during idle and closed throttle.

All the above methods for reducing NO reduce the engine power and impair performance. Alternative methods have therefore been sought. One method[22] is to subdivide the combustion chamber into two parts—one with a rich mixture and the other with a weak mixture. The rich mixture is ignited first and it, in turn, ignites the weak mixture. It is claimed that by this method the NO emissions are reduced. These engines are called stratified charge engines.

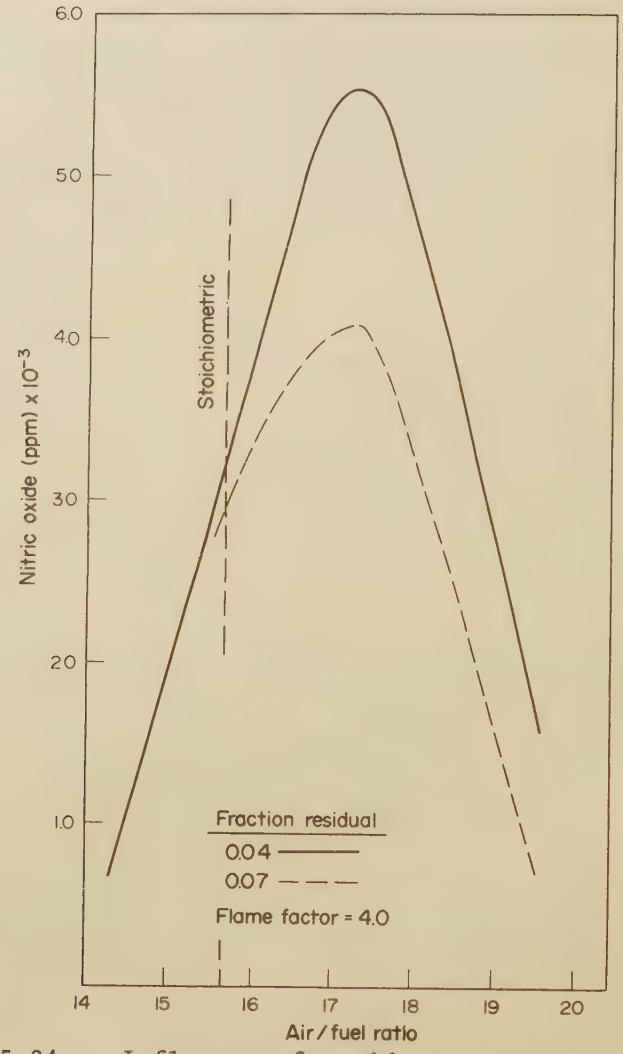

FIG. 5.24. Influence of residuals on nitric oxide concentration. (From Benson et al.[12].)

Finally, devices have been developed for mounting on the exhaust pipe to assist in the reduction of NO to oxygen and nitrogen. These are called catalytic reactors. The reaction takes place in a reducing atmosphere in the presence of a catalyst. There is evidence to show that ammonia is formed in the reduction process.[14] The catalysts are very susceptible to lead poisoning, and for their effective use lead-free fuels must be used.

5.6.3 Hydrocarbons

Hydrocarbons may appear in the exhaust gas from a number of sources; some of these can be directly related to unstable ignition

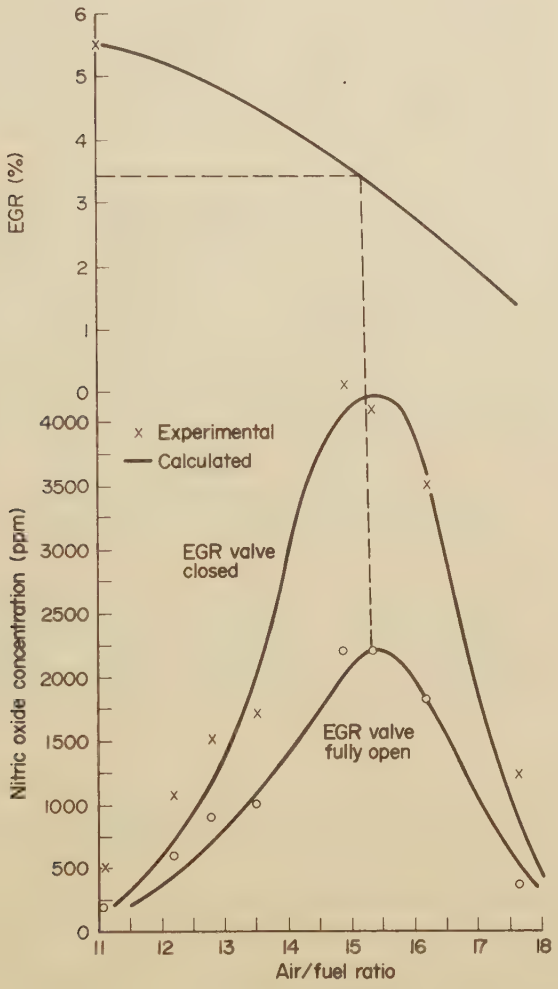

FIG. 5.25. Some typical results for a four-cylinder engine with exhaust gas recirculation.

(misfire), some to poor operation (excessive lubricating oil in exhaust due to blow-by, etc.) and some to crevices in the combustion chamber which are too narrow for the flame to enter; for example, around the valves and between the piston crown and cylinder head. The two main combustion-generated sources are the intermediate products and wall quenching.

We have already pointed out that the oxidation of hydrocarbons is a chain process with intermediate products such as aldehydes. Some of these aldehydes are stable and pass into the exhaust gas. The major source of hydrocarbon formation is wall quenching. When photographic measurements are made of the combustion process in

engines it is observed that as the flame propagates to the wall there is a thin layer adjacent to the wall where no chemical reaction except some fuel breakdown occurs. This thin layer, containing non-reacting hydrocarbons, is called the quench distance. The wall acts in two ways, firstly, as a chain breaker in the reacting mechanism, and secondly, as a heat sink which causes the temperature of the boundary layer to drop below the ignition temperature of the mixture.

The quench distance varies from 0.008 cm to 0.038 cm thickness.[24] The unburnt hydrocarbons are swept upwards by the piston ring during the exhaust stroke and the boundary layer rolls in the form of a vortex causing the hydrocarbons to enter the main stream and pass through the exhaust valve.

The quench distance is influenced by the mixture temperature, pressure, air/fuel ratio, the wall surface temperature, to the wall surface material and combustion deposits. The variation of hydrocarbon concentration with mixture strength is of similar form to the carbon monoxide curve (Fig. 5.16) with high concentration with rich mixture decreasing to a minimum at about the point of maximum temperature and then remaining almost constant, although if the mixture is too lean the concentration will increase due to misfiring.

Exhaust devices are used to reduce hydrocarbon in the gas mainly by oxidation processes in thermal or catalytic reactors. In order that the oxidation can be successfully carried out there are critical sizes for these reactors to allow for adequate residence time for the oxidation process to take place.

REFERENCES

1. Ricardo, H.R., The High Speed Internal Combustion Engine, 4th edn., Blackie, 1953.

2. Ricardo, H.R. and Hempson, J.G.G., The High Speed Internal Combustion Engine, 5th edn., Blackie, 1968.

3. Minkhoff, G.J. and Tipper, C.F.H., Chemistry of Combustion Reactions, Butterworths, 1962.

4. Lewis, B. and von Elbe, G., Combustion, Flames and Explosion of Gases, Academic Press, 1961.

5. Hewitt, D.M. and Thornes, L.S., The oxidation of propane: Part I: Products of the slow oxidation at atmospheric and at reduced pressures, J. Chem. Soc. 1656 (1937).

6. Bardwell, J. and Hinshellwood, C.N., The cool flame of methyl ethyl ketone, Proc. R. Soc. A, 205, 375 (1951).

7. Burgoyne, J.H., The combustion of aromatic and alicyclic hydrocarbons: Part V: Products of combustion of benzene and its mono-alkyl derivatives, Proc. R. Soc. A, 175, 539 (1940).

8. Downs, D. and Wheeler, R.W., Recent developments in knock research, Proc. Instn. Mech. Engrs. (AD), Pt. III, 89 (1951-2).

9. Downs, D., Griffiths, S.T. and Wheeler, R.W., The part played by the preparational stage in determining lead anti-knock effectiveness, J. Instn. Petrol, 47, 1 (1961).

10. Downs, D. and Pigneguy, J.H., An experimental investigation into pre-ignition in the spark ignition engine, Proc. Instn. Mech. Engrs. (AD) Pt. I, 125 (1950-1).

11. Phillips, R.A. and Orman, P.L., Simulation and Combustion in Gasolene Engine Using a Digital Computer, Advances in Automobile Engines, Vol.4, Pergamon Press, Oxford, 1966.

12. Benson, R.S., Annand, W.J.D. and Baruah, P.C., A simulation model including intake and exhaust systems for a single cylinder four-stroke cycle spark ignition engine, Int. J. Mech. Sci. 17, 97 (1975).

13. Pye, D.R., The Internal Combustion Engine, vol.I, Oxford University Press, 1937.

14. Institution of Mechanical Engineers, Confernece on Air Pollution Control in Transport Engines, 1971.

15. Newhall, H.K. and Starkman, E.S., Direct spectroscopic determination of nitric oxide in reciprocating engine cylinders, SAE 670122 (1967).

16. Newhall, H.K. and Shahed, S.M., Kinetics of nitric oxide formation in high pressure flames, 13th International Symposium on Combustion, Salt Lake City, 365 (1971).

17. Lavoie, G.A., Spectroscopic measurement of nitric oxide in spark ignition engines, Combustion and Flame, 15, 97 (1970).

18. Lavoie, G.A., Heywood, J.B. and Keck, J.C., Experimental and theoretical study of nitric oxide formation in internal combustion engines, MIT Fluid Mech. Lab. Report 69-10 (1969). (Also published in Combustion and Technol. Sci. 1, 313 (1970)).

19. Annand, W.J.D., Effects of simplifying kinetic assumptions in calculating nitric oxide formation in spark ignition engines, Proc. Instn. Mech. Engrs. 188, 431 (1974).

20. Blumberg, P. and Kummer, J.T., Prediction of nitric oxide formation in spark ignited engines - an analysis of methods of control, Combustion Sci. and Technol. 4, 73 (1971).

21. Huls, T.A. and Nicol, H.A., Influence of engine variables on exhaust oxides of nitrogen concentration from a multi-cylinder, SAE 670482 (1967).

22. Der CVCC - Motor vo Honda., Ansdem Report der Honda Motor GmBH Oct. 1972, MTZ 34, 130 (1973).

23. Caris, D.F., Mitchell, B.J., McDuffle, A.D. and Wyczalek, F.A., Mechanical octanes for higher efficiency, SAE Trans. 64 (1956).

24. Heywood, J.B., Pollutant formation and control in spark ignition engines, Prog. Energy Combustion Sci. 1, 135 (1976).

25. Benson, R.S. and Baruah, P.C., Performance and emission predictions for a multi-cylinder spark ignitin engine, Proc. Instn. Mech. Engrs. Vol.191, 32/77 p.339-354, 1977.

26. Baruah, P.C., Benson, R.S. and Balouch, S.K., Performance and emission predictions of a multi-cylinder spark ignition engine with exhaust gas recirculation, SAE 780663 (1978).

27. Blizard, N.C. and Keck, J.C., Experimental and theoretical investigation of turbulent burning model for internal combustion engines, SAE 740191 (1974).

28. Tabaczynski, R.J., Ferguson, C.R. and Radhakrishnan, K., A turbulent entrainment model for spark ignition engine combustion, SAE 770647 (1977).

29. Affleck, W.S., Bright, P.E. and Ellison, R.J., Run-on in gasolene engines, Proc. Instn. Mech. Engrs. 183, Pt. 2A, No. 1, (1968-9).

Chapter 6

Heat Transfer in Engines

Notation

a	constant in Annand's eqn. (6.21) and Table 6.2
A	area
b	constant in Annand's eqn. (6.21) and Table 6.2
c	constant in Annand's eqn. (6.21) and Table 6.2
C	particle mass per unit volume
c_n	constants in Woschni's eqn. (6.24) (n = 1, 2, 3)
C_p	specific heat at constant pressure
D	cylinder bore
E_b	black body energy radiated per unit area per unit time
E_g	grey body energy radiated per unit area per unit time
f	shape factor (Table 6.1)
F	shape factor (eqn. (6.10))
$\bar{h}_c$, h_c	heat transfer coefficient
I	radiant energy per unit solid angle
$I_{\lambda x}$	intensity of radiant energy at wavelength λ, distance x
k	thermal conductivity
k_f	thermal conductivity of gas
k'	monochromatic absorption coefficient
L	linear length (Table 6.1)
Nu	Nusselt number
p	pressure
p'	trapped pressure (Woschni eqn. (6.24))
p_o	motoring pressure (Woschni eqn. (6.24))
Pr	Prandtl number
q	heat flow per unit time
r	distance
Re	Reynolds number
s	particle surface area per unit mass
T	temperature, absolute
T_g	gas temperature
T_w	wall temperature
v_p	piston velocity
V	volume
V'	trapped volume (Woschni eqn. (6.24))
w	local average velocity (Woschni eqn. (6.24))
w_c	combustion induced velocity (Woschni eqn. (6.24))
x	length
$\alpha_{G\lambda}$	absorptivity of gas layer
ε	emissivity
ε_g	grey body emissivity
$\varepsilon_{G\lambda}$	emissivity of gas layer
λ	wavelength
ψ	angle (Fig. 6.2)
ω	angle (eqn. (6.4))
ϕ	angle (Fig. 6.2)
ρ	density
ρ_r	reflectivity
μ	absolute viscosity
ν	kinematic viscosity
σ	constant of proportionality in Stefan-Boltzmann law

6.1 BASIC PRINCIPLES

In Chapter 3 the limitations of the air standard cycles were discussed and heat loss to the walls of the combustion chamber from the burning gases was claimed to be the second most important reason for the deviation of such a calculation from an engine test result. Apart from performance calculations heat transfer is of importance because of the thermal loading of components—liner, piston, valves and cylinder head.

The reader is probably familiar with the principles of heat transfer, so only a brief description, of relevance to engine conditions, will be given here.

Heat transfer may be defined as the transmission of energy from one region to another as a result of a temperature difference between them. This may be accomplished by one or more of three methods—conduction, convection and radiation. In conduction, heat transfer is achieved by molecule to molecule contact without appreciable movement of the molecules. Although it may be claimed that heat transfer from a gas to a solid is dependent upon conduction, through a thin stationary boundary layer of gas molecules adhering to the wall of the solid, this concept is seldom used practically, and for our purposes conduction may be ignored.

Convection is the transport of energy by the movement of molecules over appreciable distances, the molecules acting as energy stores, picking up energy in high temperature regions and giving it up in low temperature regions. In internal combustion engines convection tends to reduce temperature gradients within the gases and also to transfer energy from the hot gases to cold walls. A major influence on the rate of convective heat transfer is the rate of movement of the gases.

Radiation is a process by which energy is transferred from one body to another without the use of molecular movement or contact. It may occur through a vacuum or any transparent medium, and is an electromagnetic phenomenon. It includes light, X-rays and radiowaves, etc.

In engines heat losses from the combustion chamber gases are due both to radiation and convection, but the losses have seldom been measured separately. An understanding of the two forms of heat transfer, as applied to engines, may be expected to become increasingly important.

6.1.1 Radiation

The essential facts about radiation for our purposes are summarized below. The reader is recommended to read elsewhere for greater depth and width of understanding.

Radiation consists of electromagnetic waves usually covering a variety of wavelengths. Solid bodies radiate at all wavelengths, producing a continuous spectrum. The proportion of the total energy radiated at any given wavelength is dependent upon the type of body and on its temperature. If a body at any specified temperature radiates the maximum possible amount of thermal radiation at all wavelengths, it is an ideal radiator, called a "black body". The energy radiated by a black body is proportional to the fourth power of its absolute temperature (Stefan-Boltzmann law). Thus

$$E_b = \sigma T^4, \tag{6.1}$$

where E_b is the energy radiated per unit area per unit time and σ is the constant of proportionality = 5.68×10^{-8} J/s m^2 K^4

Real surfaces radiate less than a black body at the same temperature. If at a given temperature the ratio of the radiative power at a given wavelength to that of a black body for the same wavelength and the same temperature is constant for all wavelengths, the body is called a grey body. For the purpose of heat transfer surfaces are usually considered to be grey. The ratio of energy radiated by a grey body to that radiated by a black body at the same temperature is called its emissivity, ε_g, so that

$$E_g = \varepsilon_g \sigma T . \tag{6.2}$$

For a true grey body the emissivity ε_g will be a constant independent of temperature, but most real bodies are not grey and their emissivities vary with temperature. Also surfaces have directional qualities, but these may be neglected for our purposes.

Kirchhoff's law states that, at thermal equilibrium, the ratio of the emissive power of a surface to its absorptivity is the same for all bodies. For any body the absorptivity for black body radiation from a surface at temperature T is the same as the emissivity of the body at the same temperature T.

So far we have considered the total radiation emitted by a black body in all directions. This concept may be visualized by placing a hemispherical surface over a surface element dA_1 as shown in Fig. 6.1.

The hemisphere will intercept all of the radiation emitted from the surface element, but only from directly above it (taking dA_1 to be horizontal) will dA_1 be seen undistorted. When viewed from a point on the hemisphere displaced by an angle ϕ from the normal to dA_1, the surface element will appear as the projected area $dA_1 \cos\phi$.

If we define the intensity of radiation from dA_1, I, as the radiant energy propagated in a particular direction per unit solid angle, per unit of area of dA_1 as projected on a plane perpendicular to the direction of propagation, the rate of radiant heat flow from dA_1 to dA_2 is

$$dq_{1-2} = I \cos\phi \; dA_1 \; dA_2/r^2, \tag{6.3}$$

$$= I \, dA_{1p} \, d\omega_1, \tag{6.4}$$

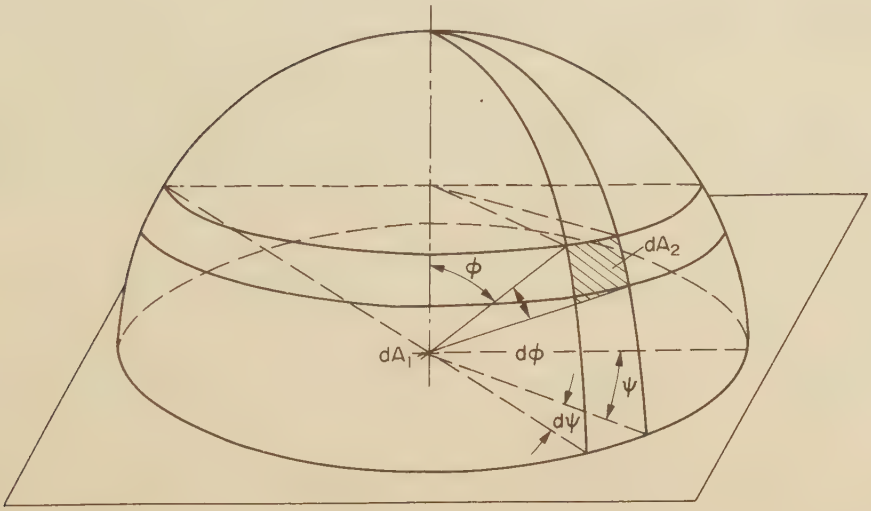

FIG. 6.1. Radiation from surface element to circumscribing hemisphere. (From Kreith[39] by courtesy of the International Text Book Co.)

where $d\omega_1 = (dA_2/r^2)$ = the solid angle subtended by dA_2 at dA_1 and $dA_{1p} = dA_1 \cos\phi$ = the projected area of dA_1 in the direction ϕ. If the intensity of radiation from surface dA_1 does not vary with the direction ϕ, as for a diffuse surface, then integrating the radiation intercepted by all such elemental areas as dA_2 over the total surface of the hemisphere, the total rate of emission per unit area of A_1, or emissive power will be

$$E = \int_{A_2}\int I \cos\phi \frac{dA_2}{r^2}, \tag{6.5}$$

but $$\frac{dA_2}{r_2} = d\omega_1 = \frac{r \sin\phi \, d\psi \; r \, d\phi}{r^2} = \sin\phi \, d\psi \, d\phi.$$

Therefore

$$E = I \int_0^{2\pi} \int_0^{\pi/2} \sin\phi \cos\phi \, d\phi \, d\psi, \tag{6.6}$$

$$= \pi I. \tag{6.7}$$

So far we have considered emission and absorption of radiation by various surfaces but not the net flow between them. To do this we have to determine the fraction of the total emission from each of the radiating surfaces which reaches and is absorbed by the others. If only black body surfaces are involved, all incident radiation is absorbed and only the geometric relation between the surfaces has to be considered.

Figure 6.2 shows the surfaces of two black bodies separated by a transparent medium.

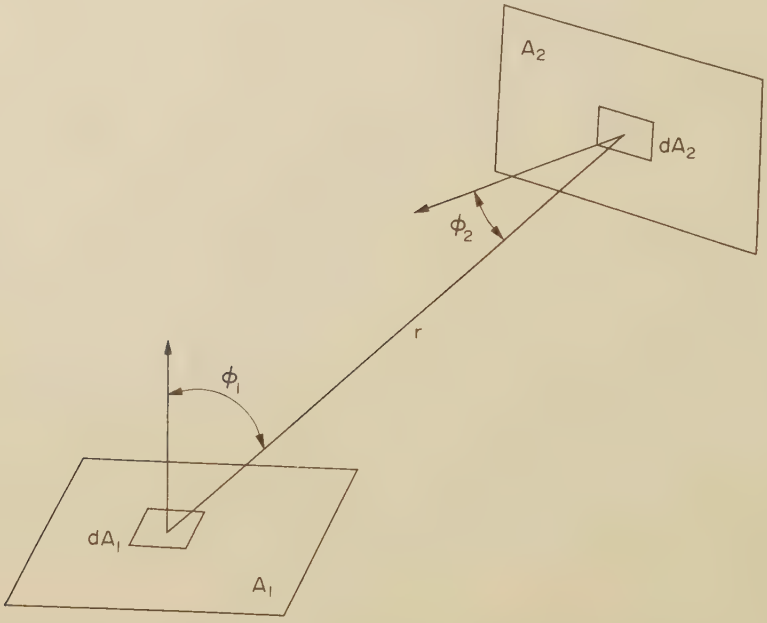

FIG. 6.2. Radiation between two elemental surface areas.

To determine the fraction of the energy radiated from surface A_1 that strikes surface A_2, consider the two elements dA_1 and dA_2, distance r apart:

$$dq_{12} = I \cos\phi_1 \, dA_1 \, d\omega_{12}, \tag{6.8}$$

where I_1 is the intensity of radiation from dA_1, $dA_1 \cos\phi_1$ = projection of area dA_1 as seen from dA_2, $d\omega_{12}$ is the solid angle subtended by dA_2 with respect to centre point of dA_1, but

$$d\omega_{12} = \cos\phi_2 \, dA_2 \, r^2$$

giving

$$dq_{12} = E_{b1} \, dA_1 \, (\cos\phi_1 \cos\phi_2 \, dA_2/\pi r^2), \tag{6.9}$$

and $\cos\phi_1 \cos\phi_2 \, dA_2/\pi r^2$ is the fraction of the total radiation emitted from dA_1 that strikes dA_2.

Similarly, $dq_{21} = E_{b2} \, dA_2 \, (\cos\phi_2 \cos\phi_1 \, dA_1/\pi r^2)$. The net rate of radiation between the two surfaces A_1 and A_2 will be

$$q = \left(E_{b1} - E_{b2}\right) \int_{A_1} \int_{A_2} \frac{\cos\phi_1 \cos\phi_2 \, dA_1 \, dA_2}{\pi r^2} .$$

This shows that the net rate of heat flow between two black bodies may be determined by evaluating the radiation from either to the other but replacing its emissive power by the difference between the emissive powers of the two surfaces.

If we divide the double integral by the total area of one of the surfaces the result is called the shape factor for the system evaluated on the basis of that surface. Thus shape factor on basis of area A_1 is

$$F_{12} = \frac{1}{A_1}\int_{A_1}\int_{A_2} \frac{\cos\phi_1 \cos\phi_2 \, dA_1 \, dA_2}{\pi r^2} \qquad (6.10)$$

F_{12} is the fraction of the total radiant energy leaving A_1 that is intercepted by A_2.

Thus

$$q = (E_{b1}-E_{b2}) F_{12}A_1 = (E_{b1}-E_{b2}) F_{21} A_2. \qquad (6.11)$$

If surface A_1 is totally enclosed by surface A_2 it can be seen that all of the net radiation that leaves A_1 will be intercepted by A_2, so that the shape factor F_{12} should be unity. This will be true unless some of the radiation from A_1 is intercepted by another part of A_1. In this latter case the true area A_1 may need to be corrected to become an effective area.

If the surfaces are opaque but not black the analysis becomes difficult because all of the incident radiation is not absorbed—some is reflected. The next simplest case is if the surfaces are grey. It is not intended to delve deeper into these fascinating complexities but of interest may be the simple case of radiation between two grey concentric spheres. Then net radiation becomes

$$q = (E_{b1}-E_{b2}) F_E F_{12} A_1, \qquad (6.12)$$

where

$$F_E F_{12} A_1 = \frac{1}{\rho_{r1}/A_1\varepsilon_1 + 1/A_1 + \rho_{r2}/A_2\varepsilon_2} \qquad (6.13)$$

and ρ_r = reflectivity and ε = emissivity (note, as surfaces are opaque, $\rho_r + \varepsilon = 1$).

Radiation may also occur from gases. Many common gases and gas mixtures, such as nitrogen, oxygen and hydrogen, have symmetrical molecules and are practically transparent to thermal radiation, they neither emit nor absorb appreciable amounts of radiation at temperatures of practical interest. However, some gases and vapours of interest, such as carbon dioxide, water vapour, carbon monoxide and hydrocarbons are not so neutral.

Gases do not radiate at all wavelengths but emit and absorb only in narrow regions of wavelength, called bands. Thus the radiation bands for carbon dioxide lie between wavelengths of 2.36 and 3.02μ,

4.10 and 4.80μ and 12.5 and 16.5μ; for water vapour between 2.24 and 3.27μ, 4.8 and 8.5μ and 12 and 25μ. Even if complete absorption/emission within these bands was achieved, i.e. the quantities of gas involved were sufficient to achieve black body conditions within these bands, the intensity of radiation (absorption) would only be a part of that obtained from an equivalent black body. At 473°K the parts would be 12% for carbon dioxide and 67% for water vapour, at 1273°K 10.5 and 46% respectively and at 2273°K 6 and 24%. These changes, which indicate that the intensity of gas radiation increases less rapidly with temperature than does black body radiation, are because the wavelength at which maximum intensity for black body radiation occurs become shorter as temperature rises, moving to shorter wavelengths than those at which the gas radiation occurs.

As is implicit in the statement above, gas radiation is not a surface phenomena as is usual for a solid body (apart from a few transparent substances and even these are relatively opaque). To calculate the radiation emitted or absorbed by a gas layer, its thickness, pressure and shape, as well as its surface area, must be taken into account.

If radiation of a single wavelength and intensity $I_{\lambda O}$ passes through a gas layer of thickness L, the radiant energy absorbed in a distance dx, distance x into the layer is

$$dI_{\lambda x} = -k'_{\lambda} \; I_{\lambda x} \, dx, \qquad (6.14)$$

where $I_{\lambda x}$ is the intensity at a distance x and k'_{λ} is the monochromatic absorption coefficient, a proportionality constant, value depending on pressure and temperature of the gas.

Integration between the limits x = 0 and x = L gives

$$I_{\lambda L} = I_{\lambda O} \, e^{-k'_{\lambda} L}. \qquad (6.15)$$

So energy absorbed by gas layer = $I_{\lambda O} - I_{\lambda L} = I_{\lambda O}\left(1 - e^{-k'_{\lambda} L}\right)$.
$\left(1 - e^{-k'_{\lambda} L}\right)$ = absorptivity $\alpha_{G\lambda}$ = emissivity $\varepsilon_{G\lambda}$ of the gas layer.
Such calculations would need to be done and summed over all the radiation bands. For large thicknesses, gas radiation approaches black body radiation within the wavelengths of the appropriate bands.

6.1.2 Radiation from Clouds of Solid Particles Such as Soot

A particle cloud may be treated as an absorbent medium similar to the gas layer described earlier, provided that the particles are large enough—compared with the radiation wavelength—not to produce scattering. The absorption coefficient of a suspension of black particles having a total particle surface per unit mass s and a total mass per unit volume C can be shown to be given by

$$k' = 0.25Cs. \qquad (6.16)$$

An isothermal cloud of grey particles may be replaced by an equivalent grey body. To do this the fraction of the energy emitted by each particle in the cloud which emerges from each element of area of the cloud boundary must be determined, making allowance for absorption on the way, and then it must be summed over all particles and all surface elements. Analytical solution is possible only in very simple cases and numerical methods must be used in others. It is found convenient to express the results in the form

$$E = 1 - e^{-fk' L}, \qquad (6.17)$$

where L is a chosen linear dimension and f a shape factor for the cloud. Some values are presented in Table 6.1 and Fig. 6.3 shows the resulting values of E[1]

TABLE 6.1. Approximate Emissivity of a Uniform Isothermal Cloud
Values of L and f for use in equation $E = 1-e^{-fk'L}$

Cloud shape	Linear dimension L	Values of f		
		k'L→0	k'L=1	k'L=2
Arbitrary convex cloud	Ratio of volume to surface	4	3.4	3.4
Sphere	Diameter	0.67	0.64	0.61
Cylinder	Diameter			
Height = dia.		0.67	0.61	0.55
Height = 5 dia.		0.91	0.82	0.75
Height ≫ dia.		1	0.91	0.84
Rectangular parallelepiped				
Cube	Edge	0.67	0.59	0.58
1:1:5	Shortest edge	0.91	0.77	0.68
1:1:∞	Shortest edge	1	0.85	0.75
1:∞:∞ (slab)	Thickness	2	1.5	1.4

Combustion of pulverised coal. (From Field et al.[1] by courtesy of the Institute of Fuel).

6.1.3 Convective Heat Transfer

When a fluid flows along a surface the fluid particles adjacent to the surface have zero velocity relative to the surface. Other fluid in the vicinity is retarded by viscous shear if the flow is laminar. If the flow is turbulent, retardation will be due to turbulent shear as well. A short distance from the surface the velocity of the fluid approaches that of the undisturbed free stream. The region of substantial velocity change is called the hydrodynamic layer. Even if the flow is turbulent there will be a very thin

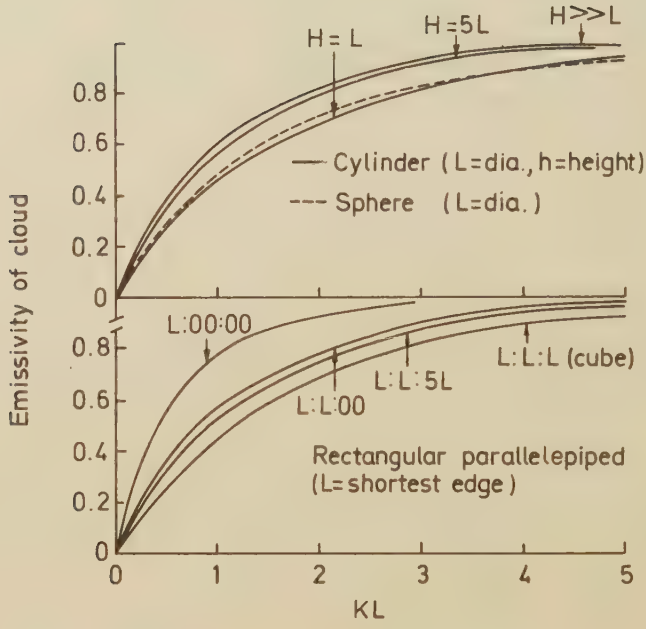

FIG. 6.3. Variation of the whole-body emissivity of a uniform cloud with shape. (From Field et al.[1] by courtesy of the Institute of Fuel.)

layer adjacent to the wall that is laminar—called the laminar sublayer.

From this brief description it may be deduced that very near to the surface heat can only flow by conduction through the stationary layer of fluid. Further from the wall the movement of the fluid helps heat transfer by transporting material and energy by turbulent motion. If the temperature gradient $\partial T/\partial y$ at the surface was known, the rate of heat transfer per unit area q/A would be $-k_f(\partial T/\partial y)_{(y=0)}$.

Usually this gradient is not known, and a heat transfer coefficient $\bar{h}_c$ is used so that, for a steady flow situation,

$$\frac{q}{A} = \bar{h}_c(T_s - T_\infty), \qquad (6.18)$$

where T_s is surface temperature and T_∞ is the bulk temperature of the fluid (usually the two temperatures known). Equating these two concepts and introducing a length L representative of the system leads to the relationship

$$\frac{\bar{h}_c L}{k_f} = \frac{-\left(\frac{\partial T}{\partial y}\right)_{(y=0)}}{\frac{(T_s - T_\infty)}{L}} \qquad (6.19)$$

$(\bar{h}_c L)/k_f$ is a dimensionless number, called the Nusselt number, and is the ratio of the temperature gradient at the surface to a representative temperature gradient of the system. If the value of the Nusselt number is known, then the convective heat transfer coefficient may be calculated from $\bar{h}_c = Nu(k_f/L)$. This shows that for similar systems the heat transfer coefficient will be inversely proportional to the significant length dimension.

There are a number of methods available for obtaining heat transfer coefficients, such as solving the boundary layer conditions, by analogy with mass and momentum transfer or by dimensional analysis combined with experiments. Unfortunately they tend to be applicable to much simpler systems than the internal combustion engine.

Nonetheless, it is of interest to note that such studies have been made and additional dimensionless groups have been found to be of value. One is the group $VL\rho/\mu$, the Reynolds number, and another is the Prandtl number $C_p\mu/k_f$, known as Re and Pr respectively. According to the principle of similarity the behaviour of two systems will be similar if the ratios of their linear dimensions, forces, velocities, etc., are the same. In geometrically similar systems with forced convection if the ratio of inertia forces to viscous forces, that is the Reynolds number, is the same the velocity fields will be similar. So similar flow conditions may be expected if the Reynolds number is the same for any two systems. Again, the ratio of kinematic viscosity μ/ρ, which affects the velocity distribution, to thermal diffusivity $k_f/\rho C_p$, which affects the temperature profile, gives the Prandtl number. So the Prandtl number may be regarded as a dimensionless group that relates temperature distribution to velocity distribution. The Nusselt number has already been shown to relate the temperature gradient at a fluid/surface interface to a reference temperature gradient. These three groups may therefore be expected to be interrelated, i.e. $Nu = f(Re, Pr)$.

The ideas developed above have been largely derived from steady flow considerations. Applying them to engine conditions may be thought to be a dubious procedure but in general has proved to be useful.

6.2 HEAT TRANSFER IN INTERNAL COMBUSTION ENGINES—A SURVEY

The processes inside the combustion chamber of an intermittent type engine are very complex, involving rapidly varying gas pressure and temperature and local fluid velocities which may also vary more or less rapidly. Heat flux into the walls varies throughout the engine cycle from a small negative value to a positive value reaching up to several megawatts per square metre, and also varies spatially due to differences in local gas temperatures and velocity and doubtless also due to differences in orientation of the wall to the radiating flames. As yet an adequate theoretical analysis of heat

transfer under these conditions has not been achieved although a number of studies aiming to improve this situation have taken place. Measurements of air movement in an engine cylinder have been made by Fitzgeorge,[2] Dent[3] and Tindal[4] during the compression stroke but not during combustion and expansion. Some attempt has also been made to predict convective heat transfer coefficients from air movement using momentum concepts.[5]

These studies do not deal with any effect due to combustion itself. At one time it was widely held that combustion would in itself produce a major increase in turbulence but recent studies indicate that this is not so.[6] However, local velocity changes can be caused by expansion of the hot burned products. In the spark ignition engine expansion of the charge produces a clearly defined difference between the rate of flame movement and the speed of propagation relative to the unburnt gas. Calculation for typical cases has given velocity changes due to this cause of the order of 10 m/s—quite large compared with fluid velocities normally found in this type of engine before the passage of the flame. This effect has also been shown by Summers[7] in a single-cycle engine simulator. Figure 6.4 shows the effect observed in which combustion increased Nusselt number considerably. Similar effects are expected in compression ignition engines. In indirect injection engines, in particular, the air motion produced by expansion is deliberately channelled and consequently produces high local velocities, and so convective heat transfer. Henein[8] presents some observations on an engine with an energy cell combustion system with analysis showing high values of heat transfer associated with charge velocities of the order of 500 m/s. In direct injection engines charge motion produced by combustion is much smaller and less well defined.

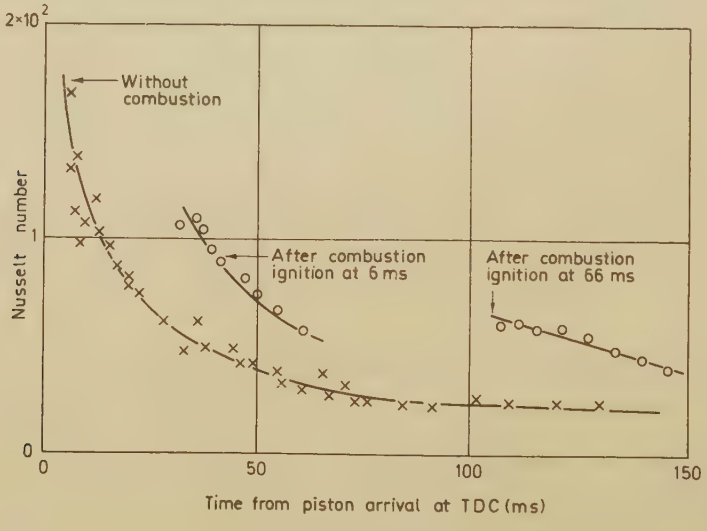

FIG. 6.4. Nusselt number variation with time, with and without combustion, in single-cycle simulator.

At one time convective heat transfer was considered to be by far the major form with radiation relatively small, perhaps negligible. The importance of radiation, at least in the compression ignition engine, is now firmly established, even if calculation on this basis is not yet usual.

Radiant heat transfer in the spark ignition engine has been investigated less than it has been in the compression ignition engine. Under the usual conditions of homogeneous deflagration no solid intermediate products are formed and only gas phase radiation has to be considered—effectively radiation from carbon dioxide and water vapour. Some assessments have given typical maximum effective emissivity about 0.1, with maximum radiant flux of half a megawatt per square metre and total maximum flux of 10 times this. As radiation diminishes much more rapidly than convection as temperature falls during expansion, the overall effect could be of negligible radiation relative to convective heat transfer.

These assessments have been quoted from Annand[6] who adds that although this view may be correct it is not substantiated, and there are grounds for doubt, such as that radiation from the flame itself has not been calculated, radiation from carbon dioxide and water vapour was based upon data obtained at lower partial pressures than exist in engine cylinders and the non-uniformity of cylinder temperature and non-equilibrium cylinder conditions may affect the result. Nonetheless, radiation from premixed flames is normally much less than from diffusion flames, and this seems to be borne out by experience of premixed combustion in the compression ignition engine, Lyn and Valdamis.[9]

For the compression ignition engine there is a considerable amount of published evidence showing that radiation can account for an appreciable fraction of the total. Thus Oguri,[10] Flynn[11] and Sitkei[12] agree in showing measured radiant heat transfer amounting to between 20% and 30% of the total, averaged over the complete engine cycle. Belinkii[13] made measurements on a small, open-chamber engine and concluded that the diesel engine flame radiated as a grey body within the rather narrow range of wavelengths covered by his experiments. He showed emissivities ranging from 1.0 at top dead centre down to about 0.6 at 50° after top dead centre. The similar but more extensive work by Flynn[11] gave a somewhat non-grey distribution. Typical observations are shown in Fig. 6.5.

So far calculation of radiation from consideration of soot cloud density and size and temperature has hardly begun although Annand[6] has made some tentative suggestions towards this end, with the flame treated as a grey body in a black box, filling the box so that form factors are not needed. Even so, soot temperature and quantity has to be estimated, and neither is as yet readily calculable though knowledge is accumulating (see Khan[14]).

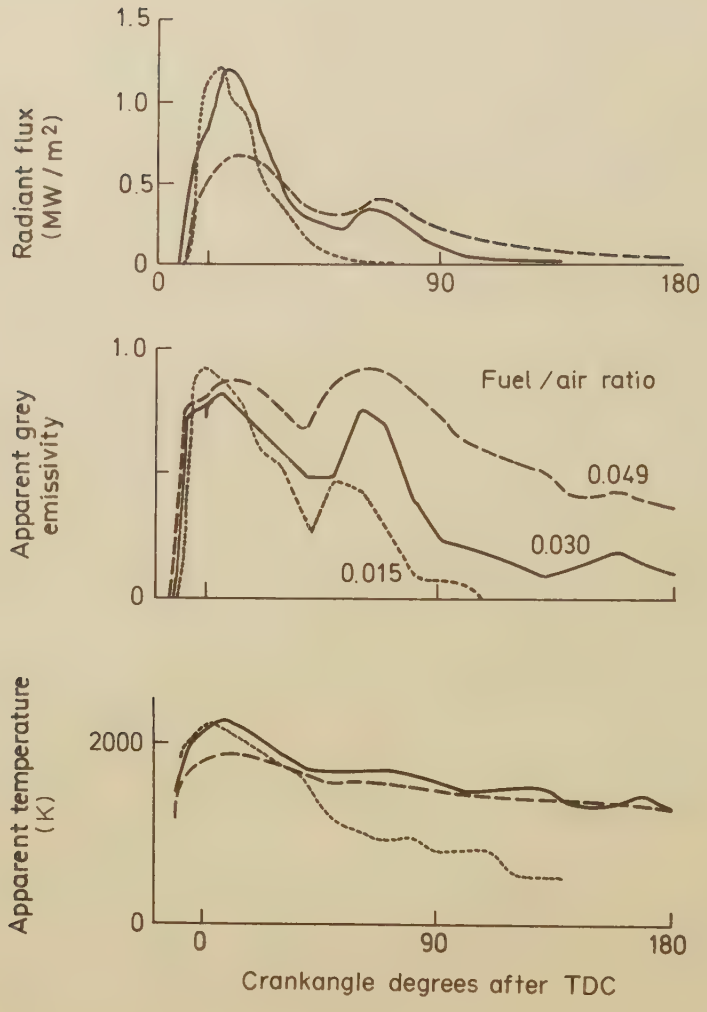

FIG. 6.5. Typical observations of radiant heat transfer in a diesel engine. (From Flynn et al.[11] by courtesy of the Society of Automotive Engineers.)

6.3 HEAT TRANSFER IN INTERNAL COMBUSTION ENGINES—SOME PRACTICAL CONSIDERATIONS

Heat transfer in engines may be considered in two ways:
(1) the overall effect which provides, if the engine is running at a

steady load and speed, a nominally steady, or mean, rate of heat loss to the combustion chamber walls and hence to a coolant; (2) the instantaneous rates that occur during a cycle of events in the engine cylinder. The second way may be integrated with respect to time to give the first. This second way is of particular interest as it is involved in the thermodynamic cycle calculations considered in Chapters 8 and 9. It also allows for a more detailed and deeper study of the heat transfer process than does the overall approach, and so gives the hope of better predictive value in the future, even though there is doubt at present. As the attempts to tackle the problem fundamentally have not yet arrived at conclusions of practical value, as may be deduced from the previous section, semi-empirical studies that have been found useful will be dealt with hereafter.

Such studies have been based mainly on temperature measurements in components forming the combustion chamber walls. These may be steady values, obtained throughout a component, from which isothermals may be drawn as outlined in Chapter 11, and mean heat fluxes deduced; or surface transient temperatures may be obtained and instantaneous heat fluxes into the combustion chamber surfaces calculated. Figure 6.6 shows typical variations in surface temperature in a medium speed engine and Fig. 6.7 the resultant calculated instantaneous heat flux diagram.

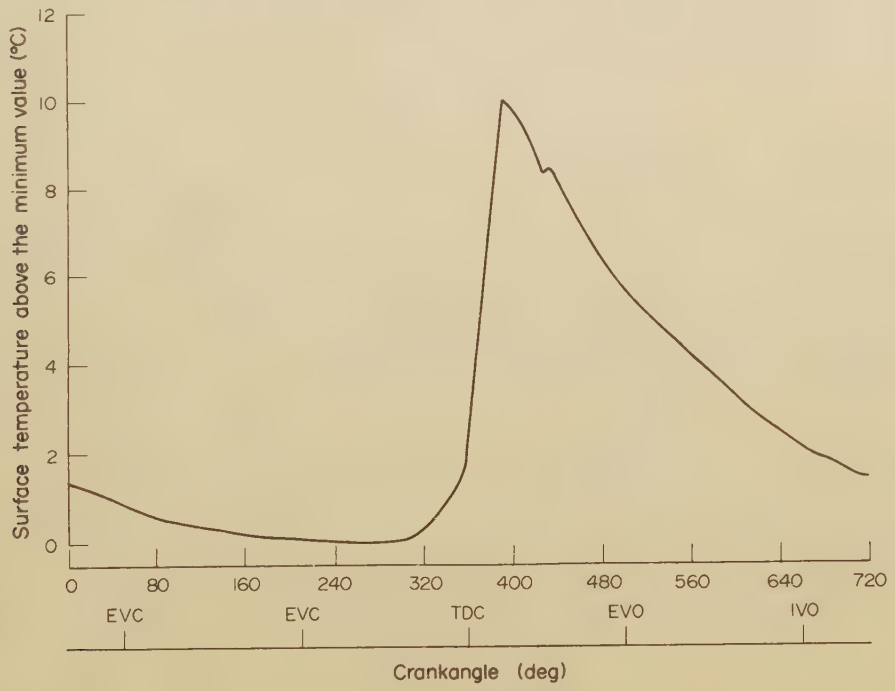

FIG. 6.6. Typical values of cyclic variation of surface temperature on cylinder head of diesel engine (b.m.e.p. 10 bar).

The fluctuation in temperature at the surface is rapidly reduced to a steady state value within a few millimetres of the surface. Typical calculated values of temperature are shown in Fig. 6.8 to illustrate this.

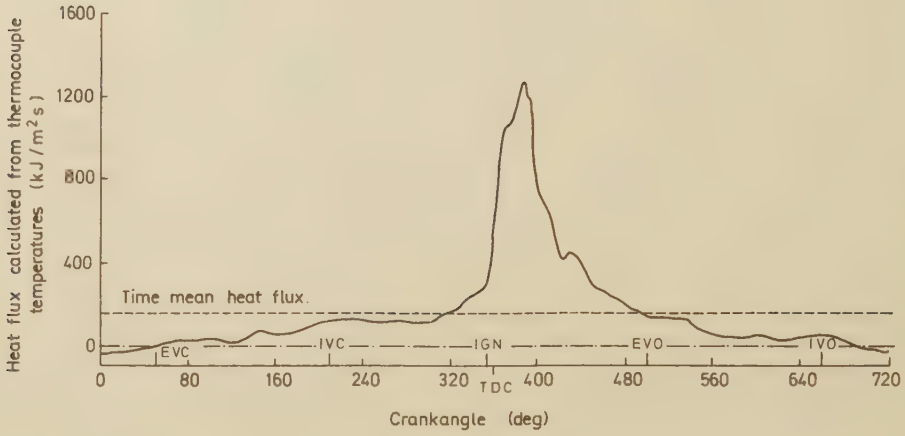

FIG. 6.7. Instantaneous heat flux at cylinder head thermocouple. (From Whitehouse,[28] by courtesy of the Institution of Mechanical Engineers.)

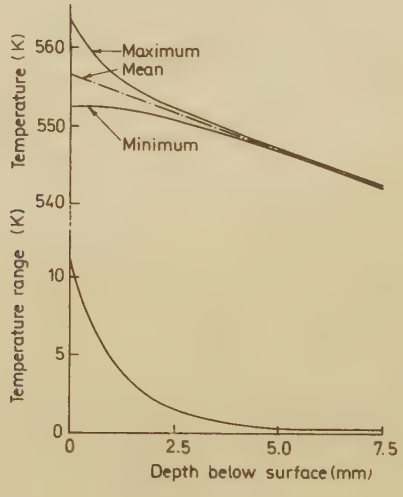

FIG. 6.8. Cyclic temperature variation in surface region of a piston crown. (From Whitehouse et al.,[15] by courtesy of the Institution of Mechanical Engineers.)

For most practical purposes the component temperatures may be taken to be the steady state values. Only rarely have the surface thermal stresses been considered to be worthy of consideration, as in one case of piston thermal loading.[15] These steady state temperatures vary widely within components, depending both upon the heat transfer into the component from the burning substances, which is our main concern, and upon the component design, particularly cooling arrangements, which is a major concern of the engine designer.

Figures 6.9-6.12 illustrate these points showing component temperatures in a medium speed two-stroke diesel engine with different piston-cooling arrangements and with two different cooling fluids (oil and water). These also show heat flux lines, normal to the isothermals, which show the direction of flow of heat through the component. The heat flux per unit area at the combustion chamber surfaces can be evaluated from such diagrams if the conductivity of the component is known.

The design engineer may use empirical information of this sort, but for prediction of heat transfer in a new engine, improvement on such direct empiricism is sought. Semi-empirical models in use are mainly based upon single-zone models of the combustion process in which it is assumed that the cylinder temperature and other factors are uniform. The method can be extended to multi-zone models. These semi-empirical models will now be examined.

6.4 INSTANTANEOUS HEAT TRANSFER CALCULATIONS

The methods outlined in the following sections show how calculations are usually performed—for practical engineering purposes—if estimates of instantaneous values are required. These methods are all dependent upon an estimate of the instantaneous conditions in the engine combustion chamber, and in practice usually form part of cycle calculations such as those shown in Chapters 8 and 9. It is also assumed that the ideas generated from the steady flow convective heat transfer concepts given in the first part of this chapter are valid for each instant of time, i.e. quasi-steady calculations are correct. This concept has been challenged by Overbye[16] who has shown that the heat flux and the overall driving temperature difference will normally be out of phase. However, the shift in phase is unlikely to be of importance and the quasi-steady approximation is unlikely to be bettered in the foreseeable future. It may also be noted that other deficiencies of greater significance can arise from the assumptions used—such as mean gas temperatures when reality involves a complex mixture of gases at different temperatures.

6.4.1 Single-zone Heat Transfer Calculations

As a matter of historical interest reference may be made to some of the numerous investigators who have reported on work of this kind (refs. 17-22). Annand's paper[23] gives a critical examination of much of the earlier published work, using dimensional analysis to indicate fundamental weaknesses in various equations put forward for

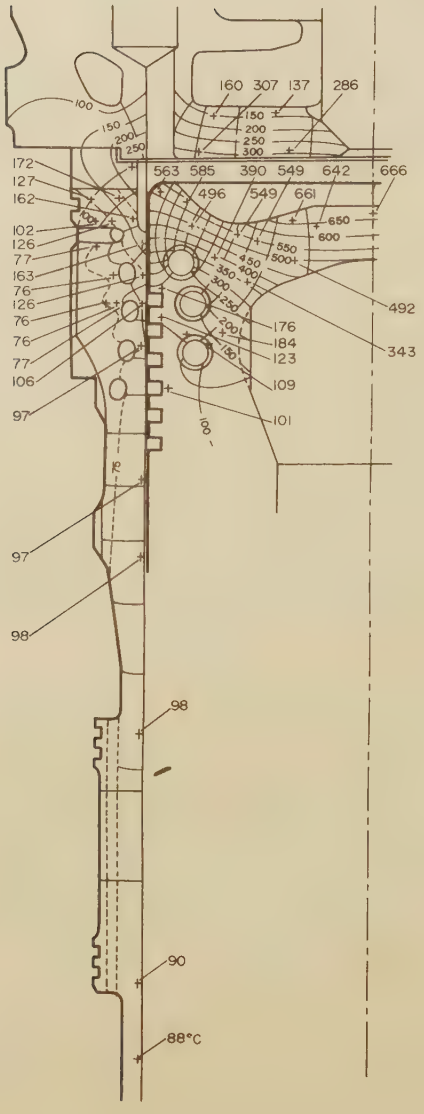

FIG. 6.9. Two-stroke engine : isothermal chart of cylinder head, liner and water-cooled piston. (From Steiger and Aue[40] by courtesy of the Institution of Mechanical Engineers.)

Engine operating data:

b.m.e.p.	6.2 bar
Mean piston speed:	7.5 m/s
Supercharging pressure:	1.0 at a
Relative air weight:	6.6 kg/h.p.h.
Scavenging air temp.:	44°C
Cooling water temp.(outlet):	62°C
Cooling oil temp.(inlet):	40°C

Remark:

Heat flow lines are spaced 2000 kcal/h apart

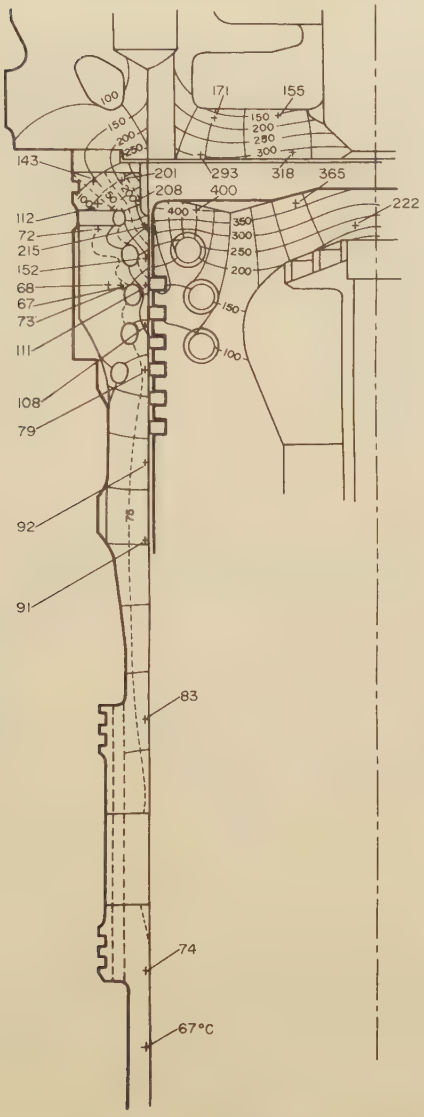

FIG. 6.10. Two-stroke engine : isothermal chart of cylinder head, liner and oil-cooled piston. (From Steiger and Aue,[40] by courtesy of the Institution of Mechanical Engineers.)

Engine operating data:		Remark
b.m.e.p.:	10.2 bar	Heat flow lines are
Mean piston speed:	7.0 m/s	spaced 2000 kcal/h
Supercharging pressure:	2.4 at a	apart
Relative air weight:	6.3 kg/h.p.h.	
Scavenging air temp.:	45°C	
Cooling water temp.(outlet)	65°C	
Cooling oil temp.(inlet)	40°C	

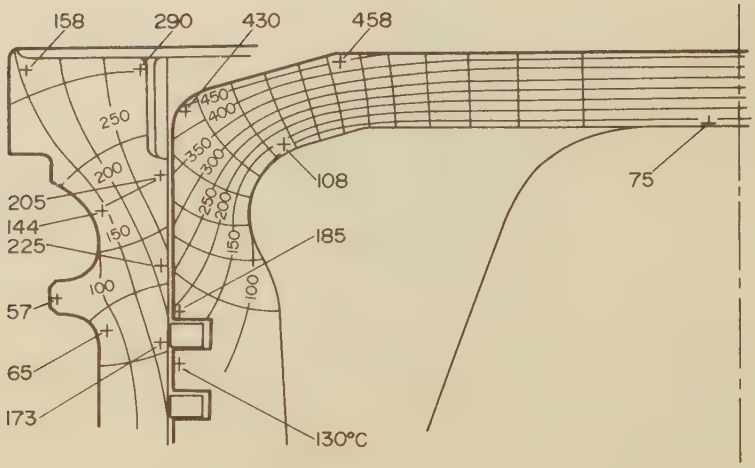

FIG. 6.11. Two-stroke engine : isothermal chart of water-cooled piston and liner. (From Steiger and Aue,[40] by courtesy of the Institution of Mechanical Engineers.)

Engine operating data:		Remark
b.m.e.p.:	9.7 bar	Heat flow lines are
Mean piston speed:	6.1 m/s	spaced 10,000 kcal/h
Supercharging pressure:	2.1 at a	apart
Relative air weight:	6.9 kg/h.p.h.	
Cooling water temp.(outlet)	57°C	
Piston cooling water temp. (outlet)	45°C	

heat transfer calculations and proposing a more satisfactory alternative.

Few of the multitude of formulae referred to are now of much more than historical interest. Three have been of use to the authors in cycle calculations at various times and are known to be still in use. These are by Eichelberg, by Annand and by Woschni, i.e.

$$\text{Eichelberg} \quad \frac{q}{A} = 10.47 \times 10^{-3} \, v_p^{\frac{1}{3}} \, (pT)^{\frac{1}{2}} \, (T_g - T_w) \quad \text{kJ/m}^2\text{s} \qquad (6.20)$$

$$\text{Annand} \quad \frac{q}{A} = a \frac{k}{D} (Re)^b \, (T_g - T_w) + c(T_g^4 - T_w^4), \text{ where } Re = \frac{\rho v_p D}{\mu}. \qquad (6.21)$$

$$\text{Woschni} \quad \frac{q}{A} = C_3 \, D^{-0.2} \, p^{0.8} \, T_g^{-0.53} \, (C_1 v_p + C_2 \frac{VT'}{p'V'}(p - p_o))^{0.8} \, (T_g - T_w). \qquad (6.22)$$

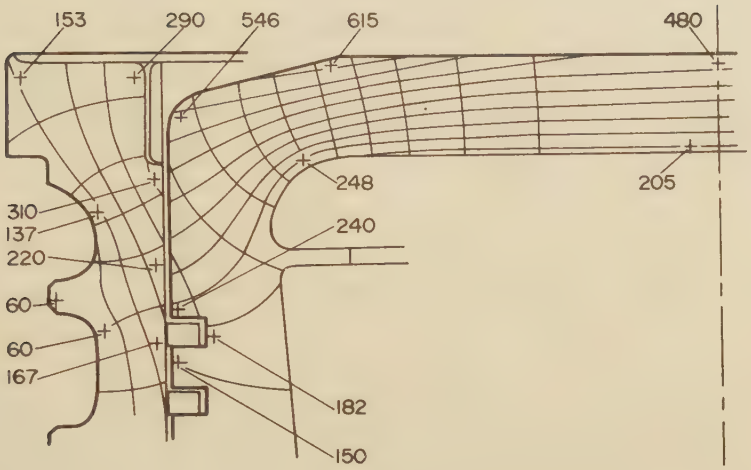

FIG. 6.12. Two-stroke engine : isothermal chart of oil-cooled piston and liner. (From Steiger and Aue,[40] by courtest of the Institution of Mechanical Engineers.)

Engine operating data:

b.m.e.p.:	9.7 bar
Mean piston speed:	6.1 m/s
Supercharging pressure:	2.1 at a
Relative air weight:	6.9 kg/h.p.h.
Scavenging air temp.:	30°C
Cooling water temp.(outlet):	57°C
Piston cooling oil temp. (outlet):	45°C

It may be noted that Eichelberg's equation has the virtues of simplicity and explicitness. There are no unknown or variable constants so it is very easy to use. It is not dimensionally homogeneous and many of the relationships appear quite arbitrary. To use such a formula in conditions outside those where experience of its reliability has been gained is therefore questionable. Modified versions, with different values of the initial constant have been used.

The Annand and Woschni expressions although different in form are both based largely on turbulent convection considerations. Annand shows that the Prandtl number for the gases forming engine cylinder contents will be approximately constant at a value of 0.7, claims that the Reynolds number is the major parameter affecting convection and that the convective heat transfer relationship may be represented by $(Nu) = a(Re)^b$, where a and b are constants. This gives the first term in Annand's equation. The second is a straightforward radiation term assuming grey body radiation.

Woschni's equation is also based upon a similar forced convection model, with the index b specified as 0.8, as for turbulent flow in pipes. The constant C_3 is a number obtained from Hausen's equation[25] for turbulent flow in pipes. The Reynolds number is replaced by pressure and temperature relationships for the gases, so that the equation is in the parameters normally used. From the above considerations Woschni's expression for the heat transfer coefficient would be

$$h_c = C_3 D^{-0.2} p^{0.8} w^{0.8} T_g^{-0.53}, \quad (6.23)$$

where w is the local average gas velocity,

$$= C_1 v_p. \quad (6.24)$$

The value of the constant C_1 was obtained from experiments with a motored four-stroke diesel engine with two inlet valves and no swirl. During combustion and expansion, however, radiation and additional combustion-induced turbulence is allowed for by adding on a velocity $w_c = (C_2(VT'/p'V'))(p-p_0)$, where the pressure difference term is the difference between cylinder pressure with combustion and cylinder pressure at the same point in the cycle, for the same conditions except for the absence of any combustion.

Both the Annand and the Woschni formulae have constants which may be adjusted to give reasonable overall heat transfer values, and this can be useful if experience or available information is adequate. Some values of the constants that have been used are given at the end of the chapter.

It should be noted that the gas temperature is the mean value for the cylinder, whereas in reality the cylinder contents are not homogeneous. These formulae have been used with single-zone cycle calculation models, and that anomalies should become apparent between calculation and experience is not unexpected. One such anomaly is that heat transfer to the cylinder walls would apparently be evenly distributed both in time and place. This has been found not to be so. Reference may be made to papers by Seale and Taylor,[26] Annand and Ma[27] and Whitehouse[28] which illustrate these points.

Figure 6.13 from the last of these three papers shows another apparent anomaly whereby instantaneous heat fluxes obtained under a variety of operating conditions are found to have much less variation in maximum values than would be expected from single-zone calculation using Annand's equation.

Accepting that any of the heat transfer equations mentioned is best thought of as unreliable except in so far as experience justifies its use and in particular the use of given values of the constants involved, it may also be remarked that for performance calculations a high accuracy is not of very great significance.

The authors must acknowledge a prejudice, compounded partly of local patriotism and greater experience, in favour of the use of the Annand equation. It may also be defended on the grounds that it does separate, as logically one should, the convective and the

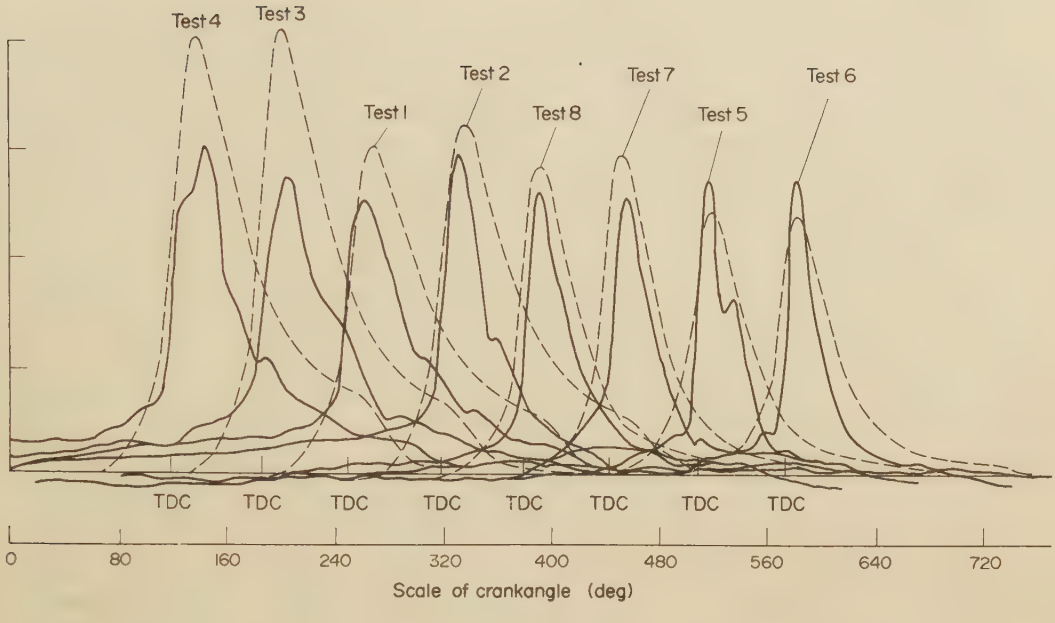

FIG. 6.13. Instantaneous heat fluxes for a range of conditions. (From Whitehouse,[28] by courtesy of the Institution of Mechanical Engineers.)

radiative components of heat transfer. Calculations with the single-zone model tend to suggest that radiation is small. The experience of some research workers suggest that it is not. Ebersole et al.[29] indicate that radiation may comprise up to 40% of the total heat transfer and mention is made by Borman et al.[30] of instantaneous values of perhaps 70% during combustion. Such quantities are thought due to radiation from hot soot particles at temperatures well above the mean gas temperature. This would also agree with comments by Alcock[31] that changes in wall temperatures have much less effect on heat transfer than would be expected from mean gas temperature considerations.

These various effects are not unexpected if the heterogeneity of engine combustion and the fourth power effect of temperature on radiation is considered.

6.4.2 Multi-zone Heat Transfer

These considerations inevitably lead to the conclusion that only a multi-zone model of the happenings in the engine cylinder during combustion and expansion can hope to produce calculations valid

enough for heat transfer to be estimated at novel conditions. This conclusion reinforces the trend towards multi-zone models for performance and pollution calculation.

As radiative heat transfer is believed to be important and as the zone temperatures in a multi-zone model are relatively very high during combustion, the importance of a heat transfer formula that deals directly and explicitly with radiation, using the fourth power of temperature relationship, is obvious. Of the formulae considered earlier, that due to Annand, or some modification of it, is undoubtedly superior. It also provides, incidentally, for both spark ignition and diesel engines.

There is comparatively little published material on multi-zone modelling (two or more). There is even less that deals with any explicitness with the heat transfer aspects of such models. Thus Shahed et al.[32] mention that heat transfer (from the cylinder contents) is calculated based on a bulk average temperature, using an Annand type correlation, with total heat transfer apportioned to the various zones in relation to their mass and temperature. Heat transfer between zones has not been modelled. Bastress et al.[33] calculated total heat transfer to the walls using a simple formula $\dot{Q} = C_4 A(T_h - T_w)$, where C_4 was a mean heat transfer coefficient, and then divided this quantity among the different zones in proportion to their volumes. Whitehouse et al.,[34, 35] with a two-zone model, calculated radiation from the burning zone to the combustion chamber walls, assuming radiation from the total surface of the burning zone. Convective heat transfer was calculated from both zones where contact was made with the walls. It was assumed that heat transfer between the zones did not occur. Annand's equation was used for the heat transfer calculations.

This use of the total surface area of a number of burning jets for radiation calculations is excessive as each jet will have some of its radiation intercepted and absorbed by the other jets. This sort of problem has been mentioned earlier in this chapter and the theoretical method of determining a shape factor indicated. Unfortunately, determination of shape factors for such complex shapes is difficult. As heat transfer by radiation as at present calculated is anyway very approximate, and the surface area and shape factor change for every step of a cycle calculation, some simple approach is required.

Saadawi[36] has used a simple "effective area" approach for this purpose. Considering black body radiation, to avoid difficulties with reflection, etc., from a hot body totally enclosed in a container, it is obvious that all the radiation is absorbed by the container irrespective of its size, so the distance from body to walls may be made large, if desired, without change to the heat radiated. Consider the radiation reaching some small area A_s of the large container. In the limit the area receives the same radiation from the body as it would from an area equal to the projection of the surface of the body on the plane normal to the line joining body and area A_s and at the centre of the body.

The actual body may thus be imagined to be replaced by a number of such projected areas. It is then necessary to determine the

appropriate number and orientation of such areas that will approximate to the original body.

Should the body be a sphere the surface area of the body would be $4\pi r^2$ and the surface area of any projected area would be πr^2. Thus any four projected areas would represent the sphere appropriately. Making the assumption that the same number would be appropriate for other shapes it is necessary to choose the most representative orientations. Saadawi chose projections from vertically above and vertically below the combustion chamber, horizontally in line with one jet and horizontally at right angles to that same jet. A three-jet model is shown in Figs. 6.14 and 6.15, before and after impingement, to illustrate the technique.

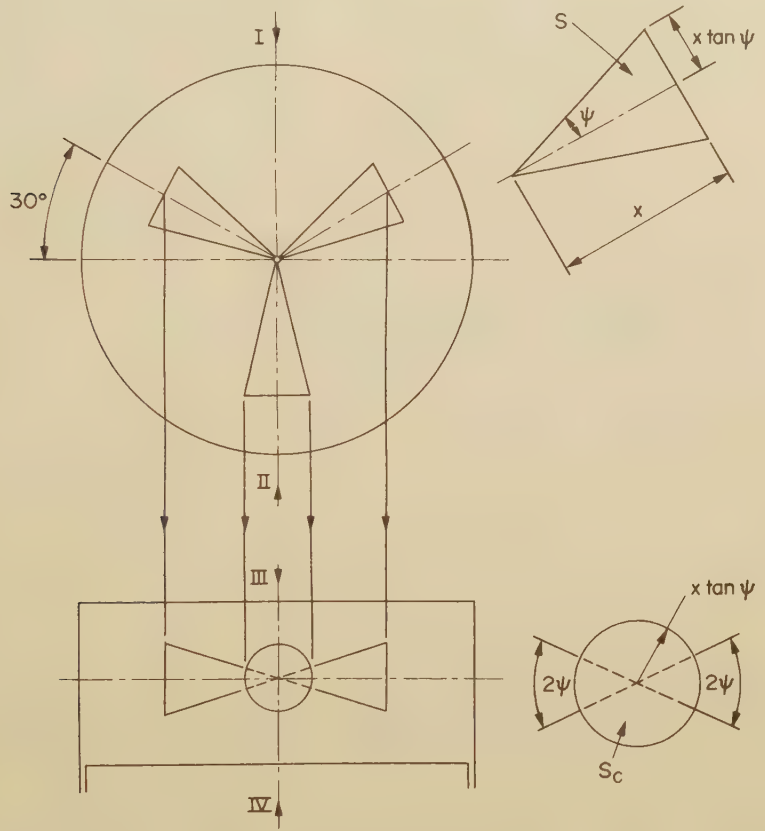

FIG. 6.14. Model for heat transfer calculations before impingement.

6.5 NUMERICAL VALUES

The value of the constants in the Annand equation for heat transfer, quoted earlier, have usually been chosen to suit empirical data, often to give overall percentage heat transfer of the correct order by comparison with estimates from steady state heat

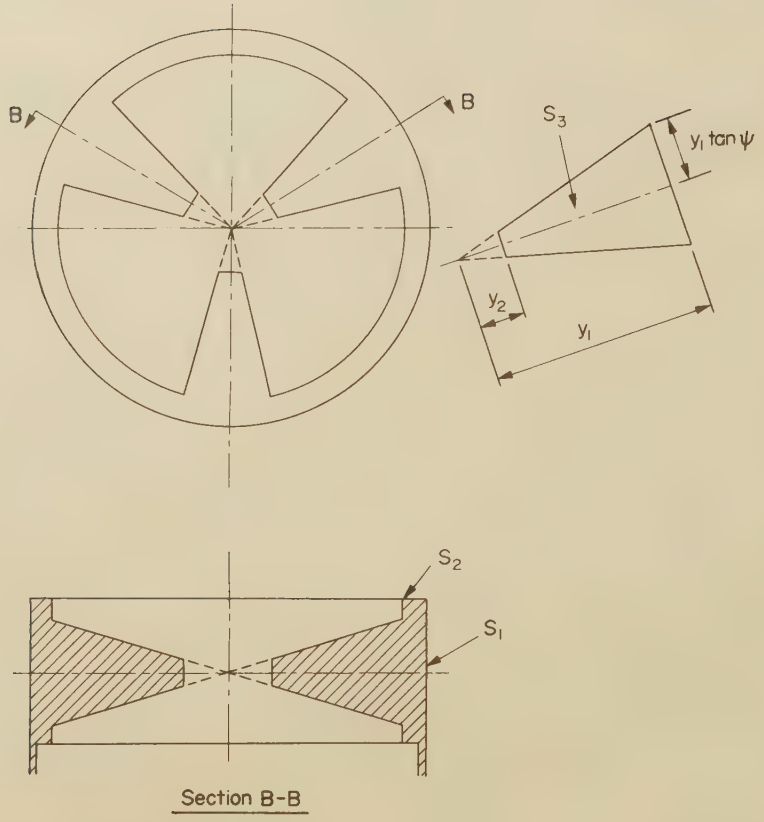

FIG. 6.15. Model for heat transfer calculations after impingement.

TABLE 6.2

Annand coefficients engine	Ref.	a	b	c
				J/s m^2 K^4
Two-stroke	(23)	0.76	0.64±0.10	3.03±1.06 x 10^{-8}
Four-stroke	(23)	0.26	0.75 0.15	3.88±1.39 x 10^{-8}
Foden FD6 (2-S)	(37)	0.3-0.5	0.7	3.28 x 10^{-8}
Rolls-Royce, K6O	(37)	0.3	0.7	
Dorman 4LBT	(37)	0.2	0.7	
Mirrlees National FV2	(37)	0.06	0.85	
Mirrlees National FV2	(37)	0.4	0.7	

balances.[37] Annand himself gave estimates based upon an analysis of a limited amount of published data. Such data is summarized in Table 6.2.

In considering these values it must be remembered that there is a considerable interaction between a and b. Thus the two sets for the Mirrlees National FV2 engine are alternative ways of achieving almost the same effect.

The values of c used with the single-zone combustion model give very low values of heat transfer by radiation, in line with beliefs current when the formula was first proposed.

Awbi,[38] comparing Woschni's formula with Annand's for heat transfer in a four-stroke medium speed engine (the Mirrlees National FV2), found they gave similar results. Woschni had given values of $C_3=3.715\times10^{-5}$, $C_2=10.63\times10^{-3}$ ft/s ^{o}C and $C_1 = 2.28$ during compression and expansion and 6.18 during the gas exchange period. Awbi used the same ratio between C_1 and C_2 but varied C_1 to give the same mean heat transfer as did the Annand equation. This resulted in $C_1 = 4.83 \pm 0.3$. These units gave heat transfer in CHU/ft^2 s K with D in feet, p_{in} lbf/in and v_p in ft/s. Converting to J/m metres, bars and m/s we have, for the Awbi values

$$\frac{q}{A} = 7.54\, D^{-0.2}\, p^{0.8}\, T_g^{-0.53} \left[(4.83 \pm 0.3) v_p + \left[(2.12 \pm 0.13) 10.63 \frac{VT'}{p'V'} (p-p_o) \right] \right]^{0.8} (T_g - T_w). \qquad (6.25)$$

REFERENCES

1. Field, M.A., Gill, B.W., Morgan, B.B. and Hawksley, P.G.W., Combustion of Pulverised Coal, British Coal Utilisation Research Association, Leatherhead, 1967.

2. Fitzgeorge, D. and Allison, J.L., Air swirl in a road vehicle diesel engine, Proc. Auto. Div., Instn. Mech. Engrs. 4, 151 (1962-3).

3. Dent, J.C. and Derham, J.A., Air motion in a four-stroke diesel injection diesel engine, Proc. Instn. Mech. Engrs. 188, 259 (1974).

4. Tindal, M.J., Williams, T.J. and Elkhafaj, A.H.A., Gas flow measurements in engine cylinders, SAE Paper 740719 (1974).

5. Knight, B.E., The problem of predicting heat transfer in diesel engines, Proc. Instn. Mech. Engrs. 179, 99 (1964-5).

6. Annand, W.J.D., Heat transfer from flames in internal combustion engines, International Seminar on Heat Transfer from Flames, Trogir, Yugoslavia (International Centre of Heat and Mass Transfer, Belgrade, 1973).

7. Summers, I.G.S., Convective heat transfer in a rapid compression machine simulating a spark ignition engine, M.Sc. thesis, University of Manchester, 1970.

8. Henein, N.A., Instantaneous heat transfer rates and coefficients between the gas and combustion chamber of a diesel engine, SAE Paper 968B (1965).

9. Lyn, W.T. and Valdamis, E., The application of high speed Schlieren photography to diesel combustion research, J. Photogr. Sci. 10, 74 (1962).

10. Oguri, T. and Ho Hsi-Tang, Radiant heat transfer in the cylinder of diesel engine, Japan Auto. Res. Inst. Tech. Memo No. 2, 263 (1971).

11. Flynn, P., Mizusawa, M., Uyehara, O.A. and Myers, P.S., An experimental determination of the instantaneous potential radiant heat transfer within an operating diesel engine, SAE Paper 720022 (1972).

12. Sitkei, G. and Ramaniah, G.V., A rational approach for calculation of heat transfer in diesel engines, SAE Paper 720027 (1972).

13. Belinkii, L.M., Thermal radiation in the combustion chamber of a high speed compression ignition engine, Trudi NILD No. 1, Moscow (1955).

14. Khan, L.M., Greeves, G. and Probert, D.M., Prediction of soot and nitric oxide concentrations in diesel engine exhaust, Conference on Air Pollution Control in Transport Engines, Proc. Instn. Mech. Engrs. 205 (1971).

15. Whitehouse, N.D., Stotter, A. and Gray, C., Piston thermal loading, Proc. Instn. Mech. Engrs. 179, Part 3C, 158 (1964-5).

16. Overbye, V.D., Bennethum, J.E., Uyehara, O.A. and Myers, P.S. Unsteady heat transfer in engines, Trans. SAE 69, 461 (1961).

17. Nusselt, W., Die Warmeubergang in den Gasmachinen, ZDVI 361, 414, 459 (1914).

18. Nusselt, W., Die Warmeubergang in den Verbrennungs-kraftmachinen, ZDVI 67, 692 (1923).

19. Eichelberg, G., Temperaturverlauf und Warmespanning in Verbrennungsmotoren. Forsch. Ing. Wes. 263 (1923).

20. Eichelberg, G., Some new investigations on old combustion engine problems, Engineering 149, 463, 547 (1939).

21. Oguri, T., On the coefficients of heat transfer between gases and cylinder walls of the spark ignition engine, Bull. Jap. Soc. Mech. Engrs. 2, 384 (1959).

22. Pflaum, W., Heat transfer in internal combustion engines, La Termotecrica N4 (April), Italy, (1963).

23. Annand, W.J.D., Heat transfer in the cylinders of reciprocating internal combustion engines, Proc. Instn. Mech. Engrs. 177, 973 (1963).

24. Woschni, G., A universally applicable equation for instantaneous heat transfer in the internal combustion engine, SAE Paper 670931 (1967).

25. Hausen, H., Warmeubergragung in Gugenstrom, Gleichstrom und Kreuzstrom, Springer-Verflag, Berlin, 1950.

26. Seale, W.J. and Taylor, D.H.C., Spatial variation of heat transfer to pistons and liners of some medium speed diesel engines, Proc. Instn. Mech. Engrs. 185, 203 (1970-1).

27. Annand, W.J.D. and Ma, T.H., Instantaneous heat transfer rates to the cylinder head surface of a small compression ignition engine, Proc. Instn. Mech. Engrs. 185, 976 (1970-1).

28. Whitehouse, N.D., Heat transfer in a quiescent chamber diesel engine, Proc. Instn. Mech. Engrs. 185, 963 (1970-1).

29. Ebersole, G.D., Myers, P.S. and Uyehara, O.A., The radiant and convective components of diesel engine heat transfer, SAE Paper 701C (1963).

30. Borman, G.L., Myers, P.S., Uyehara, O.A., Some problem areas in engine simulation, SAE Paper 710172 (1971).

31. Alcock, J.F., Introductory address, Symposium on Thermal Loading of Diesel Engines, Proc. Instn. Mech. Engrs. 179, Part 3C (1964).

32. Shahed, S.M., Chiu, W.S. and Lyn, W.T., A mathematical model of diesel combustion, in Combustion in Engines, p.119, Institution of Mechanical Engineers (1975).

33. Bastress, E.K., Chang, K.M. and Dix, D.M., Models of combustion and nitrogen oxide formation in direct and indirect injection compression-ignition engines, SAE Paper 719053 (1971).

34. Whitehouse, N.D., and Sareen, B.K., Prediction of heat release in a quiescent chamber diesel engine allowing for fuel/air mixing, SAE Paper 740084 (1974).

35. Whitehouse, N.D. and Abughres, S.M., Calculation of fuel/air mixing in a diesel engine with swirl for the purpose of heat release prediction, in Combustion in Engines, p.147, Institution of Mechanical Engineers, (1975).

36. Saadawi, H.N.H., Digital simulations of the closed part of a diesel engine cycle considering dissociation and equilibrium thermodynamics, MSc thesis University of Manchester, (1975).

37. Whitehouse, N.D. and Way, R.J.B., A simple method for the calculation of heat release rates in diesel engines based on the fuel injection rate, SAE Paper 710134 (1971).

38. Awbi, H.B., Instantaneous heat transfer in a medium speed diesel engine, MSc thesis, University of Manchester, 1969.

39. Kreith, F., Principles of Heat Transfer, 2nd edn., International Text Book Co. (1965).

40. Steiger, A. and Aue, G.K., The influence of the thermal loading criterion on the design of turbocharged two stroke diesel engines, Proc. Instn. Mech. Engrs. 179, Part 3C, 68 (1964-5).

Appendix I

Experimental Methods

Notation

c	specific heat
G_n	Fourier coefficient
h	Planck constant
I	intensity of light
k	thermal conductivity
K_n	Fourier coefficient
n	harmonic number
Q	heat transfer rate
r	coordinate
R	resistance
T	temperature
V	electrical potential, voltage
x	coordinate
y	coordinate
z	coordinate
α	thermal diffusivity
λ	wavelength
ω	angular frequency
ρ	density
ν	frequency

Our understanding of the thermodynamic processes in internal combustion engines depends on accurate experimental work. In this appendix we describe some methods currently in use to elucidate the phenomena occurring in engines. It is not intended to describe the range of equipment for engine testing (these are well reviewed by Ricardo and Hempson[1]) or to discuss in detail the accuracy of electronic measurements in internal combustion engines unless they specifically refer to the influence of the accuracy on thermodynamic analysis. The proceedings of an excellent conference on the accuracy of electronic equipment has been published by the Institution of Mechanical Engineers.[2] Nor will we describe electronic circuitry, since modern developments in this area would render description out of date. In this chapter we shall outline the principles of the instrumentation and some typical designs manufactured and tested in the authors' laboratories. We shall also refer to instrumentation developed by others and to the standard equipment now required for emissions, although for a comprehensive description of this equipment the reader is referred to the book by Patterson and Henein.[3]

The most common equipment is the pressure transducer since this enables us to study the pressure changes throughout the cycle. Special problems arise in recording the pressure accurately and analysing the subsequent record. Since these are critical to the successful analysis of the thermodynamic processes, we shall discuss the installation of transducers and the methods of recording in some detail. We shall follow with temperature measurement. This is extremely difficult, and complex equipment is normally required; we shall describe some methods successfully applied by recent workers. Studies of combustion processes involve high speed photography, gas sampling, flame speed measurement and spectrographic techniques—some of the methods in current use—will be described. Finally, we conclude with the special instrumentation used for gas analysis; this can be equally used with sampled gas from the cylinder or exhaust pipe emissions.

I.1 PRESSURE MEASUREMENT AND RECORDING

The measurement of cylinder pressures has been of interest to engineers since the birth of the steam engine for which the Watt indicator was developed. In the early days of the internal combustion engines the Watt indicator was used, but as the engine speeds increased the frequemcy response of this and similar types of indicator, as well as passage effects,militated against their use, and alternative methods have been developed. It is now widely recognized that the most satisfactory method of recording cylinder pressure is with an electrical transducer. In this type of transducer the deflection of a diaphragm subjected to the cylinder pressure is recorded electrically. For cylinder pressure

measurement the piezoelectric transducers are favoured since its frequency response and linearity hold over a wider range. Its major disadvantages are temperature drift causing a lack of pressure reference stability[4] and low electrical output. Extreme care must be taken in the correct installation of piezoelectric transducers to avoid overheating which will cause the quartz elements to break up, producing loss of sensitivity, severe electrical leakage and drift. In all cases these transducers are water-cooled.

For accurate pressure recording the transducers should be located flush with the cylinder wall surface. Unfortunately under these conditions the impingement of fuel or a hot flame causes thermal shock which produces a distortion in the pressure record similar to that shown in Fig. I.1. The expansion line drops often

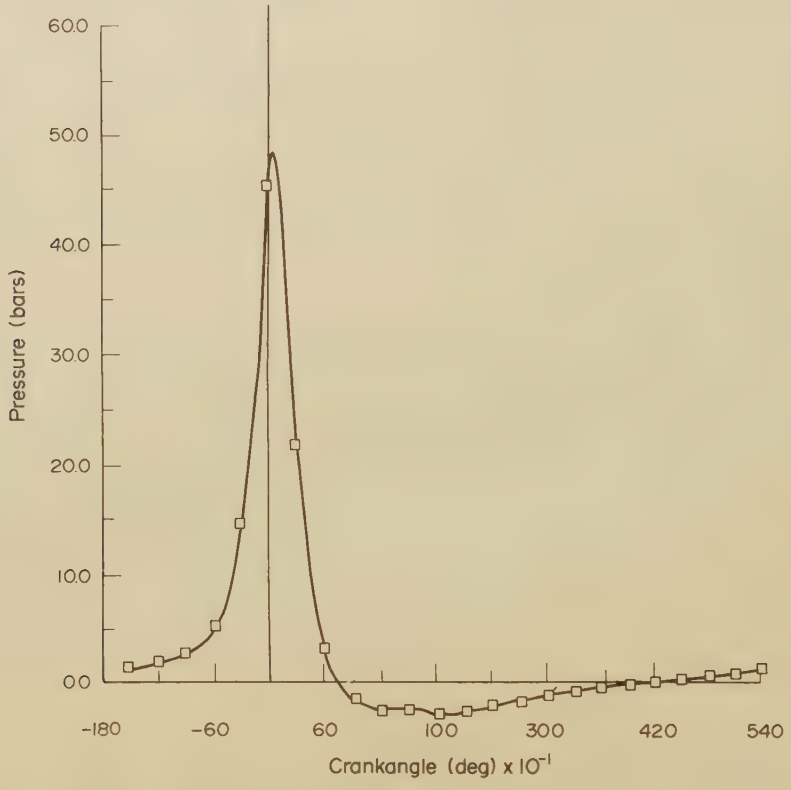

FIG. I.1. Effect of defective transducer or thermal shock.

to an apparent pressure below absolute zero, with recovery of the diaphragm during the gas exchange period. An analysis of a diagram taken with thermal shock may give an i.m.e.p. less than the b.m.e.p. To eliminate thermal shock a flame trap can be fitted in front of the diaphragm.[4] To allow for the zero drift which causes instability in the pressure reference level the authors have developed a two- or three-pressure transducer system. In the

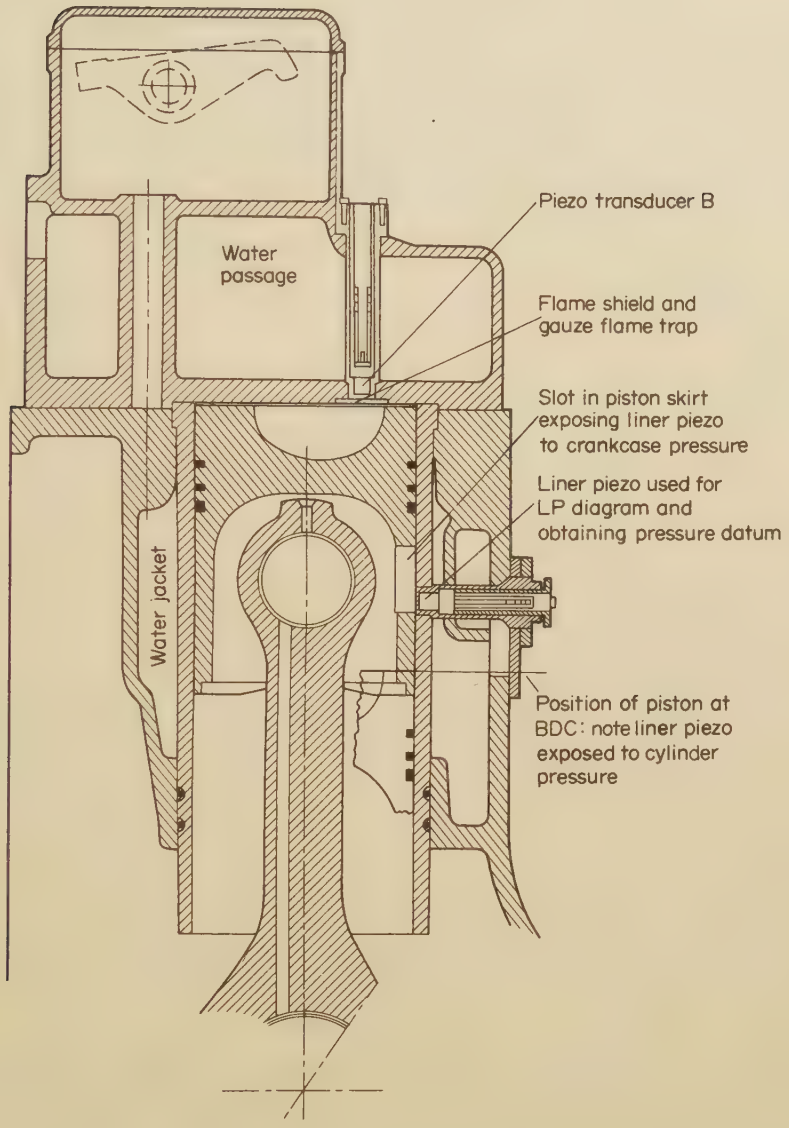
Piezo transducer B
Water passage
Flame shield and gauze flame trap
Slot in piston skirt exposing liner piezo to crankcase pressure
Liner piezo used for LP diagram and obtaining pressure datum
Water jacket
Position of piston at BDC: note liner piezo exposed to cylinder pressure

FIG. I.2. Location of pressure transducers.

example shown in Fig. I.2 one transducer (HP) is located in the combustion space and the second (LP) is located in the liner approximately mid-stroke position. The LP transducer is exposed for part of the stroke to the cylinder pressure and for part of the stroke it is in communication with the crankcase. A third transducer may be fitted in the crankcase. Since this transducer is not subject to zero drift, it can be used to set the baseline for the LP transducer when the latter is exposed to the crankcase pressure. The LP transducer is then used to calibrate the baseline

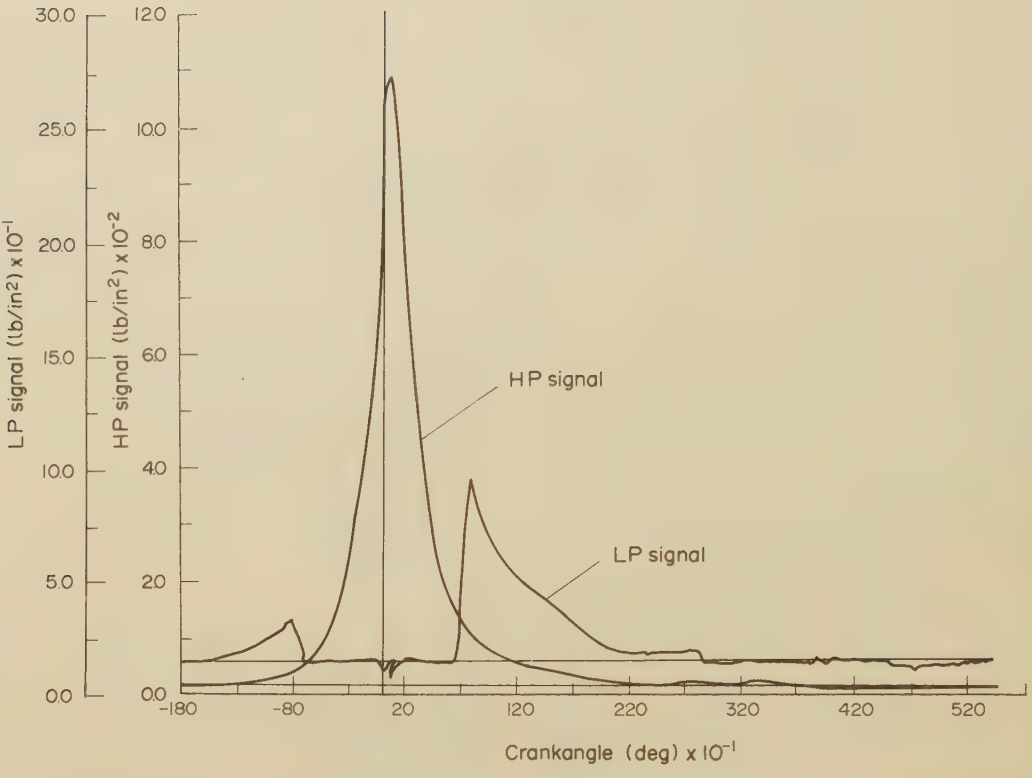

FIG. I.3. Typical cylinder pressure diagram direct output from on-line computer. (From Benson and Pick,[4] by courtesy of the Society of Automotive Engineers.)

for the HP transducer. A typical record is shown in Fig. I.3. In addition to the accurate measurement of the pressure, the phasing of the diagram is also critical. In the authors' laboratories an optical encoder is used. This is essentially a perspex disc with some 720 apertures on the periphery for the passage of light. A photocell is located on one side of the disc and a lamp on the other. There is one reference aperture which is lined up to one cylinder bottom dead centre—the final adjustment being made with the engine running with the aid of a stroboscope.

The accurate recording of the pressure is most important if a successful understanding of the cylinder phenomena is to be obtained. The signal may be recorded on a cathode ray oscillograph and subsequently photographed or the signal directly processed on an on-line computer. In this system the analogue signal is converted into digital impulses at fixed crankangles in an analogue to digital

converter (ADC). The digital signal is then transmitted to the computer where it is stored. It is immediately processed as soon as all the data for one or any number of cycles have been completed as requested. The processing may be in the form of a pressure crankangle diagram or a pressure volume diagram or a heat release crankangle diagram. A full discussion of the techniques is given by Benson and Pick[4] from which two figures are taken to illustrate the influence of zero drift (Fig. I.4) and incorrect timing (Fig. I.5) on the cumulative heat release diagrams for a compression ignition engine.

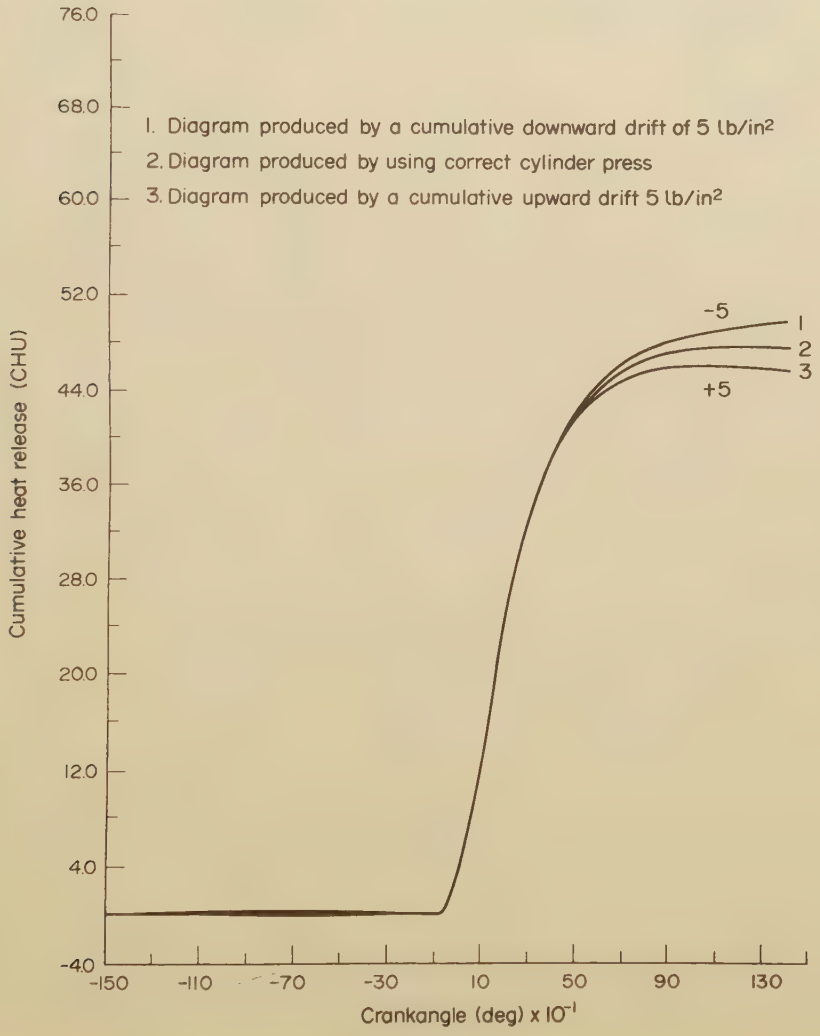

FIG. I.4. Effect of h.p. piezo drift on the cumulative heat release diagram. (From Benson and Pick[4] by courtesy of the Society of Automotive Engineers.)

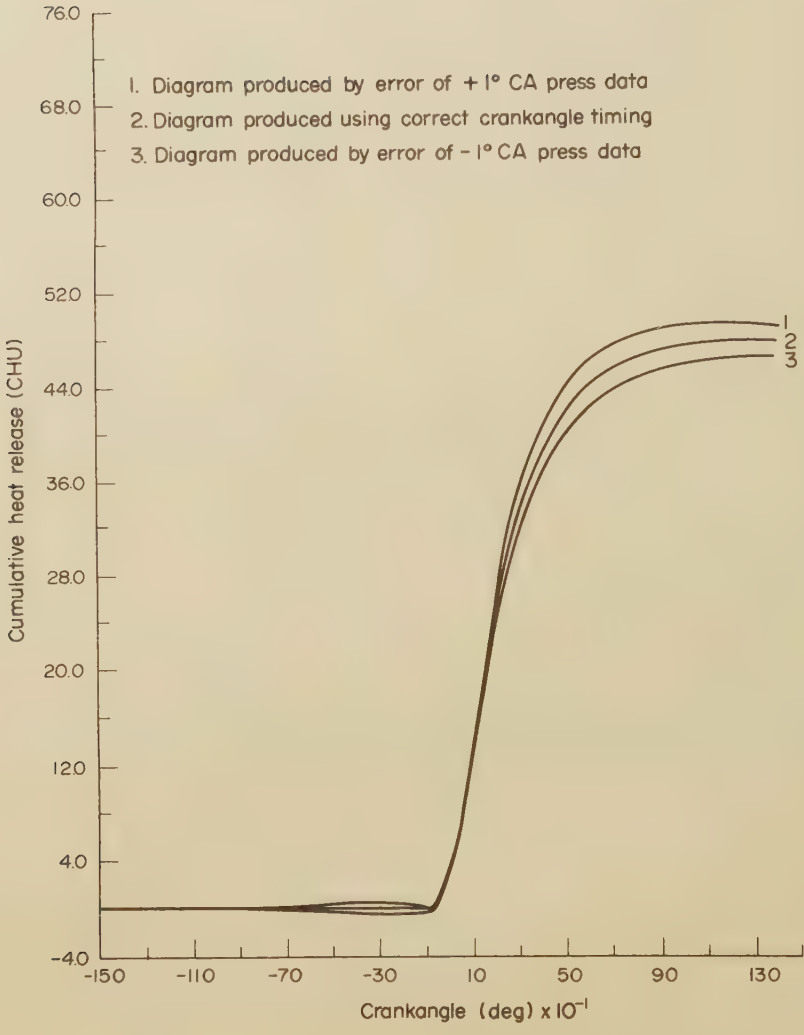

FIG. I.5. Effect of crankangle error on the cumulative heat release diagram. (From Benson and Pick,[4] by courtesy of the Society of Automotive Engineers.)

For pressure measurements in the intake and exhaust systems it is usual to use inductive transducers or strain gauge transducers. Both types of transducer must be water-cooled not only to reduce temperature drift but also to preserve transducer life.

I.2 TEMPERATURE MEASUREMENT AND RECORDING

We are interested in both surface temperature measurements as well as gas temperatures. The former are required for heat transfer studies. Because of the rapidly fluctuating temperatures the measuring techniques are complex and different approaches have to be made if the cylinder temperature is required, or the exhaust gas, or the cylinder surface fluctuating temperature, or the component mean temperature. We shall first discuss the cylinder surface temperature measurement techniques, then follow with methods for measuring mean temperature at a point following by an analogue method for using these measurements to calculate heat flow. We shall then turn to a method for measuring the cylinder gas temperature and conclude with exhaust temperature measurements.

I.2.1 Component Temperature Measurement

At the cylinder surface—gas side—the temperature fluctuates with time, but a short distance from the surface the temperature is constant. Separate techniques are therefore required for the two locations. For surface measurement a thin film thermocouple may be used (Fig. I.6). A small plug is inserted in the cylinder wall or piston surface. The plug is bored at the axis and a coated nickel wire inserted. The nickel oxide coating acts as an insulator. A junction is then made between the nickel wire and the plug with a 5×10^{-5} mm nickel film deposited under a pressure of 1×10^{-5} mmHg absolute. Details of the method are given by Benson and Pick.[5] The signals from the piston thermocouples are normally conveyed through a link mechanism of the type shown in Fig. I.7. Wires from the thermocouple pass via a C spring through a stainless steel tube as an oscillating link. Thence the wires pass a second C spring to an outside connector. A typical piston surface temperature record is shown in Fig. I.8.

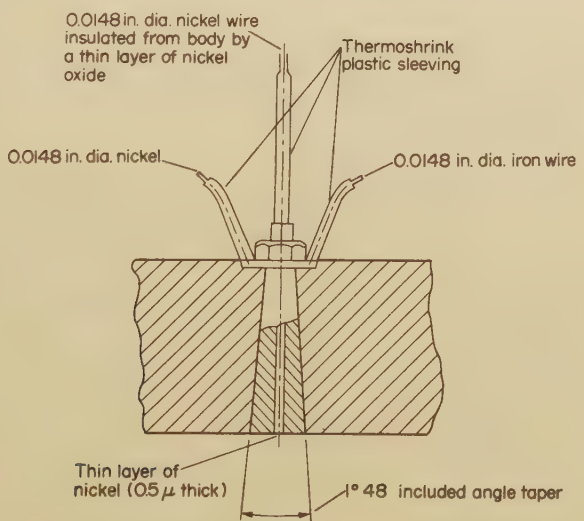
0.0148 in. dia. nickel wire insulated from body by a thin layer of nickel oxide
Thermoshrink plastic sleeving
0.0148 in. dia. nickel
0.0148 in. dia. iron wire
Thin layer of nickel (0.5 μ thick)
1° 48 included angle taper

FIG. I.6. Piston and liner surface thermocouple.

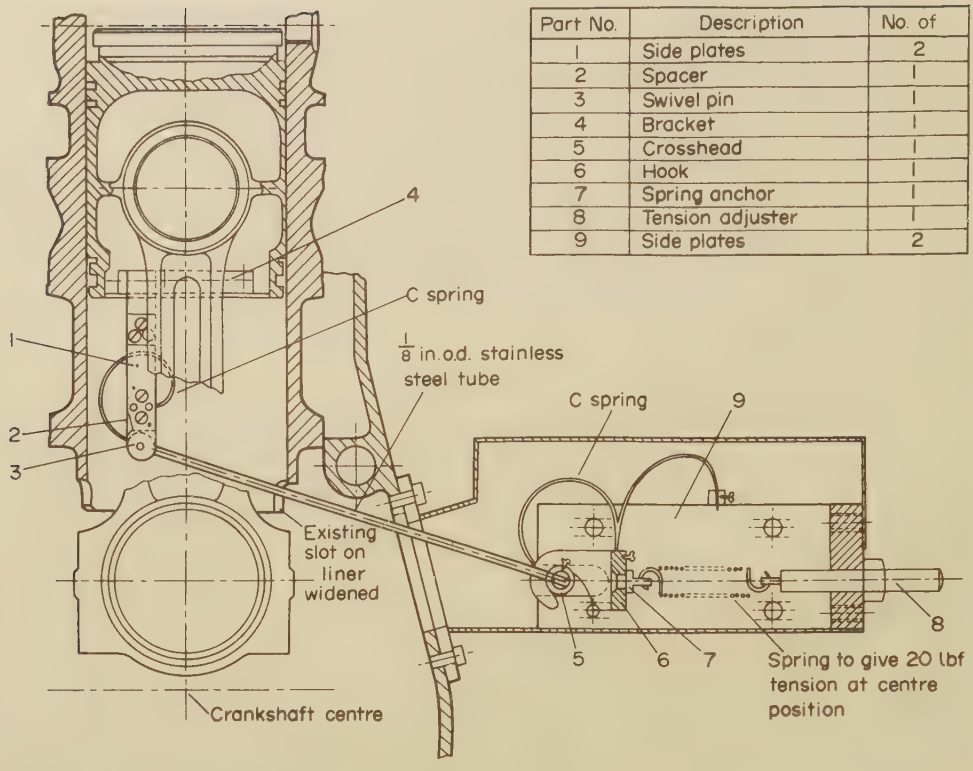

FIG. I.7. Link mechanism for recording piston surface temperatures.

The instantaneous heat flux Q through the cylinder wall surface (liner, cylinder head or piston crown) can be computed from a diagram of the type shown in Fig. I.8(a) if we can assume that heat flux is normal to the surface.

The theoretical background is given in standard textbooks.[19] It can be shown that the one-dimensional heat flow normal to the surface can be represented by the following two expressions:

$$Q = -k\left(\frac{\partial T_x}{\partial x}\right)_{x=0} \quad \text{energy units/unit area/unit time,} \qquad (a)$$

$$\frac{\partial T_x}{\partial t} = \alpha\left(\frac{\partial^2 T_x}{\partial x^2}\right), \qquad (b)$$

where T_x is the temperature of the wall material at a location x from the cylinder surface at time t, α is the thermal diffusivity of

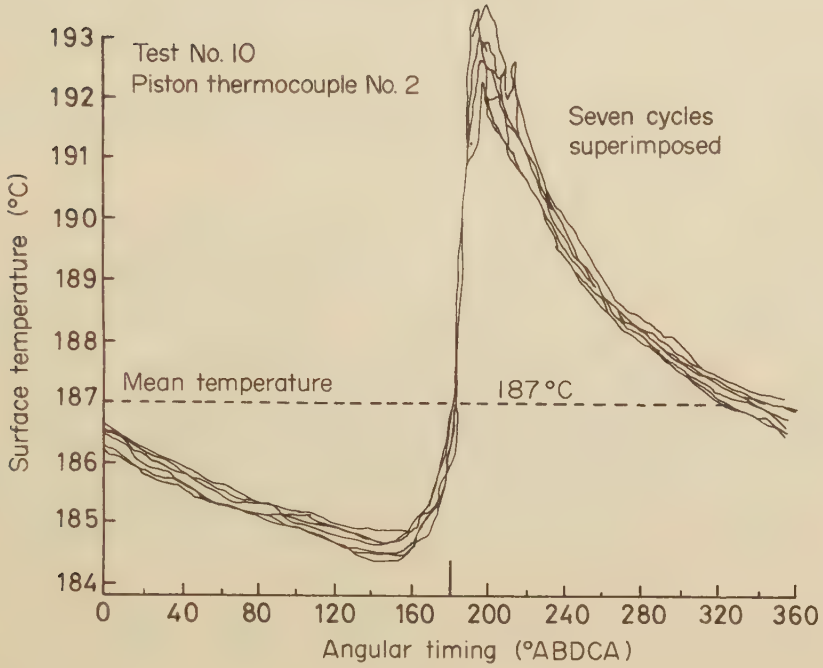

(a) Cyclic piston surface temperature

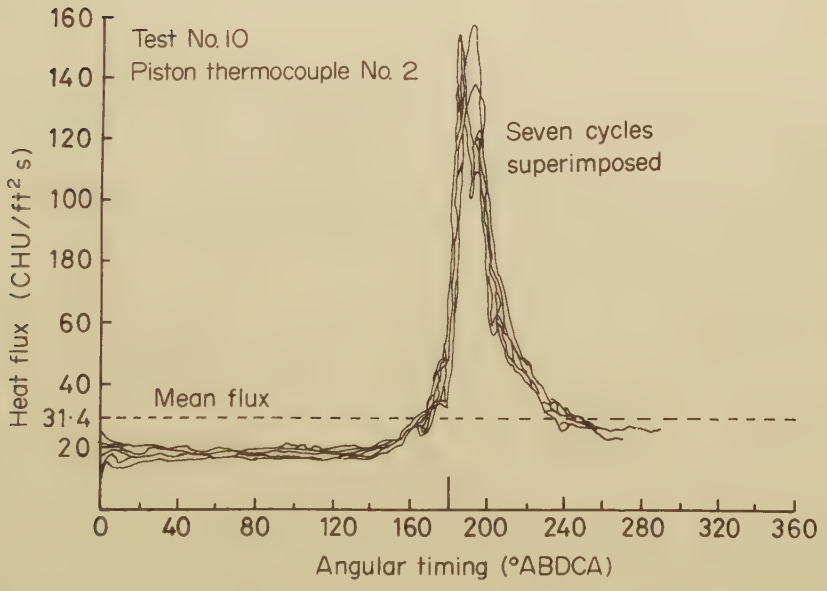

(b) Cyclic heat flux through piston

FIG. I.8. Cyclic piston surface temperature and heat flux. (From A.G. Law.[29])

the wall material given by $\alpha = k/\rho c$, and the density ρ, specific heat c and thermal conductivity k of the material are assumed to be constant.

The boundary conditions at the inner and outer wall can be represented by expressions of the form:

At $x = 0$, cylinder wall;

$$T_x = T_w = T_{wm} + \sum_{n=1}^{\infty} \left(K_n \cos n\omega t + G_n \sin n\omega t \right).$$

At $x = a$, coolant surface:

$$T_x = T_c = T_{cm} = \text{constant},$$

where T_{wm} is the time mean wall temperature in the cylinder at the point under consideration and T_{cm} is the time mean wall temperature at the coolant surface, K_n and G_n are Fourier coefficients, ω is the angular frequency equal to 2π times the cycle repetition rate, and n is the harmonic number.

Integration of the temperature differential equation (b) with the above boundary equations and substitution in the heat flux equation (b) gives the following expression for the heat flux:

$$Q = \frac{k}{a} \left(T_{wm} - T_{cm} \right) + k \sum_{n=1}^{n=\infty} r \left((G_n - K_n) \sin \omega t + (G_n + K_n) \cos \omega t \right),$$

where $r = n\omega/2\alpha$.

Law[20] has indicated that if a Fourier analysis is made of a temperature diagram of the type shown in Fig. I.8(a) with up to n = 90 harmonics, taking sample points at two-degree intervals, an accurate representation of the wall temperature may be made. Typical results are shown for the heat flux in Fig. I.8(b) taken from Law's work.[20] The heat flux and temperature curves correspond to the same test.

Two methods may be used to measure the steady temperature in the component. For a stationary component, Ricardos[1] have developed the traversing thermocouple. In Fig. I.9 an adaptation of Ricardo's thermocouple is shown to measure the temperature gradient in the bottom deck of a cylinder head.[21] It is important in this method that the plug on which the thermocouple is mounted is in contact with the surface. An alternative method used in the authors' laboratory was developed by the Shell Thornton Research Centre. This method makes use of the hardness temperature relationship for special alloy steels. Certain alloys undergo changes of hardness when subjected to elevated temperatures over a period of time. The hardness remains when the alloy returns to normal temperature so that by measuring the hardness the elevated temperature can be inferred. These alloys are used in the form of small screwed plugs called templugs. The plugs are screwed in the component whose temperature is required; the temperature of the component is measured at the point of contact of

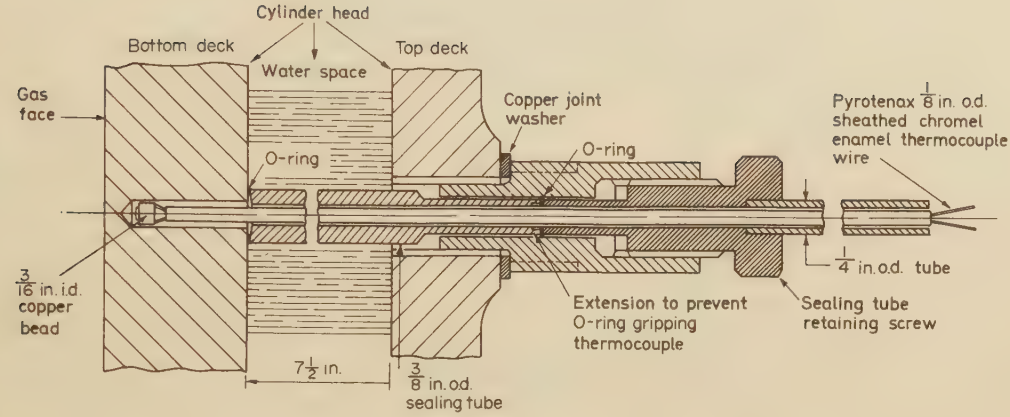

FIG. I.9. Modified Ricardo traversing thermocouple arrangement. (From Brock and Glasspoole,[21] by courtesy of the Institution of Mechanical Engineers.)

the plug and the component. In Fig. I.10 templug positions are shown in a piston in the thrust section. The engine is run at a steady load and speed for a fixed period of time after which the plugs are removed and their hardness measured. If sufficient plugs are fitted the heat flow through the component can be computed either numerically or by using an electrical analogue. In both methods the isothermals in the component are constructed to agree with the measured temperature. We shall describe the analogue method.

The analogue method is based on the similarity of the heat conduction equation and the electrical potential equations. For steady state the conduction equation, using r, z, θ coordinates, is, for axisymmetry,

$$\frac{\partial^2 T}{\partial z^2} + \frac{1}{r}\frac{\partial^2 T}{\partial r} + \frac{\partial^2 T}{\partial r^2} = 0,$$

and, for electrical potential (V),

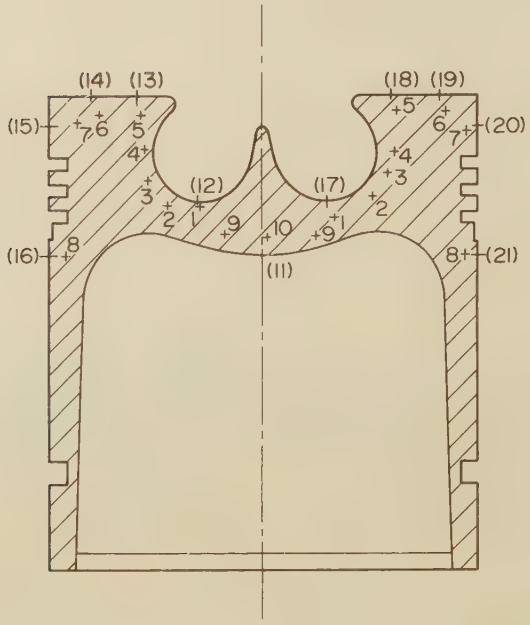

FIG. I.10. Templug positions in piston section thrust plane.

$$\frac{\partial^2 V}{\partial z^2} + \frac{1}{r}\frac{\partial V}{\partial r} + \frac{\partial^2 V}{\partial r^2} = 0.$$

Thus there is a direct analogy between T and V.

We shall illustrate the method, initially, with respect to a two-dimensional system, and then indicate how a three-dimensional system can be set up.

The two-dimensional equations for T and V in the x, y plane are

$$\frac{\partial^2 T}{\partial x^2} + \frac{\partial^2 T}{\partial y^2} = 0 \quad \text{and} \quad \frac{\partial^2 V}{\partial x^2} + \frac{\partial^2 V}{\partial y^2} = 0$$

A diagrammatic arrangement of the system is shown in Fig. I.11. A tank contains distilled water as an electrolyte. Inserted in the tank are two electrodes A and B and a probe P. The electrodes are connected to an alternating current supply (to avoid electrolysis) with resistances R_1 and R_2 forming two arms of a Wheatstone Bridge—the resistances of the electrolyte between the probe P and the electrodes A and B being the other two arms. A galvanometer D is used as a detector. The resistances R_1 and R_2 are set at fixed values to correspond to a given isothermal and the probe P moved until the detector D is zero and the current flow is balanced. To nullify polarizing effects at the probe a variable capacitor C may

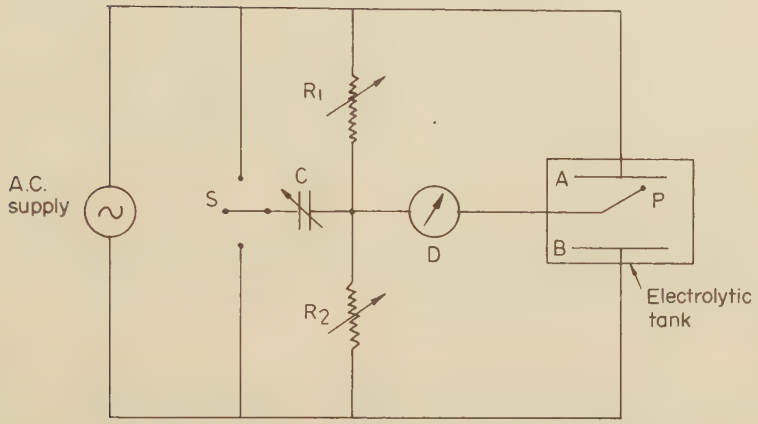

FIG. I.11. Electrical analogue system.

S, switch; C, variable capacitor;
D, detector; R_1,R_2, variable resistances;
A, B, electrodes; P, probe.

be switched into either arm at S. The probe is connected by means of a pantograph to a pencil over a plotting table. When the null point is obtained a pencil mark is made on drawing paper in the plotting table. The probe traverses the tank until a reasonable number of null points are obtained for a continuous isothermal to be plotted.

Let R_a and R_b be the electrolyte resistance from A to P and B to P respectively, and let R_1 and R_2 be set at some value, then at balance

$$\frac{R_a}{R_b} = \frac{R_1}{R_2} .$$

Let X be the ratios

$$X = \frac{R_a}{R_a+R_b} = \frac{R_1}{R_1+R_2} .$$

Now the analogue equations give:

$$V_{AB} = V_A-V_B \equiv T_A-T_B \equiv \Delta T_{AB},$$

$$V_{PA} = V_P-V_A \equiv T_P-T_A \equiv \Delta T_{PA}.$$

Then at balance for current I:

$$\frac{V_{PA}}{V_{AB}} = \frac{I\,R_a}{I(R_a+R_b)} = \frac{R_a}{R_a+R_b} \equiv \frac{\Delta T_{PA}}{\Delta T_{AB}},$$

$$X = \frac{R}{R_1+R_2} = \frac{1}{1+(R_2/R_1)} \equiv \frac{\Delta T_{PA}}{\Delta T_{AB}}.$$

Hence for a fixed ratio of R_2/R_1 we can plot an isothermal for $\Delta T_{PA}/\Delta T_{AB}$. Now if T_A and T_B are known it follows that the isothermal for T_P corresponds to the ratio R_2/R_1. Thus the resistances R_1 and R_2 give the temperature T_P.

For an engine component the temperatures are not uniform along the surfaces so that a modification is required to the analogue system. An arrangement for a piston is shown in Fig. I.12 to illustrate the modification. The electrodes A and B shown in Fig. I.11 are replaced by the system shown in Fig. I.12. A model piston—normally made of wood—is filled with distilled water.

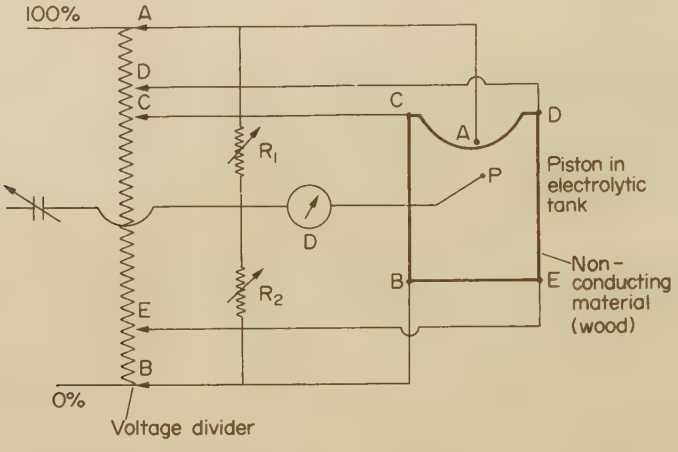

FIG. I.12. Modification to electrical analogue for non-uniform temperature boundaries.

At certain locations on the surface A, B, C, D and E the temperatures are known, say with templugs. We will assume that the maximum temperature is at A and the minimum temperature at B. The points A and B are connected either end of the voltage divider such that $V_{AB} = IR_{AB} \equiv \Delta T_{AB}$. The points C, D and E are then connected to the divider such that

$$\frac{R_{CB}}{R_{AB}} \equiv \frac{\Delta T_{CB}}{\Delta T_{AB}}, \qquad \frac{R_{DB}}{R_{AB}} \equiv \frac{\Delta T_{DB}}{\Delta T_{AB}}, \qquad \frac{R_{EB}}{R_{AB}} \equiv \frac{\Delta T_{EB}}{\Delta T_{AB}}.$$

The plotting procedure for the isothermals follow in the same manner as before.

In practice the piston cannot be represented by a simple two-dimensional pattern due to the piston shape. We normally consider two planes—the gudgeon pin plane and the thrust plane—normal to the gudgeon pin plane. One half of each plane is represented in the model as shown in Fig. I.13.

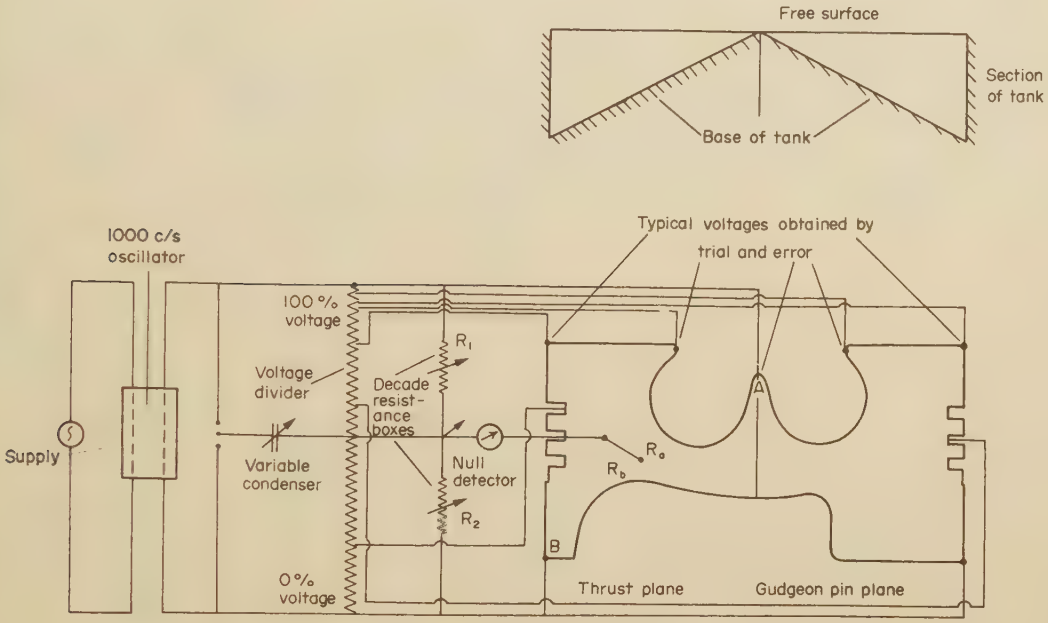

FIG. I.13. Three-dimensional electrolytic tank wiring diagram for the piston.

The axisymmetric equations are simulated by inclining the base at the tank 30° subtended from the axis (Fig. I.13). We now have a wedge of water comprising the free surface, the bottom of the tank and the piston wall. The voltage divider is connected as before on the free surface. If the templugs are bedded into the component the boundary temperature must be adjusted so that the isothermals agree with the bedded temperature. Inevitably, because of the approximations in the axisymmetric assumption for a piston, it will be difficult to obtain complete agreement between the isothermals and the measured temperature, but very close agreement can be obtained as shown in Fig. I.14.

To obtain the heat flux a "heat path" is generated as shown in Fig. I.14 (broken line). Since there is no heat accumulated in the piston it is possible to calculate the width of the heat path $\Delta\ell$ at each isothermal. The total heat flux and local heat fluxes at the surface can be computed from a knowledge of the thermal conductivity of the piston. From the heat flux, the surface temperature and the gas temperature, the heat transfer coefficients at the cylinder surface are determined. A full discussion of the electrical

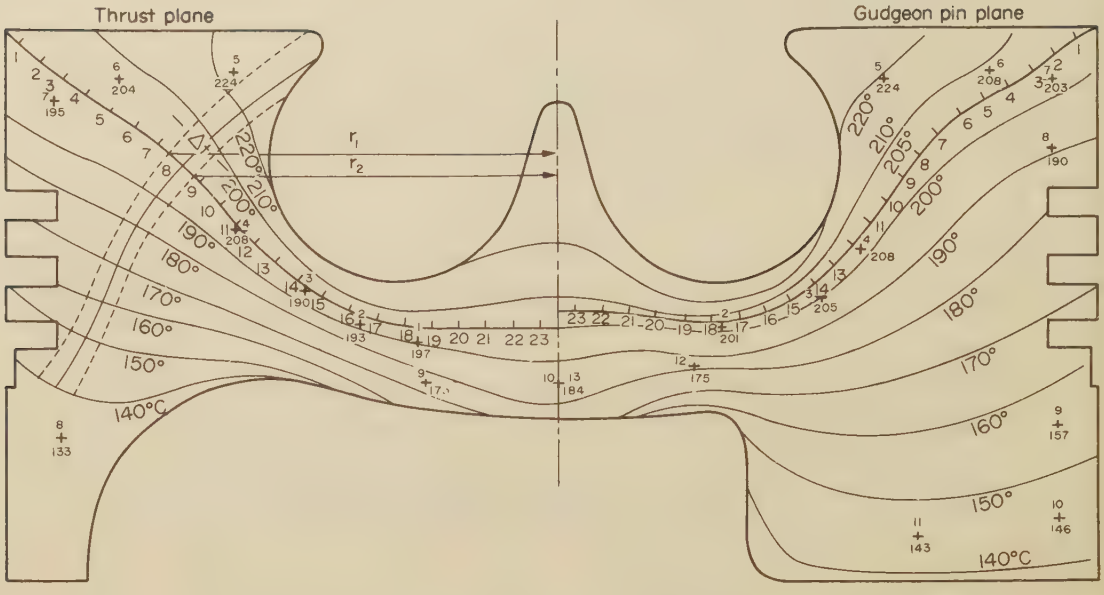

FIG. I.14. Isothermals obtained from electrical analogue.

analogue method is given by Ramchandani[6] and Jamil;[7] the former also describes a computer analysis of the problem.

I.2.2 Gas Temperature Measurement

The measurement of gas temperatures is extremely difficult, particularly in the cylinder. A number of methods have been developed but at the time of writing it seems that infrared or spectrographic methods are the most successful. These are both based on the same principle. For exhaust temperatures fine wire resistance thermometers have been successful, but there are practical difficulties in maintaining the integrity of the probes unless they are only used when the temperature is required and removed from the pipe when not required.

We shall first discuss the infrared method developed by Myers and Uyehara[8] for cylinder temperature measurement and then describe the fine wire resistance method for exhaust gas temperature measurement.

In Fig. I.15 a diagrammatic arrangement of the infrared method developed by Myers and Uyehara is shown. It is a null method. The method is based on the principle that if infrared waves from a black body source pass through a cylinder containing gas at a temperature T, then the black body temperature T_b equals the cylinder temperature when the rate of absorption of the infrared waves by the gas in the cylinder equals the rate of emission from the gas. Water vapour is taken as the sensing element (that is the detector and

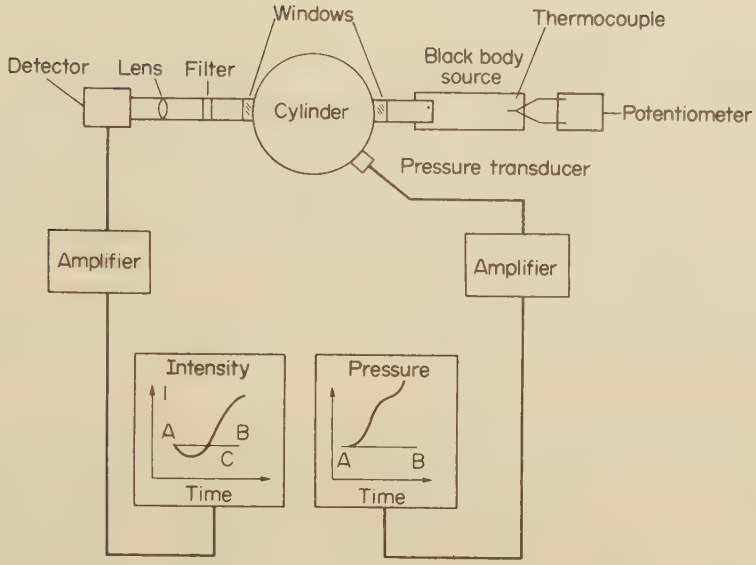

FIG. I.15. Diagrammatic arrangement of infrared method of measuring cylinder temperatures.

optical system is set to record the emissions at one of the wavelengths for water vapour—2.6 μ). A black body source is placed opposite the detector and an optical filter is placed ahead of the detector to absorb the unwanted wavelengths. The cylinder has two quartz windows so that there is a direct optical path from the infrared source to the detector. During the suction stroke there is minimum infrared absorption by the cylinder gases so that infrared waves transmitted from the black body source will pass through the cylinder with almost no change in intensity. A horizontal line AB (Fig. I.15) will be recorded. The intensity I will correspond to the black body temperature T_b measured by the thermocouple. Note this will not be the same as the gas temperature. If T_b is set above the suction temperature then at the beginning of the compression stroke as the temperature rises there will be some absorption of the infrared by the cylinder gas and the emission level will be less than from the black body. The detector will record a decrease in intensity. Further increase in temperature of the cylinder gas will produce a further decrease in recorded intensity until a minimum is reached. As the stroke continues the intensity will now increase until at C the rate of absorption of the infrared waves from the black body source equals the rate of emission from the cylinder gases. At this point the cylinder temperature equals the black body temperature T_b. The crankangle at which this occurs can be measured in the normal manner. By taking a series of black body temperatures T_b the procedure is repeated and a temperature angle diagram can be obtained. The accuracy of the method depends on the cleanliness of the quartz windows, window radiation and absorption,

homogeneity of the cylinder temperature cycle to cycle variations. A full analysis of the accuracy of the method is given by Myers and Uyehara.[8]

This method makes use of the intensity of infrared waves emitted on 2.6 μ waveband corresponding to water vapour. It is a null method. If some other chemical species can be identified participating in some chemical reaction in the cylinder whose equilibrium data are known and the relationship known between light intensity and chemical concentrations at the set wavelength, then it is possible to measure local temperatures. This method will be discussed later since it is the basis of spectrograph studies of the chemical reactions in the combustion chamber.

Another method using the relationship between the speed of sound and temperature was developed to study end gas temperatures[9] but is not now extensively used.

For measuring rapidly fluctuating exhaust gas temperatures a thin wire resistance thermometer may be used. The smaller the size of the wire the faster the response; there is, however, a limitation to the wire size before mechanical failure in service militates against its use. A full description of the construction of a resistance probe and the factors which influence its response are given by Benson.[10, 11] A typical design is shown in Fig. I.16. The element is retracted from the exhaust pipe when not in use, thus saving the wire from destruction due to solid particles in the exhaust, particularly during starting. The tungsten wire, 6.9 μ diameter and about 10 mm long, is welded to the supports after insertion in the nickel sleeves. For recording purposes the thermometer is one element of an a.c. bridge suitably offset so that the transient temperature can be measured (Fig. I.17).

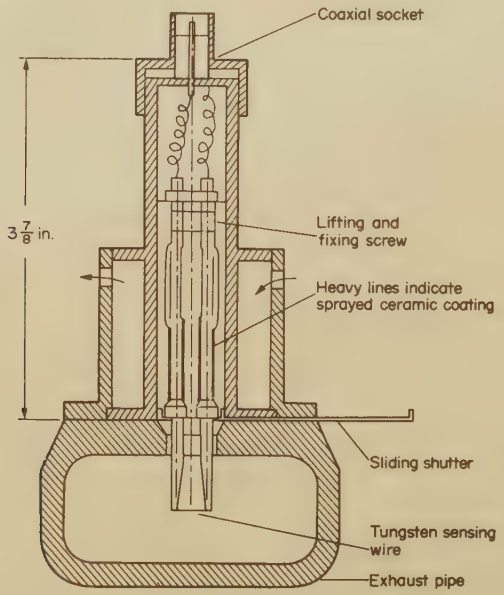

FIG. I.16. Water-cooled transient temperature probe.

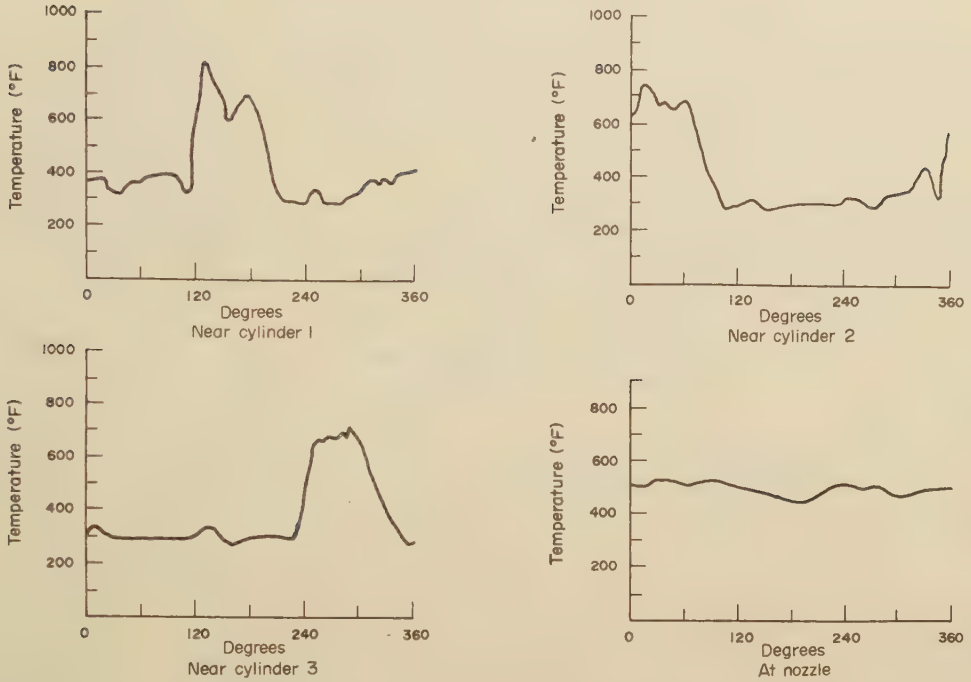

FIG. I.17. Exhaust pipe temperatures 1200 rev/min two-stroke engine. (From Benson and Pick,[4] by courtesy of the Society of Automotive Engineers.)

I.3 COMBUSTION PHOTOGRAPHY AND FLAME SPEED DETECTION

For qualitative combustion studies high speed colour photography has been successfully used, notably by Ricardo.[1] A diagrammatic layout of the system is shown in Fig. I.18. The cylinder has either a quartz or perspex window. A high speed rotating prism camera, operating up to 16,000 frames per second, is mounted on a rigid support, and mirrors are arranged to record the combustion and crankshaft simultaneously. The fuel is normally doped with copper oleate to render low luminosity flames visible. From combustion films a better understanding of the combustion process has been obtained.[12]

An alternative arrangement for photographing the combustion process, Fig. I.19, has been developed in the author's laboratory for a medium speed engine, where, due to the valve gear in the cylinder head, it is not possible to obtain a good view of the combustion space. In this apparatus the piston has a perspex crown. The combustion is viewed through the piston by means of mirrors.

A direct measurement of flame location with time may be made using ionization gauges. These consist essentially of a wire in an annulus. The wire is insulated from the body of the gauge. When a flame reaches the annulus it becomes conducting as an electrical

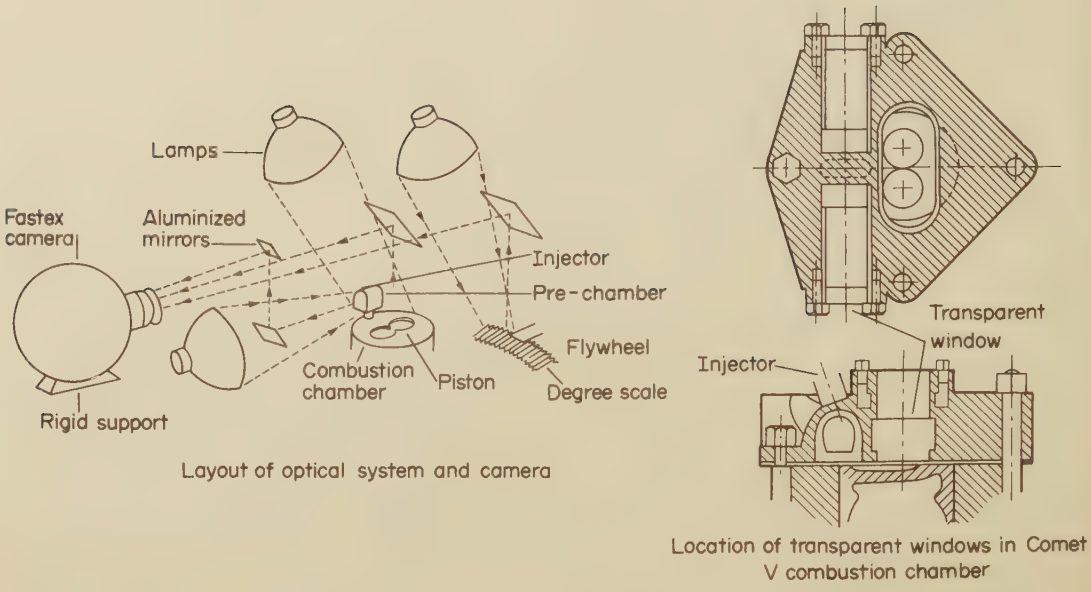

FIG. I.18. Ricardo combustion photographic rig. (From Alcock and Scott,[12] by courtesy of the Institution of Mechanical Engineers.)

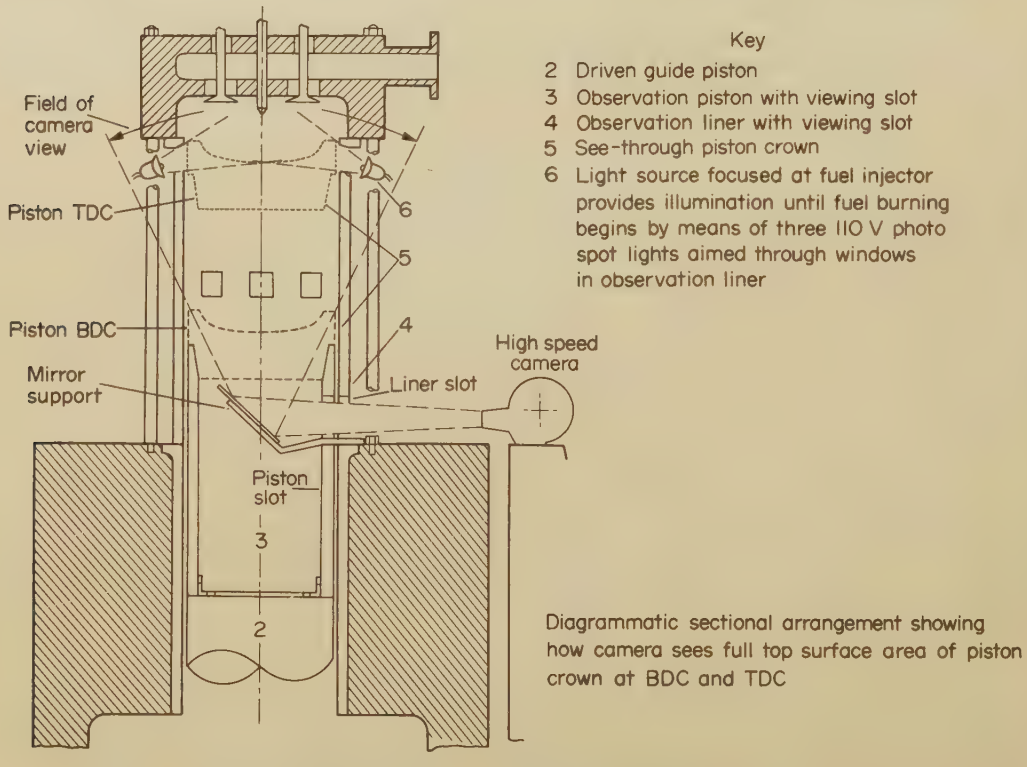
Field of camera view
Piston TDC
Piston BDC
Mirror support
High speed camera
Liner slot
Piston slot
6
5
4
3
2
Key
2 Driven guide piston
3 Observation piston with viewing slot
4 Observation liner with viewing slot
5 See-through piston crown
6 Light source focused at fuel injector provides illumination until fuel burning begins by means of three 110 V photo spot lights aimed through windows in observation liner
Diagrammatic sectional arrangement showing how camera sees full top surface area of piston crown at BDC and TDC

FIG. I.19. Diagrammatic arrangement for indirectly photographing combustion phenomena.

circuit is completed between the wire and the gauge body. A d.c. voltage is normally applied to the wire and an electronic timing circuit connected to the gauge body as well as some reference time location. When the flame arrives at the gauge the timing circuit is triggered and the time from the reference time measured. A full description of the technique is given by Harrow.[13]

By locating a sufficient number of gauges in the combustion chamber a quantitative picture of the flame propagation may be made. In analysing the results allowance must be made for expansion of the hot gas zone which is superimposed on the flame speed. The minimum voltage to trigger the ionization gauge will vary with air/fuel ratio.

I.4 SPECTROGRAPHIC METHODS

Spectrographic methods may be used for studying the chemical reactions in the cylinder as well as the local gas temperature. In these methods the light intensities associated with reacting species are measured at defined wavelengths at which the intensities are at a maximum. We will describe one method which has been successfully used to study the formation of nitric oxide during combustion.

In Fig. I.20 the rig used by Lavoie et al.[14, 15] is shown. A number of quartz windows W are fitted in the cylinder head. The light source is 2 mm by 2 mm in the cylinder combustion chamber. The cone of light emitted from the cylinder is split into four separate beams in mirror M_2, each of which is brought to a separate focus by mirrors M_3 and M_4. Three beams (2, 3 and 4) are focused onto a photomultiplier with an interference filter to pass wavelengths 0.38 μ and 0.61 μ with a bandpass of 100 Å and a wavelength of 0.75μ at a bandpass of 300 Å. The fourth channel is monitored with a monochromator and photomultiplier.

The light intensities I at the wave length 0.38 μ, 0.68 μ and 0.61 μ are recorded on a oscillograph relative to the crankangle as shown in Fig. I.20(c). The 0.38 μ wavelength corresponds to the reaction

$$CO + O \longrightarrow CO_2 + h\nu,$$

where the emitted light is associated with the discreet energy packet $h\nu$. The 0.61 μ and 0.68 μ wavelengths are associated with the reaction

$$NO + O \longrightarrow NO_2 + h\nu.$$

For the above two reactions the intensities of emitted light I associated with the energy packets $h\nu$ are related to the concentrations ( ) by

$$I_{CO} = K_1 (CO) (O),$$

$$I_{NO} = K_2 (NO) (O).$$

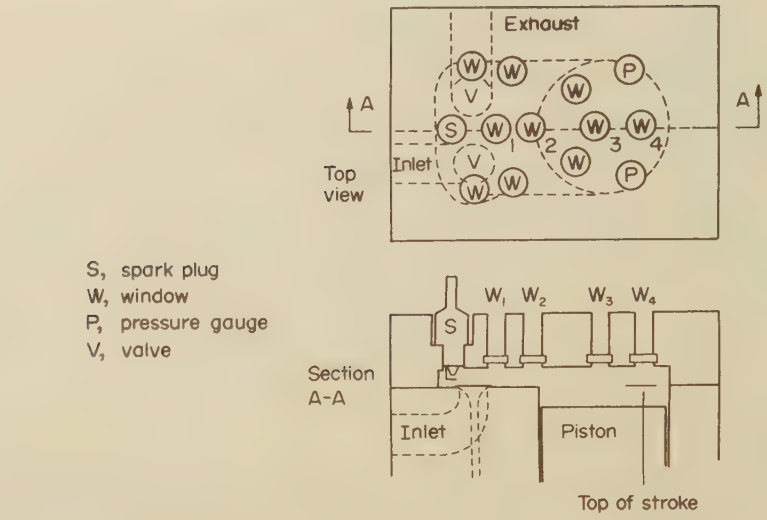

(a) Cylinder head and combustion chamber

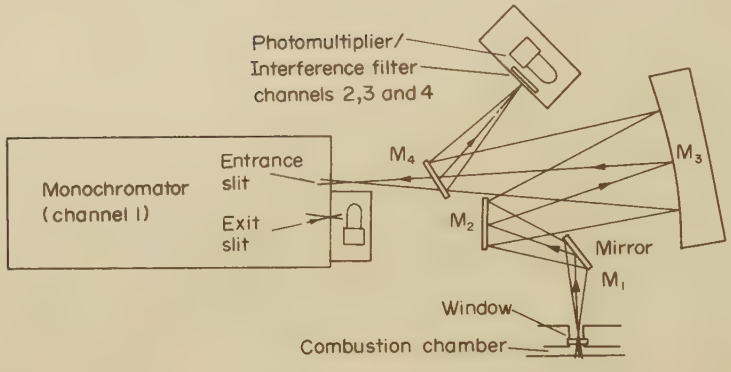

(b) Schematic of optical train

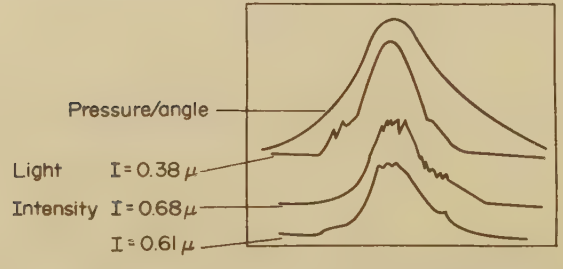

(c) Typical data record showing pressure / crankangle diagram and radiation intensity at three wavelengths

FIG. I.20. Spectrographic measurements. (From Lavoie et al.,[14] by courtesy of the Massachusetts Institute of Technology.)

The parameters K_1 and K_2 are functions of the instantaneous temperature T and the wavelength λ.

Lavoie assumed that the carbon-hydrogen-oxygen reactions were in equilibrium. Thus for each temperature T there is a known value for $(CO)(O)$ from the equilibrium constant. Furthermore, for each temperature and wavelength there is a known value for K_1. It follows therefore that at a given wavelength

$$K_1 (CO)(O) = f(T).$$

When this function equals the numerical value of the emitted light I_{CO} we know the temperature and the oxygen concentration. Thus by measuring the intensity I_{CO} at the wavelength 0.38 μ we can determine the local temperature T.

For the nitric oxide reaction, if I_{NO} is known at the appropriate wavelength, then since we know the temperature T and the oxygen concentration (O) and K_2 is a known function of the wavelength and temperature, the nitric oxide concentration can be calculated from

$$(NO) = \frac{I_{NO}}{K_2(O)}.$$

For a full discussion of the technique the reader is referred to the original papers[14, 15].

I.5 CHEMICAL ANALYSIS TECHNIQUES

Spectrographic techniques require sophisticated equipment and are limited to studying the combustion in fix positions associated with the location of the quartz windows. These windows must be kept clean and the spectrograph must be a rigid structure to cope with the optics. A more rugged method of analysis is to use a sampling valve. If this is located in a probe, then provided there is adequate clearance in the combustion space a reasonable area of the combustion chamber can be studied. With a sampling valve the chemical analysis can be carried out at some distance from the engine with fairly standard equipment which has been specifically developed for engine exhaust emissions. In this section we will describe a sampling valve and five methods of chemical analysis which are now standard equipment in engine laboratories.

I.5.1 Sampling Valve

A sampling valve should be capable of opening at a defined time and should remain open for as short a time as possible to allow an adequate sample to be drawn for analysis. There should be no chemical changes in the sample from the sample point to the point of analysis. The experiments by Downs and Wheeler referred to in Chapter 5 were carried out using a sampling valve in the end gas. A sampling valve designed in the authors' laboratories is shown in Fig. I.21. This valve is fitted in a 300 mm bore engine and opens

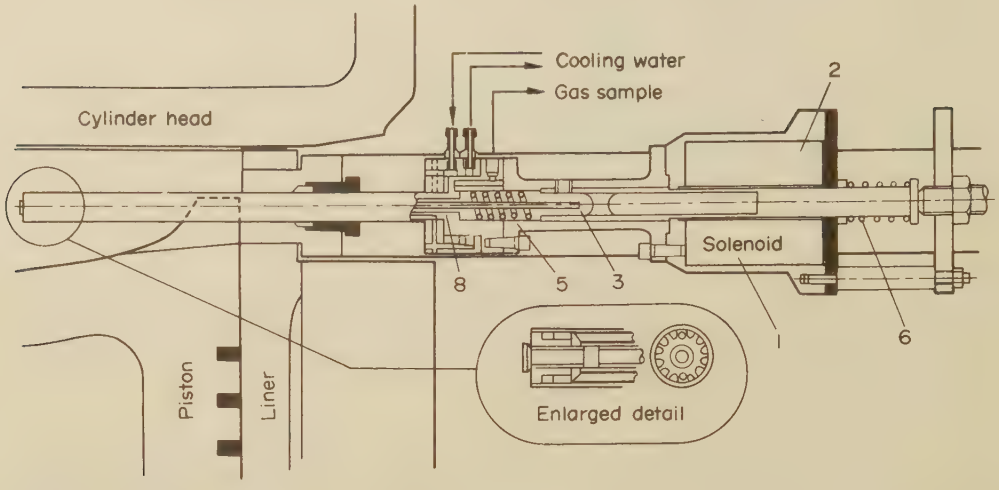

FIG. I.21. Sampling valve.

for a period of about 3 crankangle degrees at 500 rev/min with a sample withdrawal rate of some 2 ℓ/min. The timing of the valve is controlled by a crankshaft driven optical encoder which initiates current flow to the solenoid (2). This causes the steel striker (1) to be accelerated. After travelling a predetermined distance the striker hits the cap (3) on the head of the spindle (8) and rapidly opens the valve to its maximum position. The valve and the striker are returned to their original positions by the springs (5) and (6). During the opening period the gas flows from the engine cylinder through the valve annulus into a pair of hyperdermic tubes and then out of the valve body through drilled passages. The rapid expansion of the gas and the water-cooled passages provide conditions for freezing the gas composition. The sampling valve can be moved into various positions in the cylinder so that a broad spatial-temporal study of the cylinder reactions can be made. The gas samples can be analysed by the methods outlined below.

I.5.2 Orsat Apparatus

The conventional method of gas analysis is the Orsat apparatus. It is primarily used for exhaust gas analysis. If it is handled correctly it can give excellent results but cannot measure extremely small quantities or concentrations.

100 c.c. of exhaust gas is withdrawn from the pipe directly into a water-jacketed measuring burette. The sample gas is then successively passed into a solution of caustic potash to absorb carbon dioxide, a solution of pyrogallic acid in caustic potash and water to absorb oxygen and finally, a solution of cuprous chloride to absorb carbon monoxide. At each step the reduction in volume of the 100 c.c. sample corresponds to the percentage of the constituent in the exhaust gas. Accurate exhaust gas analysis will enable the air flow to an engine to be calculated from the fuel flow.

I.5.3 Non-dispersive Infrared (NDIR)

This instrument is used to measure carbon monoxide, carbon dioxide and nitric oxide although the accuracy is not very high for the latter with low concentrations.

A schematic arrangement of the instrument is shown in Fig. I.22. The detector is mounted on a cradle at one end of an optical bench. It consists of an aluminium alloy body containing a sealed sample of gas of the type to be measured and is symmetrical about the centre line, being divided by a pressure sensitive diaphragm into two chambers. The energy receiving cells, fitted with windows, communicate with each chamber. Infrared energy reaching the gas in the cells is absorbed by molecular vibration at frequencies characteristic of that gas, 4.0-4.5 μ for carbon dioxide and 4.5-5.0 μ for carbon monoxide, and then converted to translational energy which heats the gas. Since the chambers are sealed, the heat causes the gas pressure to rise and act upon the diaphragm. Insulated electrodes forming capacitors on either side of the diaphragm are connected to an electronic bridge circuit to detect diaphragm movement and hence the difference in energy received between the detector cells.

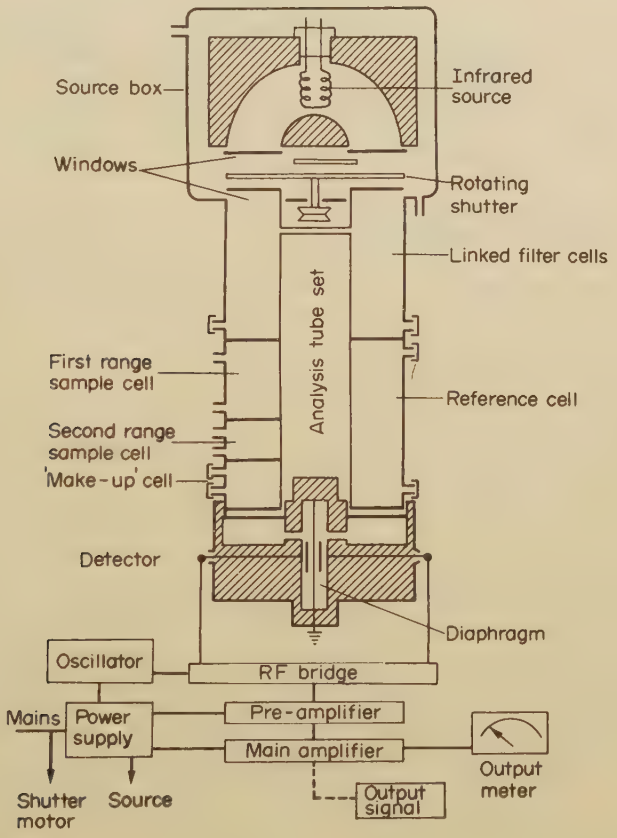

FIG. I.22. Schematic diagram of NDIR analyser.

The infrared radiation source consists of a heated wire in a quartz tube mounted in the source block located at the opposite end of the optical bench to the detector. Radiation from the source is reflected within the mounting block and passes out of a symmetrical pair of rectangular apertures into the analysis tube set. This comprises of a pair of tubes which are internally highly polished and gold-plated to ensure high transmission of radiation into the detector cells. One tube is used for the gas to be measured, whilst the opposite tube is used for reference, and is usually filled with dry air. The sample cells may be divided by windows into various lengths to give different ranges of sensitivity, the unused sample cells generally being flushed with a non-infrared-absorbing gas such as oxygen or nitrogen, or gas free of the component being measured, e.g. fresh air for carbon monoxide analysers.

The radiation from the source is interrupted by a rotating two-bladed shutter driven by a synchronous motor. Thus chopping is necessary to avoid spurious signals which would otherwise be caused by slow thermal changes, and it provides an alternating signal which is more convenient for amplification. An electronic bridge which detects the diaphragm movement is fed from a r.f. oscillator. Matched coils in series with the detector capacities on either side of the diaphragm form two arms of a bridge. When the detector diaphragm is displaced it increases one capacity and reduces the other, thus unbalancing the bridge. The unbalanced signal is then recorded directly in parts per million or per cent of the sampled gas. To change the range it is possible to switch the sample to different cells or, alternatively, to change the sensitivity of the electronic circuiting.

To zero an analyser a non-infrared-absorbing gas, e.g. dry air, is passed through the instrument. For other points on the scale calibrating gases with known concentration of carbon dioxide, carbon monoxide and nitric oxide are passed through the analyser.

I.5.4 Flame Ionization Detector (FID)

This instrument is mainly used to measure hydrocarbon concentrations in the gas sample. A pure hydrogen air flame produces very little ionization, but if a few hydrocarbon molecules are present the flame produces a large amount of ionization. The ionization is proportional to the carbon atoms present in the hydrocarbon molecule.

A diagrammatic of an FID is shown in Fig. I.23. This comprises a burner, an ignitor, an ion collector and electronic circuitry. Hydrogen, or a mixture of hydrogen and nitrogen, enters one leg of the capilliary tube and the sample enters by another leg. The length and bore of the capillary tubes are selected to control the flow rates. The mixture of H_2-N_2-C_nH_m then flows up the burner tube to a mixing chamber where a fixed proportion of air is admitted. This mixture is ignited and a diffusion flame stands at the exit to the burner tube. An electrostatic field is produced around the flame by a polarizing battery. This causes the electrons to flow to the burner jet and the ions to the collector. The collector and the burner form part of an electrical circuit. The flow of ions to

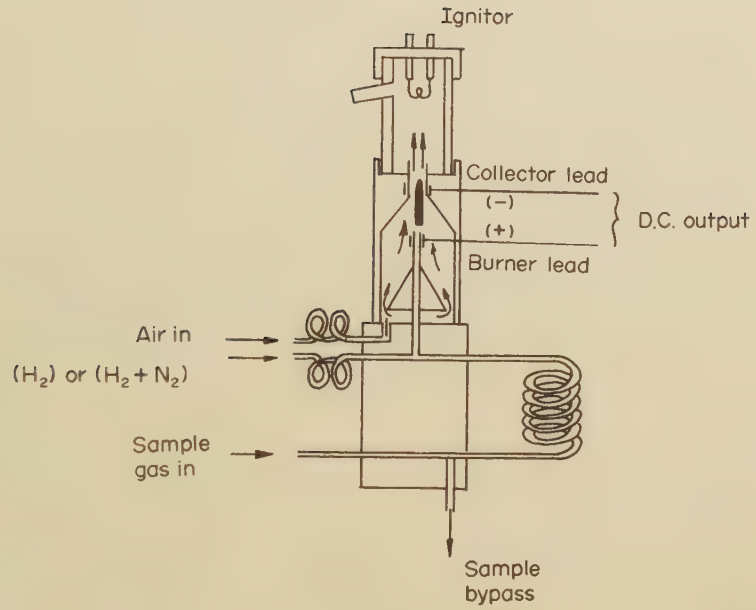

FIG. I.23. Flame ionization detector. (From Patterson and Heinan,[3] by courtesy of Ann Arbor Science Publishers Inc.)

the collector and the electrons to the burner complete the electrical circuit. The d.c. level of the current flow is recorded on a meter. This is calibrated directly in amount of hydrocarbons. To calibrate, the detector samples of known hydrocarbons are measured and the meter reading noted.

I.5.5 Gas Chromatography

Whilst the FID will give the gross hydrocarbon concentration, gas chromatography is used to identify the hydrocarbon components. Gas chromatography is a well-known chemical analysis tool for physically identifying the components in a chemical mixture. A number of chromatographic methods are used; we shall describe one only. The important section of the instrument is the column. This is a packed tube containing a solid or a solid-liquid which have certain absorbing properties. The gas to be sampled is injected into an inert gas stream called the carrier gas (or solvent) (Fig. I.24). The carrier gas is the moving phase and the solid or solid-liquid is the stationary phase. As the gas flows down the column, chemical components in the moving phase migrate into the stationary phase and then back again into the moving phase. The rate of migration into and out of the stationary phase depends on the absorbing properties of the components and the stationary phase. Some components absorb more strongly than others, so that there will be a tendency for some of the components in the carrier gas to lag behind others as the gas flows down the tube. If the column is long enough the sample will separate into discrete zones of each component in the mixture with sharp discontinuities at the zone interfaces. The gas leaving the column therefore contains slugs of the constituent substances in the original mixture.

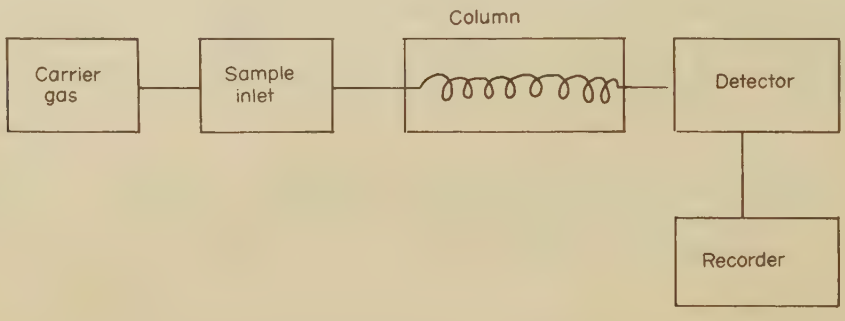

(a) Block diagram of gas chromatograph

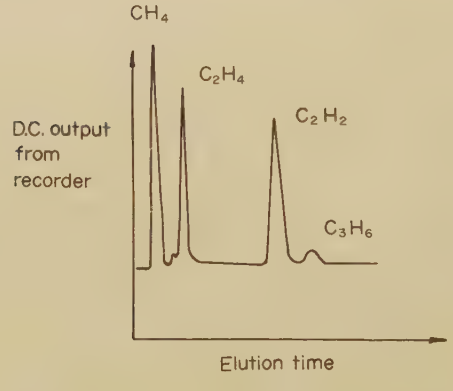

FIG. I.24. Gas chromatograph.

On leaving the column the gas enters a detector (Fig. I.24). The detector serves two functions: the first to measure the time a component is in the column called the elution time, and the second to measure the quantity of the component in the original sample. For hydrocarbon constituents we can use a FID as the detector. If the output from the detector is connected to a time base recorder, then as the carrier gas passes through the detector the product of the output signal times time will be directly related to the quantity of that component currently being detected. The signal will reach a maximum for each component and then decrease. A record of the type shown in Fig. I.24(b) will be obtained. In this chromatogram the first component is methane (CH_4); this has a sharp response, so that the quantity of methane is almost proportional to the output. There is a small bump in the record (due to C_2H_6) followed by another sharp peak corresponding to ethylene (C_2H_4), then the carrier gas contains no hydrocarbon component until acetylene (C_2H_2) appears. Once again with a sharp signal which corresponds to the quantity of acetylene in the original mixture.

To calibrate a chromatograph, fixed quantities of known substances are injected into the sample gas and the elution time is noted as well as the output calibration. Thus the hydrocarbon can be identified by the elution time and quantitatively measured. Jeffrey and Kipping[16] give a detailed review of current practice on the application of gas chromatography to exhaust emission measurement.

I.5.6 Chemiluminescence

This technique is used to measure extremely small quantities of nitric oxide. The principle of operation is identical to the spectroscopic methods described in section I.4. A mixture of a gas sample and ozone (Fig. I.25) enter a reaction vessel which is maintained at a very low absolute pressure. The reaction of the ozone and nitric oxide when heated under vacuum at 600°C produce some electronically excited molecules of nitrous oxide. When the electronically excited molecules decay they emit light which is measured on a photomultiplier. The output of the photomultiplier is amplified and recorded. The light intensity is proportional to the nitric oxide concentration in the sample.

To analyse all the oxides of nitrogen a converter is usually fitted ahead of the reaction vessel to convert all the oxides of nitrogen into nitric oxide. A full discussion on the application of the chemiluminescence technique and its application to emission testing is given by Soltau and Larbey[17] and Nicki et al.[18]

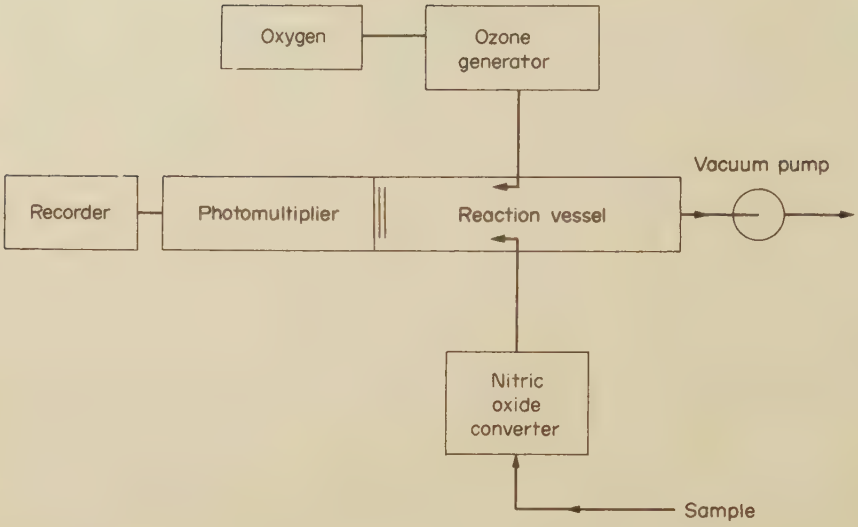

FIG. I.25. Chemiluminescent nitric oxide analyser.

REFERENCES

1. Ricardo, H. and Hempson, J.G.G., The High Speed Internal Combustion Engine, 5th edn., Blackie, 1968.

2. Accuracy of electronic measurements in internal combustion-engine development, Proc.Instn.Mech.Engrs. 180, Part 3G (1956-6).

3. Patterson, D.J. and Henein, N.A., Emissions from Combustion Engines and their Control, Ann Arbor Science, 1972.

4. Benson, R.S. and Pick, R., Recent advances in internal combustion engine instrumentation with particular reference to high speed data acquisition and automated test bed, SAE Paper 740695 (1974).

5. Benson, R.S. and Pick, R., Recent developments in internal combustion engine instrumentation in UMIST laboratories, Advance No. 9 (1970).

6. Ramchandani, M., Heat transfer in a four-stroke pressure charged diesel engine, PhD thesis, University of Manchester 1969.

7. Jamil, Q.H., Heat transfer to the piston of a naturally aspirated four-stroke diesel engine, MSc thesis, University of Manchester, 1965.

8. Myers, P.S. and Uyehara, O.A., Accuracy of and representation results obtained with an infrared pyrometer measuring compression temperatures, Proc. Instn. Mech. Engrs. 180, Part 3G, 83, (1965-6).

9. Livergood, J.L., Taylor, C.F. and Wu, P.C., Measurement of gas temperatures in an engine by the velocity of sound method, SAE Trans. 62, 503 (1954).

10. Benson, R.S. and Brundrett, G.W., Development of resistance wire thermometer for measuring transient temperatures in exhaust systems of internal combustion engines, Temperature - Its Measurement and Control in Science and Industry, 3, Pt. 2, 631 (1962).

11. Benson, R.S., Measurement of transient exhaust temperatures in internal combustion engines, The Engineer 217, 377(1964).

12. Alcock, J.F. and Scott, W.M., Some more light on diesel engine combustion, Proc. Instn. Mech. Engrs. (AD), 179 (1962-3).

13. Harrow, G.A., The effects of engine operating variables on the time of flame propagation in a spark ignition engine, J. Inst. Pet. 49 (1963).

14. Lavoie, G.A., Heywood, J.B. and Keck, J.C., Experimental and theoretical study of nitric oxide formation in internal combustion engines, MIT Fluid Mechanics Laboratory, Report No. 69-10 (1969).

15. Lavoie, G.A., Spectroscopic measurement of nitric oxide in spark ignition engines, Combustion and Flame 15, 97 (1970).

16. Jeffrey, P.G. and Kipping, P.J., Gas chromatography for the analysis of exhaust gases, Proc. Instn. Mech. Engrs. 180, Pt. 3G, 95 (1965-6).

17. Soltau, J.P. and Larbey, R.J., Sampling and measurement of exhaust emissions for motor vehicles. Air Pollution in Transport Engines. Proc. Instn. Mech. Engrs. Paper C143/71, 218 (1971).

18. Nicki, H., An ozone-NO chemiluminescence method for NO analysis in piston and turbine engines, SAE Paper 710072 (1971).

19. Rogers, G.F.C. and Mayhew, Y.R., Engineering Thermodynamic Work and Heat Transfer, Longmans, 1967.

20. Law, A.G., Instantaneous heat transfer in an opposed piston two-stroke diesel engine, PhD thesis, University of Manchester, 1968.

21. Brock, E.K. and Glasspoole, A.J., Thermal loading of cylinder heads and pistons on medium-speed oil engines, Proc. Instn. Mech. Engrs. 179, Part 3C, 3 (1964-5).

Subject Index

Absorptivity, 142
Activation energy, 50
Air-fuel mixing, 4
Air restriction, throttling, 15,21
Arrhenius equation, 50,81
Autoignition, 15,16,18,20,106,110

Bernoulli's equation, 36

Carbon monoxide, 123
Carburettor, 22
Cetane, 21
Chemical analysis, 193
Chemiluminescence, 199
Closed systems, 28
Cold starting, 10
Combustion,
  abnormal, 105
  normal, 99
  photography, 189
  uncontrolled, 118
Combustion chamber,
  air cell, 8
  automotive, 18
  Comet, 7
  compression ignition, 5
  deep bowl, 10
  hemispherical, 16
  Lanova, 8
  Meurer, 9
  overhead valve, 18
  quiescent, 12,14
  shallow bowl, 13
  side valve, 18
  squish lip, 10,11
  spark ignition, 15
  stratified charge, 20
  sub-divided, 6,14
  'T' head, 18
  turbulence chamber, 7
Compression ratio, 4,18,55
Computer, on-line, 174
Continuity equation, 35
Convection, 141
Cool flame, 106
Cycle calculations, 16
Cycles,
  air standard, 53
  diesel, 58
  dual combustion, 60
  modified Atkinson, 60,61
  Otto, 58

Diesel knock, 9
Dissociation, 44
Duration of combustion, 17,21

Efficiency, air standard, 58
Electrical analogue, 181
Electrolytic tank, 182
Emissions, 89,123
Emissivity, 142
Emissivity of clouds, 147
Engines,
  automotive, 3,4
  auxiliary, 4
  compression ignition, 4
  Doxfords, 13
  gas, 18
  indirect ignition, 4,15
  industrial, 3
  marine, 3
  Perkins, 10,11
  reciprocating, 3
  rotary, 3
  spark ignition, 4,15
  Wankel, 4,22
Enthalpy, 30,31,39
Equilibrium constant, 47,49
Equilibrium equation, 47
Excess air, 21
Expansion ratio, 4,18,56

First Law of Thermodynamics, 28, 29
Flame,
  front, 17,20,21
  ionization detector, 196
  path, 18
  propagation, 1
  speed, 17
Flammability limit, 15
Fourier analysis, 180
Fuel,
  additives, 117
  injection, 4,5
  sprays, 11

Gas,
  chromatography, 198
  mixtures, 37
  radiation, 146
  temperature measurement, 186, 188
Gaseous pollutants, 92
Grey body, 142

Heat flux, 153

Heat release, 75
Heat transfer,
  calculations, 155
  coefficients, 163,164
  convective, 147
  radiant, 151
Homentropic flow, 34
Hydrocarbons, 134

Ideal gas, 27
Ignition,
  delay, 71
  spark, 4,15
  timing, 114
  torch, 22
Indicated efficiency, 15
Induction period, 109
Infra-red, 186,195
Injection system, 21
Intensity of radiation, 142
Intermittent combustion, 3
Internal energy, 29,39

Kirchhoff's law, 142
Knock, knocking, 16,74,105,113,117

Main chamber, 22
Methane, 20
Mixture strength, 15
Momentum equation, 35

Nitric oxide, 124
Nusselt number, 149

Octane, 21
Open system, 29
Opposed piston, 12
Optical encoder, 174
Orsat, 194

Particle cloud radiation, 146
Pollution, pollutant, 15,21
Polynomial coefficients, 39
Polynomial functions, 29
Prandtl number, 149
Pre-chamber, 22
Pre-combustion, 14
Pre-ignition, 4,15,118,119
Pressure measurement, 171
Pressure, normalized, 34
Pumping work, 15

Quiescent, 14

Radiation, 141
Rate of combustion, 17,20
Reciprocating, 3
Reynold's number, 149
Ricardo, 7,8
Rotary, 3,22
Rumble, 119
Running on, 118,119

Sampling valve, 193
Sauter mean diameter, 87
Second Law of Thermodynamics, 32
Self ignition, 4
Shape factor, 145
Single zone combustion models, 75
Soot, 90
Specific heat at constant
  volume, 28,29
Spectrographic measurements, 191
Squish, 10
Steady flow-energy equation, 31
Stefan-Boltzmann Law, 142
Stoichiometric coefficients, 45
Stratified charger, 15,20
Surface area, 17
Swirl, 10,12,14,21

Temperature,
  maximum, 122
  measurement, 177
  surface, 153,177
Templugs, 180
Texaco, 21
Thermocouple, thin film, 171
Thermocouple, traversing, 180
Torch ignition, 22
Transducers,
  inductive, 176
  piezo-electric, 172
  strain gauge, 176
Troichoidal, 22
Turbulence, 17
Two-zone combustion model, 84

Universal gas constant, 27

Wall quenching, 16,135
Work, 28,30

internal combustion engines

VOLUME 1

A detailed introduction to the thermodynamics of spark and compression ignition engines, their design and development

This two volume text contains the most up-to-date presentation of the thermodynamic processes in spark and compression ignition engines. The text contains much original material related to engine design and development. A novel feature in the text is the presentation of FORTRAN listings of programs for simple cycle calculations for both compression and spark ignition engine cycles. Methods are also outlined for more complex cycle calculations of the type which are now normally carried out in design offices. The text also includes hardware features, together with a comprehensive appendix describing the latest experimental methods including emission measurements, for completeness. SI/Metric Units are used throughout.

CONTENTS

Description of internal combustion engines. Basic thermodynamics a
gas dynamics. Air standard cycles. Combustion in compression ignit
engines. Combustion in spark ignition engines. Heat transfer
engines.

KV-198-232

Low Priced Student Editions
in the
PERGAMON INTERNATIONAL LIBRARY
of Science, Technology, Engineering and Social Studies

- A complete catalogue is available from the publisher
- An inspection copy of any book in the Pergamon International Library is available to lecturers and teachers for consideration for course adoption. For details of this service see notice in the preliminary pages of this book

ISBN 0 08 022718 X f